Urban Volatile Organic Compounds in the UK: Source Apportionment, Temporal Variability, and Responses to COVID-19 Lockdown Measures

Abdulla Moussa

Doctor of Philosophy

University of York

Chemistry

August 2025

Abstract

Volatile organic compounds (VOCs) play a key role in urban air quality degradation by contributing to atmospheric ozone and secondary organic aerosol formation, in addition to their direct health risks. Despite regulatory progress in the United Kingdom, major uncertainties remain in the quantification of VOCs sources, their temporal variability, and their responsiveness to interventions. This thesis provides a comprehensive multi-scale investigation of VOC sources and behaviour in UK urban environments through receptor modelling, inter-city comparison, and a natural experiment.

First, the U.S. EPA Positive Matrix Factorisation (PMF 5.0) model was applied to long-term measurements from the London urban background Supersite, resulting in a robust seven-factor solution that identified the major VOCs sources: regional alkanes, vehicular combustion, fuel evaporation, solvents, industrial activity, and residential combustion. Secondary oxidation and solvent-related emissions were identified as key drivers of ozone and SOA generation, whereas traffic evaporative emissions exceeded vehicle exhaust.

Second, clear seasonal and spatial differences in VOCs profiles were revealed through comparative analysis between London (2023) and Birmingham (2022). Given the weaker photochemical removal and reduced boundary layer height, VOCs levels were consistently higher in winter, while oxygenated VOCs were the major contributors in summer. London demonstrated stronger contributions from solvent and evaporative emission sources, whereas Birmingham exhibited more significant combustion signatures.

Finally, the COVID-19 lockdown offered a natural assessment of emission sensitivity. At Marylebone Road, sharp declines in traffic-related alkanes and aromatics confirmed the dominance of vehicular sources, whereas Eltham displayed mixed responses, with background and meteorology masking traffic-related reductions. Random Forest meteorological normalisation and business-as-usual projections highlighted the necessity of statistical methods to separate emission changes from weather-driven variability.

Overall, this work demonstrates that effective UK VOCs policy must target solvents, fuel evaporation, and residential emissions in addition to traffic sources, with strategies tailored to local emission characteristics and secondary pollutant formation dynamics.

List of Contents

List of Tables

List of Figures

Acknowledgements

I would like to sincerely thank my supervisor, Prof Jacqueline Hamilton, for her constant support, patience, and guidance. Your constructive feedback, insightful comments, and encouragement have been so important for my development as a researcher and in shaping this thesis.

I am also very grateful to Dr Jim Hopkins for his generous support and the kind way you have always shared your time and expertise. Your advice, always patient, optimistic, and reassuring, has helped me face challenges with more confidence. I especially appreciate the way you have supported me with a smile, right up to the very last stage of this journey.

Finally, my deepest thanks go to my family for their love, support, and understanding. Your patience, sacrifices, and belief in me have carried me through the many challenges of this PhD.

Author's declaration

I declare that this thesis is original work, which I undertook at the University of York from 2020-2025. Except where stated, all the work contained within this thesis represents the original contribution of the author. This work has not previously been presented for an award at this, or any other, University. All sources are acknowledged as references.

Abdulla Moussa

August 2025

Chapter 1

1 Introduction

1.1 Volatile Organic Compounds (VOCs) Definition

The non-methane volatile organic compounds, generally called VOCs, are a group of organic species with sufficient volatility to enter the troposphere in the gas phase. Once present, they can affect air quality and exert serious direct and indirect impacts on both human health and the climate. Their effects vary depending on chemical toxicity (for instance, benzene is classified as carcinogenic to humans) and atmospheric reactivity, which influences their ability to form secondary pollutants such as ozone and secondary organic aerosols (SOA) (Vaughan et al., 2017). A more specific definition of VOCs has been given within the 2004/42/EC Paints Directive: VOCs include all organic compounds that have a boiling point, at the standard pressure (101.3 kPa), equal to or less than 250 °C (DIRECTIVE 2004/42/CE OF THE EUROPEAN PARLIAMENT AND OF THE COUNCIL, 2004). These VOCs can be classified depending on their chemical functional groups: alkanes, alkenes, ketones, organic acids, aldehydes, esters, aromatic hydrocarbons, and alcohols (Hanif et al., 2021). The process of tropospheric ozone formation by the reaction between VOCs and NOx initiates under the presence of sunlight; this light near the UV range (290–400 nm) can destroy the VOCs directly, or it oxidises the VOCs by free radicals initiated by a chain of photochemical reactions, where peroxyl radicals are being generated (Seinfeld & Pandis, 2016). These radicals can create a net photochemical ozone production route from the photolysis of NO_2, starting by converting NO to NO_2, without consuming ozone molecules, as presented in Figure 1-1.

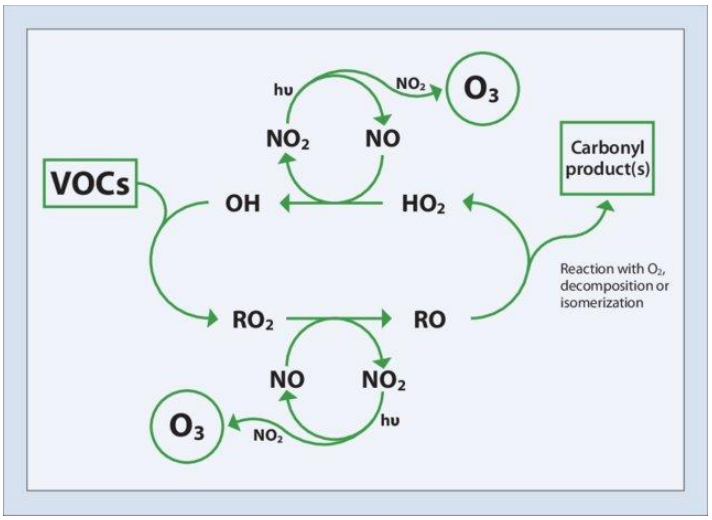

Figure 1-1 Illustration of net tropospheric ozone (O_3) formation through VOC–NO_x photochemical cycle, (WHO, 2008).

The importance of the VOCs in tropospheric ozone formation leads to a broader definition of VOCs in this respect according to the EC Air Quality Directive 2008/50/EC: VOCs are the organic species which have been emitted either from biogenic or anthropogenic sources, apart from methane, and have the ability to form photochemical oxidants under the availability of sunlight through their reaction with NO_x (Lewis et al., 2020).

The other vital role of VOCs in the atmosphere is their contribution to secondary organic aerosol (SOA) formation. As a result of the VOCs oxidation process in the atmosphere, products with low vapour pressure are being formed. These oxidation products can be easily absorbed into the pre-existing particles when they are present in the condensed phase. However, the importance of the VOCs in the SOA formation varies between VOC species, where toluene, m-xylene, ethylbenzene, benzene, and o-xylene have been found to be the five most significant anthropogenic VOC contributors to the ambient SOA formation in the UK (Derwent et al., 2010).

Where VOCs are present in the atmosphere in hundreds of different compounds, especially in the urban areas, they play a key role in determining the ambient levels of very important atmospheric species such as HO and HO_2 radicals, as shown in Figure 1-1, that are crucial to the atmosphere's oxidative capacity, which controls the rate at which pollutants like VOCs and methane are degraded (Atkinson, 2000a; Monks, 2005). Where a reduction in HO and HO_2 levels extends the atmospheric lifetimes of VOCs and methane, hence extending their environmental effects, which is particularly important for methane, given its crucial role as a greenhouse gas (IPCC, 2023). All of that emphasises the importance of the individual ambient VOCs monitoring for better understanding of VOCs emission sources to implement appropriate strategies to control their emissions, which is essential to minimise the hazardous secondary pollutants levels, which VOCs are considered one of their most important precursors (Shen et al., 2018).

1.2 General VOCs emission sources

Natural biochemical reactions in oceans, vegetation, and soil, as well as activities that are initiated by humans, including the burning of fossil fuels in a variety of industrial, commercial, and domestic processes. In addition to the extraction and distribution of both natural gas and petroleum, along with number of petrochemical industries, are all sources of VOCs that are

released into the atmosphere. These emissions are of varying significance depending on the setting in which they are released into the atmosphere. While the natural sources dominate the global VOCs emissions accounting of about 75% of them, the anthropogenic ones have vital role in the atmospheric chemistry in the urban environments (Montero-Montoya et al., 2018). This is particularly important given the majority of the worldwide population lives in urban areas, where the effects of VOC emissions, mainly atmospheric ozone formation, are more acute. Therefore, urban anthropogenic emissions possess immediate impact to human health and air quality, despite the fact that natural sources account for the majority of VOCs world budget.

Table 1-1 Volatile Organic Compounds in the UK: Atmospheric Lifetime and Main Sources.

VOC	Typical Atmospheric Lifetime	Dominant UK Emission Sources	Environment
Ethane	1–2 months	Natural gas leakage, oil & gas extraction	Regional background / Rural/ Urban
Propane	10–14 days	fuel storage and distribution	Urban / Suburban
n-/iso-Butane	4–6 days	fuel evaporation, vehicle exhaust	Urban
n-/iso-Pentane	2–4 days	Petrol evaporation, vehicle refuelling	Urban
Acetylene	2 weeks	Incomplete combustion, road transport, biomass burning	Urban roadside
Ethene	1–2 days	Vehicle exhaust, combustion sources	Urban
Benzene	7–12 days	Petrol vehicles, industrial combustion, biomass burning	Urban
Toluene	1–3 days	Solvent use (paints, coatings), vehicle emissions	Urban / Industrial
(m, o, p) Xylenes	1–2 days	Solvent use, surface coating, fuel evaporation	Urban / Industrial
Formaldehyde	Hours	Secondary formation from VOC oxidation, combustion, biomass burning	Urban & Regional
Ethanol	4 days	Plants, biofuel	Urban / Suburban
Methanol	10–15 days	Vegetation, secondary oxidation	Regional
Isoprene	1–3 hours	vegetation (biogenic) biomass burning, traffic	Rural (summer)/ Urban
Monoterpenes	Minutes–hours	vegetation (biogenic)	Rural / Woodland
Sesquiterpenes	Minutes	Vegetation (biogenic)	Rural

(Acosta Navarro et al., 2014; Atkinson, 2000; Atkinson & Arey, 2003; Derwent et al., 2010; Lewis et al., 2020; Richmond, 2025; Simpson et al., 2012).

1.2.1 Biogenic emissions (BVOCs)

Biogenic volatile organic compounds (BVOCs) are crucial to the atmospheric gas phase and heterogeneous chemistry because of their extremely high atmospheric reactivity, which causes their atmospheric lifetime to vary from a few minutes to hours. Isoprene and monoterpenes being the most abundant BVOCs as shown in Table 1-1, primarily from terrestrial vegetation emissions, as it considers the main BVOCs source (Sindelarova et al., 2014). It worth mentioning that the emission rates of BVOC species vary, under similar ambient conditions, between different plants (Acosta Navarro et al., 2014). There are several variables that can influence the emission rates of BVOCs from vegetation with sun light and ambient temperature usually considered the most important, as these have a significant impact on the rate at which a particular BVOC is released from a specific plant (Kesselmeier & Staudt, 1999). It has been estimated that an increase of 1 °C due to global warming may increase the emissions of monoterpene by almost 15% (Y. Liu et al., 2021). Consequently, the significance of BVOCs in atmospheric chemistry is expected to increase as global warming increase the natural VOCs emissions.

Plants, in general, emit BVOCs during their growth and reproduction as well as for defensive purposes. Isoprene emissions, in particular, are directly related to vital physiological functions such as mammal, insect, and parasite protection and metabolism (Ramirez-Gamboa et al., 2021), where isoprene is primarily released by plant leaves, utilising carbon substrates derived from the Calvin cycle (Sharkey et al., 2008) which explains the seasonal variability in its ambient levels. On the other hand, alcohols and carbonyls are the second predominant BVOCs groups after isoprene and monoterpenes, BVOCs also include esters, alkanes, alkenes, acids, and ethers (Kesselmeier & Staudt, 1999).

1.2.2 Anthropogenic VOCs Emissions (AVOCs)

According to the USEPA, man-made VOC emissions, as shown in Table 1-1, involve emissions from 1- fuel combustion sources which include all power plants that use fossil fuels, commercial and industrial processes, and domestic sources (boilers); 2- industrial activities, which include the production of both metal and chemicals, crude oil refining, and different industrial activities apart from fuel combustion; 3- road traffic sources: cars, motorbikes, buses, and trucks; 4- non-road engine sources: aeroplanes, ships, and generators from the farm and construction sectors. (USEPA, 2018). In 2010, the transformation industry, fuel

production processes, solvent use, land transportation, and domestic combustion were the primary sources of global emissions of anthropogenic volatile organic compounds (AVOCs), contributing roughly 18%, 16%, 12%, 16%, and 15% of total emissions, respectively. However, due to variations in fuel composition, technological procedures, and national regulations, each sector's contribution to AVOC speciation varies geographically (for example, Europe, Asia, and North America) as illustrated in Figure 1-2

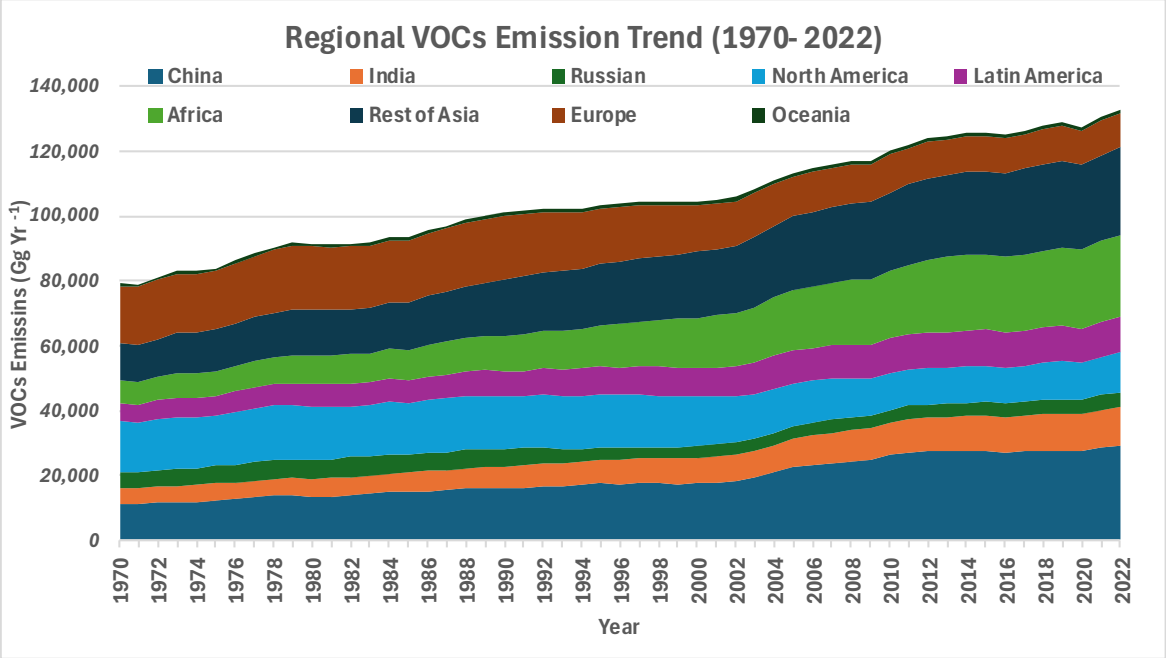

Figure 1-2 Regional AVOCs emissions from 1970 to 2022, derived from the EDGAR emission inventory (European Commission, 2024).

These three factors, fuel composition, technology improvements, and regulatory measures, also played a vital role in the total AVOCs emission reduction trend in EU and North America in the last few decades (G. Huang et al., 2017). For example, London's traffic-related VOCs have decreased significantly since the early 1990s as a result of strict emission reduction measures and fuel quality enhancements (Isobel Simpson & Claudia Volosciuk, 2019). More recently, the introduction of Ultra Low Emission Zones (ULEZ) in London has further reduced traffic-related emissions, including VOCs, and improved urban air quality (Mayor of London, 2023).

1.2.2.1 VOCs emissions from traffic sources

In the urban areas VOCs emissions from land transport sector dominate the total AVOCs emissions (C. Song et al., 2019). Traffic emissions include distinct types: exhaust emissions, fuel evaporations, and unburned fuel emissions. Gasoline fuelled vehicles, in particular, are the most contributors in these emissions (David D Parrish & William C. Kuster, 2009). Traffic related VOCs are mainly emitted due to incomplete fuel combustion in the vehicles engine (Arslan, 2020), in general, the most abundant VOCs from this sector are C_2 to C_5 alkanes, and aromatics. A study conducted by Menglei Wang and Shunyi Li in China, included 102 VOCs species, from the tailpipe emissions from different fuel powered vehicles has found that almost 39% of VOCs emissions from gasoline powered light duty vehicles were aromatics, 29% alkanes, 15% carbonyls, 7.1% halocarbons, and 7% from other groups. In contrast, for light duty diesel vehicles alkanes were dominating and accounted for almost 70% of the emissions, while aromatics have accounted of about 18%. For LPG powered cars, alkanes, aromatics, carbonyls, alkenes, halocarbons, and others accounted of 44.2%, 24.5%, 16.3%, 8.6%, 3.7% and 2.7% of these emissions respectively (M. Wang et al., 2020). It worth mentioning that LPG and ethanol powered vehicles have been found to emit more acetaldehyde and formaldehyde than regular gasoline fuelled vehicles, but they reduce the emissions in benzene and other aromatics (Arslan, 2020).

Traffic VOCs emissions, varies in VOCs species, and species ratios according to the emission source, hence some VOCs species and species ratio could be used as source or even sub source tracer, toluene, ethene and isopentane are generally enriched species in the tailpipe emissions from gasoline powered vehicles while the most abundant VOC in evaporative sector is isopentane (C. Song et al., 2020). Ratios between methyl tert-butyl ether (MTBE) to both benzene and toluene, and ratios between 2,2-dimethylbutane and i-pentane to these aromatics (benzene, and toluene) could be used to determine the specific source of emission; tailpipe, or evaporative sources (Y. Zhang et al., 2013).

Despite the steady decrease in traffic-related VOC emissions over the past two decades in the UK, due to improved traffic emission control technologies, urban and urban background measurements identify ethene, acetylene, benzene, toluene and C2–C5 alkanes as key traffic-related species. This is evident by the strong correlations between these VOCs and carbon monoxide, which confirms their association with combustion emissions (Valach et al., 2015).

Additionally, roadside and tunnel VOCs monitoring campaigns have confirmed that gasoline-powered vehicles emit substantially higher levels of aromatics and light alkenes, while diesel vehicles have greater contributions of short alkanes and combustion tracers (acetylene) in the UK (Derwent et al., 2010; NAEI, 2024; Richmond, 2025).

1.2.2.2 VOCs emissions from industrial sources

The rapid growth in the industrial section in many countries, especially developing nations like India and China, has raised the importance of this sector in the total national Gross Domestic Products (GDP) contribution. In 2012 this sector consumed almost 70% of the total energy in China and has about 40% of the total GDP (X. Wu et al., 2015), and by 2024, it still accounted for 36.5% of China's total GDP (National Bureau of Statistics of China, 2024). Consequently, the contribution of this sector in the pollution emission is serious. Industrial VOCs emissions, including both fugitive emissions and point source ones, and have vast range of VOCs species (Fu et al., 2013). The industrial sources of VOCs include wide range of industries include but not limited to industries that produce VOCs (extraction processes of both gas and oil, crude oil refining, and chemical manufacturing), industrial activities that involved VOCs as starting materials (coating and ink manufacturing, food production, production of beverage), the transportation and storage oil, and the industrial processes that use VOCs products (Papermaking, Printing and dyeing, Wood processing, etc) (Guo et al., 2021). A recent study has been conducted at industrial park in Tianjin, China has analysed the VOCs emission from different industries. It has been found that benzene, toluene, ethylbenzene, and xylene (BTEX), methyl isobutyl ketone, and ester compounds are the most emitted VOCs from the majority of industries. However, industrial VOC emissions vary depending on production process and technology, the raw materials that been used, and waste treatment processes, that study has found that car manufacturing plants, due to the variety in raw materials and the complexity in the process, emit many VOCs species including methyl isobutyl ketone, trimethylbenzene, xylene, and isobutyl alcohol (G. Liu et al., 2019).

Although industrial VOC emissions have declined substantially in the UK over recent decades due to regulatory measures, their relative contribution to total VOC emissions has increased as a result of the more rapid decline in traffic-related VOC emissions. Industrial processes (including chemical manufacturing, metal production, food and drink production, and

chemical storage) accounted for 15% of total national VOC emissions (DEFRA, 2020; NAEI, 2025).

The table below illustrate general VOCs emissions from different industries.

Table 1-2 industrial VOCs emission sources.

Industry	Substance
Petroleum refining and petro-chemistry	Benzene, toluene, xylenes, ethylbenzene; light alkanes (ethane, propane, n-butane) from fugitive emissions
Automobile manufacturing	Ethyl benzene, methyl ethyl benzene, o-xylene, trimethylbenzene
Printing and packaging printing	Propyl acetate, Ethyl acetate, Butyl acetate, Butyl acetate, m-xylene, ethanol, isopropanol
Furniture manufacturing	Sec-butyl acetate, Propene glycol monomethyl ether acetate, toluene, o-xylene, Butyl acetate, m-xylene
Paint and ink manufacture	n-hexane, BTEX, trimethylbenzenes; oxygenated solvents (ethanol, methanol)
Rubber manufacture	3-methylpentane, methyl cyclopentane, Butyl acetate, Methyl isobutyl ketone
Surface coating	Isopropyl methoxy acetate, trimethylbenzene, Ethyl acetate, o-xylene, m-xylene, 2-methyl tetrahydrofuran, toluene, ethylbenzene, trimethylbenzenes; ethanol, glycol ethers
Pharmaceutical research lab	Ethyl acetate, toluene, Methylene chloride, 2-methyl-2-methoxypropane, tetrahydrofuran, ethanol, isopropanol, acetone, methyl ethyl ketone, dichloromethane
Food & drink industry	Ethanol (whisky production), acetaldehyde; fermentation-related VOCs
Consumer products	Ethanol, methanol, acetone, n-butane (aerosol propellant)

Derived from (DEFRA, 2020; Liu et al., 2019; NAEI, 2025).

1.2.2.3 VOCs from various anthropogenic sources

Biomass burning (BB), both controlled and not controlled ones, is a very important emissions source of different VOCs species, depending on the fuel type, the biomass itself, and the combustion processes, where these measures also affect the VOCs emission factor from the BB (H. Wang, Lou, et al., 2014). Shinji Kudo, and Hiroshi Tanimoto have found that biomass burning is an anthropogenic source of isoprene, they have emphasized the importance of the BB as oxygenated volatile organic compound emission source, where BB released acetic acid, acetaldehyde, propanal, formaldehyde and butanal into the atmosphere (S. Kudo et al., 2014). Generally, biomass combustion VOCs emissions are dominated by OVOCs (ketones and aldehydes), unsaturated VOCs (alkenes), and aromatics (Gilman & Lerner, 2015).

Similarly, the production, distribution, and consumption of natural gas contribute significantly to VOC emissions and consider one of the largest industrial sources of AVOCs in the United States. These emissions include both fugitive releases (leakage and venting) and combustion-related emissions.

This contribution is mainly due to the chemical composition of natural gas, which primarily consists methane, in addition to short-chain hydrocarbons including ethane, propane, and butanes (Richard K. Lattanzio, 2020).

The importance of these emissions, in UK, is mainly due to the considerable contribution in the domestic heating, where it accounts to almost 66% of the whole domestic energy consumption, accounting for 52% and 15% of ethane and propane emissions, respectively (DEFRA, 2020). On the other hand, the biomass burning, mainly open combustion and stove wood combustion, only accounts of about 6% (BEIS, 2020). However, according to the National Atmospheric Emissions Inventory (NAEI, 2025), emissions of VOCs from domestic wood combustion increased by 56% between 2012 and 2022, mainly due to the increase of using wood burning as a secondary heating source. Recent study conducted by the University of Manchester and the National Centre for Atmospheric Science (NCAS) has concluded that wood-burning emissions leads to pollution hotspots, particularly during winter evenings (NCAC, 2024), where it emits complex mixture of VOCs, mainly oxygenated aromatics, phenols, furans and substituted benzene derivatives (Evans et al., 2025). Many of these VOCs are very reactive, oxidizes rapidly by OH and NO_3 radicals contributing significantly to the formation of secondary pollutant (Hartikainen et al., 2018; Languille et al., 2020). Hence,, despite representing a small share to domestic heating, domestic wood burning is a disproportionately important source of VOCs in residential areas, as wood smoke contains toxic and highly reactive species such as benzene, 1,3-butadiene, formaldehyde, and acetaldehyde, which possess serious health effects in addition to their vital role in the formation of ozone and secondary organic aerosols (SOA) (AQEG, 2017).

While the strict regulations and measures have achieved considerable success in VOCs emissions reduction from different sectors, mainly road transport and fuel combustion, the influence of solvents production and usage including the beverage industry, and personal care products on the AVOCs emissions has been increasing recently due to less efforts on reducing the emissions from this sector (Pearson, 2019). Solvents has become the largest contributor

in the AVOCs emission in 2017 UK, accounting of about 15% of these emissions (Lewis et al., 2020), 6.1% of the total emissions, by mass, emitted by compressed aerosol products (Yeoman & Lewis, 2021). National Atmospheric Emission Inventory (NAEI), during the same period, has reported an increase in ethanol emission, mainly from the beverage industry, and domestic solvent usage, while the main source of n-butane has become the aerosol products (Lewis et al., 2020). Where more than 90% of the emissions from these products are VOCs in addition to small contributions from fluorocarbons, slightly less than 0.5% and about 6.5% of compressed air. In general, the majority of hydrocarbon-based aerosol propellants are a mixture of iso/n butane and propane in addition to smaller amounts of both iso/n-pentane (Yeoman & Lewis, 2021). The importance of non-aerosol personal care products (PCPs) hair conditioner, shampoo, and similar products is way less than the aerosol ones; however, it still contributes to ethanol, limonene, benzene, and methanol emissions (Yeoman et al., 2021). In 2015 a study conducted about the VOCS emissions from 37 different types of personal products included but not limited to PCPs, air fresheners, and laundry products, has concluded that different types of these products emit several VOCs species: α-/ β pinene, acetaldehyde, ethanol, methanol, and acetone (Steinemann, 2015). Another study on the use of domestic solvents has summarised those aromatics and alkane dominate the VOCs emissions from indoor solvents accounting of 50% and 30% respectively, in the painting case (furniture, domestic and indoor paints) the contribution of aromatics emission was considerably higher than in the indoor solvent case, while printing emission are dominated by C2–C5 VOCs, and C8–C9 aromatics (H. Wang, Qiao, et al., 2014).

Figure 1-3 shows total UK VOC emissions (kt) by sector from 2005 to 2023, illustrating the overall decline in national emissions and the changing contribution of source sectors over time, with reductions in transport and fugitive emissions and an increasing relative importance of solvent-related sources.

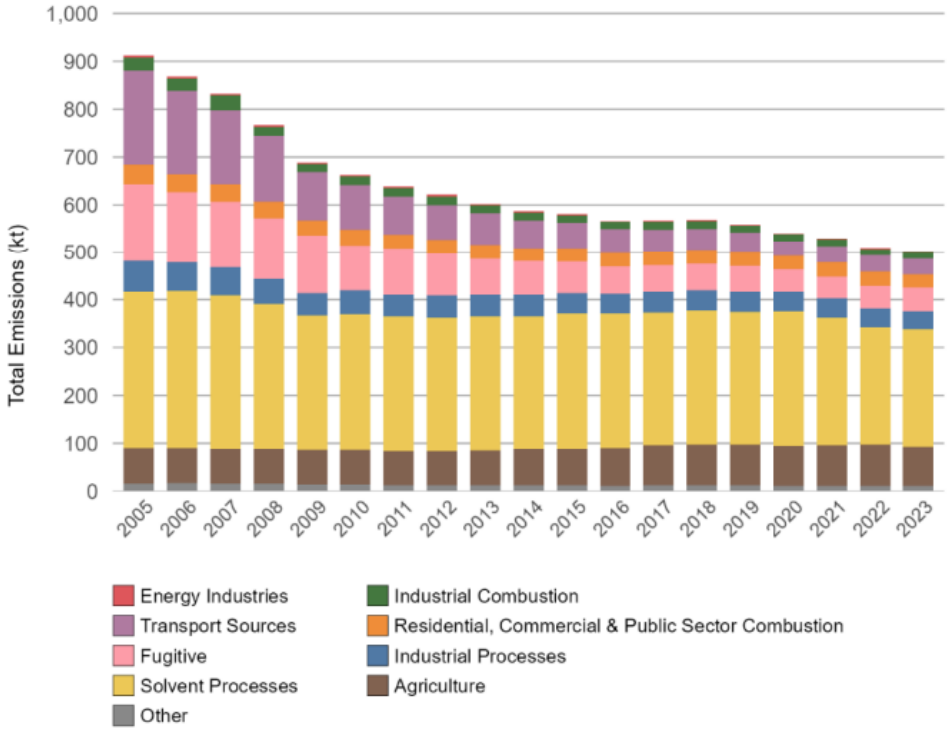

Figure 1-3 *T*otal UK *VOCs* emissions (kt) by source sector from 2005 to 2023, (NAEI, 2025).

1.3 Atmospheric Sinks of VOCs

In addition to VOCs emission strength, VOCs ambient concentrations are also determined by their chemical and physical removal processes, with gas-phase oxidation dominants atmospheric sink for most of VOCs (Jacob, 1999). During the daytime the hydroxyl radical (OH), mainly formed through ozone photolysis followed by reaction with water vapour, is the main oxidant. VOCs reactivity to OH varies considerably depending on molecular structure with alkenes and aromatic compounds reacting substantially faster than saturated alkanes (Atkinson, 2000; Atkinson & Arey, 2003), eventually leading to the formation of peroxy radicals (RO_2), which facilitate NO -NO_2 cycling, promote tropospheric ozone production, and contribute to SOA formation (Monks et al., 2015).

Ozone, itself, has an important sink effects through the ozonolysis of unsaturated VOCs, which can happen during daytime and nighttime, leading to the formation of carbonyl compounds, consequently, enhancing secondary pollutant formation (Atkinson & Arey, 2003).

Nitrate radicals (NO_3), on the other hand, are the dominant oxidant during nighttime, as they react with alkenes and other reactive species, contributing to nocturnal SOA formation,

particularly in polluted urban environments (Brown & Stutz, 2012). Moreover, chlorine atoms (Cl), especially in marine-influenced regions, during early-morning hours can oxidize certain VOCs with reaction rates may exceed those of OH (Finlayson-Pitts & Pitts Jr, 2000).

In addition to chemical sinks, VOCs are also removed through physical processes, including dry deposition onto surfaces and wet deposition of more soluble oxygenated species. However, gas-phase oxidation remains the most dominant atmospheric sink route (Jacob, 1999).

1.4 Atmospheric implication of Volatile organic compounds

1.4.1 Impact of VOCs on Air Quality and Climate

VOCs have a serious climate and air quality effect, due to their reactivity and atmospheric transformation characteristics. Following their emissions into the troposphere, from various sources, they participate in complex photochemical reactions, primarily initiated by oxidation from hydroxyl (OH) radicals, consequently, generates peroxy radicals (RO_2 and HO_2). These radicals in the presence of UV radiation and high-NOx concentrations, facilitate the conversion of NO to NO_2 and the subsequent formation of ground-level ozone (O_3), mainly in urban settings. (ICCP, 2014; Swamy et al., 2012). Additionally, VOCs degradation is a key reason of SOA formation. This can lead, as a result of these tropospheric formations, to degradation in the general air quality, and the production of photochemical haze in certain conditions (EDP, 2025).

Figure 1-4 presents a schematic summary of ethane (C_2H_6) oxidation pathways, illustrating how NO_x levels regulate ozone production. In high-NO_x environments, peroxy radicals react with NO, leading to NO_2 formation and subsequent ozone production. In the contrast, under low-NO_x conditions, peroxy radicals are removed through reactions forming hydroperoxides (e.g., CH_3OOH) and other species, limiting radical availability and reducing net ozone formation.

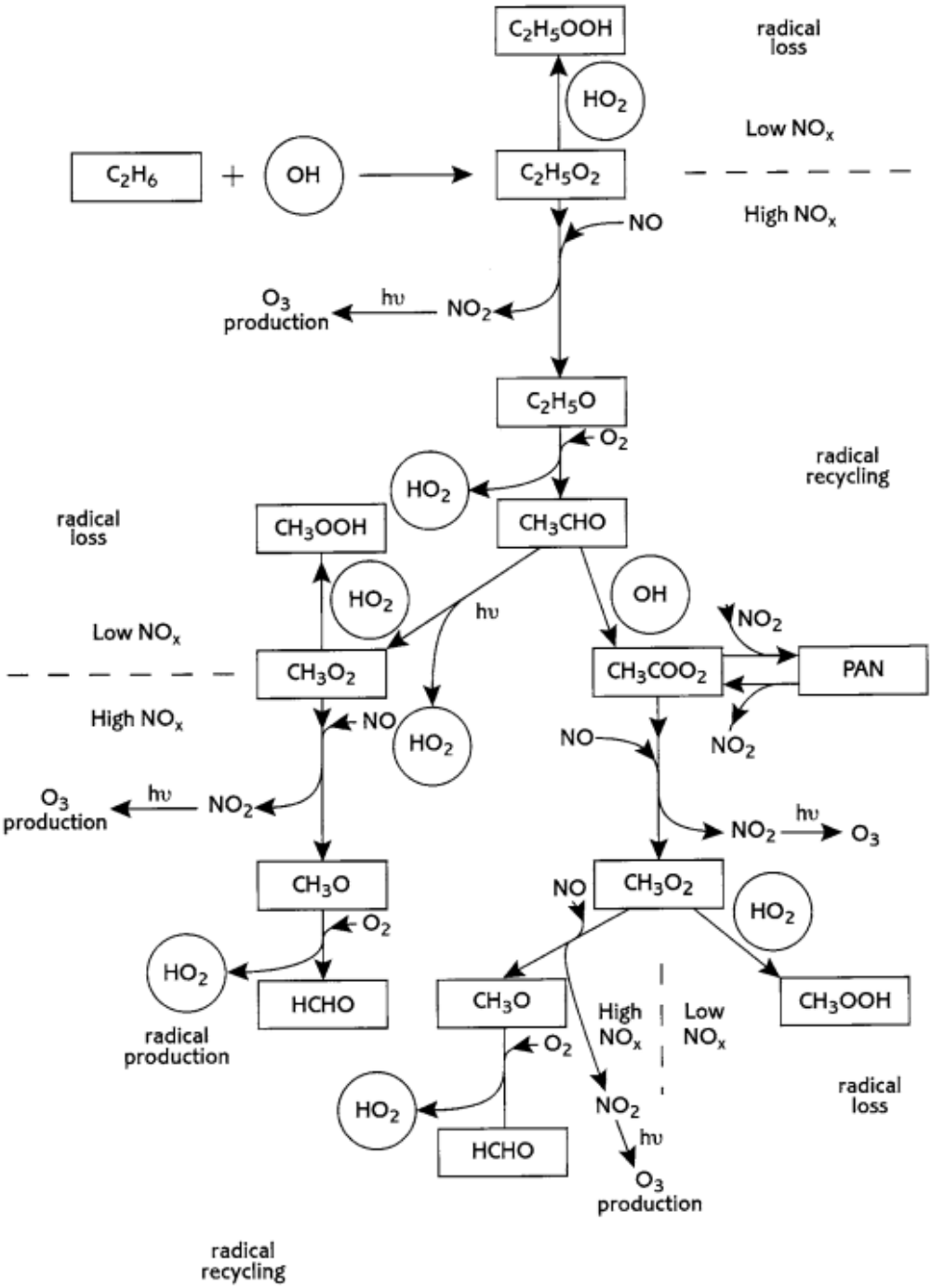

Figure 1-4 oxidation mechanism of ethane (C_2H_6) initiated by OH radicals under high NOx and low NOx conditions (Collins et al., 2002).

Furthermore, the vast majority (90%) of ozone global emissions, is due to photochemical processes that are driven by VOCs (Wild, 2007). Ozone, with effective radiative forcing of +0.47 W m^{-2} in 2019 relative to 1750, is the third most significant anthropogenic warming molecular after CO_2 and CH_4 (IPCC, 2021), as shown in Figure 1-5.

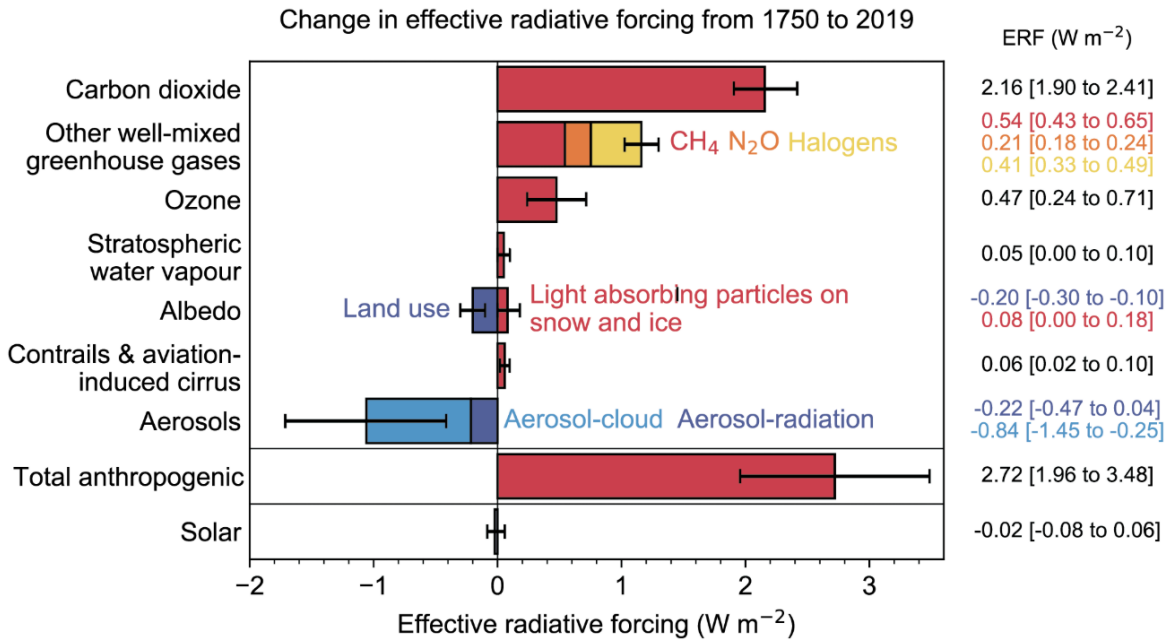

Figure 1-5 Change in effective radiative forcing (ERF, W m^{-2}) from 1750 to 2019 for major anthropogenic and natural climate agents.

Various scientific studies have concluded that urban areas are generally VOC-limited Ozone formation environments (Lyu et al., 2016). Ground level Ozone is formed in the atmosphere by the photochemical reactions between its procuress VOCs and NOx (NO + NO_2) in the presence of the sun light, following the ozone formations chain presented below (Sillman, 1999):

$$\begin{aligned}
&\mathrm{VOC} + \mathrm{OH} \xrightarrow{[O_2]} \mathrm{RO_2} + \mathrm{H_2O} \\
&\mathrm{CO} + \mathrm{OH} \xrightarrow{[O_2]} \mathrm{HO_2} + \mathrm{CO_2} \\
&\mathrm{RO_2} + \mathrm{NO} \xrightarrow{[O_2]} \text{secondary VOC} + \mathrm{HO_2} + \mathrm{NO_2} \\
&\mathrm{HO_2} + \mathrm{NO} \rightarrow \mathrm{OH} + \mathrm{NO_2} \\
&\mathrm{NO_2} + h\nu \rightarrow \mathrm{NO} + \mathrm{O} \\
&\mathrm{O} + \mathrm{O_2} + \mathrm{M} \rightarrow \mathrm{O_3} + \mathrm{M}
\end{aligned}$$

Equation 1-1

The production of Ozone is sensitive to VOCs and NO_x emissions but the formation response to their reduction is not linear, leading to two atmospheric production regimes depending on the VOC/NO_x ratios (J. Ren et al., 2022). A reduction in NO_x emissions at low VOC/NOx ratios could lead to increase O_3 formation, where high concentrations of fresh NO react with O_3 leading to the production of NO_2, depleting the Ozone.

$$NO + O_3 \rightarrow NO_2 + O_2$$

Equation 1-2

Additionally, high NO_2 emissions consumes the OH radical by reacting with it forming products like nitric acid, preventing the first step of VOCs oxidation in the Ozone formations chain.

$$NO_2 + OH \rightarrow HNO_3$$ Equation 1-3

This is called a VOC-limited regime, where reducing the Ozone levels can be done more efficiently by controlling the emissions of VOCs rather than reducing the NO_x concentrations (European Environment Agency, 2016), Figure 1-6 shows estimated Ozone concentration for different VOC and NO_x concentrations.

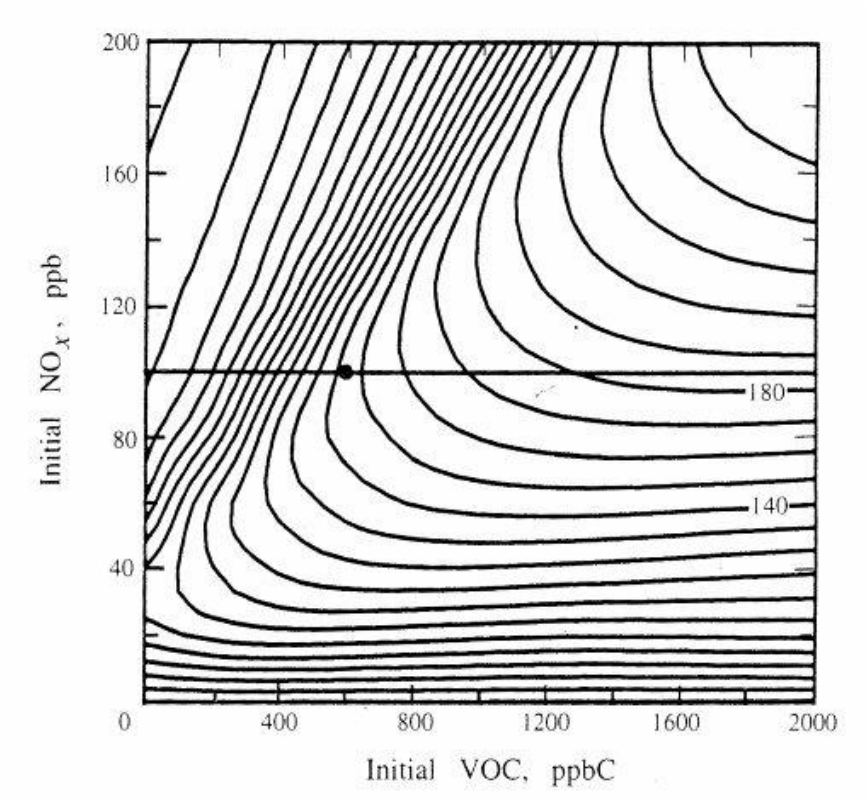

Figure 1-6, O_3 isopleth diagram presenting the estimated ozone concentration for different VOC and NO_x concentrations (Dubois, 2008).

Finally, due to the role of VOCs in the formation of these secondary pollutants, they have been considered as indirect contributor to acid deposition, atmospheric warming, and climate change by disrupting the chemical balance of the troposphere (Bauguitte et al., 2010).

1.4.2 The importance of OVOCs in atmospheric chemistry

The importance of OVOCs in atmospheric chemistry arises from their high reactivity, which is often greater than that of the parent hydrocarbons from which they are formed through photo-oxidation. Consequently, they play a vital role in tropospheric ozone formation under

both clean and polluted atmospheric conditions. The ozone formation reaction initiated by HO radical, can be present by the following alcohols general scheme chain of reactions, illustrated by methanol, (Mellouki et al., 2015), summarized by Equation 1-1:

$HO + CH_3OH \rightarrow H_2O + CH_2OH$

$CH_2OH + O_2 \rightarrow HCHO + HO_2$

$HO + HCHO \rightarrow H_2O + HCO$

$HCO + O_2 \rightarrow HO_2 + CO$ **net: $CH_3OH + 6O_2 \rightarrow 2H_2O + 3O_3 + CO_2$** Equation 1-4

$HO + CO \rightarrow H + CO_2$

$H + O_2 + M \rightarrow HO_2 + M$

$3\ (HO_2 + NO \rightarrow HO + NO_2)$

$3\ (NO_2 + h\nu\ (\lambda < 420\ nm) \rightarrow NO + O(^3P))$

$3(O + O_2 + M \rightarrow O_3 + M)$

Similarly, Figure *1-7* shows atmospheric ozone formation by the oxidation of Formaldehyde initiated by HO radical (Mellouki et al., 2015).

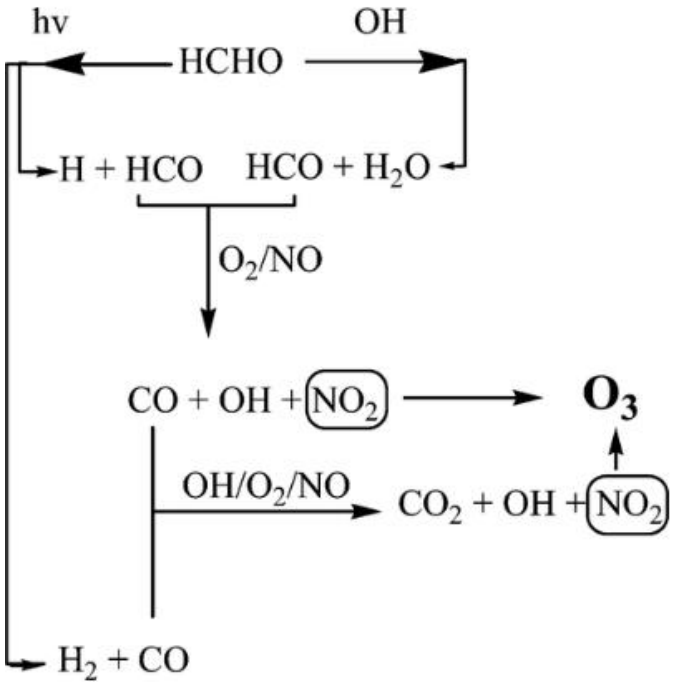

Figure 1-7 Scheme of Ozone Formation through the Atmospheric Degradation of Formaldehyde.

OVOCs include carbonyls (aldehydes RCHO, ketones RCOR), alcohols (ROH) and carboxylic acids (RCOOH) (Sommariva et al., 2011). This species can be emitted directly, primary pollutants, into the atmosphere from both biogenic (plant metabolism is an important source

of acetaldehyde, acetone, and methanol) and anthropogenic sources (fuel additive is a source of ethanol, ETBE, and MTBE) (Mellouki et al., 2015), and they can be formed in the atmosphere, secondary pollutants, by alkoxy and peroxy radicals' reaction (Atkinson & Arey, 2003). Some oxygenated VOCs, due to their long atmospheric lifetime, acetone as example, could be subjected to long distance transportation from their original location, and contribute to the photo-oxidation of many VOCs in different environments, as a result to their role in providing radicals (McKeen et al., 1997). The degradation process of saturated OVOCs is mainly due to their reaction with OH radicals, while the oxidation of unsaturated OVOCs could be by their reaction with ozone, OH radical or nitrate (NO_3), in all cases the OVOCs degradation considerably contribute to many secondary pollutants' formation: highly oxidized volatile organic compounds, SOA, peroxyacyl nitrates (PAN) and ozone, which explains their huge influence on the tropospheric oxidizing capacity (Mellouki et al., 2015).

1.5 The effects of VOCs on Human health

Although VOCs from food and drink contribute to sensory attributes like taste and smell, many VOCs are extremely harmful to human health (Carter, 2009). Where the respiratory system is the primary route of exposure to VOCs since they are released into the air and easily inhaled, which is particularly crucial in urban and industrial settings as VOCs concentrations are considerably elevated comparing to other environments.

Acute and long-term health impacts have been linked to VOC exposure. Symptoms of short-term exposure include headaches, dizziness, irritation of the eyes, nose, and throat, in addition to worsening of bronchitis and asthma (Dunmore et al., 2016; Miller et al., 2011).

More seriously, long-term exposure to VOCs raises the risk of many critical disease cancer and cardiovascular disease and can seriously harm important organs such as the liver, kidneys, and central nervous system (Montero-Montoya et al., 2018; S. K. Song et al., 2019). Many substances have identified as carcinogenic species by the International Agency for Research on Cancer (IARC), namely, vinyl chloride and benzene. Benzene, in particular, is linked to leukaemia and haematologic diseases (Kampa & Castanas, 2008). However, VOCs' health risks vary depending on the concentration, functional group, and exposure time of species. Where aromatic, specifically BTEX (benzene, toluene, ethylbenzene, and xylenes), due to their abundance and toxicity, have serious health effects. These species, commonly linked to land

transport and industrial emission sources, can be transferred to the indoor environments and concentrate in such relatively small space leading to elevated, usually ten times than outside, levels (Hou et al., 2024). Recent studies have demonstrated the substantial contribution of land traffic and solvent emissions to ambient VOC concentrations, as well as their key role in the production of secondary particulate matter and ozone formation, in mega-urban environments such as Mexico City and Seoul (Montero-Montoya et al., 2018; S. K. Song et al., 2019), where respiratory problems are more likely to occur, particularly during the summer when photochemical activity is at its highest. Likewise, an industrial health study has demonstrated that elevated ambient levels of VOCs, namely, perchloroethylene, and ethylbenzene exceeds the recommended exposure limits and pose significant carcinogenic risks, leading to severe occupational complications (Hou et al., 2024).

Children represent a particularly vulnerable population group due to their developing respiratory and immune systems., Low birth weight, asthma, neurodevelopmental abnormalities, and a higher risk of respiratory infections have all been linked to VOC exposure throughout pregnancy and the early years of life. When benzene levels are higher than 1 $\mu g/m^3$, the risk of getting cancer over a person's lifetime increases dramatically, which could be the case in many industrial and polluted urban areas (Montero-Montoya et al., 2018).

Generally, the negative health effects of VOC exposure vary from moderate sensory irritation to serious chronic conditions, such as cancer and cardiovascular disease.

1.6 UK General VOCs trends in the last 15 years.

Comparison between general VOCs trend over the past 15 years across three different environments: the rural monitoring site (Auchencorth Moss), the suburban monitoring site (London Eltham), and the urban traffic monitoring site (London Marylebone Road), has been conducted. Site's locations and the surrounding areas are shown in Figure 1-8, Figure 1-9, and Figure 1-10.

Figure 1-8 Location of the Auchencorth Moss rural air quality monitoring site in Scotland, shown using a satellite image from Google Earth.

Figure 1-9 Location of the London Eltham, suburban air quality monitoring site, shown using a satellite image from Google Earth.

Figure 1-10 Location of the London Marylebone road, traffic air quality monitoring site, shown using a satellite image from Google Earth.

The data used in this comparison were obtained from UK Automatic Urban and Rural Network (AURN) (AURN, 2020). Figure 1-13, Figure 1-12, and Figure 1-13 illustrate the monthly mean, median and the general smooth VOCs trends at these three hydrocarbons monitoring sites between 2010 and 2024, respectively. An example of the temporal variability of selected VOC species across these sites is shown in Figure 1-14.

At the rural environment (Auchencorth Moss), despite the low data capture percentage for many species, a general downward trend is observed across most VOC species. In contrast, combustion related VOCs (ethene, ethyne, and propene) (An et al., 2014; Cai et al., 2010) exhibited progressive increases, indicating the possibility of ongoing or new combustion-related sources in rural settings. Similarly, with an atmospheric lifetime about two months (Angot et al., 2015), the most long-lived measured VOC, ethane, had a weak upward trend over the studied period, which could be due to a slight increase in its background levels. The relatively constant levels of isoprene, however, indicate steady biogenic emissions. A general gradual decline was observed in BETX compounds (benzene, ethylbenzene, toluene, xylenes) trends.

The Eltham suburban monitoring site showed generally consistent downward trends across all VOCs species, including BETX compounds, i-pentane, and i-octane, which could be an indicator of achieving reduction in VOCs emissions from several sectors in London during the reported period. However, a slight upward trend in isoprene levels was observed, which could be due to changes in temperature or vegetation activities in this semi-urban region.

Similarly, the general VOCs trend at the Marylebone Road site, which is significantly skewed to traffic emissions, was sharp decline evident by most VOCs trends, particularly BETX compounds, reflecting success in traffic VOCs emissions reduction strategies in London over the reported period. However, ethane, propane, iso-butane, and n-butane levels appeared relatively stable, indicating steady emissions from natural gas or evaporative sources that have not decreased at the same rate as other traffic-related VOCs.

As presented in Figure 1-15, ethane was the most abundant measured VOC in all environments, throughout the studied period flowed by propane, reflecting its long atmospheric lifetime (two months, and 14 days respectively), and widespread presence (Angot et al., 2015; Rosado-Reyes & Francisco, 2007).

At the rural site, illustrated in Figure 1-15 (a), n-butane was the third most abundant VOC, followed by i-butane, ethyne, ethene, and i-pentane which were among the most prevalent VOCs at this site. While, at the suburban site, illustrated in Figure 1-15 (b), propane and n-butane annual sum concentrations were very closed to each other, closely followed by i-butane. Ethene, toluene, and i-pentane were among the most prevalent VOCs at this site. Similarly, at the urban traffic site illustrated in Figure 1-15 (c), ethane remains the highest measured VOC, with substantial contribution from propane, n-butane, and i-butane. Again, ethene, toluene, and i-pentane were among the most prevalent VOCs at this site.

A close inspection of the most abundant VOCs annual mean trends at each monitoring site from 2010 to 2024 was conducted for further detailed analysis presented in Figure 1-16. At Auchencorth Moss, a remote rural site, ethane had slight fluctuations with a gradual upward trend after 2015 and hit a peak in 2021. Similarly, propane displayed a relatively fluctuated trend up to 2016 then it is stabilised until 2020. i-butane, n-butane and ethene also displayed mostly stable levels, however, ethyne hit a peak between 2019 and 2020 then it levelled off from 2021 onward.

In the suburban environment, Eltham site, ethane exhibited a more distinct declining trend, particularly after 2012, propane and n-butane showed nearly parallel trends, remaining relatively stable with only modest declines after 2019. I-butane, i-pentane, and ethene followed similar patterns, while toluene showed a steady drop trend since 2010.

In the traffic monitoring site, Marylebone Road, all major VOCs showed a high fluctuating trend. However, ethane tended to have downward trend since 2019, while propane, n-butane and i-butane levels increased between 2020 and 2022. Toluene showed a clear and steady decline, ethene and i-pentane showed gentle overall downward trends.

In terms of the chemical functional groups, presented in Figure 1-17, alkanes were consistently the most dominant contributors to total VOC concentrations across all three environments: rural (Auchencorth Moss), suburban (Eltham), and urban traffic (Marylebone Road). Although alkenes and aromatics were found in lower quantities, a substantial difference was observed in their proportional contributions among sites. At the Marylebone Road traffic site and the suburban site of Eltham, aromatics, such as benzene, toluene, and xylenes, comprised a larger portion of the VOC profile compared to alkenes. In contrast, at the rural background site (Auchencorth Moss), alkenes had a slightly more balanced presence relative to aromatics.

In terms of the annual sum of VOCs concentrations per location between 2010 and 2024, Figure 1-17, reveals a consistent pattern, with Auchencorth Moss consistently recording the lowest concentrations, followed by Eltham, and then Marylebone Road, which continuously reported the highest levels. This shows a clear difference in VOC pollution between urban, suburban, and rural environments, reflecting the obvious variations in traffic volume, industrial activity, and local emissions sources. It should be noted that the drop in total observed VOC concentration at Auchencorth Moss in 2015 is due to data availability issues, only 41.7% of hourly measurements were valid in 2015, compared with 63.2% in 2014 and 89.7% in 2016, suggesting substantial instrument downtime during that year. Interestingly, Eltham's sum VOC concentrations dropped significantly after 2021, while the concentrations at Marylebone Road increased sharply in 2022, and then back to normal levels, similar to 2020 and 2021, in 2024, which could be due to meteorological variability effects on VOCs levels.

These observations emphasise the importance of long-term monitoring networks in assessing general pollution trends. Due to the significant impact of meteorological variability and seasonal patterns on ambient VOC concentrations, only long-term datasets are able to clearly reveal the key changes in emission trends. However, short-term campaigns still provide an important picture of VOCs levels during specific pollution events.

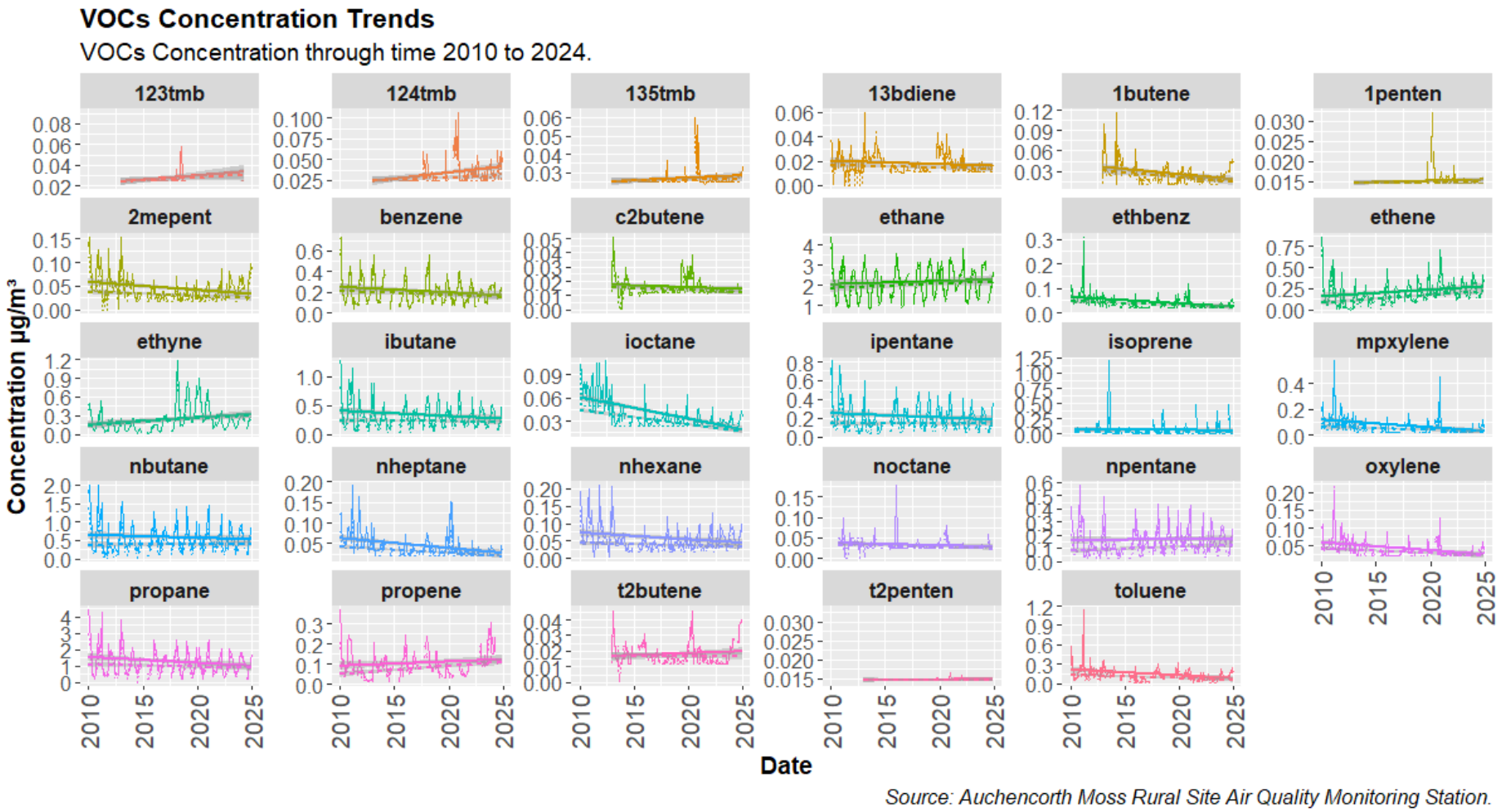

Figure 1-11 VOCs general trends from 2010 to 2024 at Auchencorth Moss. Solid lines represent the mean concentrations; dashed lines represent the median concentrations for each pollutant. A grey linear regression line is overlaid to show the long-term trend in VOC levels.

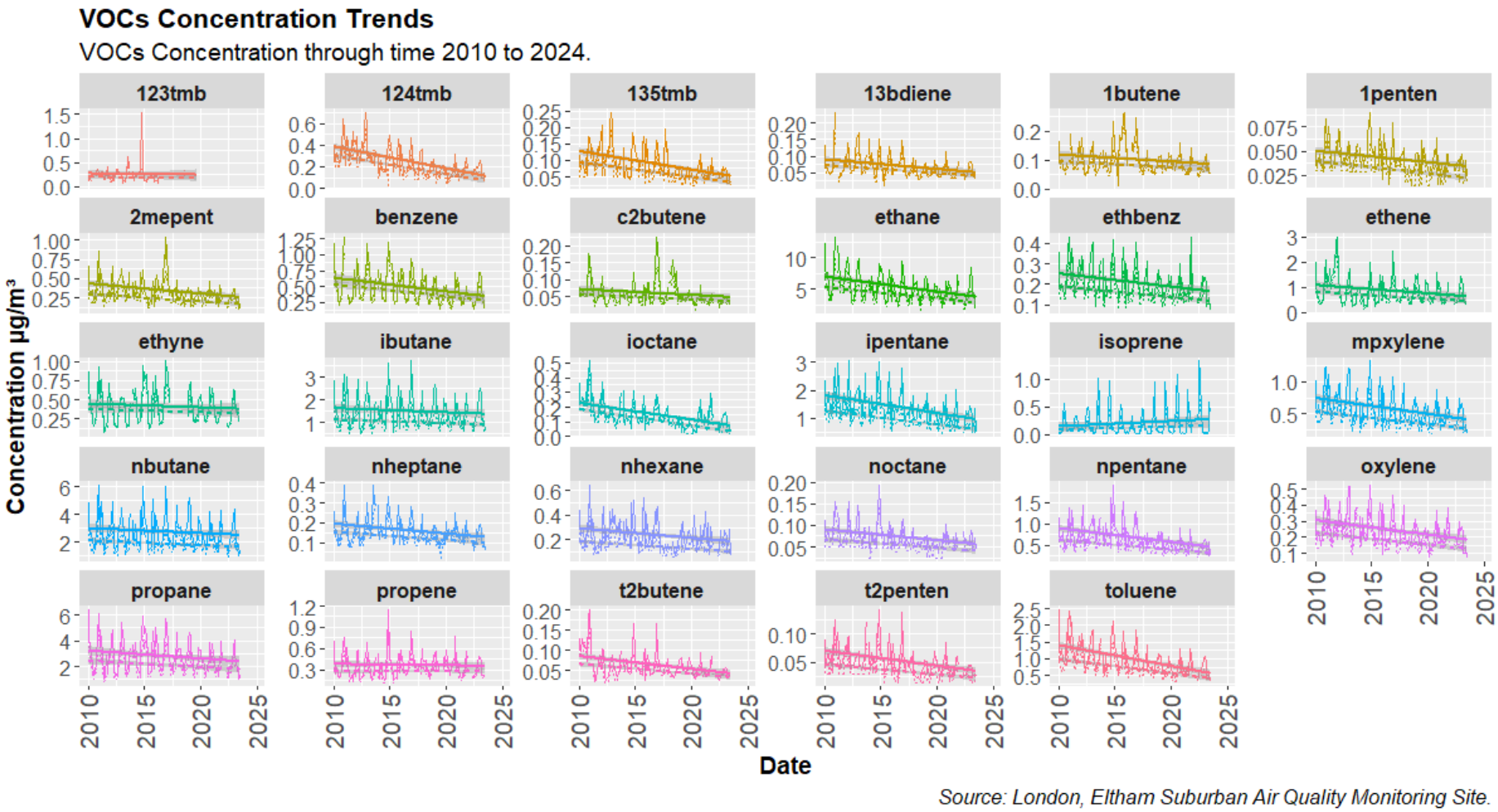

Figure 1-12 VOCs general trends from 2010 to 2024 at London Eltham. Solid lines represent the mean concentrations; dashed lines represent the median concentrations for each pollutant. A grey linear regression line is overlaid to show the long-term trend in VOC levels.

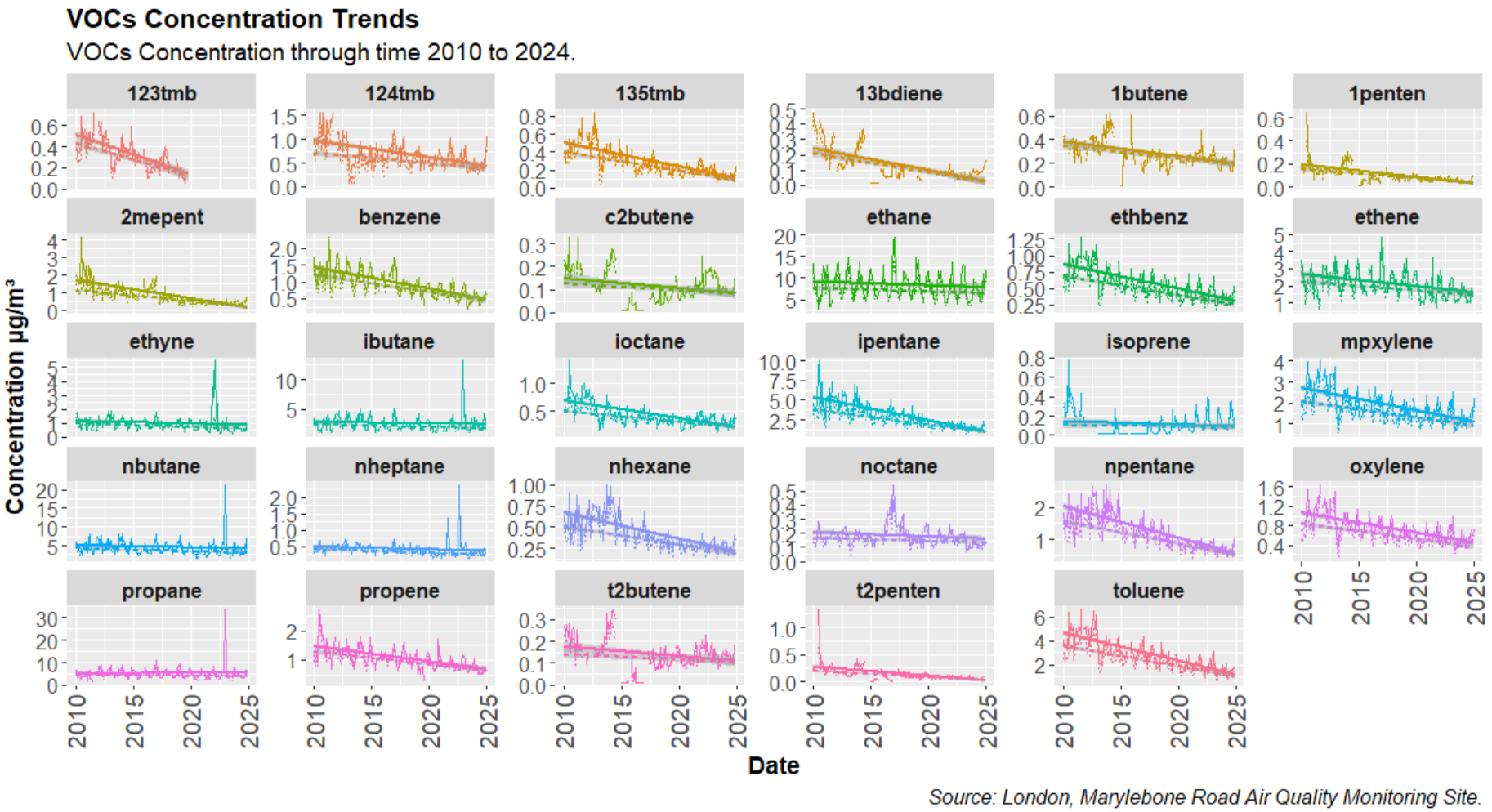

Figure 1-13 VOCs general trends from 2010 to 2024 at Marylebone Road. Solid lines represent the monthly mean concentrations, and dashed lines represent monthly median concentrations, for each pollutant. A grey linear regression line is overlaid to show the long-term trend in VOC levels.

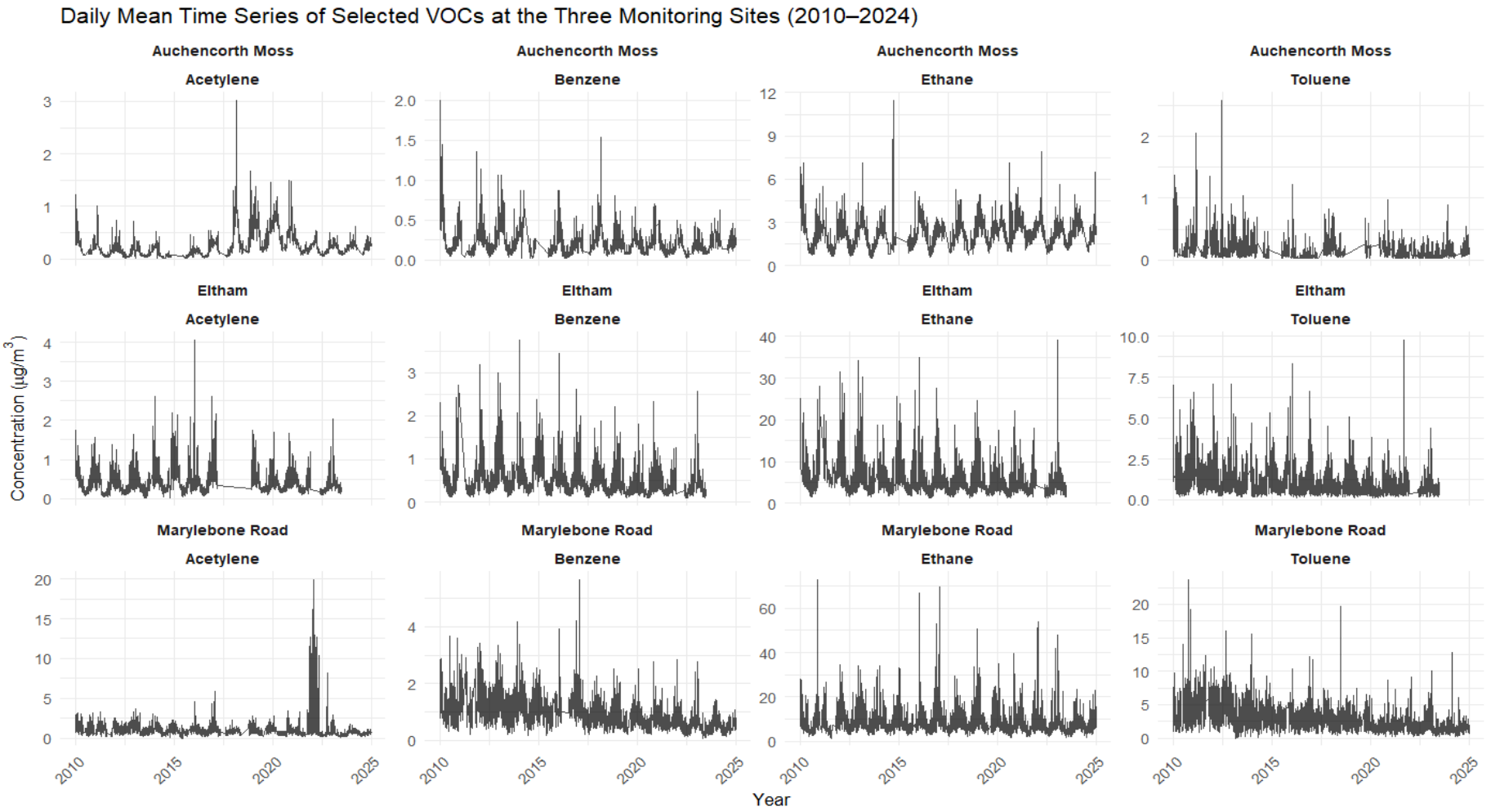

Figure 1-14 Daily mean time series of selected VOCs (benzene, ethane, acetylene, and toluene) measured at three UK monitoring sites—Auchencorth Moss (rural background), Eltham (urban background), and Marylebone Road (kerbside), between 2010 and 2024.

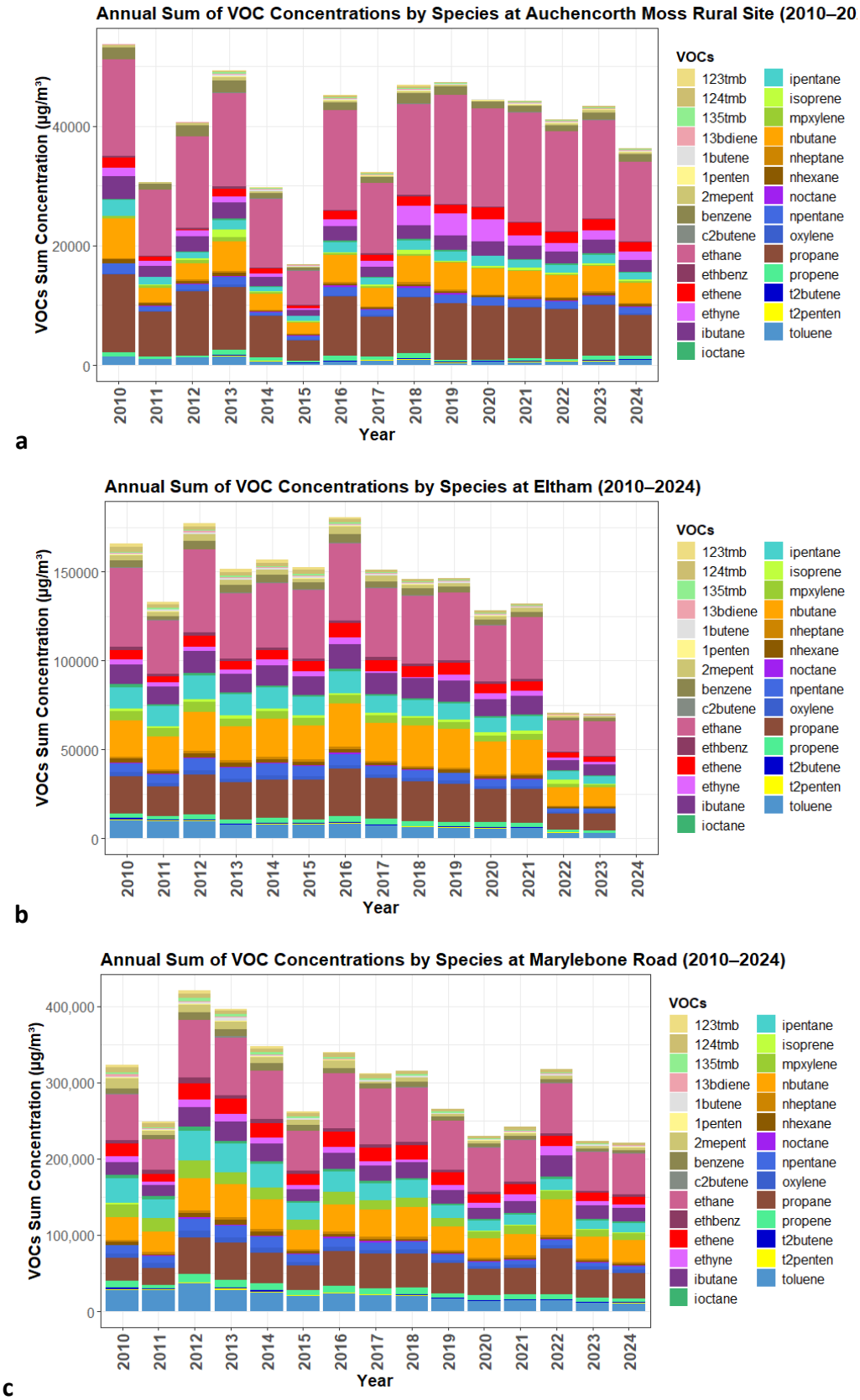

Figure 1-15 Annual Sum of VOC Concentrations by Species (2010–2024), a) Auchencorth Moss, b) London Eltham, and c) Marylebone Road.

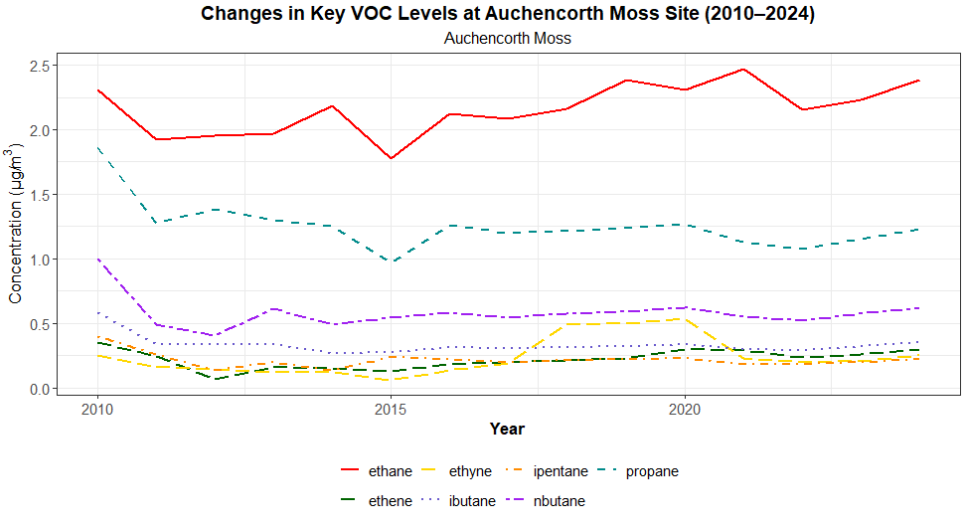

a

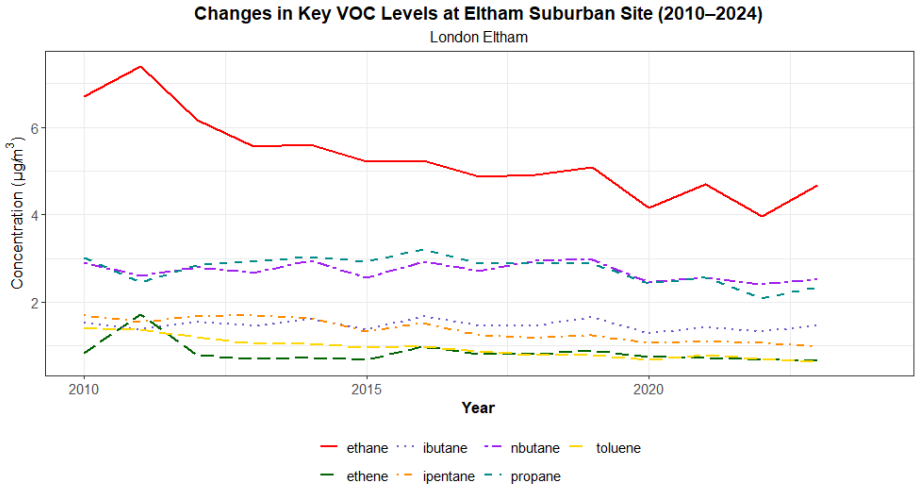

b

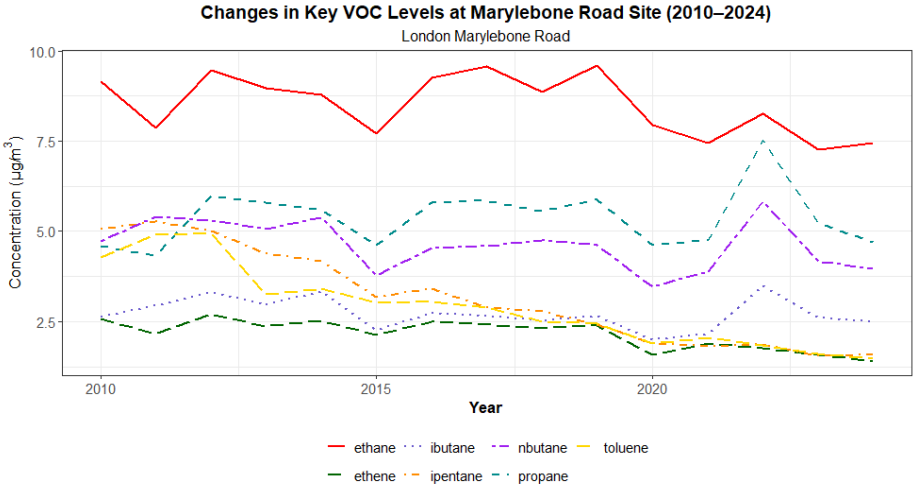

c

Figure 1-16 Changes in Key VOC Annual Mean Concentrations Between 2010 and 2024. **a**) Auchencorth Moss, **b**) London Eltham, and **c**) Marylebone Road.

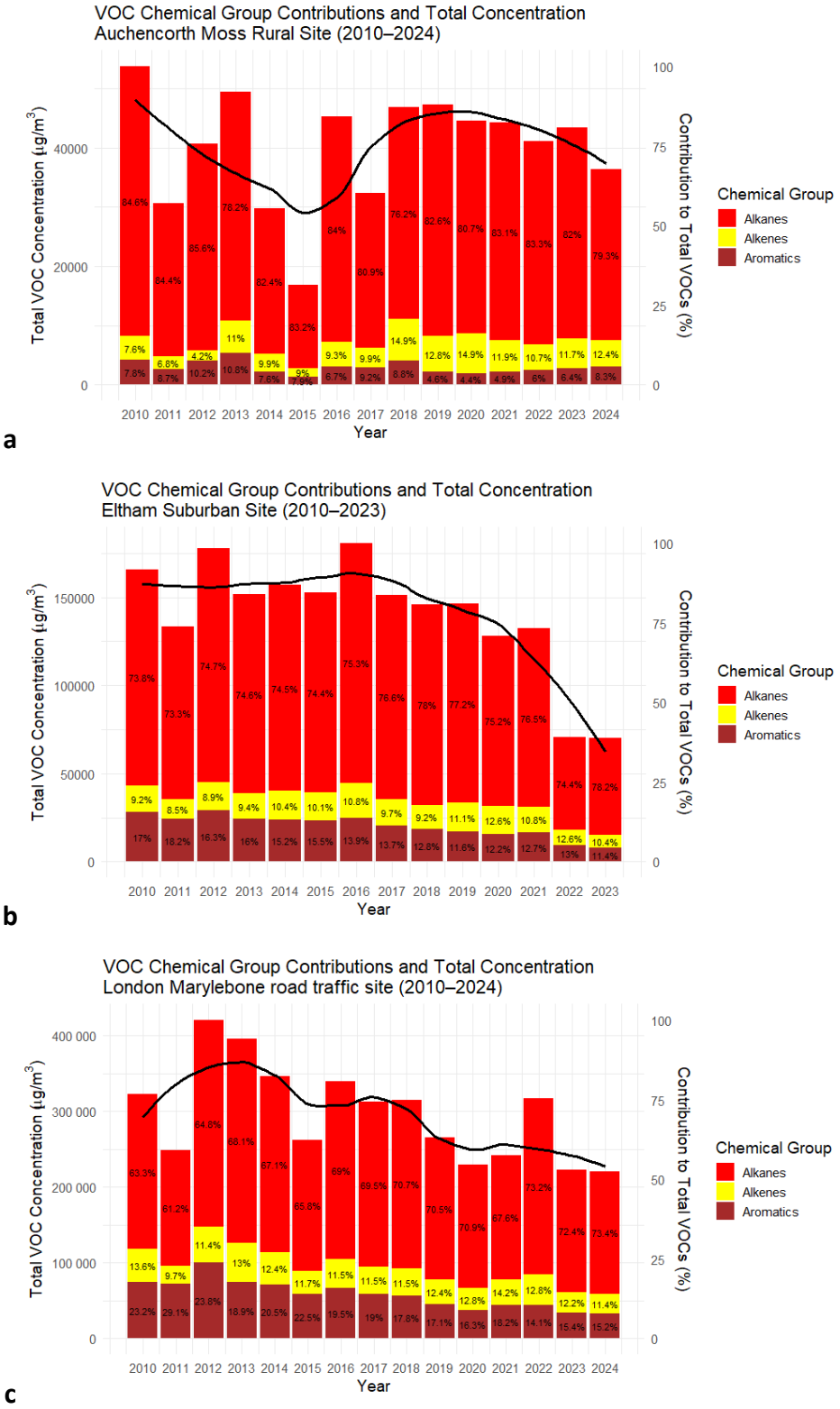

Figure 1-17 Annual Sum of VOC Concentrations and the contribution of major chemical groups 2010-2024. The black line represents the overall temporal trend in total VOC concentrations. **a**) Auchencorth Moss, **b**) London Eltham, and **c**) Marylebone Road.

1.7 Study Objectives and Aims

The main aim of this thesis is to improve understanding of VOCs sources, temporal variability, and policy-relevant impacts in UK urban environments. This was achieved through a combination of receptor modelling, inter-city comparison, and the assessment of a natural experiment (the COVID-19 lockdown). The specific objectives were:

Firstly, to apply the U.S. EPA Positive Matrix Factorisation (PMF 5.0) model to long-term VOCs measurements at the London urban background Supersite in order to identify and quantify the contributions of major emission sources. This included evaluating the role of traffic exhaust, evaporative emissions, solvent use, industrial activity, residential combustion, and secondary atmospheric processes in shaping urban VOC concentrations. In addition to assessing their relative importance in driving atmospheric ozone formation and secondary organic aerosol production.

Secondly, to investigate VOCs seasonal and diurnal variability at the two most populated UK cities, London and Birmingham, by identifying the most ten abundant VOCs in each location and determining how seasonal changes in photochemistry and boundary-layer dynamics influence their importance and distribution, emphasising how site-specific characteristics result in distinct VOC patterns under comparable meteorological and photochemical conditions.

Thirdly, to explore the effects of the COVID-19 lockdown on VOC concentrations at two contrasting London monitoring sites: Marylebone Road (roadside) and Eltham (urban background), by examining the response of traffic and non-traffic related VOCs to extraordinary decreases in transportation activities. This was done by utilising historical comparisons, trend analysis, meteorological normalisation with Random Forest models, and predicting business-as-usual scenario, hence, distinguishing between VOCs emission-driven changes and meteorological variability.

Overall, we aimed to provide a thorough assessment of VOC speciation and behaviour across multiple spatial and temporal scales. This thesis addresses critical gaps in understanding VOCs sources, their chemical composition, and their atmospheric impacts in the UK, providing scientific based evidence to develop effective VOCs management strategies.

Chapter 2

2 Atmospheric Sources of non-methane hydrocarbons in London

2.1 Introduction

Ambient air pollution is the most substantial environmental threat to public health in the United Kingdom (Environment Agency, 2023; Smith, 2025). Anthropogenic air pollution-related mortality accounts for 28,000 to 36,000 deaths annually. Notably, it is predicted that from 2017 to 2025, the cumulative economic loss of the National Health Service (NHS) and the social care system due to atmospheric air pollution will reach up to £1.6 billion (Office for Health Improvement and Disparities, 2022).

Non-methane hydrocarbons (NMHCs), a vital subset of VOCs, play a key role in atmospheric chemistry by contributing to the formation of both tropospheric ozone (Atkinson & Arey, 2003) and secondary organic aerosols (SOAs) (Hallquist et al., 2009; McFiggans et al., 2019), mainly due to their oxidation process by hydroxyl (OH), ozone (O_3), chlorine (Cl) and nitrate (NO_3) radicals in the troposphere, consequently, producing organic peroxy (RO_2), and hydroperoxyl (HO_2) radicals. This leads to the increase in atmospheric oxidation (Claeys et al., 2004; Tham et al., 2016), promoting the formation of secondary pollutant, with repercussions for air quality and human well-being in urban settings, while also exerting an indirect influence on global climate change. Additionally, some VOCs are themselves toxic to humans and can cause both immediate and long-term negative health effects (Azuma et al., 2016; Kim et al., 2019), including BTEX (benzene, toluene, ethylbenzene and xylene), which have been classified as carcinogenic species (Kumar et al., 2020).

VOCs can be emitted from diverse anthropogenic and biogenic origins. Yet, the significance of anthropogenic and biogenic VOC emissions differs across geographical regions. Biogenic VOC sources are the primary cause of the elevated VOC mixing ratios in rural and wooded areas (T. Karl et al., 2003). In contrast, anthropogenic emissions dominate in urban environments (Borbon et al., 2013). The primary sources of biogenic VOCs are emissions from terrestrial plants, making a substantial contribution to the composition of regional VOCs (Y. Ren et al., 2017) that includes isoprene and various terpenoids, along with minor constituents OVOCs and alkenes). On the other hand, anthropogenic sources contain operations related to oil and natural gas (ONG) including extraction, storage, refining, and distribution processes, in addition to traffic and stationary fossil fuel and biofuel combustion activities, industrial manufacturing, chemical and petrochemical processes, and the production and use of solvents (Abeleira et al., 2017; Cai et al., 2010; H. Zhang et al., 2017).

In major urban areas like London, there has been comprehensive research on the emissions of VOCs (Langford et al., 2010; Vaughan et al., 2017), where vehicles are identified as a key emission source. This contribution arises either through emissions from exhaust gases or by the evaporation of incompletely burnt fuel (Vaughan et al., 2017). Nevertheless, a recent study, based on the National Atmospheric Emissions Inventory (NAEI) data, revealed a notable reduction in the road transport sector's contribution to the overall VOC emissions in the UK. This decline is a direct result of the implementation of strict vehicle emission standards (Lewis et al., 2020), mainly the enforcement of the use of three-way catalytic converters in vehicle production (Langford et al., 2009). By 2017, the road transport sector accounted only for 4% of the total UK VOC emissions, a substantial decrease from the 30% reported in 1990. In the same year, the most substantial contribution to VOC emissions was from the solvent sector. While emissions from this sector have seen an overall decrease, the reduction is considerably low compared to road transport and fugitive emissions reduction levels. The industrial processes sector also experienced relatively smaller reductions, contributing about 15% to the total emissions in 2017 (Lewis et al., 2020). Therefore, it is crucial to determine the up-to-date key sources of atmospheric VOCs and their contribution to the total ambient VOC concentrations in major cities in order to set proper policies and regulations to tackle their health and environmental effects (Ou et al., 2015).

2.1.1 Receptor Models for Source Apportionment

Various receptor-oriented source apportionment analyses, which are mathematical techniques used to quantify the contributions of sources to measured samples based on their chemical composition or source signatures, can be applied to identify the key VOC emission sources contributing to ambient VOC levels (J. Li et al., 2018; S. K. Song et al., 2019). Chemical Mass Balance (CMB), Positive Matrix Factorisation (PMF), and UNMIX are among the most established and well-known receptor models, each of them has its unique benefits and drawbacks based on the study's goals and the nature of the data.

The deterministic Chemical Mass Balance (CMB) model is a receptor model that applies linear least-squares regression of measured ambient concentrations against a database of known source profiles to estimate source contributions. With the availability of precise and representative source profiles, CMB is highly interpretable and provides direct measurement of source impacts (Watson et al., 2002). However, its efficacy is severely dependent on the

completeness and representativeness of the input profiles. This makes it less useful in intricate urban environments with a wide variety of sources or inadequately described sources. Emission sources need to be pre-determined in the model for the model to resolve them (Hopke, 2016). In addition to the complications that arise from the reactive atmospheric species like VOCs, the chemical conservation assumption, coupled with the absence of atmospheric changes, leads to systematic errors.

In contrast, Positive Matrix Factorization (PMF), a multivariate factor analysis method, requires adequate atmospheric measurements and scientific knowledge of the potential sources (Brown et al., 2007; Lee et al., 2008), without requiring prior knowledge of source compositions. The dataset is divided, in the PMF method, into two matrices: factor contributions (G) and factor profiles (F), which facilitate the identification of distinct source composition profiles, each including a combination of compounds corresponding to a specific emission source or category (Pinthong, Thepanondh, & Kondo, 2022). This approach provides more accurate factor solutions and error analysis (Norris & Bai, 2014). It is worth mentioning that PMF incorporates uncertainty estimations and non-negativity constraints.

Low signal-to-noise ratios and missing values are common challenges in VOC monitoring datasets. However, these challenges can be effectively addressed by Positive Matrix Factorisation (PMF) (Brown et al., 2015; Paatero & Tapper, 1994). Finally, PMF factor identification is still subjective and generally assigns factors to real-world sources using tracer species or external information.

UNMIX, a receptor model also developed by the U.S. EPA, uses self-modelling curve resolution to identify sources based on geometric features in multidimensional space and extracts source profiles and contributions from ambient data (Đorđević et al., 2013). Although UNMIX depends less on a priori source profiles compared to CMB and requires less statistical assumptions than PMF, it is prone to outliers and requires larger datasets with clear source contrasts for optimal performance. Furthermore, its applicability is constrained by sparse or noisy datasets, and it is unable to handle uncertainty robustly as in PMF. On the other hand, PMF has a number of benefits over other receptor models, this includes its realistic uncertainty estimations, individual data points weighting, and improved handling of missing and below-detection-limit observations. Additionally, by incorporating external constraints, the advanced model's rotational tools improve resolving rotational ambiguity and provide solutions that more accurately reflect real-world emission patterns.

Following its endorsement by the U.S. Environmental Protection Agency (EPA), Positive Matrix Factorization has become one of the most extensively used methods for source apportionment (Hopke, 2016). Hence, the PMF method has been used in this study to identify the main sources of VOCs in London measured at the London Honor Oak Park urban background supersite.

2.2 Volatile organic compounds atmospheric measurement methods

Several analytical methods, depending on the chemical specificity, sensitivity, and temporal resolution, have been used in order to measure the ambient VOCs. Where high-time-resolution instruments, reaching a 1 second time scale (De Gouw & Warneke, 2007), providing a real-time total VOC measurements, such as the Selected Ion Flow Tube Mass Spectrometry (SIFT-MS) and Proton Transfer Reaction Mass Spectrometry (PTR-MS), have become very common methods in the ambient air monitoring field (Blake et al., 2009). Despite their excellent sensitivity and suitability for time-series analysis of reactive species, these direct-injection mass spectrometric techniques lack chemical species identification, specifically for compounds with the same mass or fragmentation patterns, i.e. isomers. Xylene isomers (m-, p-, and o-xylene) and combinations of C_9 aromatics and C_{10} alkanes, for example, cannot be specified using these techniques. Using the PTR-MS method, ambient m- and p-xylene levels are generally summed up as a single compound. However, given their distinct OH reactivity and emission ratios from traffic and solvent sources (Borbon et al., 2002), their important distinctions in sources and atmospheric reactivity will be lost if these are combined into summed ion masses, and therefore, precise secondary pollutant generation, particularly ozone formation and secondary organic aerosol (SOA) potential, in addition to comprehensive source apportionment studies are difficult to achieve.

On the other hand, gas chromatographic methods continue to be the most reliable approach for VOC speciation in order to tackle the above-mentioned restrictions, where VOCs are separated by gas chromatography (GC) following their volatility or polarity, which is commonly used in conjunction with mass spectrometry (GC–MS) or flame ionisation detection (FID). Consequently, accurate identification and measurement of individual compounds, including structural isomers and co-eluting species is achievable (Mcnair & Miller, 2011). Due to the requirement for sample pre-concentration and column separation, which usually takes 30 minutes to several hours (Poole, 2019), GC-based methods often low

time resolution, compared to MS based methods, however, they provide improved speciation, where precise VOC speciation is vital for comprehensive source apportionment studies and emission inventory validation, GC-based methods are essential for atmospheric chemistry research (Barletta et al., 2005; Warneke et al., 2004).

2.2.1 Gas Chromatography (GC)

The physical characteristics of gaseous mixtures, such as their affinity for the stationary phase and retention time, as well as their thermal stability at the evaporation temperature, make gas chromatography (GC), a sensitive and highly selective analytical technique, particularly suitable for their separation. GC has found extensive application in the long-term monitoring of ambient air samples. The isomeric speciation of emissions can be determined using GC, which has settings that enable ambient measurements of a variety of alkanes, alkenes, and oxygenated volatile organic compounds (OVOCs) (Hopkins et al., 2003).

It consists of a carrier gas (typically 99.99% pure helium; (mobile phase), sample injector, separation column (stationary phase), oven (heat up samples), and detector (signals eluted component from the column). The sample component is introduced via the sample injector into the column, which contains a flowing inert carrier gas within a temperature-controlled oven. The elution process, or material extraction, is carried out inside the column, which is frequently a small, coiled tube of stationary phase coated on the inside. The differing elution durations of the sample components, which reach the detector and are recorded as signals on the data system, cause the mobile phase to interact with the stationary phase in distinct manners, leading to separation (Ellis & Mayhew, 2014).

The varying physical properties of the analytes including polarity, volatility, and molecular size, influence their interaction with both the stationary and mobile phases, consequently, affecting their separation. The fundamental principle of gas chromatography is to utilise these differential interactions in order to achieve distinct migration rates of analytes through the column, which leads to effective separation of species (Bartle & Myers, 2002; Tranchida, 2019). The length and type of column, the pressure or flow rates in the mobile phase, and the oven temperature ramp can all affect the separation. One of the most crucial decisions is which column to choose because the molecular characteristics of the stationary phase determine the degree of interaction between the analyte and column and, consequently, the

retention duration (Pravallika, 2016). A chromatogram is a two-dimensional depiction of a sequence of signals that illustrates the detected compounds organised by ascending elution time on the x-axis and the detector signal of the compound (relative abundance) on the y-axis, reflecting a characteristic of the constituent chemical (Bartle & Myers, 2002; Poole, 2019). For these reasons, gas chromatography remains one of the most widely used analytical techniques for the separation and quantification of atmospheric VOCs in long-term air quality monitoring networks.

2.2.2 Flame Ionization Detector (FID)

After the separation stage, a detector is used to measure the analytes. The electron capture detector (ECD), mass spectrometer (MS), and flame ionisation detector (FID) are among the several types of detectors that can be employed. FID is usually the preferred detector for quantitative analysis (McNair et al., 2019; Mondal et al., 2021) because it can directly compare peaks in a chromatogram, measure organic substances at very low concentrations (10 - 13g/s), is easy to use, has a linearity response range of up to 107 g/s, is robust, inexpensive to acquire and maintain, and has detection limits in the low pg. C/s (picogrammes carbon per second).

The FID is a highly popular analytical GC detector that responds to organic compounds and is a destructive mass-sensitive detector with a good linear dynamic range. It needs support gases of hydrogen and air that burn slightly above a flame jet, as seen in Figure 2-2, with an average air to hydrogen ratio of 10:1. A negatively polarised voltage is provided between the jet tip and the collector electrode as the analyte elutes from the column, igniting in the flame and generating ions and electrons. During the period, the number of ions created is determined by the number of reduced carbon atoms that enter the detector per unit of time. The space between the jet tip and the electrode is where a current flows due to electrons created in the flame. A negatively charged collector picks up the positive ions, creating a current that flows. This current is then amplified and converted into digital signals (Poole, 2015; Vozka et al., 2019).

Crucially, organic materials can be selectively detected in intricate atmospheric matrices since the FID is insensitive to inorganic molecules (such as CO_2, H_2O, and NOx). A Schematic diagram of the main components of GC-FID system and a Diagram of a flame ionization detector (FID)

are shown in Figure 2-1, and Figure 2-2, respectively, from (Diane Turner, 2024b; Patricia Atkins, 2022).

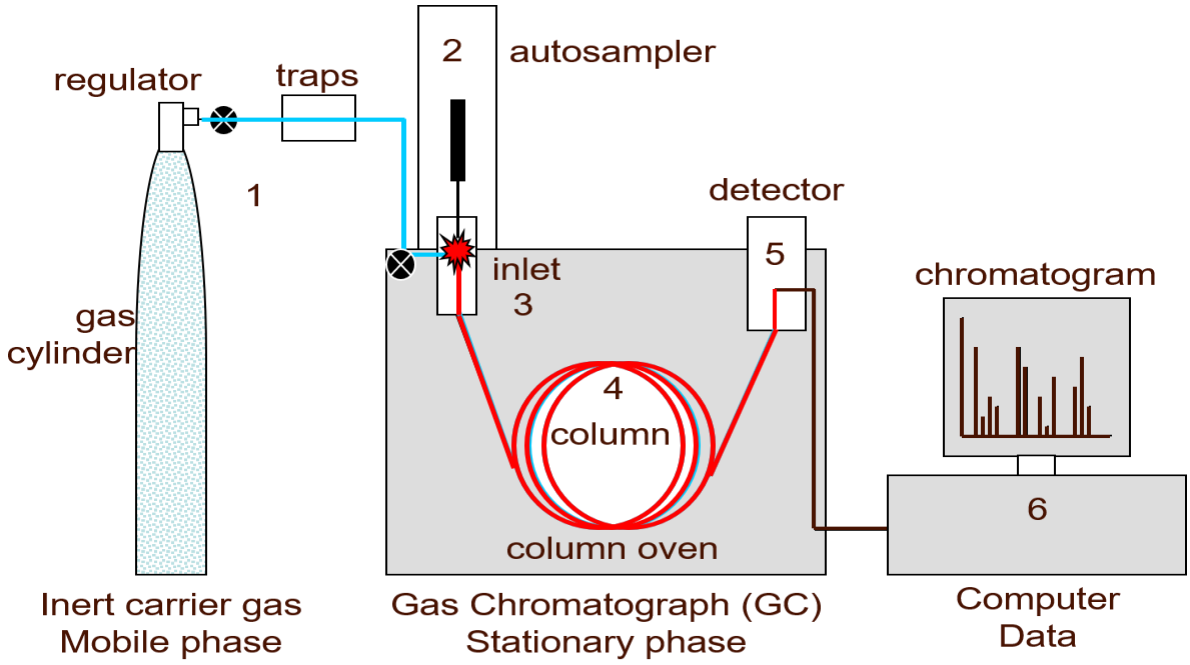

Figure 2-1 A simplified diagram of a gas chromatograph showing: (1) carrier gas, (2) autosampler, (3) inlet, (4) analytical column, (5) detector and (6) PC.

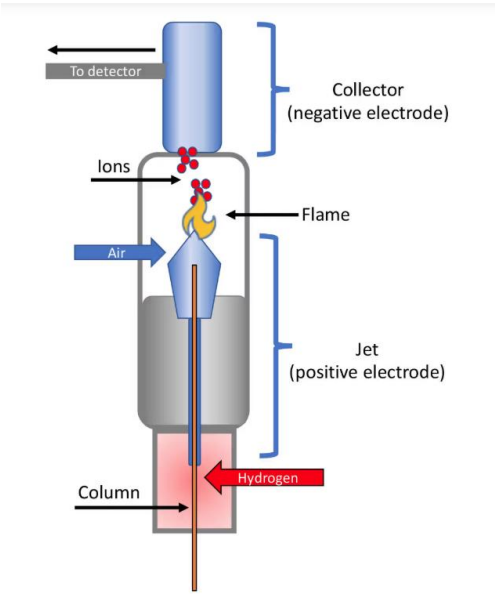

Figure 2-2 Diagram of a flame ionization detector (FID).

2.2.3 Mass spectrometry (MS) detector

Mass spectrometry (MS) is another widely used detection technique coupled with gas chromatography for the identification and quantification of VOCs. MS utilizes molecular

fragmentation patterns to identify compounds, which makes it a highly important detection method for complex atmospheric mixtures (Kännaste et al., 2014; McNair et al., 2019). Hence, GC–MS is commonly applied in atmospheric chemistry studies where detailed speciation of VOCs is required (Sobrado et al., 2016).

Following their elution from the gas chromatographic column, compounds enter the ionisation chamber, commonly electron ionisation (EI), of the mass spectrometer under high vacuum conditions, where molecules being bombarded with high-energy electrons (typically 70 eV). Consequently, positively charged molecular ions as well as characteristic fragment ions that are specific to each compound, are produced. These ions are then separated based on to their mass-to-charge ratio (m/z) by utilizing a mass analyser (quadrupole, ion trap, or time-of-flight analyser) and (De Hoffmann & Stroobant, 2007; Gross, 2011).

After that, the ion abundance is measured as the ions reach the detector, producing a mass spectrum that represents the distribution of fragment ions. By comparing the resulting spectra with reference libraries (such as NIST or Wiley), individual VOC species can be accurately identified, even when compounds have similar chromatographic retention times. Therefore, GC–MS is a reliable technique for the analysis of complex atmospheric VOC mixtures where both compound identification and quantification are required (Hajšlová & Čajka, 2007; B. Liu et al., 2024).

Although MS offers higher-level compound identification compared with FID, it has a narrower linear dynamic range in general, and it is more complex and expensive to operate. Therefore, GC–MS has been commonly used for qualitative identification and detailed speciation, whereas GC–FID is still widely applied for the routine quantitative monitoring of VOCs in long-term atmospheric measurements. (Pacchiarotta et al., 2010; Shuttleworth & Johnson, 2022). A Schematic diagram of a GC/MS is shown in Figure 2-3, from (Diane Turner, 2024a).

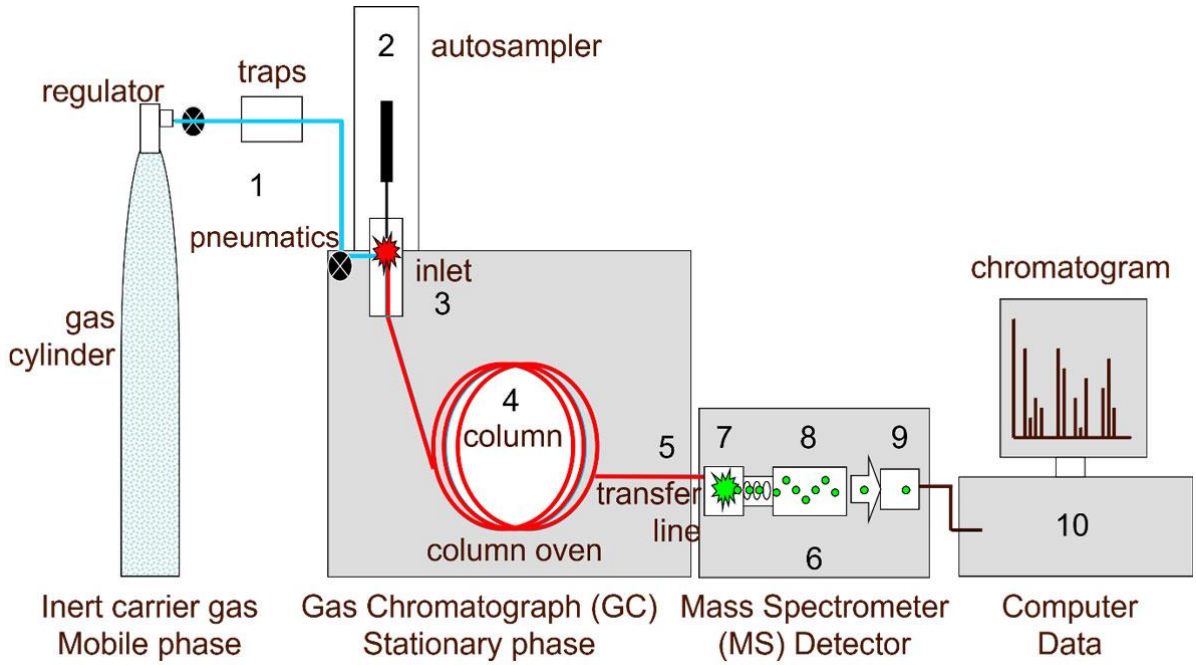

Figure 2-3 Schematic diagram of a gas chromatograph–mass spectrometer showing (1) carrier gas, (2) autosampler, (3) inlet, (4) analytical column, (5) interface, (6) vacuum, (7) ion source, (8) mass analyzer, (9) ion detector and (10) PC.

2.3 Methodology

2.3.1 Monitoring site description

The London Supersite monitoring station, located in Honor Oak Park within the Royal Borough of Greenwich in the southeast area of London (51°26'58.9"N, 0°02'14.6"W). Site Address: King's College Sports Ground Brockley Rise London SE23 1NW, ideally represents a suburban background environment within the Greater London region. It is part of the UK Air Quality Supersites network, funded by the UKRI Strategic Priorities Fund and managed, maintained and operated by King's College London in association with the Department for Environment, Food and Rural Affairs (Defra) (UK Air, 2023). As a suburban monitoring site, it is typically placed to monitor the air pollutants in a residential area with low traffic activity, and hence, observing the impact of several pollution sources in the regional and metropolitan background setup, which includes local, long-distance transported, and dispersed emissions from all urban activities. The site is not dominated by any major primary emission sources such as industrial facilities or heavily busy motorways (European Environment Agency), and therefore it is ideally relevant for monitoring and evaluating baseline atmospheric pollutants in London's suburban environment as shown in Figure 2-4 and Figure 2-5. The station is equipped with advanced online instrumentation that monitor various ambient pollutants,

including VOCs, , particulate matter (mass, number, and size distributions, PM1, PM4, PM2.5 and PM10), gases such as carbon monoxide (CO), nitrogen oxides (NOx), ozone (O_3), sulphur dioxide (SO_2), methane (CH_4), carbon dioxide (CO_2), ammonia (NH_3), reactive nitrogen compounds (NOy), and meteorological variables (air temperature, humidity, pressure, wind speed and direction, cloud cover and aerosol layer height), complying with established protocols such as those outlined by the European Monitoring and Evaluation Programme (EMEP) and the UK Automatic Urban and Rural Network (AURN). All that makes the atmospheric measurements conducted at the London Supersite vital and reliable for analysing the spatial and temporal patterns of urban air pollution and provide scientific based evidence for regulatory, emission inventory evaluations and exposure analyses (McNabola et al., 2011; Sokhi et al., 2022), in addition to its suitability for urban source apportionment studies.

Figure 2-4 London Supersite, urban background environment (google earth).

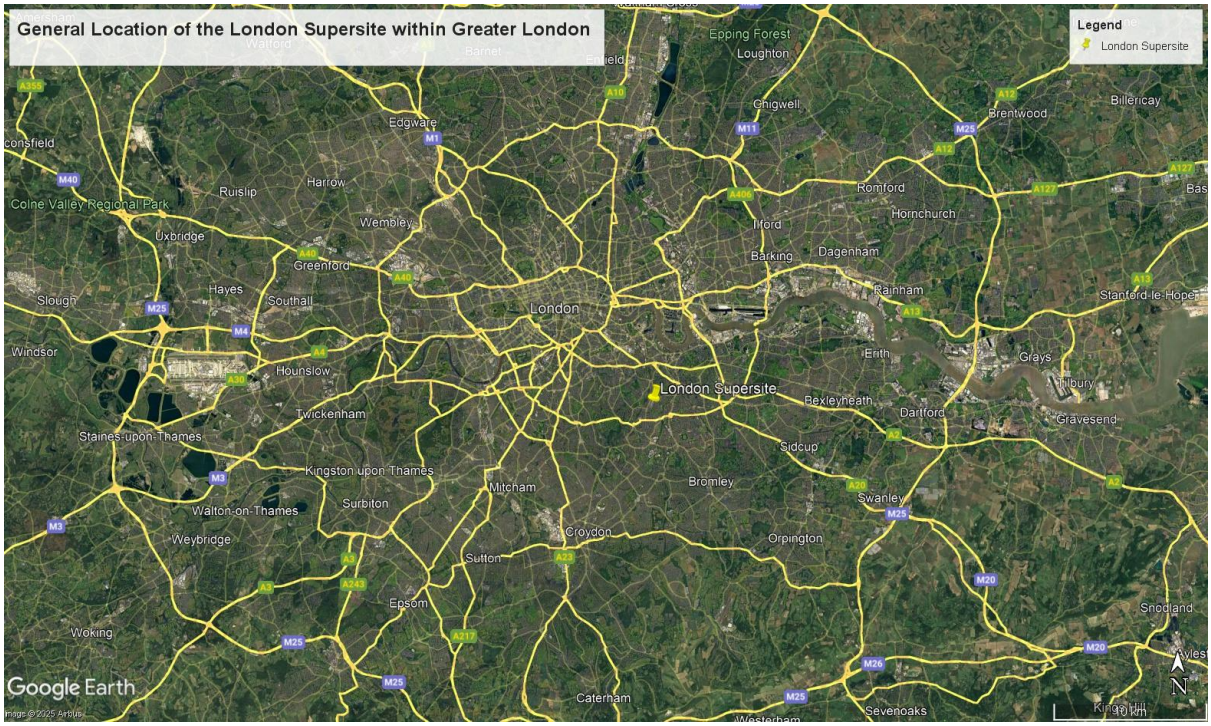

Figure 2-5 Geographical Location of the London Supersite within Greater London (google earth).

2.3.2 Dual GF-FID setup

A dual-column GC-FID (gas chromatography with flame ionization detection) analyser has been used to monitor the ambient VOCs concentrations, including some oxygenated VOCs (OVOCs), at the London supersite monitoring station, a suburban background environment site (51°26'58.9"N 0°02'14.6"W). The system was configured, and the resulting data were processed by Dr. Jim Hopkins, who designed the analytical platform to maximise the accuracy and the reproducibility of VOCs quantification. As the instrumental configuration and operational details have not been published yet, a comprehensive description of the setup and methodology is provided in this section.

This method gets over the problems with single-column GC, especially when it comes to differentiating oxygenated VOCs (OVOCs) from the more common hydrocarbon VOCs. Where Dual-column GC can identify chemicals with the same polarity but different volatility within a single analysis, one-dimensional GC cannot achieve it (Beens et al., 2000, 2001). This is a key feature, specifically, in industrial and urban settings where intricate ambient samples are presented.

Additionally, the peak area in the dual column GC-FID has a higher capacity compared to the single column one, and therefore dual columns GC has a higher sensitivity (X. Xu et al., 2003) However, pre-treatment steps including water removal and optimising the injection conditions are still necessary for accurate quantification of oxygenated and complex mixtures (Melder et al., 2023), this pre-treatment steps can limit the analysis's volatility range that result in carryover between samples. Separations typically take minutes to hours due to the nature of chromatographic separations (Feldhausen et al., 2022; G. Fernández-Martínez et al., 2000; T. G. Karl et al., 2007; US EPA, 1997).

The air samples were collected using a stainless-steel metal bellows pump from glass inlets at the rooftop level via PTFE tubing with an outer diameter of ¼ inch, at a controlled pressure of 5 psig. These samples were subsequently sent to a specially constructed thermal desorption unit (TDU). A gas chromatograph (GC) Agilent 7890A with flame ionisation detectors (FID) (Agilent Technology, 2023) was coupled to the TDU for analysis. Figure 2-6 illustrates the schematic of the analytical flow channel. A dedicated software was used to control the system's continuous operation, this software coordinated automated sequences that included periodic analysis of calibration, blank gases, and ambient air samples. Additionally, in order to preserve instrument performance, daily calibrations were conducted to account for any sensitivity drifts.

Firstly, 500 mL sample volume was passed through a water removal trap, which was consisted of a 30 cm length of 1/16" silica-coated stainless-steel tubing that was kept at -40 °C, where moisture was removed by cryogenic freezing, with a mass flow controller controlling the flow of the sample downstream of the water trap. Then, after purging at 25 mL min^{-1} for 10 minutes, sampling was started by introducing the pre-concentration trap in-line. This trap consisted of a 30 cm stainless steel tube coated with silica and filled with CarbopackTM X (40–60 mesh) and CarbopackTM B (60–80 mesh) adsorbents (Sigma-Aldrich, Germany) The tube was kept at cryogenic temperatures lower than -120 °C. Following collection, the trap was heated to -80 °C and purged for 4 minutes with hydrogen carrier gas in a forward direction to eliminate CO_2, which can obstruct the detection of VOC. Target compound desorption was accomplished by switching the flow of the carrier gas and heating the trap to 190 °C for three minutes. Following that, the analytes were transferred to a second cryogenic focus trap. This trap, a 20 cm 1/32" stainless steel tube coated with silica and filled with the same adsorbents,

was used to concentrate the analytes before they were quickly heated to 200 °C for thermal desorption. For separation and detection, analytes were subsequently fed to the GC oven via a 1 m fused silica capillary (250 µm ID). The traps were back-flushed with carrier gas and heated to 220 °C during GC analysis in order to remove any remaining organics, and the water trap was back-flushed and heated to 100 °C in order to remove any moisture that had accumulated.

The analytes then were passed into the GC through a 60 m VF-WAX column (150 µm ID, 0.50 µm film thickness; Agilent Technologies), which runs at a pressure of 22 psig and a carrier gas flow rate of 3.5 mL min^{-1}. The unresolved analytes (C2–C8 VOCs) that eluted from the WAX column were first transferred via a Deans switch to a Na_2SO_4-deactivated Al_2O_3 porous-layer open tubular (PLOT) column (50 m x 320 µm ID, with a film thickness of 5 µm) for separation and FID detection. Next, the analytes were forwarded to the second FID. The Deans switch approach focuses on eliminating any mechanical valves in the analytical flow path. Exposing physical valves to elevated temperatures in the oven, makes flow switching a real challenge, as mechanical issues such as material deterioration, leakage, and inadequate inertness can cause potential issues. The Deans' switch principle, on the other hand is based on valveless switching mechanism to adjust the pressure levels in a continuous network of flow resistors, which the pressures and flows are controlled by valves located outside of the analytical flow channel. Figure 2-7 presents the basic Deans' switch diagram, where three Y-type press-fit connectors make Deans switch a reliable process. A 3-way solenoid valve is connected to the two outside connectors (1 and 3), when the carrier is fed to one of these two Y-connectors, the other is turned off.

Figure 2-7 shows that carrier gas is supplied to connector 1. Here, connector 1 experiences pressure due to the increased flow of carrier gas, as a result, connection 3 receives the GC effluent and transfers it to the PLOT column and then to FID1 detector, meanwhile a pure carrier gas is used to power the other detector. A countermeasure against diffusion into the closed column line is the fourth minor restriction (Boeker et al., 2013).
A heart-cutting dual-column gas chromatographic system was used in this study where air sample pass through a non-polar primary column (Aluminium Oxide (Al2O3) PLOT column), and a high polarity secondary column (column (LOWOX)) offering the species independent separation. The primary column separates compounds mainly based on polarity, but the

initial few minutes of the chromatogram often contain a large number of unresolved compounds with very similar polarity. These early-eluting compounds are then selectively transferred, via a heart-cutting technique, to the secondary column, which separates them based on their volatility. Compounds with similar polarity but different boiling points, which were not resolved in the primary column, become separated in the secondary one, while the remaining compounds continue to be resolved on the first column based on their polarity.

This setup is similar, generally, to comprehensive two-dimensional gas chromatography (GCGC), but it is different because it continuously modifies and moves small amounts of sample from the first column to a second column at regular intervals (usually every 1–2 seconds), creating a structured 3D chromatogram from thousands of modulation cycles.

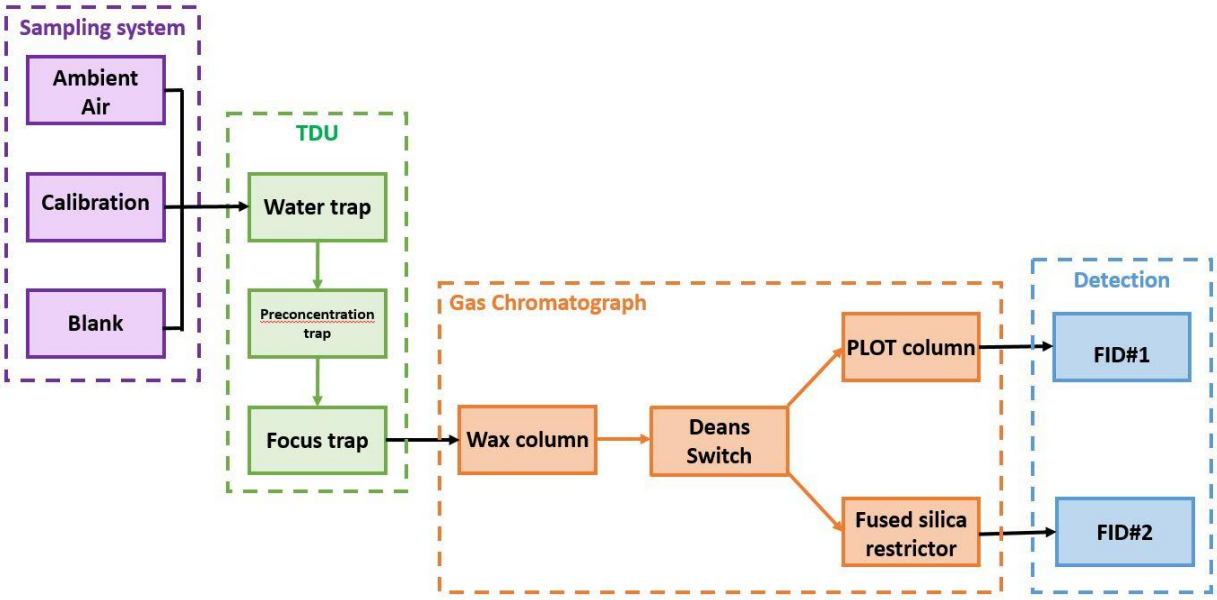

Figure 2-6 Schematic representation of the sample analysis system and flow pathways utilised at London supersite.

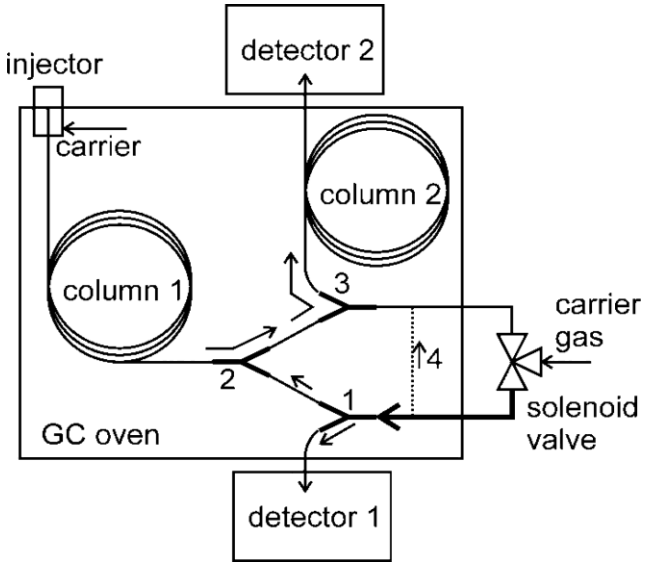

Figure 2-7 Fundamental configuration of a Deans' switch with press-fit connectors (Boeker et al., 2013).

The calibration of the instrument was done using 10-litre Target Gas (TG) cylinder that contained a blend of 36 VOCs, all presented in Table 2-1, that were prepared by adding known amounts of standards to evacuated cylinders and then pressurising them to 100 bar with pure nitrogen. Each TG cylinder's contents were measured using a certified reference cylinder (No. D933515) provided by the National Physical Laboratory (NPL) (National Physical Laboratory (NPL)), Teddington, UK, in accordance with the Global Atmosphere Watch (GAW) scale for VOCs (Global Atmosphere Watch). The quantification was carried out utilising a GC system with a mass spectrometric detector. A similarly developed and certified standard replaced each TG cylinder after it had been in use for up to 24 months. It is worth noting that in the gas cylinders, 1,3-butadiene and isoprene exhibited instability. Therefore, a relative response approach was employed to determine their levels, this method is commonly used in gas chromatography for unstable or missing standards (Korban et al., 2022, 2024; Y. Kudo et al., 2023). For similar reasons, this method was applied to oxygenated VOCs (acetaldehyde, acetone, methanol, and ethanol). A schematic depiction of the GC configuration is presented in Figure 2-8.

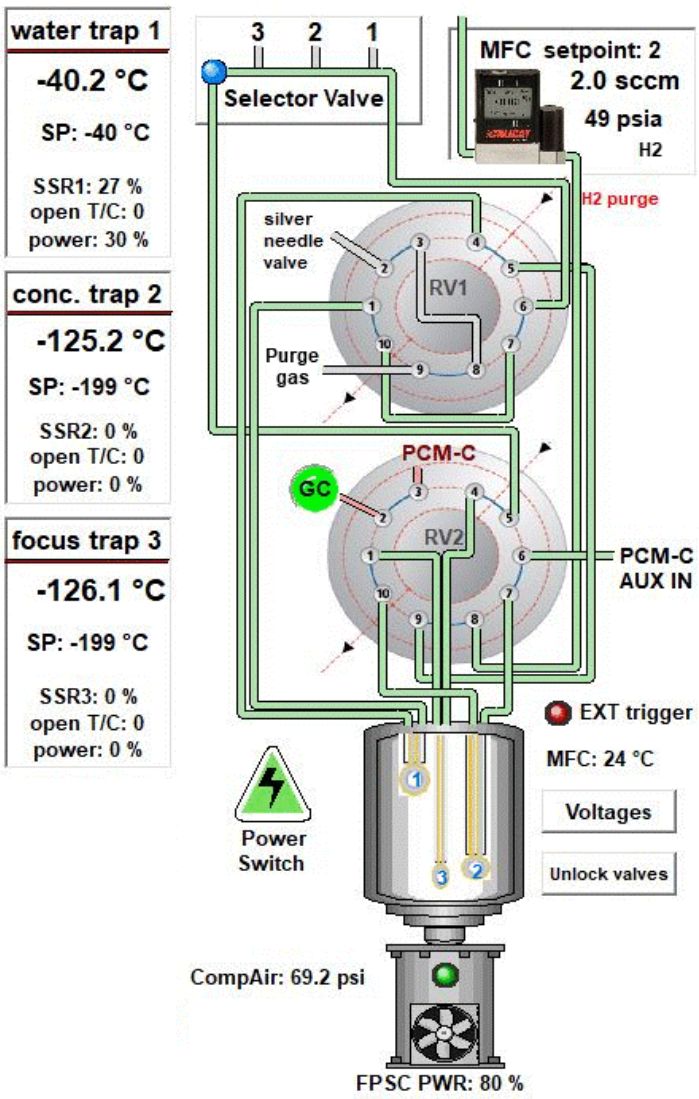

Figure 2-8 Schematic representation of the thermal desorption unit (TDU) and the flow pathways utilised at London supersite. The water trap (1), pre-concentration trap (2), and focus trap (3) are depicted and marked within the cooling block of the unit.

2.3.3 VOCs Measurements uncertainties:

Many factors contribute to measurement uncertainties in the dual-column GC-FID monitoring method. Firstly, the calibration gas concentration, which has 5% fixed uncertainties. The volume of the ambient air sample also has a 5% uncertainty due to the mass flow measurements process. The analyser reproducibility, which reflects instrument precision, can be evaluated by repeated analyses of a calibration standard. It is typically expressed as the relative standard deviation (RSD) from the mean and also accounts for uncertainties arising from peak integration. Generally, the peak integration uncertainty is negligible in the high concentration ranges (such as in calibration gas). However, it is highly variable and depends on the chromatogram peak area, and it can be important near the detection limit range,

where the measurements are detected at ppt levels. The data are reported as mixing ratios with uncertainties including both the fixed components and the variable integration ones that depends on the peak area and can be calculated for each analyser based on the experimental data, using root-sum-square propagation as expressed in Equation 2-1:

$$U_{total} = \sqrt{U_{cal}^2 + U_{flow}^2 + U_{repro}^2 + U_{int}^2}$$ Equation 2-1

Where U_{cal} is the calibration gas uncertainty, U_{flow} is the sampling volume uncertainty, U_{repro} is the analyser reproducibility, and U_{int} is the integration uncertainty.

2.3.4 GC FID Data validation and verification:

The ambient mixing ratio of 36 VOC species has been measured using a dual-column GC-FID at the London supersite since 2020. VOCs data from November 2022 to August 2023 were obtained from this supersite, presented in Table 2-1, to for input to the source apportionment analysis using US-PEA Positive Matrix Factorization 5 (PFM 5). This period was chosen as it offers the most continuous data capture that properly represents VOCs emissions' seasonality patterns, mainly between summer and winter, despite missing data between February to May 2023. VOCs time series were examined to identify any data issues, such as instrument failures or localised emission spikes, before being used by the PMF 5 model, in order to prevent biasing the source apportionment findings.

Isoprene data were dropped, categorised as bad, from this study as there was no clear seasonality of isoprene concentrations as shown in Figure 2-14, indicating issues with the data quality or detection reliability. Isoprene is mainly emitted from biogenic sources, with various physiological and environmental variables including leaf area index (LAI), ambient air temperature, leaf age and UV, considerably impacting its emission rates (Mishra & Sinha, 2020). Although some studies have shown that anthropogenic sources play a key role in isoprene emissions in highly polluted urban environments along with biogenic ones (Bryant et al., 2023), it is not the case in our studied suburban site, and we still expect isoprene levels to show clear seasonality patterns. Additionally, there were instrumental issues and doubts about ethanol and benzene measurements, as their chromatographic peaks sometimes overlapped. Consequently, ethanol and benzene data were categorised as invalid and excluded from the PMF analysis.

Table 2-1 Summary of VOCs measured at the London Supersite, including compound name, chemical formula, chemical group, molecular weight, and mean and median mixing ratios (ppb).

VOC Name	Chemical Formula	Chemical Group	Molecular Weight (g/mol)	Mean Mixing Ratio (ppb)	Median Mixing Ratio (ppb)
Ethane	C2H6	Alkane	30.07	3.921	2.214
Propane	C3H8	Alkane	44.1	1.413	0.820
iso-Butane	C4H10	Alkane	58.12	0.706	0.306
n-Butane	C4H10	Alkane	58.12	1.313	0.666
cyclo-Pentane	C5H10	Alkane (cycloalkane)	70.1	0.049	0.032
iso-Pentane	C5H12	Alkane	72.15	0.401	0.234
n-Pentane	C5H12	Alkane	72.15	0.171	0.112
Methyl_2_pentane	C6H14	Alkane	86.18	0.108	0.068
Methyl_3_pentane	C6H14	Alkane	86.18	0.070	0.043
n-Hexane	C6H14	Alkane	86.18	0.061	0.038
n-Heptane	C7H16	Alkane	100.21	0.043	0.029
2,2,4 Trimethylpentane	C8H18	Alkane	114.23	0.019	0.011
n-Octane	C8H18	Alkane	114.23	0.015	0.010
Ethene	C2H4	Alkene	28.05	0.542	0.295
Propene	C3H6	Alkene	42.08	0.138	0.058
Trans-2-butene	C4H8	Alkene	56.11	0.014	0.008
1-Butene	C4H8	Alkene	56.11	0.030	0.017
Iso-Butene	C4H8	Alkene	56.11	0.063	0.051
cis-2-butene	C4H8	Alkene	56.11	0.011	0.007
1,3-butadiene	C4H6	Alkene	54.09	0.011	0.004
Trans-2-pentene	C5H10	Alkene	70.13	0.008	0.001
1-pentene	C5H10	Alkene	70.13	0.008	0.003
Acetylene	C2H2	Alkyne	26.04	0.318	0.180
Benzene	C6H6	Aromatic	78.11	0.188	0.127
Toluene	C7H8	Aromatic	92.14	0.318	0.199
Ethylbenzene	C8H10	Aromatic	106.17	0.056	0.033
m-Xylene	C8H10	Aromatic	106.17	0.124	0.062
p-Xylene	C8H10	Aromatic	106.17	0.054	0.031
o-Xylene	C8H10	Aromatic	106.17	0.067	0.038

VOC Name	Chemical Formula	Chemical Group	Molecular Weight (g/mol)	Mean Mixing Ratio (ppb)	Median Mixing Ratio (ppb)
1,3,5-Trimethylbenzene	C9H12	Aromatic	120.19	0.012	0.004
1,2,4-Trimethylbenzene	C9H12	Aromatic	120.19	0.050	0.021
1,2,3-Trimethylbenzene	C9H12	Aromatic	120.19	0.016	0.008
Acetaldehyde	C_2H_4O	Carbonyl	44.05	1.121	0.978
Acetone	C_3H_6O	Carbonyl	58.08	1.382	1.190
Ethanol	C_2H_6O	Alcohol	46.07	3.055	1.994
Isoprene	C5H8	Diene	68.12	0.004	0.001
Total VOCs	-	Total	-	15.88	10.414

Figure 2-9 to Figure 2-14 show the time series of selected VOCs (acetaldehyde, n-hexane, methyl-3-pentane, iso-pentane, iso-butane, and isoprene) measured at the London Supersite between November 2022 and August 2023. Each data point represents an individual GC measurement cycle, illustrating the extreme concentration events, and occasional step changes observed in the dataset.

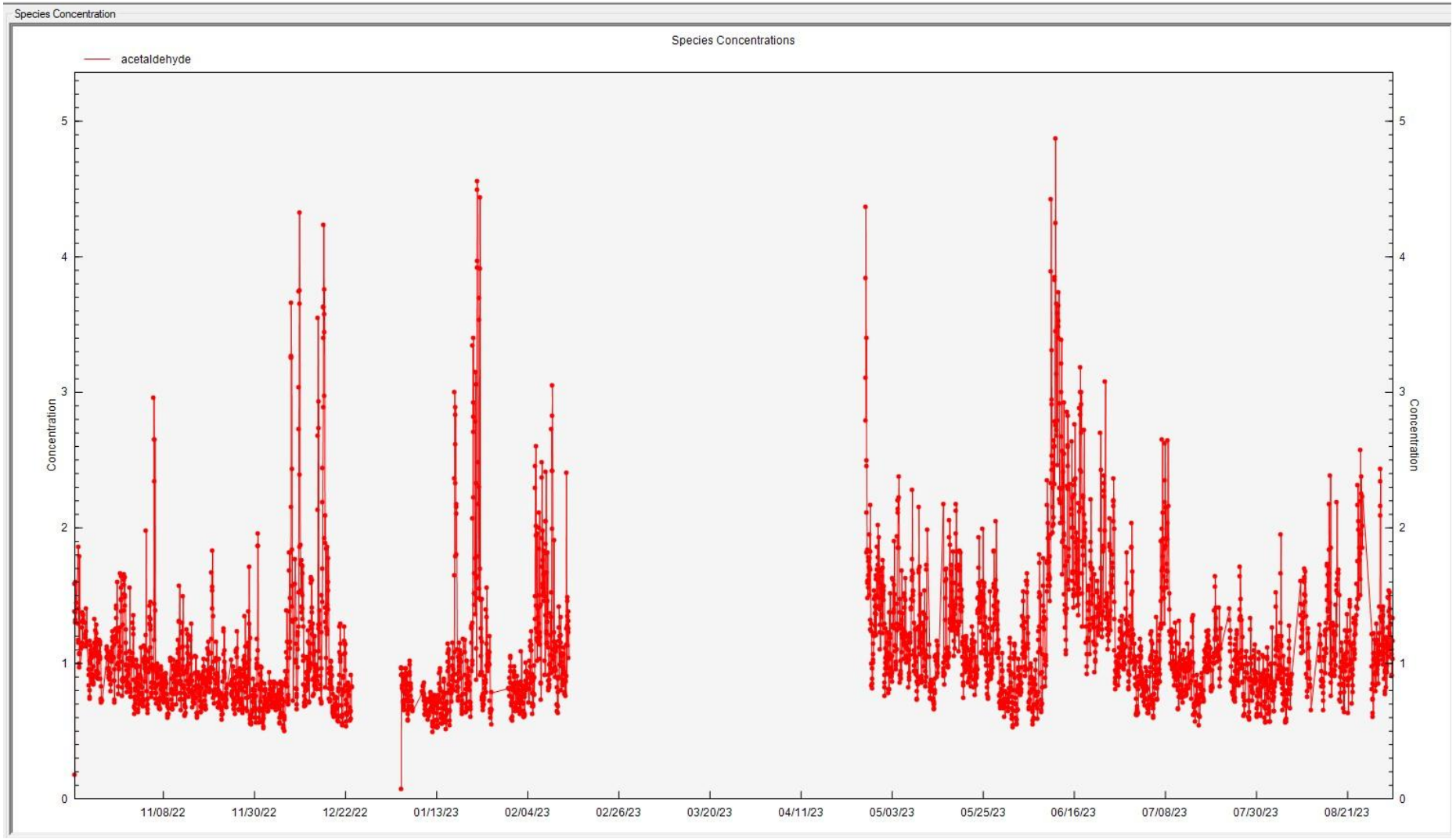

Figure 2-9 Time series of acetaldehyde concentrations (ppb) measured at the London Supersite between November 2022 and August 2023, based on GC–FID cyclic measurements (1–1.2 hour resolution).

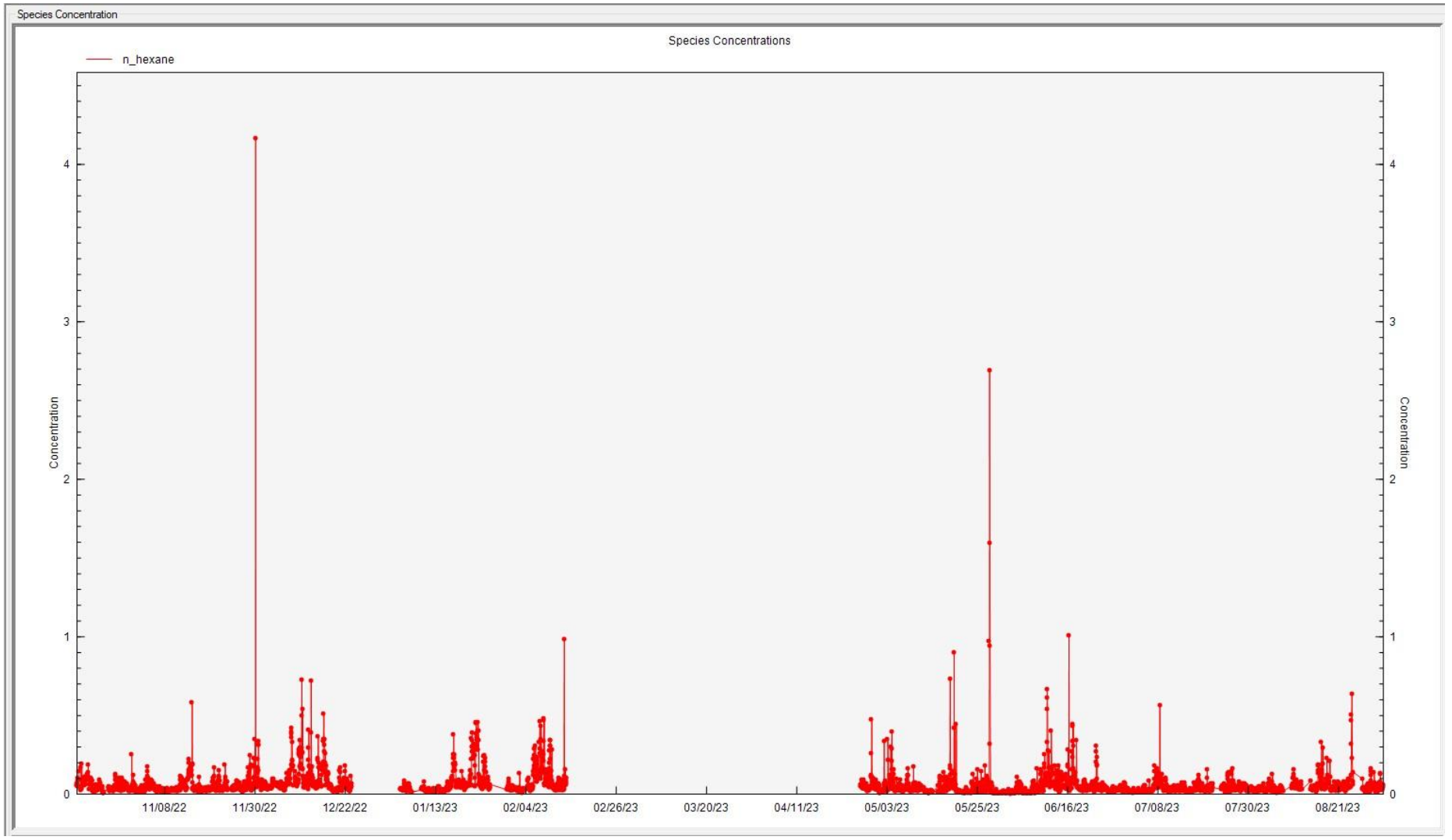

Figure 2-10 Time series of n-hexane concentrations (ppb) measured at the London Supersite between November 2022 and August 2023, based on GC–FID cyclic measurements (1–1.2 hour resolution).

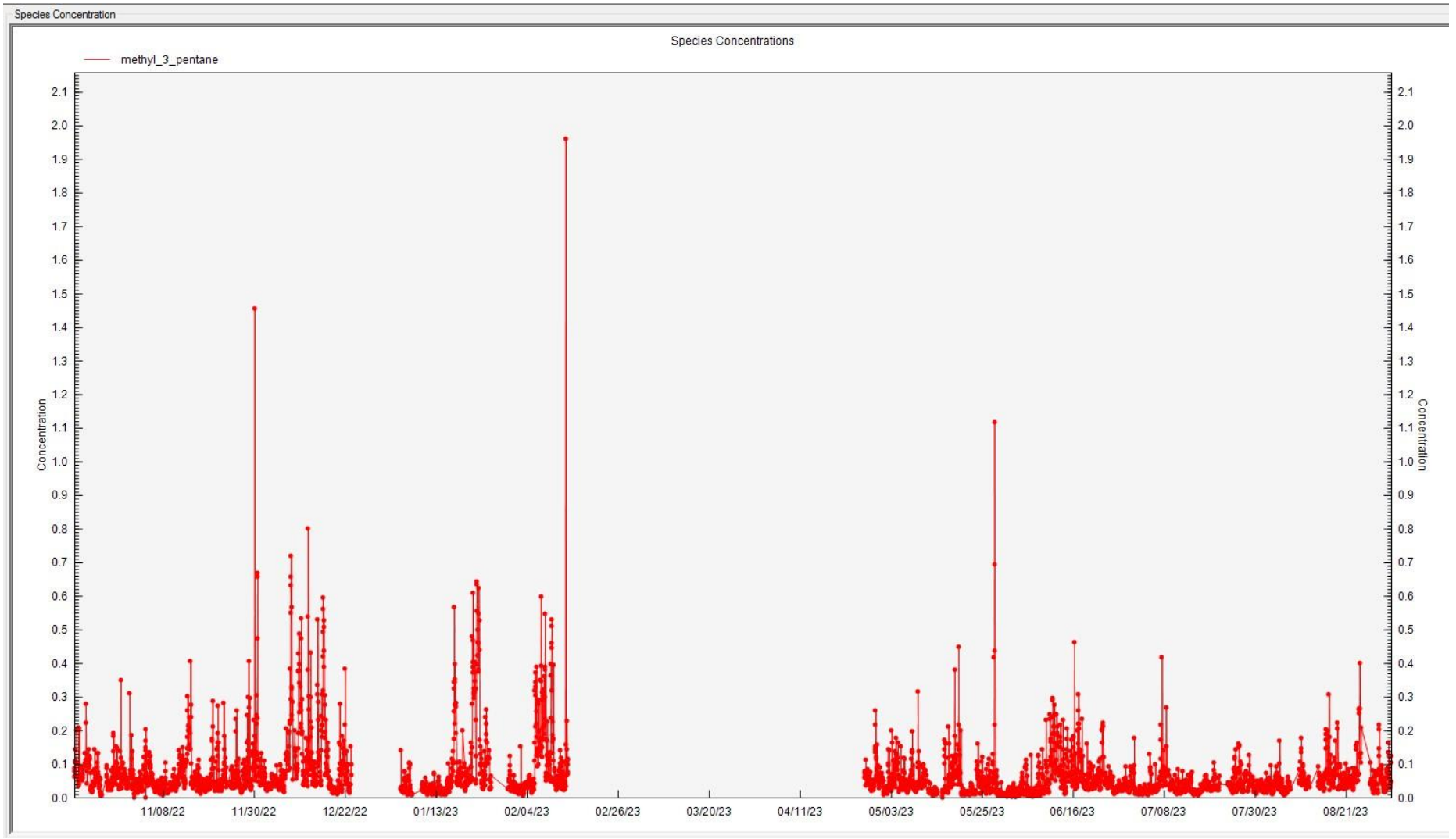

Figure 2-11 Time series of methyl_3_pentane concentrations (ppb) measured at the London Supersite between November 2022 and August 2023, based on GC–FID cyclic measurements (1–1.2 hour resolution).

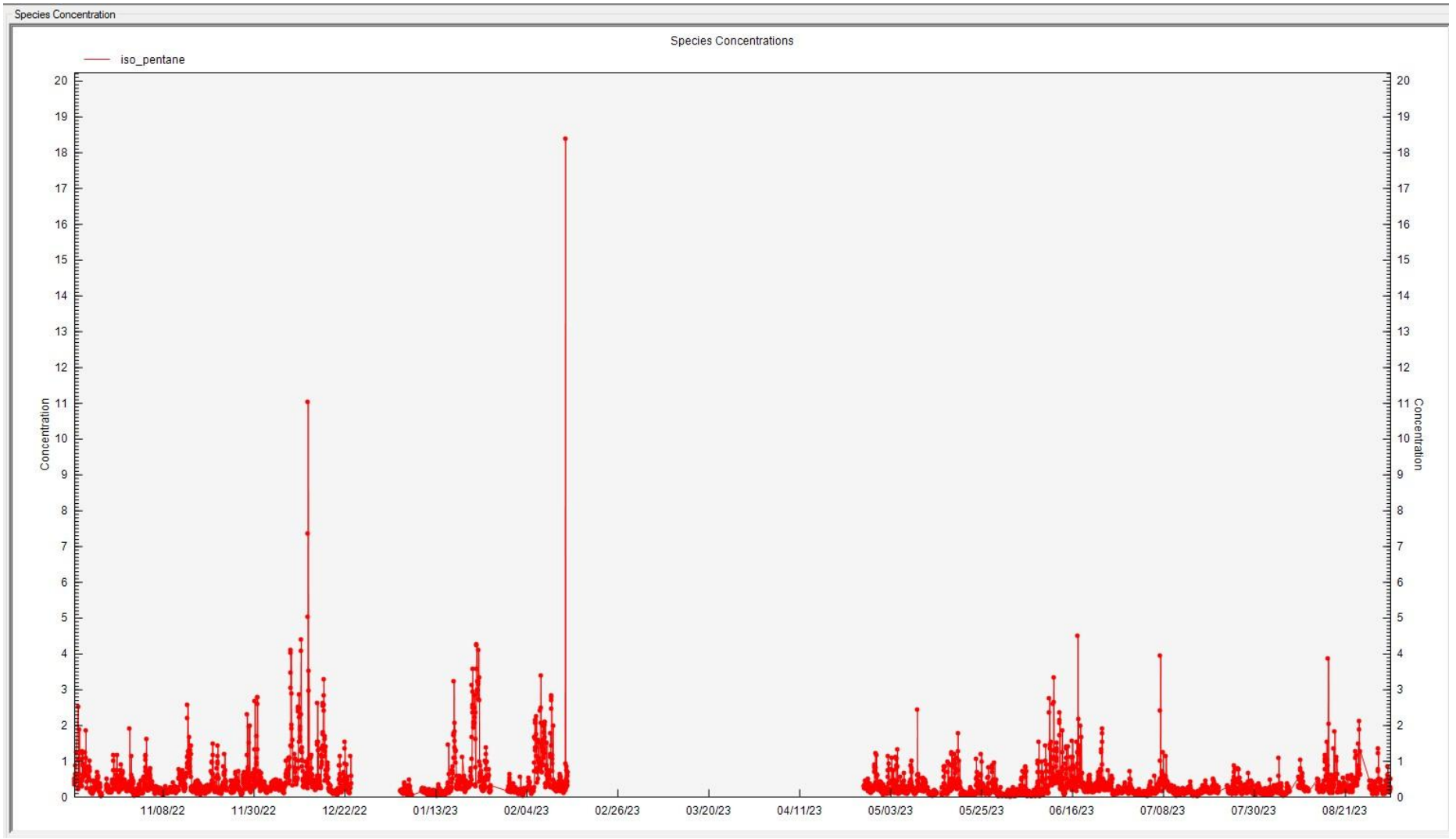

Figure 2-12 Time series of iso pentane concentrations (ppb) measured at the London Supersite between November 2022 and August 2023, based on GC–FID cyclic measurements (1–1.2 hour resolution).

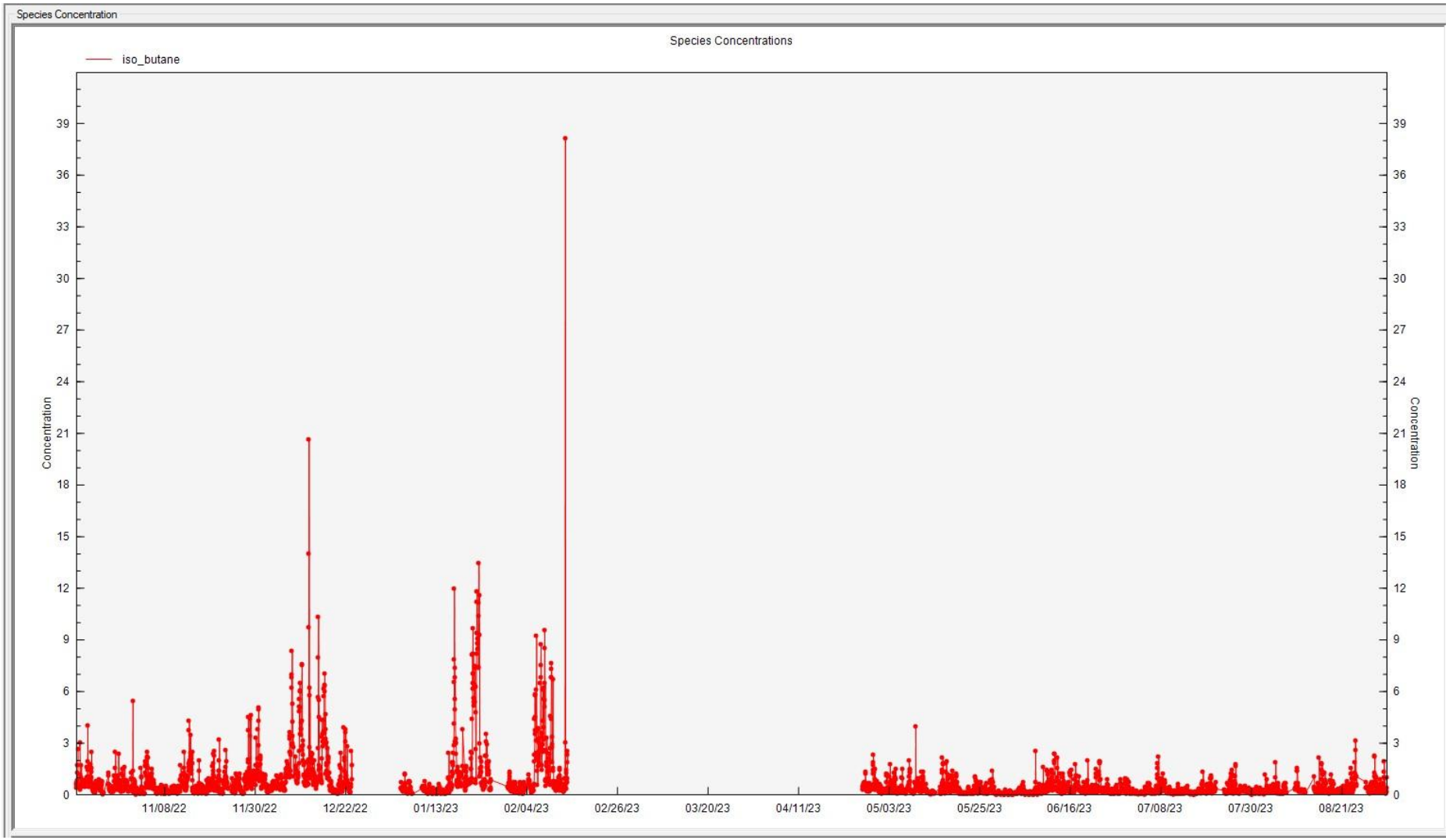

Figure 2-13 Time series of iso butane concentrations (ppb) measured at the London Supersite between November 2022 and August 2023, based on GC–FID cyclic measurements (1–1.2 hour resolution).

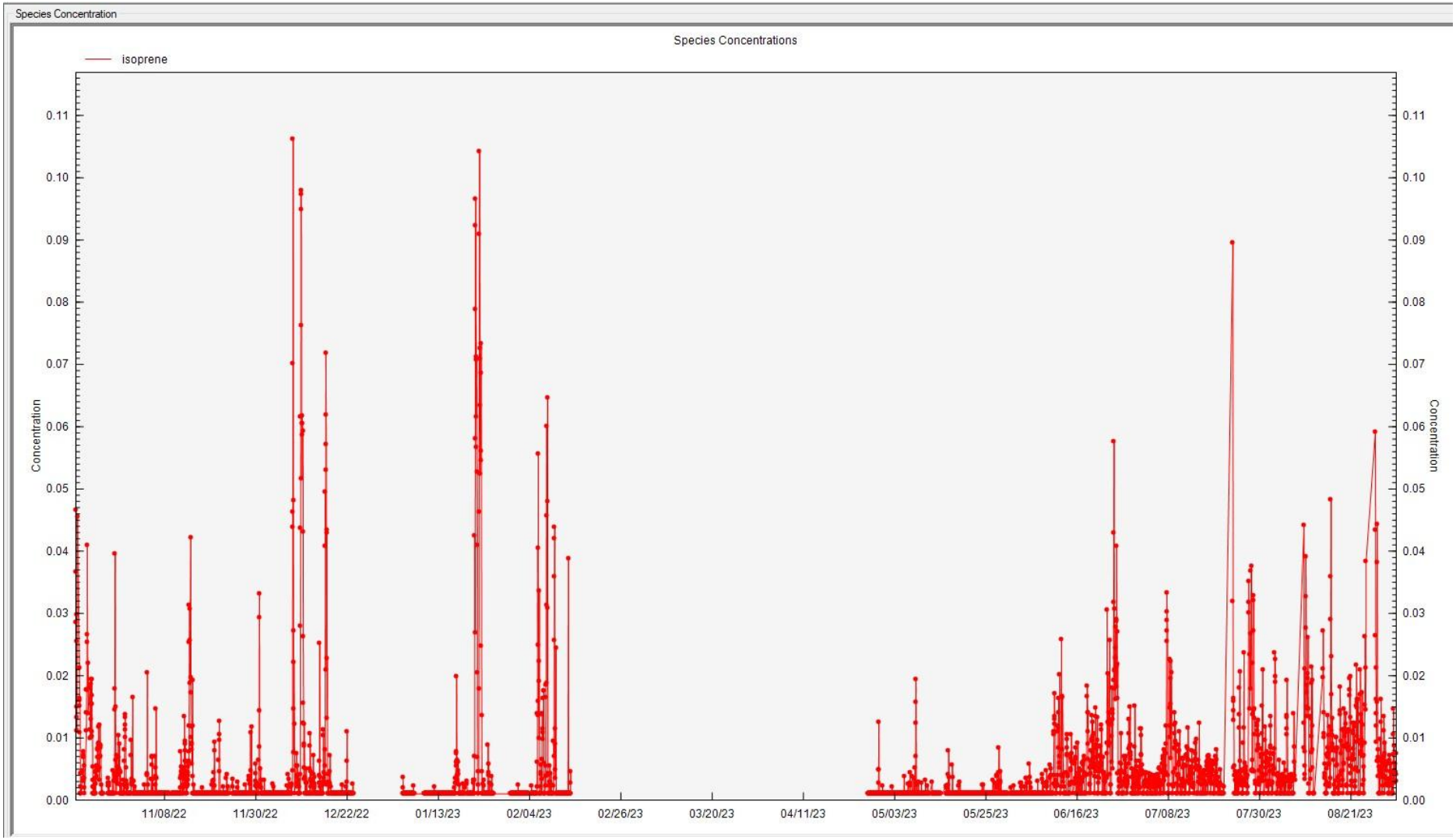

Figure 2-14 Time series of isoprene concentrations (ppb) measured at the London Supersite between November 2022 and August 2023, based on GC–FID cyclic measurements (1–1.2 hour resolution).

2.3.5 Positive Matrix factorization

In this study, ambient concentrations of VOCs were appointed to their corresponding sources by utilising the U.S. EPA's Positive Matrix Factorisation (PMF) version 5.0 receptor model. A matrix of residuals (E) and two non-negative matrices, the factor contribution matrix (G) and the factor profile matrix (F) were created from a matrix of recorded pollutant concentrations using multivariate factor analysis techniques. The relationship is mathematically expressed as in Equation 2-2:

$$X_{ij} = \sum_{k=1}^{p} G_{ik} F_{kj} + e_{ij} \qquad \text{Equation 2-2}$$

X_{ij} denotes the measured concentration of species j in sample i, p signifies the number of sources, G_{ik} indicates the contribution of source k to sample i, F_{kj} represents the chemical profile of source k, and e_{ij} is the residual (Norris & Bai, 2014; Paatero & Tapper, 1994). The PMF technique uses a least squares method to continuously adjust the values of the G and F matrices in order to minimise the quality of fit parameter Q, defined as in Equation 2-3 :

$$Q = \sum_{i=1}^{n} \sum_{j=1}^{m} \left(\frac{e_{ij}^2}{s_{ij}^2} \right) \qquad \text{Equation 2-3}$$

where s_{ij} is the uncertainty linked to each observation X_{ij}. Non-negativity requirements are imposed on both G and F matrices to guarantee physically meaningful solutions (Hopke, 2016). The scaling factor is the specified error value of the data point being fitted, and Q is the sum of the squares of the scaled residuals. "Q Expected" (Qexp), a theoretical value of Q, is equivalent to the degrees of freedom of the fitted data:

$$Q_{exp} = mn - p(m+n) \qquad \text{Equation 2-4}$$

A crucial stage in PMF analysis is to specify the optimal number of the solutions (factors) that effectively reflect the appropriate sources, and ideally represent the data variability without overfitting the data (including additional factors) which can lead a false factor splitting, in which the relevant actual physically meaningful factors (sources) are separated into multiple irrelevant factors (sources) (Ulbrich et al., 2008). To assess the goodness of model fit (Q/Qexp), the accuracy of species profiles reproduced by the model was evaluated based on the selected number of parameters. The chosen number of factors offers a statistically

consistent solution when the Q/Qexp ratio is close to one, which means that the genuine inaccuracy in the measurements is accurately described by the estimation of errors in the input error matrix (Abeleira et al., 2017).

Matrix values for concentration (X) and uncertainty (U) are essentially required in the PMF input files. The method detection limit (MDL) and the error fraction were combined to compute uncertainties using the following formula Equation 2-5:

$$U_{ij} = \sqrt{(0.5 \times MDL_j)^2 + (error\_fraction \times X_{ij})^2} \qquad \text{Equation 2-5}$$

For concentrations below the MDL, values were substituted with half the MDL, and uncertainties were set at 5/6 multiplied by MDL (Kuo et al., 2014; Reff et al., 2007)

The EPA PMF model's signal-to-noise (S/N) ratio computation is crucial for evaluating each species' reliability in the dataset. In the previous versions, the S/N was calculated by dividing the total concentrations by the total uncertainty, which was considered generally effective. However, that approach was biased, where species with a few high concentrations could appear as "strong," and immoderate uncertainty values may lead to truly strong species being categorised as "weak," which was a common issue in that practice. The computed signal was further affected by slightly negative concentration values, which are typical in environmental datasets. A revised S/N strategy was implemented in EPA PMF 5.0 to address these constraints and better reflect each species' actual signal contribution, where only concentration values that are greater than their corresponding uncertainties are regarded as having a meaningful signal in the updated methodology. Consequently, the signal can be calculated as the difference between the measured concentration (xi), and the signal (si), and therefore, it may be distinguished from measurement noise using Equation 2-6:

$$d_{ij} = \left(\frac{x_{ij} - s_{ij}}{s_{ij}} \right) \text{ if } x_{ij} > s_{ij} \qquad \text{Equation 2-6}$$

This was then used to calculate S/N ratios. This guarantees that only statistically reliable measurements impact species' classification, where concentrations below the uncertainty threshold do not contribute to the signal. This approach improves both the accuracy and consistency of species classification in PMF analysis by avoiding the overestimation or

underestimation of S/N values due to the effects of outliers, negative readings, or overstated uncertainty (Norris & Bai, 2014). Hence S/N is calculated as per Equation 2-7:

$$\left(\frac{S}{N}\right)_j = 1/n \sum_{i=1}^{n} d_{ij}$$ Equation 2-7

2.3.6 PMF Factors Optimal Number Selection

The most critical step in PMF analysis is specifying the optimal number of PMF solutions, as it possesses significant impact on the accuracy and explainability of source apportionment results. Determining the optimal number of factors is a vital step in order to avoid overestimating or underestimating the number of factors, which can lead to factor splitting (introducing extra factors that have no physical meaning) or merging of disparate sources (ambiguous or mixed profiles), respectively (Bressi et al., 2014). Various methods can be used together to identify the optimal number of PMF solutions, including PMF generated diagnostic indicators (Pernov et al., 2021), receptor area's emission inventories (C. Song et al., 2019), literature review (Zhao et al., 2020), and field investigations (Gu et al., 2020). However, the diagnostic metrics derived from the PMF model are among the most commonly used methods, which consist of: the correlation coefficient between observed and modelled species' concentrations, the Q value (PMF solution's goodness-of-fit metric) (Salameh et al., 2016), the error estimation (EE) diagnostic index (measuring model uncertainty) (Pernov et al., 2021), Fpeak rotational tools (assessing solution stability and interpretability) (Norris & Bai, 2014), the distribution of scaled residuals (identifying potential model misspecifications(Guan et al., 2020), and the physical interpretability and realism of resolved source profiles (M. Wang et al., 2021). Defining the optimal number of solutions can be achieved through the combination of these PMF tools, guaranteeing the statistical validity and the physical meaning of the PMF outputs.

The coefficient of determination (R^2) between the observed and modelled concentrations of VOCs, provided by the PMF output, is obtained from an unweighted least-squares fit. High R^2 values suggest a generally satisfactory model performance (Fan et al., 2021), but this may not accurately reflect the actual relationships between the measured and modelled values. Therefore, when evaluating the quality of PMF solutions, relying solely on R^2 can prove to be an unreliable approach, and hence we used R^2 values just as an initial indication for the optimal number of PMF solution (Factors) in this study. We then applied the three advanced

error estimating (EE) procedures included in EPA PMF v5.0 to handle the main uncertainties and ambiguities related to factor resolution: classical bootstrap (BS), displacement of factor elements (DISP), and bootstrap enhanced by displacement (BS-DISP), as they provide complementary information about the stability and dependability of resolved factors. Both BS and BS-DISP tools are effective for characterising uncertainty in source profiles and contributions, while the DISP tool is reliable for evaluating rotational ambiguity, a serious challenge in receptor models (Hopke et al., 2023). A robust PMF solution can be achieved by evaluating and combining these EE statistical tools together as they validate the reproducibility and physical plausibility of the PMF solution. Additionally, we examined the change in the normalized objective function value (Q/Q_{exp}), when the steady decrease in Q/Qexp slope becomes gradual or negligible with the addition of extra factors, this generally indicates that the model has reached an optimal balance between underfitting and overfitting (Brown et al., 2015; Hemann et al., 2008). It is worth noting that while Fpeak model runs evaluates the rotational ambiguity, this strategy is considered subjective because of its dependence on user interpretation and lack of statistical analysis (Yang et al., 2022).

Finally, a solution is considered robust when all factors are mapped in more than 80% of bootstrap (BS) runs, and there is no rotational ambiguity or factor swapping in displacement (DISP) analysis (Fan et al., 2021).

2.3.7 PMF Data Preparation

A total of 36 VOC species were monitored, resulting in 4,065 ambient VOC samples measured between November 2022 and August 2023. Matrix values for associated concentration (X) in mixing ratio units and uncertainty (U) were fed to the US EPA PMF 5.0 model. The time series of each VOC was thoroughly examined prior to the PMF model's execution, in order to detect and exclude any extreme observation events and step changes that could affect the accuracy of the model performance. Rare events can skew the model's results and may not be representative of typical source profiles, such as short-term spikes from unfamiliar sources, where adding these extreme events could result in the identification of unrealistic factors or alter the composition of physically meaningful existing ones. Likewise, including step changes, usually related to instrumental issues, such as sudden, unexpected shift in the VOCs mixing ratios, could introduce false sources. Therefore, all extreme events and step changes were excluded. These were identified through visual screening of the time series prior to PMF

analysis, extreme events were defined as short-duration concentration spikes substantially exceeding the surrounding background levels while step changes were identified as sudden changes in the baseline concentration that remained elevated or reduced over a sustained period of consecutive measurements as shown in Figure 2-9 to Figure 2-13. All improved the physical interpretation of the source profiles (Grover & Eatough, 2008). Any ambient sample that contained a missing observation was entirely excluded (Su et al., 2019). In addition to the calculated uncertainty described in Equation 2-5, an extra 5% modelling uncertainty was added for all species in the PMF input in order to account for any unquantifiable issues not captured by the experimental or the analytical uncertainties, this approach is advised in the EPA PMF 5.0 recommendations to address unquantified sources of error such as sample handling, interferences, and slight variations in detection limits over time. Adopting this additional uncertainty mitigates overfitting and improves solution stability (Norris & Bai, 2014). Then we conducted two-stage analysis regarding species categories. Firstly, to minimise their impact on model solutions, species with moderate data quality (S/N < 2) were initially down weighted by a factor of 3 (status = "weak"), while species with low signal to noise ratios (S/N < 1) were eliminated (status = "bad"). In the second stage, and after the initial model run, we conducted thorough residual, scatter plot, and time series analyses (observed against predicted), where poorly fitted species, those with scaled residuals higher than 4.0 or unfitted peak concentrations in scatter or time series plots, were assigned to the weak category (Brown et al., 2015b; Norris & Bai, 2014). These VOCs are acetylene, cyclo_pentane, iso_pentane, methyl 2pentane, methyl 3pentane, n_heptane, n_hexane, n_pentane, 1,2,3-Trimethylbenzene, 2,2,4 Trimethylbenzene, toluene, and trans 2pentene, shown in Table 2-2.

Table 2-2 Summary of VOC input data used in the PMF model. Including signal-to-noise (S/N) ratios, descriptive statistics (minimum, 25th percentile, median, 75th percentile, maximum mixing ratios) and the percentage of samples included in modelling against total raw samples.

VOCs Species	Category	S/N	Min	25th	Median	75th	Max	% Modelled Samples	% Raw Samples
ethane	Strong	10	0.77	1.53	2.20	3.66	87.45	99%	100%
ethene	Strong	9.9	0.01	0.14	0.29	0.63	6.66	99%	100%
propane	Strong	10	0.05	0.43	0.81	1.56	22.13	99%	100%
propene	Strong	9.6	0.01	0.04	0.06	0.10	2.96	99%	100%

VOCs Species	Category	S/N	Min	25th	Median	75th	Max	% Modelled Samples	% Raw Samples
isobutane	Strong	10	0.01	0.15	0.30	0.68	13.45	99%	100%
n-butane	Strong	10	0.03	0.37	0.66	1.27	23.21	99%	100%
acetylene	*Weak*	7.6	0.02	0.11	0.18	0.34	3.86	99%	100%
Trans-2-butene	Strong	5	0.00	0.01	0.01	0.01	0.25	99%	100%
but_1_ene	Strong	8	0.00	0.01	0.02	0.03	0.55	99%	100%
isobutene	Strong	8.1	0.01	0.04	0.05	0.07	0.53	99%	100%
Cis-2-butene	Strong	4.3	0.00	0.00	0.01	0.01	0.19	99%	100%
cyclopentane	*Weak*	7.3	0.01	0.02	0.03	0.05	0.88	99%	100%
isopentane	*Weak*	10	0.01	0.14	0.23	0.42	4.49	99%	100%
n_pentane	*Weak*	10	0.01	0.07	0.11	0.19	1.65	99%	100%
buta_1_3_diene	Strong	2.7	0.00	0.00	0.00	0.01	0.35	99%	100%
trans_2_pentene	*Weak*	1.4	0.00	0.00	0.00	0.00	0.19	99%	100%
pent_1_ene	Strong	2.3	0.00	0.00	0.00	0.01	0.19	99%	100%
methyl_2_pentane	*Weak*	9.9	0.00	0.04	0.07	0.12	1.14	99%	100%
methyl_3_pentane	*Weak*	9.1	0.00	0.03	0.04	0.08	0.72	99%	100%
isoprene	**Bad**	0.8	0.00	0.00	0.00	0.00	0.11	0%	100%
n-hexane	*Weak*	9.5	0.00	0.02	0.04	0.06	1.01	99%	100%
n-heptane	*Weak*	9.1	0.00	0.02	0.03	0.05	0.47	99%	100%
tmp_224	*Weak*	6.1	0.00	0.01	0.01	0.02	0.34	99%	100%
n_octane	Strong	5.7	0.00	0.01	0.01	0.02	0.14	99%	100%
benzene	**Bad**	10	0.04	0.09	0.13	0.20	2.54	0%	100%
toluene	*Weak*	10	0.02	0.12	0.20	0.34	3.72	99%	100%
ethylbenzene	Strong	8.6	0.00	0.02	0.03	0.06	0.69	99%	100%
m-xylene	Strong	9.3	0.00	0.03	0.06	0.12	1.98	99%	100%
p-xylene	Strong	8.3	0.00	0.02	0.03	0.06	0.70	99%	100%
o-xylene	Strong	8.9	0.00	0.02	0.04	0.07	0.87	99%	100%
tmb_135	Strong	2.8	0.00	0.00	0.00	0.01	0.30	99%	100%
tmb_124	Strong	5.6	0.00	0.01	0.02	0.05	1.15	99%	100%
tmb_123	*Weak*	3.3	0.00	0.01	0.01	0.02	0.31	99%	100%
acetaldehyde	Strong	8.1	0.49	0.80	0.98	1.26	4.87	99%	100%
acetone	Strong	8.2	0.39	0.84	1.19	1.65	7.62	99%	100%
ethanol	**Bad**	8.2	0.29	1.35	1.99	3.40	32.94	0%	100%

VOCs Species	Category	S/N	Min	25th	Median	75th	Max	% Modelled Samples	% Raw Samples
TVOCs	*Weak*	10	3.09	7.52	10.37	16.2	212.16	99%	100%

2.3.8 Evaluation of Ozone Formation Potential (OFP)

In order to determine the relative contribution of VOC sources to the photochemical production of ozone, the ozone formation potential (OFP) for each PMF resolved VOC source was estimated by calculating the sum of ambient concentration of each non-methane hydrocarbon (NMHC) species within each factor multiplied by its relevant maximum incremental reactivity (MIR) factor, using Equation *2-8*:

$$OFP_{source} = \sum_{i=1}^{n} [VOC_i]_{source} \times MIR_i$$ Equation 2-8

where $[VOC_i]$ is the mass concentration of species i attributed in that source, and MIRi is the maximum incremental reactivity of species i (g O_3/g VOC). Prior to the OFP calculation, molecular weights and standard temperature and pressure (STP) assumptions were used to convert VOC concentrations that were first reported in ppb to µg/m³, and the calculated values are given in Table 2-3

2.3.9 Evaluation of Secondary Organic Aerosol Potential (SOAP) per Source

Using the secondary organic aerosol potential (SOAP) for each PMF-resolved source factor, the relative contribution of VOC sources to the generation of secondary organic aerosols (SOA) was estimated, where the mass concentration (µg/m³) of each VOC species within a source was multiplied by the corresponding SOAP factor that represents the relative potential of that VOC to form SOA mass on a mass basis (relative to toluene =100), using the following Equation *2-9*:

$$\mathrm{SOAP}_{\mathrm{source}} = \sum_{i=1}^{n} [\mathrm{VOC}_i]_{\mathrm{source}} \times \mathrm{SOAP}_i$$ Equation 2-9

where $[VOC_i]$ is the mass concentration of species i attributed in that source, and SOAPi is the SOA factor of species i (relative to toluene = 100). Similar to OFP, prior to the SOAP calculation, molecular weight and standard temperature and pressure assumptions were used to convert

VOC concentrations, originally reported in ppb, into μg/m³. The values used are illustrated in Table 2-3.

Table 2-3 VOCs used in OFP and SOAP calculations, including molecular weights, maximum incremental reactivity (MIR), and SOAP factors representing relative SOA formation potentials on a mass basis (relative to toluene = 100).

VOCs	MIR ($g O_3/g$ VOC)[a]	SOAP factor[b]	VOCs	MIR ($g O_3/g$ VOC)[a]	SOAP factor[b]
Ethane	0.28	0.1	pent_1_ene	12.22	0
Ethene	9	1.3	methyl_2_pentane	1.5	0
propane	0.49	0	methyl_3_pentane	1.8	0.2
propene	11.67	1.6	n-hexane	1.24	0.1
isobutane	1.23	0	n-heptane	1.07	0.1
n-butane	1.15	0.3	tmp_224	1.26	0
acetylene	0.95	0.1	n-octane	0.9	0.8
Trans-2-butene	15.16	4	Toluene	4	100
but_1_ene	9.73	1.2	ethylbenzene	6.57	111.6
isobutene	6.29	1.2	m-xylene	9.75	84.5
Cis-2-butene	14.24	3.6	p-xylene	9.75	84.5
cyclopentane	2.39	0	o-xylene	7.64	95.5
isopentane	1.45	0.2	tmb_135	5.59	94.8
n_pentane	1.31	0.3	tmb_124	8.87	20.6
buta_1_3_diene	12.61	1.8	tmb_123	11.97	43.9
trans-2-pentene	10.56	3.1	acetaldehyde	6.54	0.6
-	-	-	acetone	0.62	0.3

a; (CCR, 2001), b; (M. Song et al., 2018).

2.3.10 Conditional Bivariate Probability Function (CBPF) for source identification

Conditional bivariate probability function is a simple method for providing information about potential pollution sources depending on their location distance and direction from a monitoring point (Bennett et al., 2013). It mainly includes wind direction, wind speed and the pollutant concentration to identify the probability of certain concertation percentile associated with a specific wind direction following the Equation 2-10:

$$\mathrm{CBPF}(\Delta\theta, \Delta u) = \frac{m_{\Delta\theta,\Delta u \mid c \geq x}}{n_{\Delta\theta,\Delta u}}$$ Equation 2-10

where θ is the wind sector; $m_{\Delta\theta,\Delta u}$ is the number of samples with wind speed Δ_u whose concentration C is higher than or equal to a specified concentration x from that wind sector; and $n_{\Delta\theta,\Delta u}$ is the total number of samples from the same wind group (Uria-Tellaetxe & Carslaw, 2014).

2.4 Results and Discussions

2.4.1 Statistical Selection of PMF Optimal Factors Number

A series of base model runs were conducted using EPA PMF 5.0, evaluating factor numbers from three to nine, where each solution was initially conducted by 20 base model runs using a fixed seed number of 25 in order to ensure reproducibility and assess model stability. To determine the most statistically appropriate solution the variation of Q(true)/Q(expected) value as a function of the number of factors was evaluated. As presented in Figure 2-15 the Q/Qexp ratio decreases steadily with increasing number of factors, starting from a high value of 4.35 for a three-factor solution and dropping to 1.55 for the nine-factor solution. Although this ongoing decline is anticipated given that models with more degrees of freedom are better able to minimise residuals, the rate of improvement just gradually decreases after the seven-factor solution, where the switch from six to seven factors lowers Q/Qexp to just below 2.0, falling below the suggested threshold of 2, where Q/Qexp ratios near 1 are generally indicative of an ideal solution; ratios below 2 are nevertheless acceptable and show a reasonable agreement between observed and model-predicted values (Norris & Bai, 2014). Furthermore, in the eight and nine-factor solutions, the Q/Qexp ratio drops to 1.71 and 1.55, respectively.

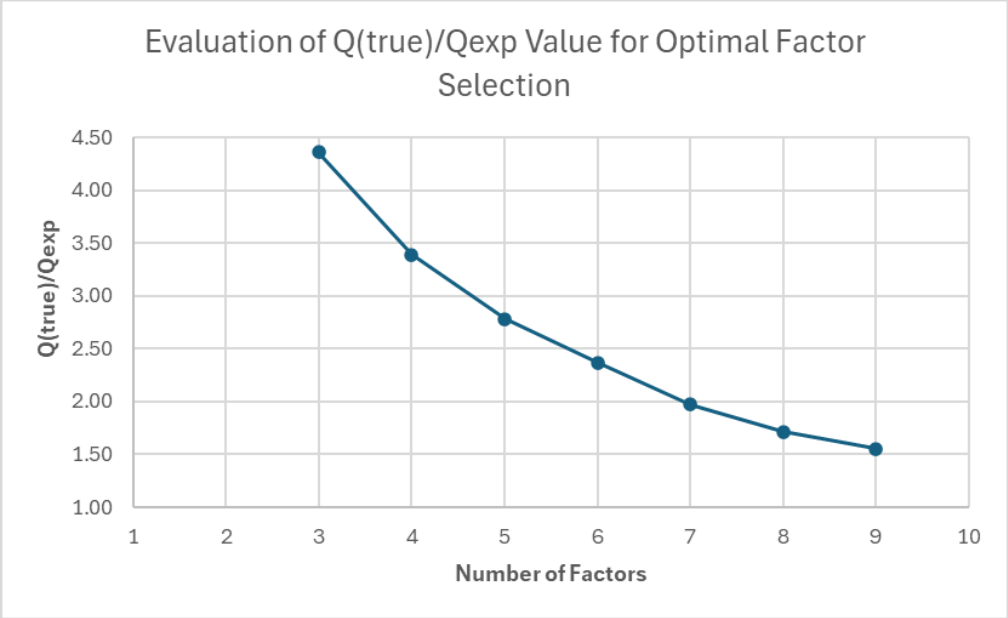

Figure 2-15 Evaluation of Q(true)/Q(exp) Value for Optimal PMF Factor Selection of VOCs sources in London November 2022 to August 2023.

Secondly, the fluctuation in Q(Robust) and Q(True) values was assessed throughout 20 base runs for 6,7 and 8-factor solutions to evaluate model stability as shown in Table 2-4.

The 6-factor solution had the most variation, with Q(True) ranging from 142,126 to 143,262 and Q(Robust) ranging from 135,867 to 139,087, a spread of more than 1,100 and 3,200 units, respectively. This level of variation signifies possible rotational ambiguity, indicating that the solution may lack complete stability (Norris & Bai, 2014). The 7-factor solution, in contrast, showed outstanding consistency, with Q(True) values between 110,519 and 110,520 and Q(Robust) values between 108,744 and 108,747; a difference of only 1 and 3 units, respectively. This minimal variance confirms a highly stable and well-converged solution. With Q(True) ranging from 88,927.1 to 88,928.1 and Q(Robust) ranging from 87,506.1 to 87,509.1; varying by just 1 and 3 units, respectively, the 8-factor solution similarly showed high stability. This indicates that both seven and eight-factor solutions could be statistically valid at this stage.

Table 2-4 Q Value Comparison for PMF 5.0: 6, 7 and 8- factor solution of VOCs sources in London November 2022 to August 2023.

Factor Solution	Q(Robust) Min	Q(Robust) Max	Q(Robust) Range	Q(True) Min	Q(True) Max	Q(True) Range
6 Factors	135867	139087	3220	142126	143262	1136
7 Factors	108744	108747	3	110519	110520	1
8 Factors	87506.1	87509.1	3	88927.1	88928.1	1

Then we progressed the 7 and 8-factor solutions for Error Estimation (EE) statistical analysis, starting with Bootstrap (BS) to evaluate the stability and reproducibility of the identified factors, where 100 BS runs were performed. The correlation of bootstrap factors to base model factors explains the consistency of the solution during resampling, an essential criterion for assessing the robustness of the factor structure.

In the seven-factor solution, all bootstrap factors correlated distinctly and solely with their respective base factors, where every bootstrap factor mapped 100% to one base factor (with the exception of Boot Factor 5, which mapped 98% to Factor 5 and had 1% cross-mapping to Factors 1 and 3) as presented in Figure 2-16 (a), with no unmapped factor at all. The great stability of the seven-factor solutions under data perturbation suggested by this clear and unambiguous one-to-one mapping across all factors, indicates that this solution is a resilient and interpretable PMF solution as it has a consistent factor structure that is insensitive to slight variations in the input data.

In contrast, the 8-factor solution demonstrated relatively high degree of instability, as Boot Factor 1 was mapped between Factor 1 (78%) and Factor 6 (22%) as shown in Figure 2-16 (b), suggesting that some degree of factor ambiguity or overlap may exist, which indicates that this solution does not have consistent factor structure and it is sensitive to slight variations in the input data, and therefore the 8-factor solution was considered statistically not robust and was not considered (Fan et al., 2021).

a

```
Base model run number:          12
Number of bootstrap runs:       100
Bootstrap random seed:          25
Min. Correlation R-Value:       0.6
Number of factors:              7
Extra modeling uncertainty (%): 5


Mapping of bootstrap factors to base factors:

                Base Factor 1   Base Factor 2   Base Factor 3   Base Factor 4   Base Factor 5   Base Factor 6   Base Factor 7        Unmapped
Boot Factor 1           100               0               0               0               0               0               0               0
Boot Factor 2             0             100               0               0               0               0               0               0
Boot Factor 3             0               0             100               0               0               0               0               0
Boot Factor 4             0               0               0             100               0               0               0               0
Boot Factor 5             1               0               1               0              98               0               0               0
Boot Factor 6             0               0               0               0               0             100               0               0
Boot Factor 7             0               0               0               0               0               0             100               0
```

b

```
Base model run number:          14
Number of bootstrap runs:       100
Bootstrap random seed:          25
Min. Correlation R-Value:       0.6
Number of factors:              8
Extra modeling uncertainty (%): 5


Mapping of bootstrap factors to base factors:

                    Factor 1        Factor 2        Factor 3        Factor 4        Factor 5        Factor 6        Factor 7        Factor 8        Unmapped
Boot Factor 1             78               0               0               0               0              22               0               0               0
Boot Factor 2              0             100               0               0               0               0               0               0               0
Boot Factor 3              0               0             100               0               0               0               0               0               0
Boot Factor 4              0               0               0             100               0               0               0               0               0
Boot Factor 5              0               0               0               0             100               0               0               0               0
Boot Factor 6              0               0               0               0               0              99               0               1               0
Boot Factor 7              0               0               0               0               0               0             100               0               0
Boot Factor 8              0               0               0               0               0               0               0             100               0
```

Figure 2-16 Base Model Bootstrap Results. Mapping of bootstrap factors to base factors for the 7-factor PMF solution (a) and 8-factor PMF solution (b).

Additionally, the degree of rotational ambiguity associated with the resolved factor profiles was assessed by conducting the DISP (Displacement Error Estimation) analysis using increasing Q displacement thresholds (Qmax = 4, 8, 15, and 25) on the 7-factor PMF solution, where a successful execution was confirmed by the diagnostic error code being 0 with no factor swaps occurring at any Qmax level and a largest observed Q drop of 0.000, which strongly indicates that the solution lies at or near a global Q-minimum and is not susceptible to alternative rotated solutions, a key marker of solution uniqueness and robustness as presented in Figure *2-17*. As per the PMF guidelines, EPA PMF charts default to dQmax = 4 for routine diagnostics, and dQmax values of 4 and 8 generally produce the most cautious and trustworthy estimates of error boundaries.

The results confirm that there is no evidence of instability or overlapping factor identities observed, even at the highest tested dQmax value (25), providing high confidence in the structural integrity of the factor solution. It is worth mentioning that DISP does not take into consideration random observational errors or inaccurate uncertainty specification, even

though it does capture the implications of rotational ambiguity. Therefore, poorly defined uncertainty estimates may appear artificially wide if uncertainty estimates are poorly defined, especially for weak or down-weighted species. However, the lack of swaps and 0% Q-reduction across all examined displacements in this study confirms that the chosen 7-factor solution is well-resolved, distinctly characterised, and appropriate for source interpretation of our ambient VOC data.

Finally, the EPA PMF 5.0 error estimation concentration summary for the seven-factor solution explains the uncertainty limits regarding species contributions to each factor, where both DISP (which accounts for rotational ambiguity) and bootstrap (which accounts for random sample variability) are used to calculate these uncertainty intervals, in which a comparison of these two methods across factors reveals important differences in source profile stability. As illustrated in Figure 2-17 the DISP-derived error bounds are more consistent and narrower for all seven factors, which is consistent with the limited rotational behaviour that has been verified by earlier diagnostics, while bootstrap intervals are generally wider, especially for species with minimal contributions or those associated with several factors such as ethane due to its long atmospheric life time and variety of its atmospheric sources (Simpson et al., 2012) indicating random variability in the input data (Norris & Bai, 2014).

However, this analysis highlights the robustness and interpretability of the 7-factor PMF solution for this VOC source apportionment study by confirming that, even though data-driven variability may introduce greater uncertainty for specific species, the 7-factor solution is still well-constrained under both rotational and sampling variability.

The impact of outliers on the optimal 7-factor PMF solution was also assessed by analysing the difference between Q(True) and Q(Robust) in a representative run (Run 12), where the Q(Robust) was 108,744 and Q(True) was 110,520. This low difference with Q(robust) only 1.6% lower than the Q(true) suggests that only a few outlier points with excessively large residuals had an impact on the Q-value, and the robust algorithm performed effectively, limiting the influence of outliers without changing the main structure of the solution (Brown et al., 2015).

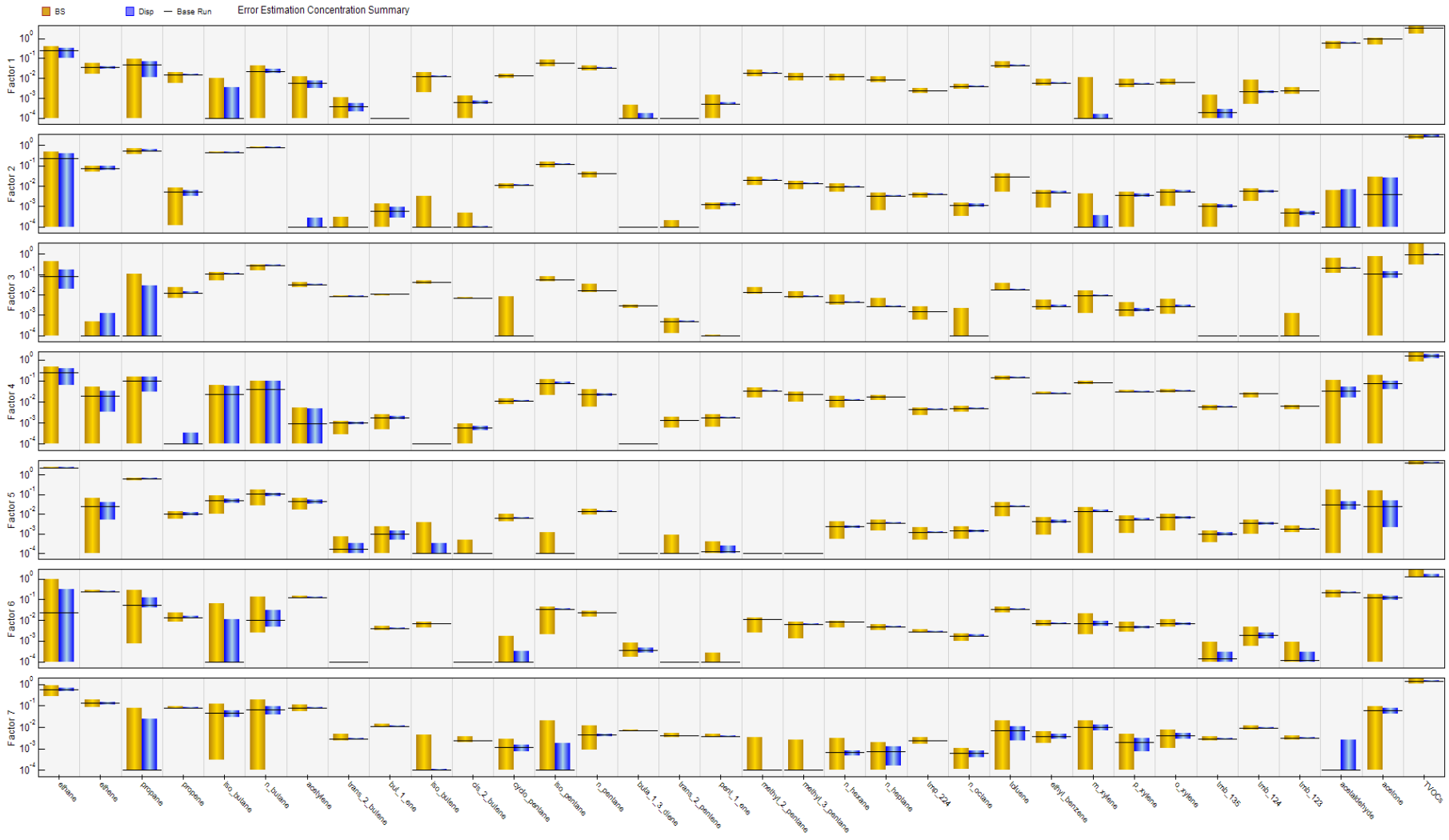

Figure 2-17 Error Estimation Concentration Summary for all seven PMF factors (Run 12). The figure presents the uncertainty ranges of species concentrations for each factor, derived from Bootstrap (BS, yellow bars) and DISP (blue bars) analyses. Black horizontal lines represent base run estimates. DISP intervals reflect rotational ambiguity, while BS intervals represent random sampling uncertainty.

2.4.2 Sources Profiles

The statistical robustness of the PMF solution as described in 2.4.1 (Statistical Selection of PMF Optimal Factors Number) was combined with chemical compositions of factors profile to confirm the interpretability of the PMF solution. Three supplementary PMF output matrices were analysed to assess the interpretability of the resolved factors: species concentrations, the percentage of each species allocated to each factor (% of species sum), and the contribution of each species to the total factor mixing ratio (% of total variable). Furthermore, factor profiles were compared to existing VOC source apportionment studies, including Positive Matrix Factorisation (PMF) and tracer-based evaluations (Arsene et al., 2009; Borbon et al., 2002; Borlaza-Lacoste et al., 2024; Kumar et al., 2020; Li et al., 2022; C. Liu et al., 2017; Su et al., 2019; Ulbrich et al., 2008; Yuan et al., 2012; Zhao et al., 2020; Zheng et al., 2019). These studies investigated VOC sources in a range of urban and suburban environments across Europe, North America, and Asia, identifying common emission sources; traffic exhaust, fuel evaporation, solvent use, industrial emissions, and biogenic sources based on characteristic chemical tracers. Comparison with these published factor profiles and tracer relationships helped to ensure that sources were both contextually suitable and chemically reasonable. This multiapproach method made it possible to identify the sources of VOC emissions that contribute to the urban background environment of London in a reliable and literature-informed manner.

In addition to the chemical interpretation of factor profiles, the temporal variation of source contributions was examined. In PMF, the source contribution represents the model-estimated concentration of VOCs assigned to each resolved source factor at a given time period, expressed in ppb as shown in Figure 2-19. Analysing the temporal behaviour of these contributions helps to assess the identified sources seasonal and episodic patterns, providing additional details that improve the interpretation confidence of the PMF factors.

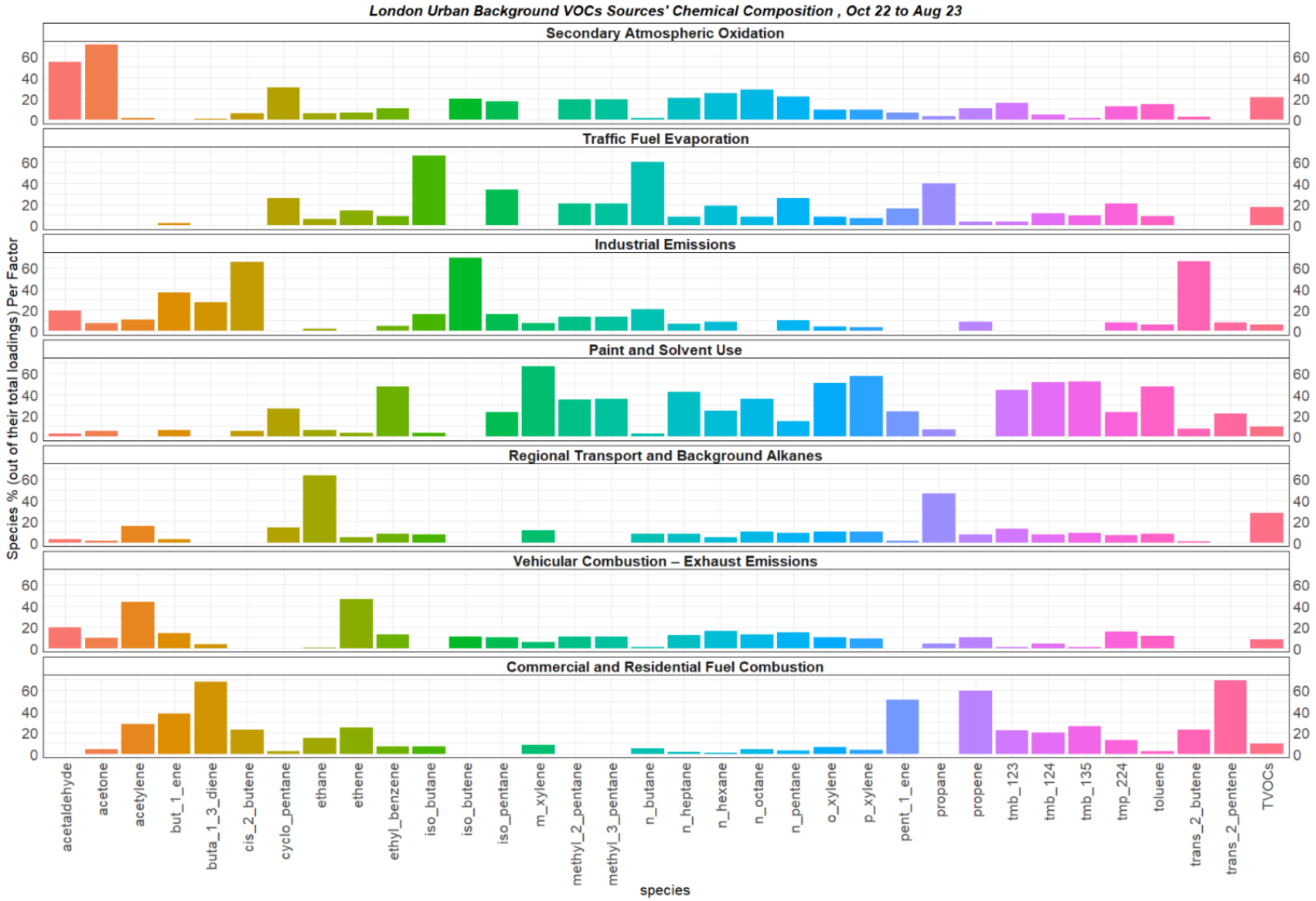

Figure 2-18 Chemical profiles of VOC sources identified by Positive Matrix Factorisation (PMF) at a London urban background site (October 2022 – August 2023). Bar plots show the percentage contribution of each individual VOC species to each resolved source factor.

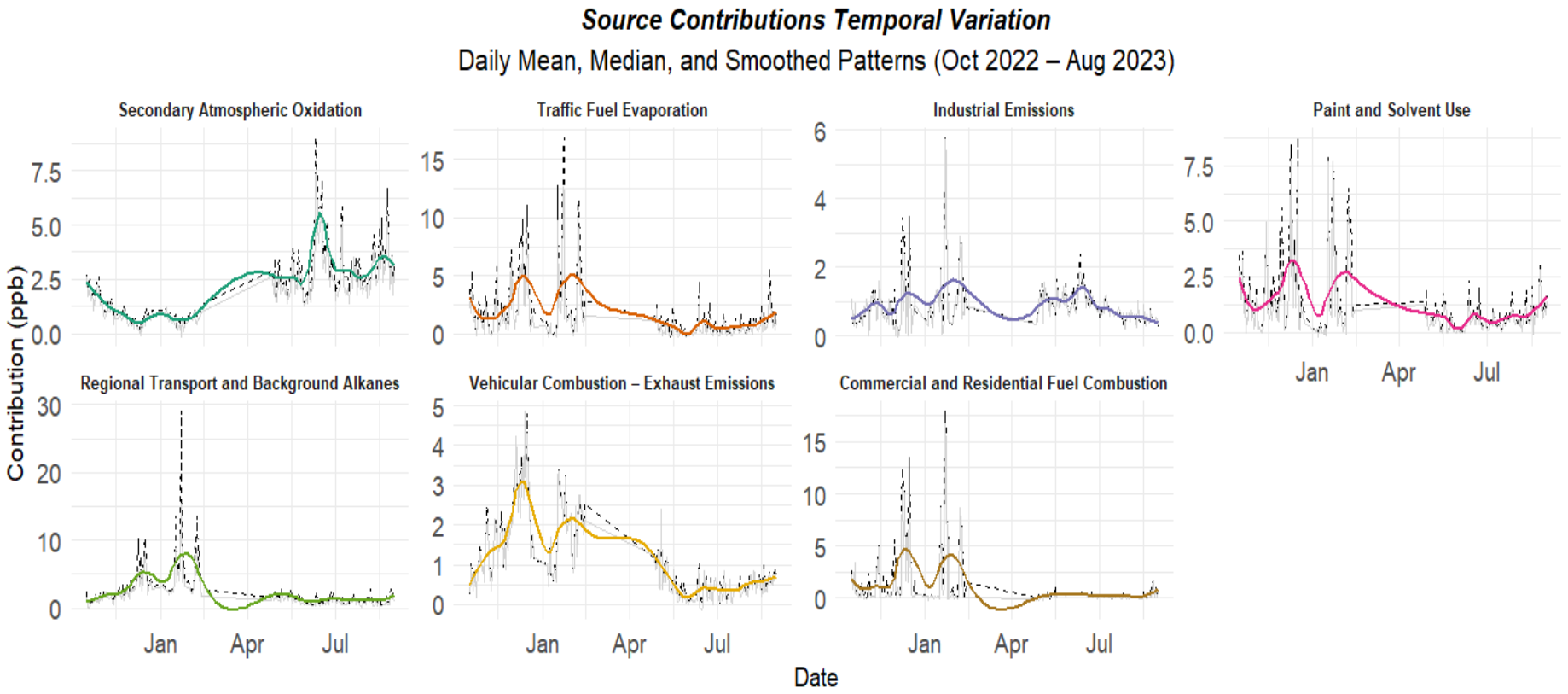

Figure 2-19 VOC source contributions' temporal variation at the London urban background site between October 2022 and August 2023. Dashed black lines represent the daily mean maxing ratio, the solid light grey lines show the daily median maxing ratio. both aggregated from ~1.2-hourly time-resolved data. Coloured bold lines smoothed trends (span = 0.2).

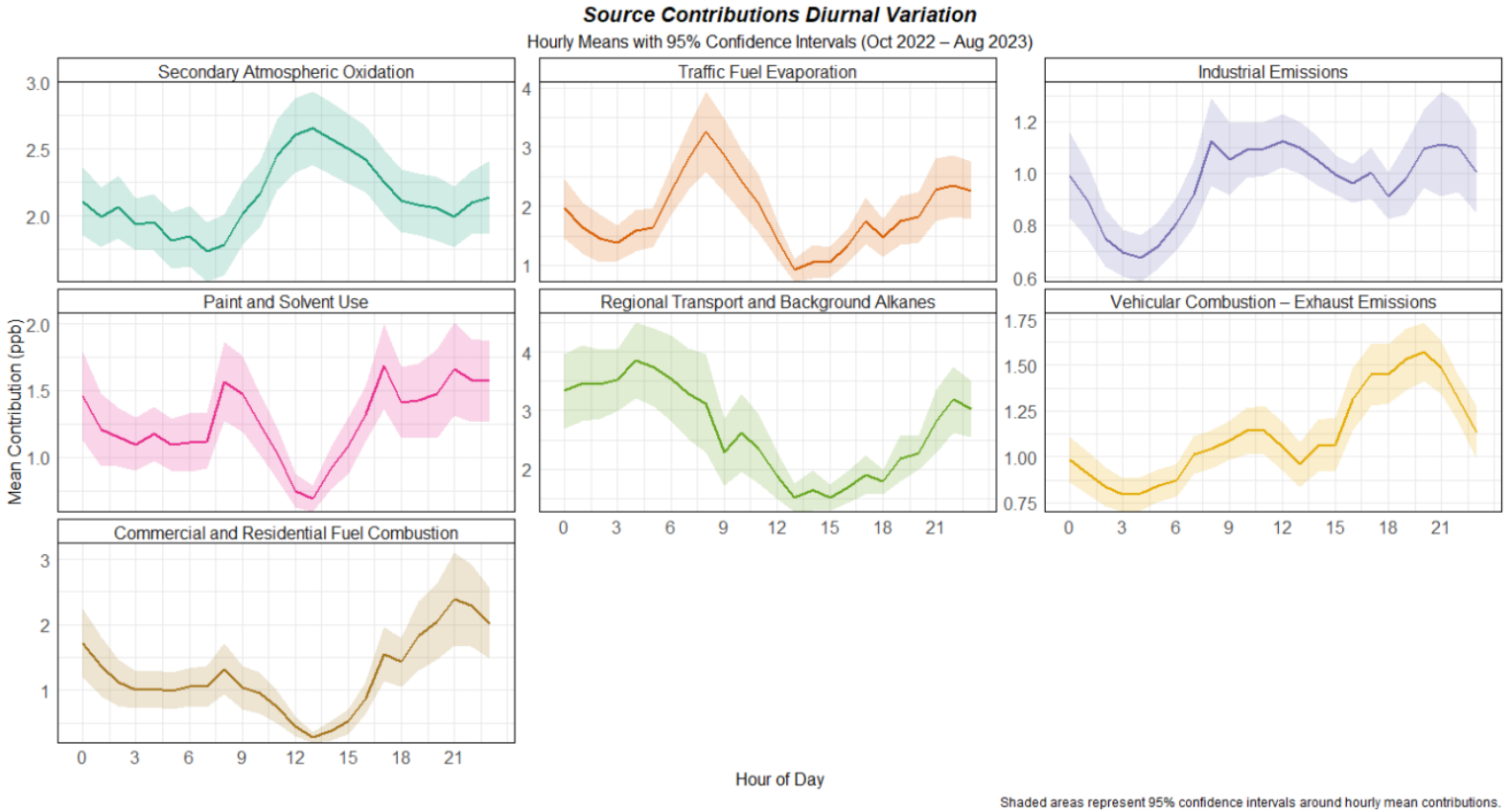

Figure 2-20 VOC source contributions diurnal variation at the London urban background site, averaged by hour across the entire study period (October 2022 to August 2023). Solid coloured lines represent the hourly mean contribution for each factor; shaded ribbons show the 95% confidence intervals around the mean.

CPF – Secondary Atmospheric Oxidation

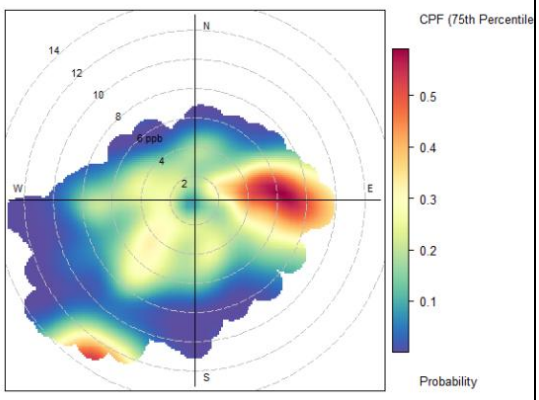

CPF at the 75th percentile (=2.9)

CPF – Traffic Fuel Evaporation

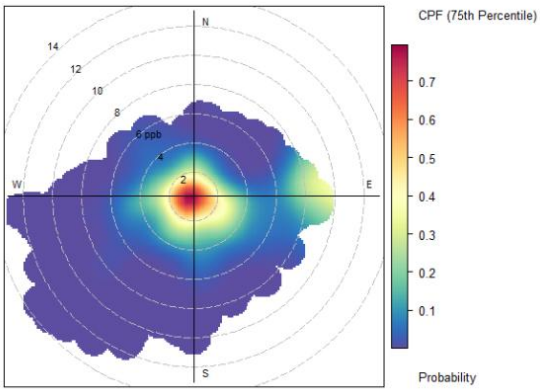

CPF at the 75th percentile (=1.9)

CPF – Industrial Emissions

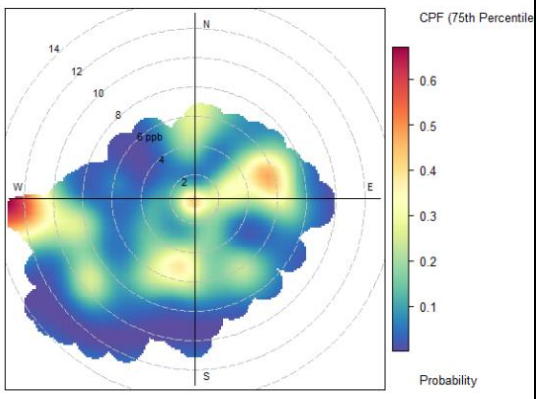

CPF at the 75th percentile (=1.1)

CPF – Paint and Solvent Use

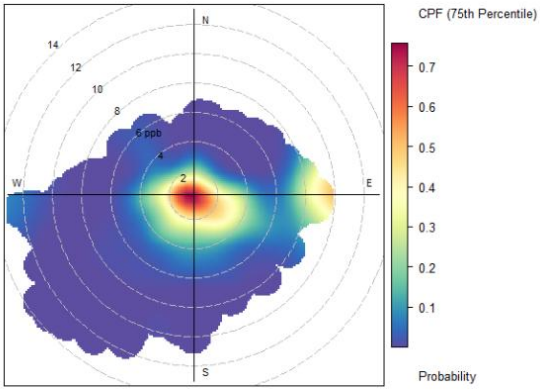

CPF at the 75th percentile (=1.3)

CPF – Regional Transport and Background Alkanes

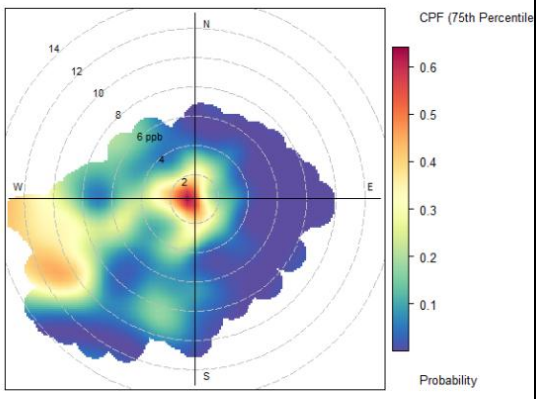

CPF at the 75th percentile (=3)

CPF – Vehicular Combustion – Exhaust Emissions

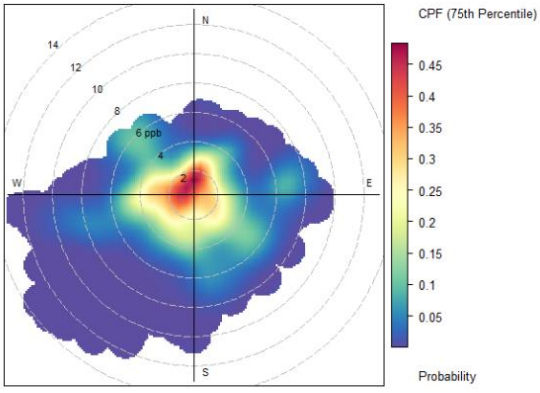

CPF at the 75th percentile (=1.7)

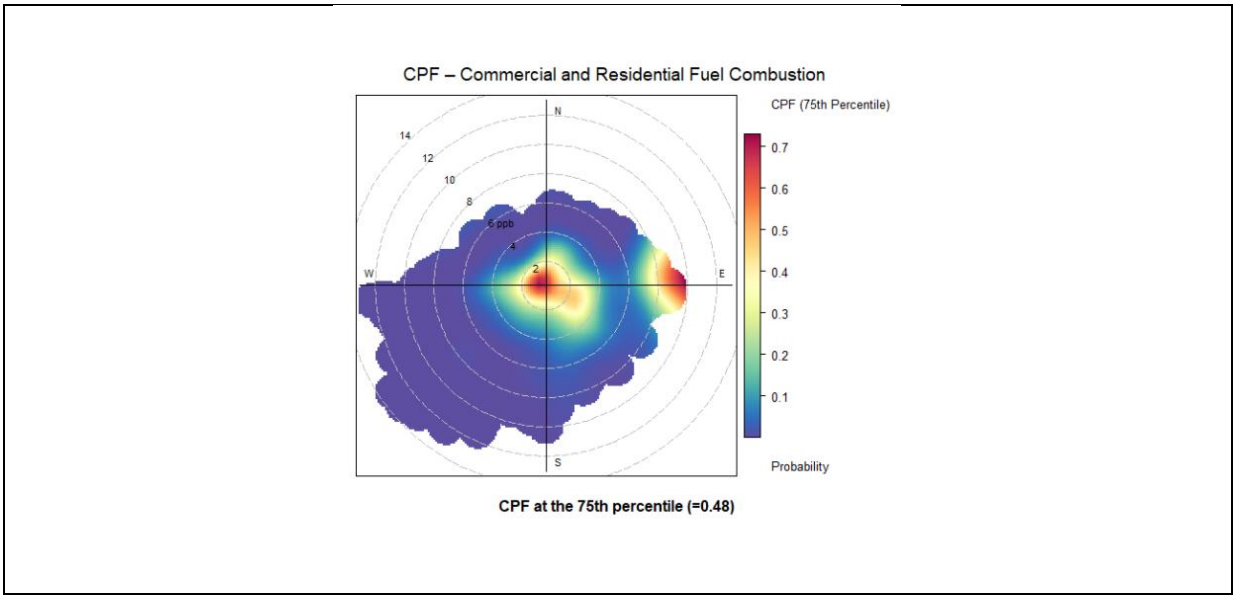

Figure 2-21 Conditional Probability Function (CPF) plots for 7 factor contributions identified by the PMF model. Each plot shows the CPF calculated for the 75th percentile occurring from specific wind directions and speeds.

Factor 1 (Secondary Atmospheric Oxidation)

Factor 1 is defined by significant contributions from oxygenated volatile organic compounds (OVOCs) particularly, acetone and acetaldehyde. These two species account for about 70% and 55% of their total ambient mixing ratios in this factor as shown in Figure 2-18, and comprise a significant fraction of the overall factor mixing ratio, distinguishing Factor 1 from the other six factors. These two species are well established as secondary products of atmospheric photochemistry through the photochemical degradation of anthropogenic and biogenic VOC precursors such as ethanol, isobutane, alkenes, and isoprene, under high NOx and solar radiation conditions (Millet et al., 2010; Seinfeld & Pandis, 2016; H. Singh et al., 1994) with acetaldehyde mainly formed through the atmospheric oxidation of primary anthropogenic precursors (Russo et al., 2010; Sommariva et al., 2011), in addition to its direct emissions from ethanol-blended fuelled vehicle exhaust (Mellouki et al., 2015), while acetone has equally important secondary and primary anthropogenic origins (Fischer et al., 2012; Yáñez-Serrano et al., 2016) in urban areas. These two OVOC species have relatively different atmospheric lifetime, with acetone lifetime ranging from 15 to 20 days while acetaldehyde has a relatively shorter lifespan of up to one day (Atkinson, 2000b; Jacob et al., 2002), which enable them to accumulate at regional scales and, following significant atmospheric processing, build up in urban environments like London, not only from local emissions but also due to their persistence in regionally aged air masses. Hence this source can be linked to regionally aged air masses.

Factor 1 designation as a secondary atmospheric oxidation source is further supported by its clear seasonal and distinct diurnal patterns, which are consistent with these mechanistic routes. As illustrated in Figure 2-19, the seasonal trend in Factor 1 contribution shows a consistent rise from early spring to hit its peak in summer, especially in June and July, this then followed by a gradual decrease until autumn, which is a direct result of increased photochemical activity in warmer months due to longer daylight hours, increase in temperatures, and higher solar radiation levels which expedite photochemical processes. The increase in precursor availability, greater biogenic emissions, and more effective photochemical oxidation, all combined enhance the oxidation of VOC precursors and the generation of OVOCs like acetone and acetaldehyde (Atkinson, 2000b; Jacob et al., 2002; Millet et al., 2010; H. Singh et al., 1994). In addition to being higher in the summer, Factor 1

showed several episodic peaks at times of high photochemical activity indicating a rapid in situ oxidation of VOC precursors under favourable meteorological conditions, as confirmed by the smooth trend shown in Figure *2-19*.

Additional evidence for photochemical influence is demonstrated by the diurnal cycle of Factor 1, as presented in Figure 2-20, The early morning hours (04:00–08:00) have the lowest contributions, which then rapidly increased until reaching a peak at 13:00 local time, which corresponds with the increase in the height of the boundary layer, solar irradiation, and availability of OH radicals (L. Liu et al., 2022). This midday peak, which has been noted in urban settings, is typical of OVOCs that are produced photochemically (Millet et al., 2010; H. Zheng et al., 2018). Following its peak, the contribution slowly decreases over the evening and early night, consistent with declining photochemical activity and potential loss through oxidation and deposition, suggesting a low and stable background level of OVOCs.

Finally, the origin of air masses linked to this factor can be analysed spatially from the Conditional Probability Function (CPF) plot at the 75th percentile threshold (2.9 ppb) illustrated in Figure 2-21. The highest CPF probabilities (>0.5) were observed for winds from the east to southeast sectors, particularly at moderate wind speeds of 3 to 6 m/s, suggesting the transport of photochemically aged air masses from more distant upwind regions toward the monitoring site. However, a secondary spot of elevated CPF values also emerges from the southwest associated with high wind speed between 12 to 14 m/s, suggesting that this factor is influenced by a number of transport channels, including air masses that pass over sub-urban and semi-rural areas southwest of the city, in which a combination of atmospheric oxidation and anthropogenic and biogenic precursor emissions may raise OVOC levels in certain areas.

The complex nature of such overlapping source processes emphasises the importance of PMF analysis in separating the contributions of various source areas and mechanisms, particularly for multifunctional secondary species like acetone and acetaldehyde. In contrast to time-series analysis by itself, which is typically unable to distinguish between sources due to concurrent temporal profiles, PMF is capable of unravelling mixed-source contributions and achieving more accurate assignment of observed concentrations to both primary and secondary sources.

Based on its chemical composition, atmospheric lifetimes, diurnal and temporal patterns, and conditional probability function, Factor 1 is confidently assigned to secondary atmospheric oxidation source that represents regional photochemical processing of VOCs.

Factor 2 (Traffic Fuel Evaporation)

The main chemical composition of Factor 2, as presented in Figure 2-18, are light alkanes which are commonly identified as important tracers of traffic related fuel evaporative sources (Borlaza-Lacoste et al., 2024; Salameh et al., 2016; Xue et al., 2017), since petrol consists of high concentrations of C_4 and C_5 alkanes, particularly isopentane (Y. Liu et al., 2008; Xue et al., 2017). This factor contains light alkanes includes isobutane at about 66% of its total amount across the 7 factors, n-butane, which is a key tracer for gasoline use in urban areas as the gasoline evaporative is its major source in such environments (Tiwari et al., 2010), at almost 60% of its total amount. Propane and iso-pentane contribution in this factor was about 39% and 34% respectively, both are key tracers for petrol powered vehicles and evaporative emissions (Huang & Hsieh, 2019; Kumar et al., 2020). All the above-mentioned VOCs have been well identified as unburned evaporative gasoline emissions (Arsene et al., 2009), where these compounds are usually emitted by gasoline-powered vehicles through non-combustion pathways such as refuelling losses, diurnal tank breathing, engine hot soak, and running losses (Pandit et al., 2011). Additionally, this factor contained a small fraction of 2/3methyl-pentanes at 20% each. It is worth mentioning that iso/n butane and iso/n-pentane can also be emitted from non-aerosol personal care products (PCPs) (Yeoman & Lewis, 2021), however, their association with fossil fuel related tracers such as 2- and 3-methylpentane provides clear evidence that the dominant source of these compounds in this factor is gasoline evaporation.

With a contribution reaching its peak between December and March, Factor 2's seasonal trend, shown in Figure 2-19, reveals an unexpected wintertime enhancement. Although, evaporative emissions are generally linked to warm seasons due to higher vapour pressure and ambient temperatures, nevertheless, this profile shows how a lower Boundary Layer Height (BLH) and fewer photochemical oxidations during cold seasons can lead to increased VOC concentrations in the atmosphere. This could indicate that the variations in atmospheric BLH have a greater impact than other factors (Rajabi et al., 2020). Under such atmospheric conditions, with negligible vertical dilution and atmospheric dispersion, VOCs emissions are more likely to concentrate near the surface. Similarly, recent PMF study, conducted at a

remote site in Corsica (north-western of Mediterranean Sea), reported the domination of evaporative emissions during autumn and winter (Debevec et al., 2021). Crucially, the persistence of these species aligns with their moderate to long lifetimes in the atmosphere. Assuming average OH radical levels (1×10^6 molecules cm^{-3}), propane has an atmospheric lifetime of around 13 days, n- and isobutane about 2 to 4 days, and iso-pentane about 1-2 days (Atkinson, 2000). This allow them to accumulate significantly in winter months, particularly when photochemical loss pathways are inhibited by decreased solar radiation and OH radical concentrations.

The daily trend, presented in Figure 2-20further supports this interpretation, with limited vertical mixing due to low boundary layer height. Morning rush hour traffic coincides with a noticeable peak about 8:00–10:00, then the factor contribution decreases due to enhanced turbulence and convective mixing during midday period, another but less sharp peak occurred around 20:00 represents both boundary layer reduction and evening traffic emissions. The persistence of prominent levels in the morning and evening, especially throughout the winter, is mainly due to the weather-controlled accumulation of slowly degrading VOCs.

Finally, as illustrated in Figure 2-21, the Conditional Probability Function (CPF) plot at the 75th percentile threshold (1.9 ppb) can be used to investigate the origin of air masses contributing to this factor, where calm wind speed conditions just below 2 m/s, are highly related with a centralised area of maximum probability (CPF > 0.7) in the CPF distribution for Factor 2, which suggests that emissions associated with this factor are mostly local in origin, coming from sources close to the monitoring location, like parked cars experiencing evaporative losses, adjacent petrol stations, or small scale fuel handling facilities. Under low boundary layer height and weak wind dispersion during stagnant conditions, locally emitted VOCs have minimal chance to mix with cleaner background air, and hence, elevated source contribution occurred. This central probability signal is consistent with the temporal and diurnal trends of this factor, which both show increased factor contribution under low boundary layer height and stationary dispersion circumstances.

A secondary region of elevated CP about 0.4 from the east, associated with moderate wind speeds 3 to 5 m/s, is also presented on the CPF plot, which could be a result of additional contributions from commercial gasoline-handling zones or transportation routes east of the site.

Based on its chemical composition, diurnal and temporal patterns, and conditional probability function, Factor 2 is confidently allocated to Traffic Fuel Evaporation source that represents traffic-related evaporative VOCs sources.

Factor 3 (Industrial emissions)

The preponderance of highly reactive alkenes, including iso-butene at just above 69% of its total amount across all factors, trans-2-butene at almost 66%, cis-2-butene at just nearly 66.8%, 1-butene at 36.5% 1,3-butadiene at 27.5%, and about 20% of acetaldehyde is a defining feature of factor 3, as shown Figure 2-18. With a short atmospheric lifetime typically of few hours (Atkinson, 2000b; Baker et al., 2005) these substances are distinctive markers of fresh emissions. Butenes, which are versatile chemical compounds for industrial activities due to their double bond, can be emitted into ambient air from various sources in urban and suburban areas due to the combustion of fossil fuels and emissions from petrol plants and refineries (Kilty & Sachtler, 1974; Lv et al., 2021; TEXAS COMMISSION ON ENVIRONMENTAL QUALITY, 2008). Trans-2-butene and cis-2-butene are two isomers predominantly released to the atmosphere from identical sources (Xue et al., 2020). Additionally, the presence of 1,3-butadiene, a recognised incomplete combustion tracer, further indicates the association with combustion emissions (Hughes, 2001). Finally, and despite its major presence in the secondary atmospheric production (factor1), acetaldehyde (CH_3CHO) can also be emitted directly from a variety of anthropogenic and biogenic sources, with anthropogenic emissions the key source in cities, particularly, stationary combustion and mobile sources (Dunmore et al., 2016; Jailson de Andrade et al., 1998; Luecken et al., 2012). In addition, reactive alkenes like butenes involve in rapid atmospheric oxidation process via reactions with hydroxyl radicals (OH) and ozone (O_3) (Atkinson & Arey, 2003). The ozonolysis of these alkenes cleaves carbon-carbon double bonds, forming of Criegee intermediates, which eventually decompose into various oxygenated volatile organic compounds (OVOCs) like acetaldehyde (Johnson & Marston, 2008). The ozonolysis represents an important atmospheric sink for unsaturated VOCs, as the reaction rate of some alkenes with ozone can be faster than their reaction with OH, particularly under high ozone levels environments or during nighttime (Newland et al., 2022). This means that the acetaldehyde associated with this factor could be also generated from secondary formation via alkene ozonolysis in addition to direct primary emissions.

However, these VOCs are also recognised as key tracers for vehicles tailpipe emissions (Ho, Lee, Ho, Blake, Cheng, Li, Fung, et al., 2009; M. Song et al., 2018).

The seasonal pattern of Factor 3 reveals a clear winter increase from November to February, followed by a gradual decrease during spring and summer as shown in Figure 2-19. Apart from the obvious seasonal cycle, there are a number of episodic increases that occur during the winter, suggesting sporadic but significant release events. The seasonal pattern is mainly due to meteorological condition and atmospheric reactivity. In winter, the accumulation of short-lived VOCs due to lower boundary layer heights and lower OH and O_3 concentrations align with a recent seasonal study in Houston that reported a 20% increase in wintertime VOC concentrations compared to summer, with alkenes being especially high (Sadeghi et al., 2021). However, these key reactive species; iso-butene, 1-butene, and 1,3-butadiene experience a relative drop in their concentrations during summer due to enhanced photochemical oxidation, sinks via ozonolysis and greater atmospheric mixing, which explains the higher seasonal contribution of this source in winter. While the observed peaks might be the result of sporadic emissions from fuel handling, petrochemical processes, or industrial processes involving heating.

As illustrated in Figure 2-20 this source has a diurnal fluctuation, where factor contribution starts to rise dramatically at around 03:00 reaching their highest point between 8:00 and 12:00, and continue to be relatively high into the late morning. Industrial start-up operations or morning shifts at adjacent sites could be the cause of this early spike, while reduced emission rates and enhanced vertical mixing during peak atmospheric dispersion hours are predicted to cause a slow fall from midday to 18:00. A combination of additional operational peaks, nighttime process cycles, or changes in boundary layer dynamics that reduce dilution may be responsible for the factor contribution's slight increase between 18:00 and 21:00. This then followed by a period of lower industrial activity and stable overnight conditions sharp decline after 21:00 occurs reaching its lowest point at approximately 03:00. This diurnal profile does not reflect traffic-related sources that typically exhibit powerful bimodal peaks during commuting hours. In contrast, it appears more compatible with operational or batch-processing emissions, such as those from light manufacturing, airport support operations, or gasoline handling infrastructure. The curve's shape, especially the early morning rise and wide

midday plateau supports the continuous daily emissions pattern with atmospheric buildup controlled by boundary layer dynamics (M. Song et al., 2018).

Factor 3's CPF plot, Figure 2-21, displays a dispersed non-local emission. Under the highest wind speed, the west is the source of the strongest directional signal with CPF just above 0.6, suggesting a substantial emission source upwind of the monitoring site, which is consistent with Heathrow Airport's location, about 25 km to the west of the monitoring site, and the light industrial sectors that surround it, both of which are known to release butenes and other VOCs due to fuel storage, aircraft support services, and chemical handling (An et al., 2014). This is supported by the recently published National Atmospheric Emissions Inventory (NAEI), NMVOC Speciation Information 2025, which considers the industrial activities and aircraft landing and take-off to be key sources for butenes in the UK (Richmond, 2025). The east, southeast, and northwest also show secondary spots with lower CPF values between 0.3–0.4, which may indicate that several industrial areas under various wind regimes contributed to this source. It is further supported by the lack of a strong CPF signal in low wind circumstances that Factor 3 is influenced by dispersed industrial activities related sources rather than by adjacent sources like local traffic.

Based on its chemical composition, diurnal and temporal patterns, and conditional probability function, Factor 3 is confidently allocated to Industrial emissions sources.

Factor 4 (Paint and Solvent emissions)

Factor 4, as shown in Figure 2-18, is distinguished by the significant contributions of aliphatic species and aromatic hydrocarbons, which are generally linked to evaporative solvent emissions. Around 50% of total Trimethylbenzenes (TMBs) mixing ratios present in this factor, 70% of m-xylene, around 50% of p- and o-xylene and 48% of toluene mixing ratios, in addition to a notable contribution from n-heptane that has 42% of its total amount in this factor. These chemicals are extensively recognised as key markers of paint, varnish, adhesive, and solvent usage in both domestic and industrial sectors due to their volatility and solvation properties (An et al., 2014; Chen et al., 2014; Jaimes-Palomera et al., 2016; C. Liu et al., 2017; Mugica et al., 2002). Additionally, n-heptane, generally used in industrial facilities as a solvent and cleaning agent (Xiong et al., 2020; Y. Xu et al., 2021), significant contribution indicates that this factor represents emissions related to solvents from various settings. This fraction of total

mixing ratio attributable to this factor and its overall species-level composition are in line with its assignment to evaporative emissions from solvent and paint sources. It is worth mentioning that traffic related activities, both evaporative and tailpipe emissions, is also a possible source of these species (C. Song et al., 2020; Y. Zhang et al., 2013).

A clear seasonal pattern can be seen in the temporal profile of Factor 4 presented in Figure 2-19, with the biggest contributions taking place between November and February due to reduced boundary layer heights (BLH) and limited atmospheric chemistry promote the buildup of semi-volatile evaporative emissions which is reflected in this wintertime enhancement (Debevec et al., 2021; Rajabi et al., 2020). The contributions progressively decline after February, reaching a low point in spring (May), reflecting enhanced atmospheric dispersion conditions. A minor increase in summer may correlate with occasional renovations or industrial activities in the locality of the observatory.

A distinct bimodal structure can be seen in the diurnal pattern of Factor 4 (Figure 2-20) which is possibly due to the cycles of interior ventilation and daily human activities. Early morning operations like cleaning, maintenance, or industrial opening hours, all can lead to the first peak that happens between 8:00 and 9:00, then the contributions progressively drop until midday, reaching its lowest between 11:00 to 15:00, presumably due to increased air mixing which has a negative correlation with pollutant levels (Sangiorgi et al., 2011; K. Zhang et al., 2018). Furthermore, a rapid removal of aromatics with higher chemical reactivity occurs in daytime due to their reactions with hydroxyl radicals (OH) (X. B. Li et al., 2022; C. Wu et al., 2020). A subsequent increase is observed beginning in the middle of the afternoon and peaking at around 17:00, which could be due to a decrease in atmospheric dilution and degradation conditions as paint and solvent emissions continue.

The CPF plot for Factor 4, Figure 2-21, indicates a robust signal associated with calm conditions, wind speed less than 2 m/s, with probability exceeding 0.7, suggesting localised sources of paint and solvent emissions, presumably from indoor or nearby commercial sources. A sustained low-level signal around 0.3 CP is evident under wind speeds of up to 4 m/s from almost all directions, further confirming the prevalence of distributed local sources, such as small-scale domestic renovations and decorating. Furthermore, under 8 to 10 m/s winds, a secondary hotspot appears from the east, with CPF values ranging from 0.5 to 0.6, indicating contributions from farther-off light industrial or commercial sectors.

Based on its chemical composition, diurnal and temporal patterns, and conditional probability function, Factor 4 is identified as Paint and Solvent emissions, representing residential and commercial sources.

Factor 5 (Regional Transport and Background Alkanes)

Ethane and propane, two long-lived, low-reactivity alkanes, dominate Factor 5's chemical composition, as shown in Figure 2-18, accounting for 63% and 46% of the total species loadings within this factor, respectively. Both species can persist at regional to global scales and accumulate in stagnant weather circumstances due to their atmospheric lifespan with ethane lifetime ranging between 20 days in summer and two months in winter as its main sink is reaction with OH radicals, and propane lifespan of 13 days (Derwent et al., 2012; Rudolph & Ehhalt, 1981). The main source of atmospheric ethane. In the UK is fugitive emission from natural gas distribution, while propane is not solely linked to natural gas distribution emissions (AQEG, 2020; Derwent et al., 2017). Additionally, several intermediate-lived hydrocarbons showed minimal contributions to this factor: n-butane and i-butane, along with i-pentane, each contribute around 20% in addition to acetylene, which also contributes about 23% of its total loading to Factor 5. Although these VOCs are moderately represented in this factor, they contribute more significantly to other factors, and their contribution has been ignored due to their negligible contribution compared to ethane and propane.

These relatively low contributions can be explained by the complexity of the urban atmospheric environment, where a variety of spatially distributed and small-scale emission sources including fuel storage or handling activities, micro-scale industrial activities, and household combustion sources, can elevate species with comparatively low average contributions. Therefore, source profiles may overlap or mix in such situations at short spatial and temporal scales, which presents serious challenges for receptor models such as PMF. Consequently, receptor models' results must be analysed in light of the dynamic and fragmented emission landscape that characterises urban environments.

A distinct seasonal cycle can be seen in the temporal variation of Factor 5 shown in Figure 2-19. This source contribution begins to rise in November, peak in January and February, where limited sun exposure during the winter slows the oxidative loss of alkanes by reducing the formation of OH radicals in addition to low winter boundary layer heights that limit

vertical dispersion, which both promote near-surface VOC accumulation, leading to this winter peaks (M. Li et al., 2022; Rajabi et al., 2020). The increase in Natural Gas (NG) use for heating during these cold months also contributes to this factor winter peak. After that the contribution steadily declined until falling to low, stable levels around 1-3 ppb in the summer due to the increase in chemical removal and atmospheric mixing strengthened as a result of the increase in solar intensity and boundary layer depth in summer.

Factor 5's diurnal profile, presented in Figure 2-20reveals high contributions during the night and early morning (00:00–07:00), peaking between 04:00 and 05:00, then there was a steep drop in this source contribution, with a minimum occurring between 13:00 and 15:00. This pattern, which is comparable to the seasonal dynamics previously reported, is determined by the daily change in OH radical concentrations and boundary layer height (BLH). Low OH levels and a shallow boundary layer prevent oxidative loss and vertical mixing at night, allowing long-lived alkanes like propane and ethane to build up close to the surface. Following sunrise, solar heating raises the BLH and starts the creation of OH, which improves dispersion and photochemical breakdown (WMO, 2007). This leads to the noted midday reduction in Factor 5 contribution. When taken as a whole, these temporal trends demonstrate that Factor 5 is a background source that is oxidant-limited and regional in nature, influenced by photochemical and climatic conditions rather than local emissions.

The CPF analysis for Factor 5, illustrated in Figure 2-21, identifies two primary characteristics: a centre high-probability area >0.6, and an extensive west to south-westerly region with increased probabilities linked to wind speeds of 10–12 m/s. The centre zone can be explained by the localised natural gas fugitive emissions from natural gas distribution systems, in addition to the overnight accumulation of the VOCs in low wind conditions and a shallow nighttime boundary layer. On the other hand, the west to southwest sector where elevated CPF values were associated with high wind speeds, indicates regional scale transported emissions, and not variability in the urban background. Similar findings were reported in VOCs transmission studies, where emissions associated with fossil fuel combustion and industrial activities produced higher CPF values in specific wind directions, indicating transported emissions (Gilman et al., 2013; Shan et al., 2025). Overall, the CPF indicates that both episodic regional travel and nighttime meteorological conditions have a key impact on Factor 5.

Based on its chemical composition, diurnal and temporal patterns, and conditional probability function, Factor 5 can be confidently identified as Regional Transport and Background Alkanes, mainly from natural gas origin.

Factor 6 (Vehicular Combustion – exhaust emissions)

This factor is dominated by ethene, acetylene and acetaldehyde, those have about 47%, 45%, and 20% of their total loadings within this factor, respectively, as shown in Figure 2-18, These species are highly indicative of direct emissions from internal combustion engines' tailpipes as they are well-known combustion tracers, and all significantly contribute to the overall chemical composition of this factor.

Ethene can be emitted from anthropogenic and biogenic sources in urban environments its dominant source is combustion, particularly from road transport (Toon et al., 2018), where it is mainly produced from combustion engines and has been widely recognised as a tracer for gasoline powered Vehicles (Y. Liu et al., 2008). Ethene has been found to be a major contributor to tailpipe emissions in a number of studies (Gentner et al., 2009, 2013). In addition, several source apportionment studies have identified ethene as a main VOC in traffic-related factors (An et al., 2014; Cai et al., 2010; Chen et al., 2014). Moreover, ethene has also been identified as one of the most prevalent VOCs in real traffic situations using tunnel measurements conducted in Nanjing and Hong Kong (Ho, et al., 2009; Q. Zhang et al., 2018). Due to its relatively short atmospheric lifetime (1–3 days through OH oxidation), ambient ethene levels generally indicate local traffic emissions (Olivella & Solé, 2004).

Unlike ethene, acetylene is primarily emitted by combustion activities and does not have any biogenic, or evaporative sources (Stemmler et al., 2005; Suthawaree et al., 2010). Hence, its atmospheric presence is directly linked to fuel burning, mainly in fuel-rich situations. Consequently, acetylene is broadly considered a reliable traffic emission marker due to its strong correlation with motor vehicle exhaust (Alam et al., 2024; Guicherit, 1997; Jobson et al., 2004). Additionally, acetylene and ethene were reported among of the five most common VOCs emitted from vehicles, according to tunnel-based observations study conducted in the Shing Mun Tunnel in Hong Kong, which again highlight their importance as traffic emission markers (Ho, et al., 2009). Similarly, when defining vehicle exhaust profiles, acetylene is frequently grouped with ethene, and light alkanes as one of the primary markers of mobile

sources in the larger hydrocarbon characterisation of traffic emissions (Araizaga et al., 2009; Q. Zhang et al., 2018). Moreover, the association between ethene and acetylene provides an accurate indicator of emissions from mobile sources (Sagebiel et al., 1996), where the ratio of ethene to acetylene can reveal details about the vehicle's operating conditions, especially whether a catalytic converter is operational, as this ratio under a functioning catalytic converter should be ranging between 1 to 3, with a lower value implying the opposite (Araizaga et al., 2009). The ethene to acetylene ratio in factor 6 was precisely 1.96, associated with negligible contribution of one-ring aromatics, such as 1,2,4 TMB, 1,3,5 TMB, and 1,2,3 TMB, suggesting post-catalyst emissions from warm engines under normal driving conditions (D. D. Huang et al., 2024).

Finally, and despite being primarily linked to secondary atmospheric production (factor1), acetaldehyde (CH_3CHO) can also be emitted directly from a variety of anthropogenic and biogenic sources. Anthropogenic emissions are the key source in cities, particularly, stationary combustion and mobile sources, such as gasoline-powered vehicles that use ethanol-blended fuels (Dunmore et al., 2016; Jailson de Andrade et al., 1998; Luecken et al., 2012). In addition to its secondary role in Factor 1, its notable presence in Factor 6 suggests vehicle emissions.

A clear seasonal pattern is observable in the temporal fluctuations of Factor 6, as illustrated in Figure 2-19, where the contribution from this source increases sharply through November and December with further peak around 2 to 3 ppb in January and February. As already explained in the previous traffic related factors, wintertime peaks are associated with low boundary layer heights and decreased photochemical activity, which encourage the near-surface accumulation of VOCs linked to near surface emission sources. Subsequent to the winter peak, the factor's contribution progressively declines during spring and stabilises at reduced levels about 0.5 ppb throughout the summer months, due to enhanced air mixing and higher photochemical degradation during the warmer months, which dilutes and eliminates VOCs more effectively.

In line with increased vehicle activity and increased evening traffic, Factor 6's diurnal profile Figure 2-20 shows a slow increase starting at 6:00 and a wide peak between 18:00 and 21:00, the higher evening peak is a direct result of the atmospheric persistence of its primary components, acetylene that has a lifetime of two weeks, and ethene that has a shorter but still noteworthy lifetime of about 1.4 days (Atkinson, 2000b; Xiao et al., 2007), which enable

emissions from the morning traffic peak to build up throughout the day and gather with the evening traffic emissions. However, the noon dip, between 12:00 and 15:00, is less noticeable, which could be due to the increased boundary layer mixing in addition to the partial elimination by OH radicals and ozone. The shape of this profile supports the assumption that Factor 6 is a combustion-related source primarily composed of engine vehicle exhaust, with contributions increasing during the day but not rapidly degrading or dispersing.

Under light winds up to 4 m/s almost from all directions, the CPF plot for Factor 6 Figure 2-21 shows a concentrated, nearly uniform signal with high probabilities up to 0.45. This local, spatially distributed emissions are reflected in the broad CPF signal, with wind-speed-limited footprint, which is in line with normal transportation activity in the vicinity of the monitoring station. In contrast to Factor 3, which indicates the effect of arterial corridors or main roads and displays stronger directional signals at high wind speeds, Factor 6's more restricted confined, consistent CPF pattern indicates the presence of adjacent dispersed traffic sources, such as secondary or residential roads. Further evidence that Factor 6 is influenced by background vehicle activity at the urban scale rather than concentrated fresh exhaust plumes carried from a distance comes from the absence of a prevailing wind direction and the highest CPF values under calm to low wind speeds.

Based on its chemical composition, diurnal and temporal patterns, and conditional probability function, Factor 6 can be confidently identified as Vehicular Combustion – exhaust emissions source.

Factor 7 (Commercial and Residential Fuel Combustion)

As shown in Figure 2-18, Factor 7 has high contributions from 1,3-butadiene, 2-pentene, propene, 1-pentene, and 1-butene (68%, 70%, 60%, 51%, and 38% of their total loadings within this factor%, respectively) along with the existence of acetylene, ethene and trimethylbenzenes (TMBs). Together, these species, which are connected to a range of combustion and evaporative sources, provide a profile that is consistent with emissions from combustion activities.

The combustion of petrol and diesel is the main 1,3-butadiene emission source, which has historically been linked to on-road traffic emissions (Dollard et al., 2001). However off-road equipment and stationary combustion sources, also account for a sizable portion of the UK's

1,3-butadiene emissions (NAEI, 2025). Additionally, 1,3-butadiene is also known to be produced by burning wood and biomass (Barrefors & Petersson, 1995; Ye et al., 1998). These activities are usually related to cooking and heating in homes and small businesses (AQEG, 2020).

Propene is a common byproduct of internal combustion processes and has been widely employed as a marker of combustion emissions (An et al., 2014; Cai et al., 2010). Apart from combustion, propene, 1-butene, cis-/trans-2-butene, and 1-pentene can also be release to the atmosphere from fuel evaporation processes that use diesel, petrol, or LPG/NG (Geng et al., 2009). However, butene in general has been linked to industrial combustion sources (Y. Liu et al., 2008). Similarly, 1-butene has also been discovered as a byproduct of combustion processes in industrial environments (Watson et al., 2001) and 36.5 % of 1-butene has been assigned to Industrial emission factor 3 in this study. Acetylene has also been directly associated with fuel burning (Alam et al., 2024; Jobson et al., 2004). All of ethene, propene, acetylene, and isobutene can be used as incomplete combustion markers associated with fuel-burning activities (Gentner et al., 2009, 2013).

Prior research has interpreted the high contribution of cis- and trans-pentenes and butenes in related source profiles as indicative of evaporative emissions (Alam et al., 2024). Nonetheless, the presence of combustion-associated species such as propene and butadiene in Factor7, along with these unsaturated hydrocarbons, raises the prospect of mixed or overlapping origins.

Finally, although not specifically diagnostic, the presence of trimethylbenzenes (TMBs) indicates the possible contribution of aromatic species that could be connected to the composition of fuel or evaporative processes related to combustion sources.

A noticeable seasonal trend can be seen in the temporal profile of Factor 7, Figure 2-19, with peak contributions during colder months (November to March) and a noticeable reduction during the warm months, when contributions are almost to background levels. This factor's seasonality clearly indicates heating-related combustion sources which are more active in colder climates. With wintertime heightened levels are consistent with increased use of solid and liquid fuels for space heating, in conjunction with low vertical mixing height and atmospheric degradation. In contrast, the decline to near-background levels from May to

August indicates a significant drop in heating demand, which is in line with these combustion sources' seasonal operation, associated with enhanced atmospheric degradation and vertical mixing conditions in warmer months. This temporal pattern further sets Factor 7 apart from mobile traffic emissions, which often occur throughout the year, and links it with weather-dependent, periodic combustion activities, which are typical of non-industrial fuel use in buildings and off-road applications.

Factor 7's diurnal pattern presented in Figure 2-20 shows no distinct morning peak, and a steady decline from around 09:00, reaching a minimum between 14:00 and 15:00, followed by steady raise from early afternoon to a peak between 18:00 and 22:00, which is incompatible with emissions linked to traffic activities and points to a non-road fuel combustion source, like the burning of fuel in fixed off-road machinery or heating systems in homes or businesses. With a strong evening increase and lack of a morning peak could be due to building usage or heating during the colder hours. This diurnal pattern points to non-traffic combustion activities, rather than mobile emission sources, as the main contributors to this factor.

Factor 7's CPF plot displays two different high probability hotspots of around 0.7 shown in Figure 2-21. The first is centred under calm wind conditions, suggesting that there is a local source close to the monitoring location. However, the second one is to the east of the site associated with moderate-to-high wind speeds between 8 to10 m/s, suggests contributions from sources located downwind in commercial or mixed-use zones. This regionally oriented signal points to non-road combustion activities, local and transported emissions, potentially linked to commercial fuel burning and residential heating. Similarly, solvent-related, and evaporative emissions factors also showed eastern hotspot which supports the existence of mixed residential-commercial activity in that sector. The significance of the calm-wind hotspot reinforces the evidence for a nearby emission source, typical of residential or small-scale fuel consumption. These findings support the hypothesis that Factor 7 represents non-industrial combustion emissions rather than mobile or industrial point sources.

Based on the chemical composition, temporal, and diurnal trend in addition to the CPF analysis we have been identified this factor as stationary combustion sources mainly from Residential, and Commercial fuel consumption.

2.4.3 Sources Contribution to Total VOCs

The contributions of each VOC factor to the total average ambient VOC mixing ratio in London is illustrated in Figure 2-22. Regional Transport and Background Alkanes (factor 5) accounted for 28% of the total measured VOCs, making it the most abundant over the entire measurement period. This illustrates the impact of aged air masses, regional-scale transport processes in addition to the natural gas fugitive emissions on urban VOC concentrations, especially in the presence of stagnant weather conditions. The second most abundant VOC source was Secondary Atmospheric Oxidation (factor 1), which accounted for 18% of the total measured VOCs, reflecting the substantial importance of atmospheric oxidation and photochemical transformation of primary VOC precursors within the urban atmosphere. Therefore, reflecting the importance of considering both direct emissions and secondary production pathways in any VOC management regulations. On the other hand, anthropogenic sources in the vicinity of the monitoring site were also crucial, where the traffic fuel evaporation emissions from vehicle refuelling, diurnal evaporation, and fugitive losses from fuel systems accounted for about 19% of the total VOCs mixing ratio. Paint and Solvent Emissions, which include contributions from the use of solvents in homes, businesses, and industries, accounted for 9 %, which is aligned with the extensive use of VOC-containing products in urban settings.

Similarly, commercial, and residential fuel combustion accounted for 9 % of the overall observed VOC mixing ratio, which comprises combustion emissions from space heating, and small-scale fuel burning. These emissions are particularly significant during colder months and in urban areas with a high residential building density.

Industrial emissions accounted for 9% of the total VOCs mixing ratio, this relatively small contribution, generally includes both point and fugitive emissions from smaller-scale industrial operations spread around the city.

The contribution from vehicular combustion-exhaust emissions, including both petrol and diesel cars running under a variety of operation conditions throughout the London fleet, was about 8%. Despite being lower than many other sources, reflecting the successful approach of engine control technologies and Ultra Low Emission Zone (ULEZ) by reducing traffic related emissions, it continues to be an important urban VOC contributor, particularly during

congestion or cold-start scenarios. However, it is worth mentioning that collectively traffic related VOCs emissions sources, both vehicular combustion-exhaust emissions and Traffic fuel evaporative, account for 27% of VOC emissions in London's atmosphere.

These findings show that VOCs in London have a complex origin, with significant contributions from both local and regional processes. Consequently, reflecting the need for an integrated approach to air quality management strategies that tackles not just vehicle and solvent emissions, but also residential combustion and transboundary pollution. This is further supported by the near equivalence between background/secondary sources and primary anthropogenic emissions.

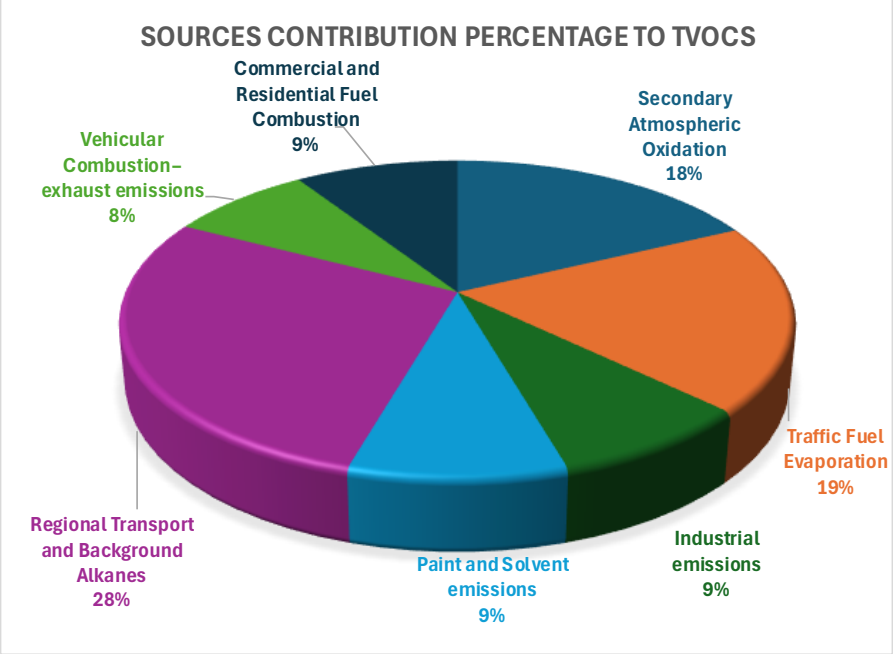

Figure 2-22 Relative contributions of the seven PMF-resolved VOCs source to total measured VOC mixing ratio over the entire measurement period at the London urban background site.

2.4.4 Secondary Organic Aerosol Potential (SOAP) of each VOC Sources

The results reveal significant variation in VOCs sources contribution to SOAP in the London background monitoring site. With a SOAP-derived SOA potential of just above 129 µg SOA/m³, Paint and solvent emissions, despite their relatively low contribution to the total VOCs emissions by mixing ratio at just 9%, clearly dominate the total SOAP. This is mainly due to the significantly high SOAP factors of aromatics associated with evaporative solvent use as shown Figure 2-23, specifically aromatics, presented in this source compared to the rest of other sources chemical composition. It is worth mentioning that Paint and solvent source, by

itself, has a higher contribution to the total SOAP, than the rest of the six VOCs sources combined.

Having a SOAP value of about 26.6 µg SOA/m³, secondary atmospheric oxidation source was the second highest contributor, despite the relatively low SOAP factors of its major chemical composition, acetone and acetaldehyde, this was elevated by the high mass concentrations of this factor. The significance of atmospheric processing beyond direct emissions is underscored by its contribution, especially in background conditions where oxidised organics build up and play a leading role in the generation of aerosols. It is worth mentioning that oxygenated VOCs (OVOCs) and SOA are two products of atmospheric oxidation process. Consequently, the SOAP potential of this factor is lower, as part of the oxidation process has already occurred.

Vehicular Combustion - Exhaust Emissions with calculated SOAP about 24.4 µg SOA/m³, and Regional Transport and Background Alkanes with SOAP of 23.4 µg SOA/m³ were the third, and fourth largest contributors to SOAP, respectively. These sources are dominated by alkenes and alkanes, which possess comparatively low relative SOA formation potentials, and therefore, they have low contributions to SOAP compared to solvent-related emissions. Similarly, Traffic Fuel Evaporation source with contribution of exact 18.0 µg SOA/m³, played a relatively minor role in the total SOAP, reflecting the low SOAP factors of its chemical composition.

Lastly, the lowest SOAP contributors were commercial and residential fuel combustion and industrial emissions sources, with values of 14.5 µg SOA/m³ for and 14.3 µg SOA/m³, respectively. These results imply that although these sources release VOCs due to their chemical profiles, and mass emissions values, would not significantly contribute to the total SOAP.

In this study, the identification of aromatics as the dominant contributors to secondary organic aerosol formation was only possible through compound-specific resolution, which facilitated the separation of solvent-related evaporative emissions from combustion and regional background sources. This illustrates the importance of high-resolution VOC speciation in source apportionment and atmospheric reactivity assessments, otherwise the

significant impact of solvent-related emissions on SOAP would be masked within the total VOC burden.

Overall, the findings clearly confirm that the most significant VOC source category for SOA formation in London background environment is evaporative emissions from solvent and paint application, exceeding the combined contribution of all other sources, emphasising the necessity of including solvent-related VOCs in urban air quality management plans, especially in areas where classical combustion sources have already been partially reduced.

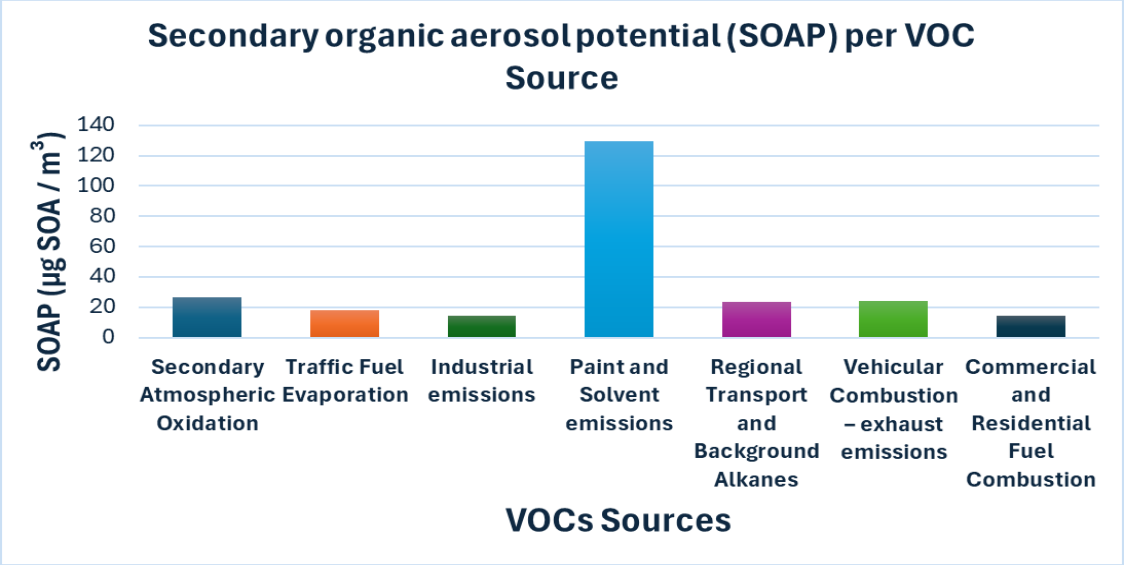

Figure 2-23 Secondary Organic Aerosol Potential (SOAP) per PMF-resolved VOC source over the entire measurement period at the London urban background site.

2.4.5 Ozone Formation Potential (OFP) per VOC Sources

Evaluation of the ozone formation potential (OFP) using PMF-resolved VOC factors offers vital information on the photochemical effects of different emission sources. As illustrated in Figure 2-24 the highest contributor to total OFP, with an estimated value of 12.7 µg O_3/m^3, was the Paint and Solvent source, based on reactivity-weighted concentrations using maximum incremental reactivity (MIR) factors. This is mainly due to highly reactive aromatics, including ethylbenzene, xylenes, and toluene, which possess high MIR coefficients (Carter, 2010). The increased contribution from this source highlights the rising role of non-combustion anthropogenic sources in urban ozone formation. The Secondary atmospheric oxidation source had an OFP value was very close to the Paint and Solvent source, with an overall OFP of just below 12 µg O_3/m^3, dominated by photochemically processed OVOCs particularly, acetone and acetaldehyde which are known to be key ozone precursors and

oxidation products (N. Li et al., 2025; Yan et al., 2024), emphasising the importance of secondary atmospheric oxidation products in local ozone levels formation.

With a contribution of almost 8 μg O_3/m^3 from vehicular combustion and exhaust emissions, the influence of traffic-related pollutants on urban ozone formation is still present, this moderate OFP is consistent with the presence of reactive short-chain alkenes, including acetylene and ethene. Although, vehicles after-treatment technologies and fleet emission improvement have caused exhaust emissions to decrease over time, their photochemical significance is still present (Lewis et al., 2020). The other source of traffic related VOCs emissions, traffic fuel evaporation (Factor 2), had the fourth largest contribution to OFP by 7 μg O_3/m^3. Together, traffic related emissions, tailpipe and fuel evaporative, had the largest contribution to OFP in the studied environment. The OFP values from Industrial Emissions at about 6.9 μg O_3/m^3, and Commercial and Residential Fuel Combustion at 6.2 μg O_3/m^3, were comparable but less significant, mainly due to the low mass concentration of their components.

Interestingly, although being the largest contributor to the total VOCs mixing ratio, Regional Transportation and Background Alkanes had the lowest OFP, measuring just 4.75 μg O_3/m^3. With a chemical profile dominated by long-lived VOCs, which typically have lower reactivity than alkenes or aromatic hydrocarbons (Atkinson, 2000), this explains the minor contribution to OFP from this source.

In metropolitan settings like London, where solvent usage, secondary processes, and local traffic emissions are now the main contributors to OFP, and in order to comply with ozone air quality regulations, future ozone mitigation strategies should prioritise the reduction of reactive non-combustion VOCs emissions.

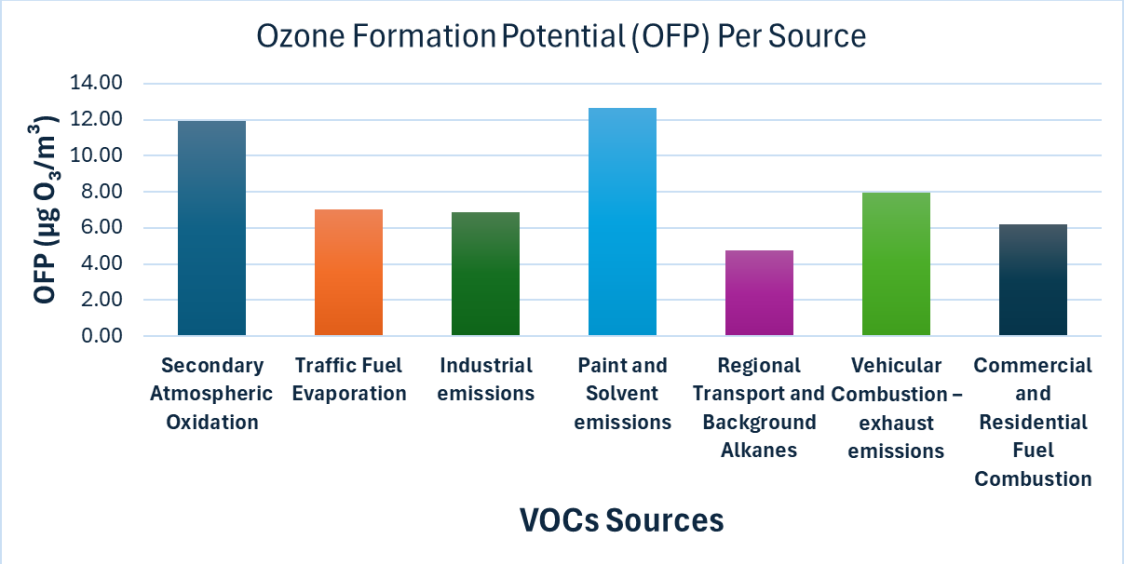

Figure 2-24 Ozone Formation Potential (OFP) per PMF-resolved VOC source over the entire measurement period at the London urban background site.

2.4.6 Research Limitations

Although this study offers a thorough and reliable source apportionment of VOCs at an urban background site in London utilising PMF, it must be noted that this work has some limitations because of instrumental constraints. Firstly, the determination of a specific biogenic emission source was hampered by the unreliable detection of isoprene, as detected isoprene levels did not exhibit a distinct seasonal trend, contrasting with their known emission dynamics that are influenced by temperature and solar radiation and hence this PMF study did not include isoprene data. At the time of writing, work is underway to understand and resolve these limitations. This could be due to calibration gas standard's volatility and possible pre-concentration losses during thermal desorption or chromatographic interference, which led to a notable lack of biogenic emissions source contribution.

Additionally, the model input excluded all of methanol, ethanol, and benzene due to instrumental peak separation issues, as there were overlapping chromatographic peaks that made it difficult to quantify their precise peak areas. Although VOCs sources were still detected using a variety of other specific sources' tracer species, this lack of ethanol, methanol and benzene may have limited the complete representation of oxygenated and aromatic VOCs within their respective source profiles. This illustrates a few drawbacks of using GC-FID techniques for source apportionment studies, as compound-specific resolution

and standard stability are critical for accurate species identification, and consequently for reliable interpretation of source profiles. The anticipated integration of a mass spectrometer into the monitoring system would enhance compound-level resolution, especially for oxygenated and aromatic VOCs, and would address these limitations in future analyses.

Finally, NO_x, a commonly used as tracer of traffic-related emissions (Beevers et al., 2012), and black carbon (BC), a well-established tracer of diesel combustion (Choi et al., 2021), data were measured at the site, but they were not included in the PMF input matrix. The inclusion of these co-emitted tracers could potentially improve source identification and interpretation, mainly for traffic-related sources.

2.5 Conclusion

This work used GC-FID VOCs data obtained from the London Supersite and the U.S. EPA Positive Matrix Factorisation (PMF 5.0) receptor model to provide a thorough source apportionment of VOCs in the background environment of London, where complex interactions between primary anthropogenic, secondary, regional, and local VOC sources in an urban background setting were reflected in the identification and interpretation of a robust seven-factor solution. Regional transportation and background alkanes, secondary atmospheric oxidation, traffic fuel evaporation, vehicle exhaust emissions, industrial emissions, paint and solvent use, and commercial and residential fuel combustion activities were the key sources that have been identified. The seven-factor solution demonstrated high consistency and minimal rotational ambiguity, supporting the interpretation of the source profiles, and was statistically confirmed using advanced error estimation approaches (Bootstrap, DISP, and BS-DISP).

Regional transport and background alkanes, notably ethane and propane, had the largest contribution (28%) to the overall measured VOC mixing ratio on average across the measurement period, highlighting the impact of stable species and transboundary air mass transport. This was followed by the vehicular sources, including traffic fuel evaporation and exhaust, which accounted for 27%, underscoring the persistent importance of road traffic in urban VOC profiles, despite the obvious efficacy of modern emission control measures like exhaust control technologies and the Ultra-Low Emission Zone (ULEZ). Notably, secondary atmospheric oxidation comprised 18%, indicating that photochemically produced VOCs from both biogenic and anthropogenic precursors substantially influence urban background concentrations, especially during the warmer months.

Source-specific evaluation of ozone formation potential (OFP) and secondary organic aerosol potential (SOAP) indicates that emissions linked to solvents had the biggest potential for both SOA and photochemical ozone production. In addition to paint and solvent emissions the other main contributors to SOAP and OFP were the secondary oxidation source, Vehicular exhaust, and traffic fuel evaporative emissions respectively, which indicates a transition from fossil fuel combustion sources to evaporative and secondary sources of urban atmospheric reactivity. The findings suggest that, especially during winter when air dispersion is limited, VOC-related policy measures must consider solvent utilisation, traffic fuel evaporation,

mainly from fuel storage, and home combustion in addition to the applied transportation regulations.

In conclusion, the detection of biogenic emissions and key aromatic and oxygenated VOCs (isoprene, ethanol, methanol, and benzene), was constrained by instrumental limitations. However, we have tried tackle these issues through comprehensive model diagnostics coupled with detailed chemical interpretation, in combination with validation against existing literature, which collectively ensured that this study provides a robust and r reliable source apportionment of VOCs at London's urban background site. These findings are crucial for developing tailored VOC management strategies that mitigate secondary organic aerosol and ozone production in urban settings.

Chapter 3

3 Seasonal Variability and Inter-City Comparison of Volatile Organic Compounds in London and Birmingham

3.1 Introduction

This chapter describes the analysis of VOCs seasonal variability in London 2023 and Birmingham 2022, in addition to inter-site comparisons for summer 2023 and winter 2021–2022. These cities are the two largest urban areas in the UK, both experiencing significant demographic and spatial evolution, and are known for their complex land use patterns, dynamic urban landscapes, and extensive transportation networks, hence, they contribute significantly to the nation's total anthropogenic VOCs emissions. However, because of their varied population, geographic locations, and human activities, they present a valuable case study to investigate how seasonal and spatial factors affect the composition and total concentration of VOCs in two different urban environments.

With the 2022 mid-year estimate (MYE) population of about 8.95 million and 1.6 million in London and Birmingham, respectively, (Birmingham city council, 2024; London Data Store, 2024), these two cities are home to 17.5% of the total England population (ONS, 2024). The elevated urban population contributes, directly and indirectly, to VOC emissions due to higher domestic fuel consumption, and solvent production and utilisation, which are highly positively correlated with the city population and density. Moreover, energy demand for heating and the use of goods that contain VOCs, such as paints, cleaning supplies, and personal hygiene products, is greater in higher population centres, all of which are consider key sources of VOCs emissions in the UK (NAEI, 2024).

About 19.4 billion vehicle miles were driven on London's 9,200 miles of roads in 2024, while 3.66 billion vehicle miles were driven in Birmingham in the same year (Department of Transport, 2025). Together, the 23.06 billion vehicle miles from these two cities accounted for about 8.0% of the 287 billion vehicle miles of road traffic in England in 2024 (Department of Transport, 2025). These traffic statistics highlight the critical role that London and Birmingham play in determining the country's VOCs emission profile and urban air quality dynamics, especially considering the significance of land transport as a source of urban VOC emissions through both exhaust and evaporative fugitive processes.

Non-traffic VOCs sources dominate the VOCs profile in both cities. Volatile Chemical Products (VCPs) , including cleaning agents and personal care products, have become an import VOCs emission source in London (Kelly et al., 2023; Vohra et al., 2021). In addition, commercial

cooking and small-scale activities are also significant emission sources in London due to its high population density compared to other UK cities (Vohra et al., 2021).

In contrast, industrial VOCs emissions in Birmingham dominate its VOCs profile reflecting its higher concentration of manufacturing and point-source emissions (NAEI, 2025). However, the contribution of VOCs emissions from household solvent use, in both cities, are becoming a key emission factor, with alcohols now being the most abundant VOC group in their urban backgrounds (Vohra et al., 2021). Furthermore, London, due to its geographical location, is more exposed to transboundary VOC precursors from continental Europe (28%) compared to Birmingham (16%), where domestic emission sources remain the major influence (Kelly et al., 2023).

The substantially high population density of 10,660, 4,000 and 4,275 residents per square kilometre in inner London, outer London and Birmingham, respectively, compared with England's average population density of 434 residents per square kilometre in 2021 (birmingham city council, 2022; Centre for London, 2023) in addition to the significant vehicle traffic volumes of London and Birmingham, highlight their critical influence on the urban VOC emission profile in the UK. Taking into account London's higher population and more congested traffic, suggests greater anthropogenic emissions than Birmingham.

Therefore, this chapter evaluates the changes in VOCs levels over a year within each city and compares the patterns of VOCs from summer to summer and winter to winter in London and Birmingham by evaluating the seasonal behaviour of ambient VOCs, considering the variations in urban scale, traffic intensity, and geographic location.

3.2 Data and Methods

3.2.1 Site Descriptions

The VOCs data used in this chapter were measured and extracted from the Birmingham Air Quality Supersite (BAQS) and London Honour Oak Park Supersite, two urban background sites in the UK Air Quality Supersite network. This network main aim is to provide high-resolution monitoring of the atmospheric composition in key UK cities. Initially, this project was funded by the Natural Environment Research Council (NERC, part of UKRI) and was then supported by the Department for Environment, Food and Rural Affairs (Defra) and the Environment Agency (University of Birmingham, 2023).

Section 2.3.1 presents a detailed description of the London Honour Oak Park urban background supersite, located within a residential neighbourhood in southeast London and influenced by diverse emission sources including traffic, residential heating, and regional transportation.

Located at the University of Birmingham (52°27'19.8"N, 1°55'44.3"W), the Birmingham Air Quality Supersite (BAQS), part of the West Midlands Air Quality Observatory, is a highly instrumented urban background monitoring station. The site is equipped with a full range of cutting-edge instruments for continuous atmospheric measurement. In addition to VOCs measurements operated by the University of York, particulate matter (mass, number, and size distributions, PM1, PM_4, $PM_{2.5}$ and PM_{10}), gases such as carbon monoxide (CO), nitrogen oxides (NOx), ozone (O_3), sulphur dioxide (SO_2), methane (CH_4), carbon dioxide (CO_2), ammonia (NH_3), reactive nitrogen compounds (NO_y), and meteorological variables (air temperature, humidity, pressure, wind speed and direction, cloud cover and aerosol layer height) are also monitored and measured at this site. This full range of atmospheric measurements allows for the thorough investigation of detailed atmospheric processes, regional atmospheric composition, sources of pollution, and variations in air quality trends, which all have vitally important atmospheric implications. (University of Birmingham, 2023). The geographical setting of the Birmingham Air Quality Supersite (BAQS) is shown in Figure 3-1.

Together, the London and Birmingham supersites facilitate high-quality VOCs measurements for a comparable analysis of VOCs' seasonal variation and diurnal patterns between similar urban environments across two different geographically located cities with different populations and distinct patterns of anthropogenic and biogenic activity.

Figure 3-1 Geographical location of the Birmingham Air Quality Supersite (BAQS), satellite image from Google Earth imagery.

3.2.2 Species Selection and Measurement Method

VOCs measurements at the London and Birmingham urban background supersites were conducted with a heart-cutting dual-column gas chromatograph equipped with flame ionisation detection (GC-FID), as thoroughly explained in Chapter 2, Section 0. High-resolution separation and quantification of a wide range of VOCs and OVOCs, with slightly over one-hour time resolution and parts-per-trillion (ppt) detection limits was achieved by the thermal desorption-based setup. Additionally, the dual-channel arrangement, consisting of non-polar and polar capillary columns, enables the selective identification of alkanes, alkenes, aromatics, and OVOCs, in addition to the heart-cutting process that facilitate the separation of co-eluting species more effectively, especially in complex urban settings.

The best year (year with the most available data) within a site (intra-site) and the best winter and summer, in term of data capture, of the same year between the two sites (inter-site) comparisons were identified by analysing VOC data from the London and Birmingham Supersites for the years 2021 to 2024. Preliminary time series screening was conducted in order to find and eliminate any significant issues with data quality, such as extended or recurring measurement gaps. Additionally, the data capture rate for each species was calculated and evaluated both annually and seasonally in order to determine the best period

of adequate temporal coverage. This procedure eventually informed the selection of specific full years and seasons from specific years that would provide a reliable comparison between locations (urban contrasts) as well as within individual sites (seasonal variation). As a result of this method, the following measured VOCs were excluded from our analysis, and they did not contribute to the total VOCs calculations.

- n-octane, a major gasoline component and is widely used as a tracer of petrol vehicle emissions (Gentner et al., 2017): not measured at the London site (2021 to 2023) and absent in Birmingham (2023 and 2024)
- n-heptane: only measured at the London site in 2024.
- Butanol: not measured at the Birmingham site.
- n-nonane: removed because of consistently poor rates of data capture, even during periods with adequate coverage of most VOCs.

In order to facilitate direct comparison, a list of 32 validated VOC species, which were consistent between the two sites, was employed in the analysis presented in this chapter, as shown in Table 3-1.

Table 3-1 VOCs species by chemical group employed in this chapter analysis.

VOC Group	**Species**
Alkanes	Ethane, Propane, n-Butane, Isobutane, n-Pentane, Isopentane, n-Hexane, Isooctane, cyclopentane, Methyl-2-pentane, Methyl-3-pentane
Alkenes	ethene, propene, But-1-ene, cis-2-Butene, trans-2-Butene, Pent-1-ene, trans-2-Pentene, 1,3-Butadiene, 2-methylpropene
Aromatic Compounds	Benzene, Toluene, Ethylbenzene, m-Xylene, p-Xylene, o-xylene, 1,2,4-Trimethylbenzene (tmb_124), 1,2,3-Trimethylbenzene (tmb_123), 1,3,5-Trimethylbenzene (tmb_135)
Oxygenated VOCs (OVOCs)	Ethanol, Acetone, Acetaldehyde

Additionally, we employed an outlier trimming process based on percentiles for each VOC time series to mitigate the influence of odd values on statistical analysis and data presentation, and this approach also preserves the core distribution of the data. Outliers were identified as values that fell below the first percentile or above the 98.5th percentile and were removed from further analysis by replacing them with missing data (NA). It is worth

mentioning that these percentile values were chosen after a series of trimming calculations and post trimming time series evaluation. By utilizing this trimming technique, we reduced the impact of localised emission spikes and instrumental errors, on the statistical descriptors that include mean, variance, and correlations. Moreover, percentile-based filtering is a common approach in environmental and air quality studies, particularly in pollution concentration trends research and machine learning applications for forecasting air quality (Dash et al., 2023; Dongre et al., 2025).

Following the data screening and trimming processes mentioned above, London 2023 and Birmingham 2022 were chosen for intra-site seasonal variation analysis due to their elevated data capture and representative seasonal coverage, with data coverage of VOCs species ranged between 90.8% and 94.5% in Birmingham 2022 and from 74.9% to 76.3% in London 2023, mainly due to instrumental issues at the London site during March and April. This indicates that these years had fewer data gaps in both the summer and winter seasons. Figure 3-2, and Figure 3-3 present the time series of selected VOC species (ethane, ethanol, acetone, and acetaldehyde) measured at the London supersite (2023), and the Birmingham supersite (2022) using dual GC–FID (about 1.2 hour resolution). These compounds were selected to illustrate the temporal variability of VOC concentrations.

For inter-site comparisons, two specific years were selected. Summer 2023, in which VOC levels in both Birmingham and London were compared during the same photochemically active season (Atkinson, 2000a; Pripdeevech et al., 2025), was chosen due to its high data collection, covering almost all species of interest, with ranges between 97.0% and 99.9% in London and 85.0% and 95.5% in Birmingham. However, London winter 2023 VOCs data coverage was insufficient for winter comparison with Birmingham. Consequently, winter 2021-2022 (December 2021, January, and February 2022), was selected to compare the two cities' wintertime VOC profiles, with the majority of species surpassing 90% data capture in London during this period ranged between 87.8% and 95.2%. Similarly, Birmingham data ranged from 81.5% to 92.2%. This winter coverage is adequate for site-to-site comparison in DJF conditions, when boundary-layer height and photochemistry conditions are generally comparable, and hence reducing, as possible, the effects from meteorological variability on VOC concentrations.

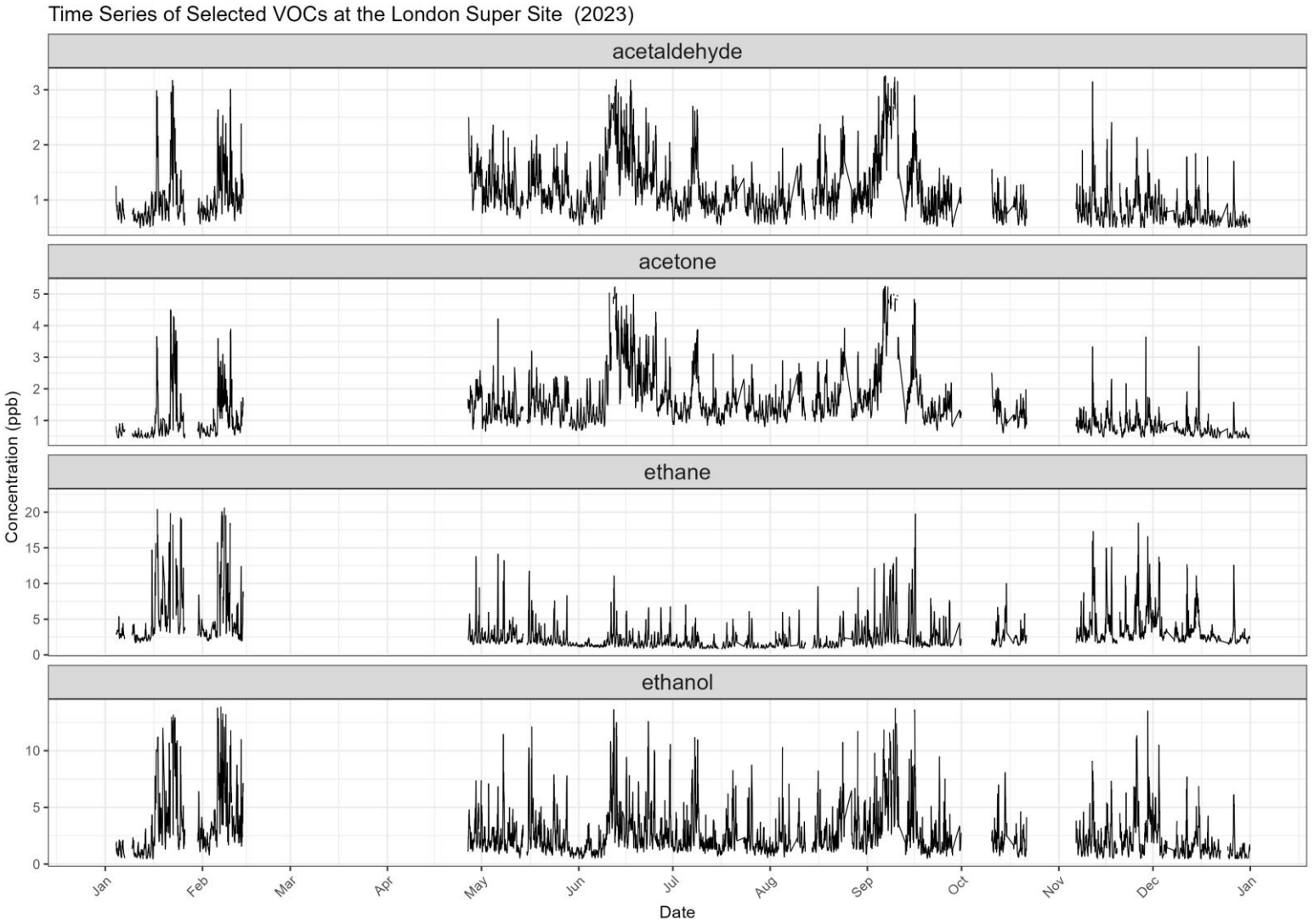

Figure 3-2 Time series of selected VOC species (acetaldehyde, acetone, ethane, and ethanol) measured at the London supersite (2023).

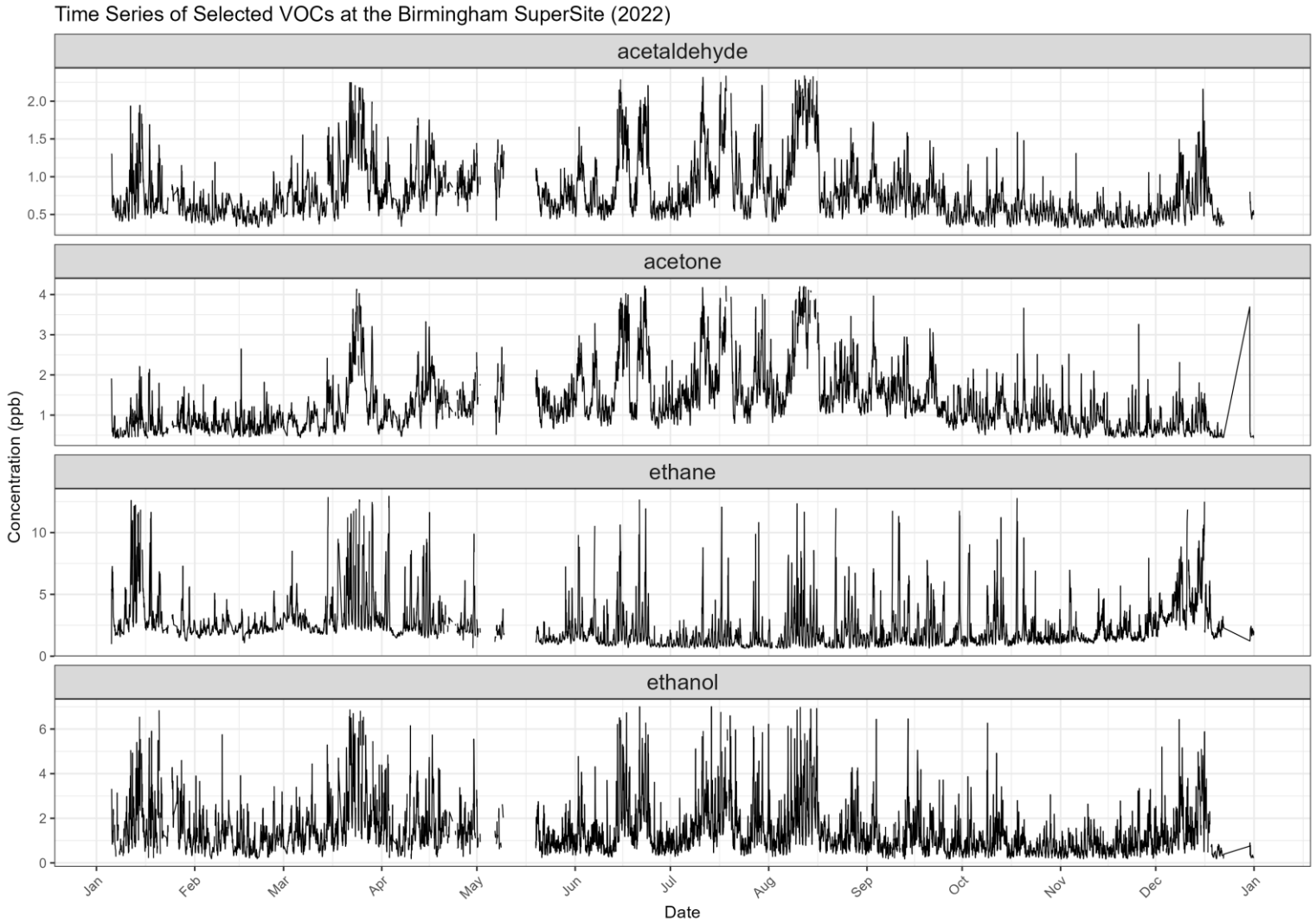

Figure 3-3 Time series of selected VOC species (acetaldehyde, acetone, ethane, and ethanol) measured at the Birmingham supersite (2022).

3.3 Results and Discussion

3.3.1 London 2023 VOCs Seasonality

The results in Table 3-2 present the daily average seasonal (summer and winter) and annual mean +/- standard deviation (SD) mixing ratios of measured VOC species in London 2023, gathered based in their chemical group. It shows that VOCs daily means' average mixing ratios in winter were consistently higher than summer ones for all VOCs chemical groups, except for oxygenated VOCs, with light alkanes and combustion alkene tracers showing the strongest enhancement in their levels. Propane, for example, rose from 0.78 +/- 0.47 ppb in the summer to 1.70 +/- 1.09 ppb in the winter. Likewise, ethane showed a winter mean of 4.37 +/- 2.78 ppb compared to 1.84 +/- 0.67 ppb in the summer. Which was also the case for n-butane, iso-butane, ethene, propene, and acetylene (the only measured alkyne). All of these compounds are directly associated with natural gas leaks, vehicle exhaust and fuel evaporative emissions (AQEG, 2020; Gentner et al., 2013; Stemmler et al., 2005; Tiwari et al., 2010).

In contrast, two of three measured oxygenated VOCs, acetone and acetaldehyde, showed higher daily mean values in summer (1.78 +/- 0.72, 1.20 +/- 0.42 ppb) than in winter (0.85 +/- 0.45, 0.87 +/- 0.30 ppb), respectively, reflecting their stronger influence from secondary photochemical production in warmer months (Fischer et al., 2012; Russo et al., 2010). However, ethanol, the third measured OVOC, showed smaller seasonal differences, with slightly higher winter values, consistent with combustion emissions from ethanol-blended gasoline-powered vehicle exhaust dominating in winter, and evaporative emissions from fuel use and storage which dominating in summer (Dunmore et al., 2016; Florêncio et al., 2024)

Aromatics, specifically toluene and benzene, followed the overall winter enhancement trend, which is consistent with lower photochemical loss rates during colder months when traffic and solvent emissions strongly accumulate (Debevec et al., 2021; Rajabi et al., 2020; Sadeghi et al., 2021).

As shown in Figure 3-4, in terms of the contribution by the chemical group, alkanes dominated London's total observed VOC mixing ratio in 2023, accounting for 49% of the total annual VOCs level based on the sum of daily means' mixing ratio, followed by oxygenated VOCs (OVOCs), which contributed by 38%. Aromatics and alkenes contributed only by 6% and 5% of the annual total VOCs, respectively, whereas acetylene, the only measured alkyne, had the

lowest contribution, at just 2%. However, as presented in Figure 3-5, these contributions varied between winter and summer. Alkanes significantly contributed (by 57%) to total VOCs levels in winter while they only accounted for 39% in summer. In contrast, oxygenated VOCs had the highest contribution, among all groups, in summer (51%), but only 28% in winter. Alkenes, aromatics, and alkynes had higher winter contribution of 6%, 6% and 3%, compared to 4%, 5% and 1% in summer, respectively. Alkanes and OVOCs were the main contributors in summer and winter seasons. The considerable alkanes' contribution during winter, is mainly due to the lower vertical mixing (BLH), and the less photochemical degradation rates, in addition to the increase emissions from their main emission source (NG and traffic) (Derwent et al., 2017; Salameh et al., 2016; Xue et al., 2017). In contrast, the highest contribution of OVOCs during summer, is a direct result of the enhanced photochemical reactions (Jacob et al., 2002; Millet et al., 2010).

As shown in the VOCs daily means' mixing ratio seasonal distributions by chemical group Figure 3-6, alkanes had the highest median and maximum in their distribution during the winter months, while OVOCs had highest median and maximum values in summer. Notably, excluding outliers, the summer alkanes distribution was comparable to the winter OVOCs distribution. Aromatics, alkenes, and alkynes, despite their lower annual contributions, showed distinct winter elevation distribution, compared to their summer levels, this could be mainly due to higher boundary layer hight and enhanced photochemical degradation in summer months (Atkinson, 2000a; Grange et al., 2021).

These distribution results confirm that the observed seasonal contributions are genuine and not driven by extreme values.

Table 3-2 London 2023 Ambient VOCs Levels (daily mean average +/- standard deviation).

Group	VOC	Summer (ppt)	Winter (ppt)	Annual (ppt)
Alkanes	ethane	1835 ± 669	4370 ± 2781	3035 ± 2040
	propane	778 ± 470	1700 ± 1086	1211 ± 897
	n-butane	677 ± 376	1340 ± 1223	1029 ± 867
	isobutane	329 ± 225	746 ± 745	550 ± 526
	isopentane	308 ± 212	354 ± 317	351 ± 280
	n-pentane	134 ± 86	178 ± 134	159 ± 114

Group	VOC	Summer (ppt)	Winter (ppt)	Annual (ppt)
	methyl_2_pentane	83 ± 48	99 ± 84	97 ± 69
	methyl_3_pentane	53 ± 32	65 ± 54	63 ± 46
	n-hexane	47 ± 28	62 ± 46	55 ± 39
	cyclopentane	42 ± 23	44 ± 40	47 ± 32
Alkenes	ethene	243 ± 129	662 ± 492	443 ± 363
	propene	65 ± 33	138 ± 135	97 ± 88
	isobutene	59 ± 22	51 ± 20	54 ± 22
	but_1_ene	14 ± 6	30 ± 26	21 ± 17
	iso-octane	11 ± 7	19 ± 15	16 ± 12
	cis-2-butene	8 ± 3	11 ± 8	9 ± 5
	trans-2-butene	9 ± 4	14 ± 10	11 ± 7
	pent_1_ene	4 ± 4	8 ± 11	6 ± 7
	buta-1,3-diene	4 ± 2	10 ± 12	7 ± 7
	trans-2-pentene	2 ± 4	7 ± 12	4 ± 8
Alkyne	acetylene	122 ± 44	446 ± 260	257 ± 202
Aromatics	toluene	221 ± 118	304 ± 254	273 ± 195
	benzene	131 ± 48	241 ± 113	179 ± 94
	m-xylene	67 ± 38	123 ± 122	88 ± 83
	o-xylene	40 ± 21	65 ± 59	55 ± 44
	p-xylene	35 ± 20	54 ± 50	47 ± 38
	ethylbenzene	35 ± 19	56 ± 50	47 ± 38
	tmb_124	26 ± 18	50 ± 53	40 ± 39
	tmb_123	11 ± 5	15 ± 15	14 ± 10
	tmb_135	5 ± 4	12 ± 14	9 ± 10
Oxygenated	ethanol	2629 ± 1247	2677 ± 2134	2661 ± 1572
	acetone	1779 ± 716	852 ± 454	1418 ± 794
	acetaldehyde	1199 ± 424	871 ± 301	1096 ± 431

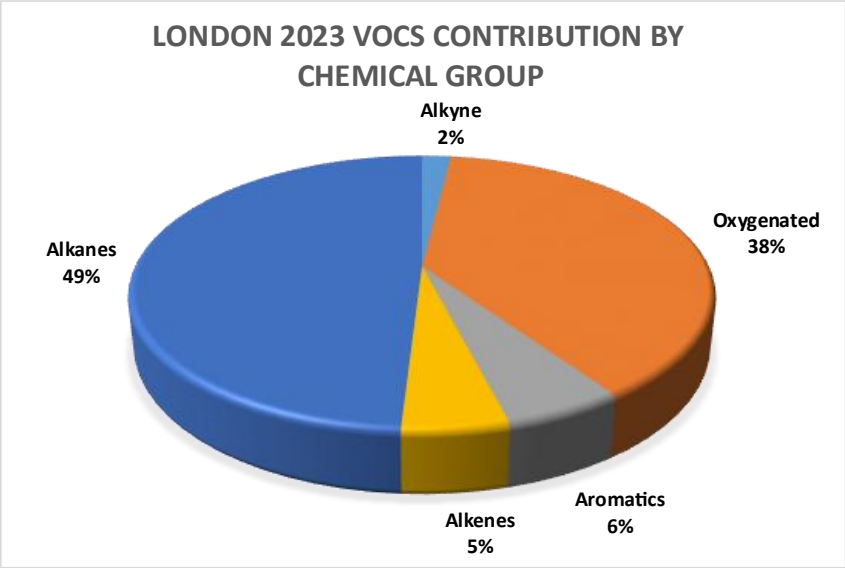

Figure 3-4 VOCs chemical groups contributions to the total VOC mixing ratio (based on the sum of VOCs daily means), London 2023.

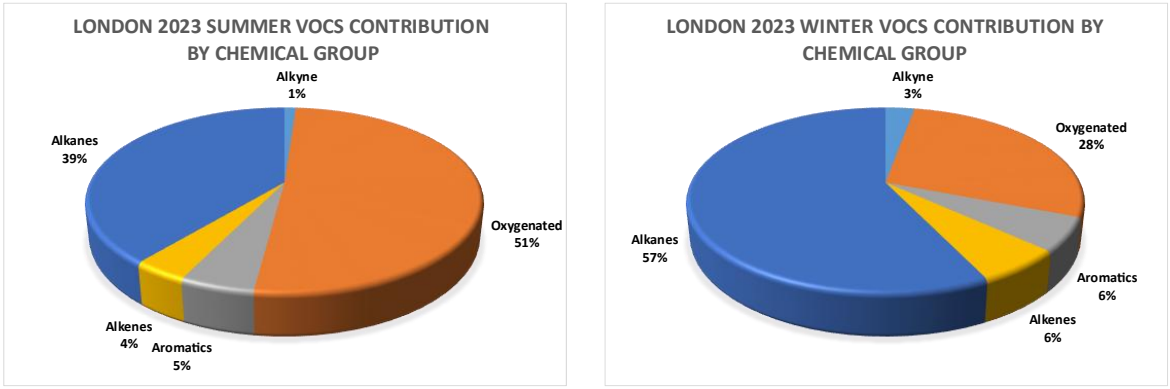

Figure 3-5 Summer and winter VOCs chemical groups contributions to the total VOC mixing ratio (based on the sum of VOCs daily means), Summer (to the left), Winter(to the right), London 2023.

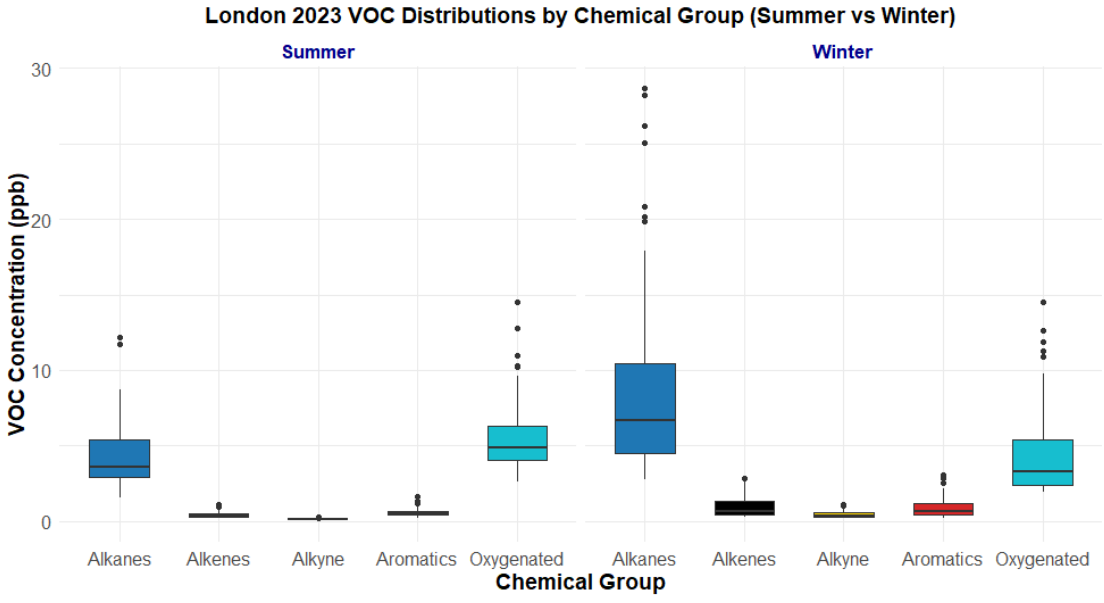

Figure 3-6 Summer vs. Winter VOCs chemical group daily means distributions.

Despite the exclusion of March and April from interpretation due to insufficient data collection, and the missing data for almost half of February and October, these months were analysed cautiously, London's monthly distribution of daily mean total VOC concentrations in 2023 as presented in Figure 3-7, shows a distinct seasonal pattern. Winter months, especially January and February, had the highest concentrations and variability. February recorded the highest VOC concentrations of the year, in terms of mean, median, and all quartiles, with a median and mean concentration of about 18ppb and 22ppb, respectively, and a maximum TVOCs daily mean concentration of about 46 ppb. Similarly, January showed higher levels with a wider range of daily mixing ratios, but marginally lower than February. The winter high concentration is a direct result of the combined effects of cold-season meteorology that decreases air dispersion, and increased emissions from heating sources and vehicle exhausts, which collectively contribute to pollutant accumulation (Rajabi et al., 2020). Moreover, as shown in Figure 3-8, this seasonal accumulation is mostly driven by dramatic rises in alkane concentrations, which were accompanied by noticeable increases in some oxygenated volatile organic compounds. The overall VOC mixing ratio was further increased by the relatively higher levels, compared to their levels across the entire year, of aromatics, alkynes, and alkenes during these winter peaks. With TVOCs medians of approximately 15 and 14 ppb and means of 18 and 15 ppb associating with broad interquartile ranges, a secondary peak in was noted in September and November, where elevated concentration of both alkanes and OVOCs, along with relatively high aromatics levels contributed to the September peak, as illustrated in Figure 3-8.

Conversely, late spring to summer, May to August, exhibited decreased and more consistent concentrations with monthly medians of total observed VOCs mixing ratio between 8 and 12 ppb, reflecting stronger air mixing and enhanced photochemical degradation (Seinfeld & Pandis, 2016b; H. B. Singh et al., 1994), where the chemical group time series showed in Figure 3-8 indicates that this seasonal minimum was influenced by relatively reduced concentrations of alkanes and oxygenated VOCs, despite a peak of OVOCs in the mid of June, similar to the September one. Additionally, alkynes, alkenes, and aromatics all continued to be present in relatively low concentrations in this season compared to their levels over the rest of the year.

Oddly, December concentrations were notably lower than the September and November values, with December TVOCs mixing ratios' distributions comparable to those in summer

months, this could be due to the minimal contribution from oxygenated VOCs under the lack of sunlight (X. B. Li et al., 2022) during this month in combination with meteorological conditions, mainly wind speed, favouring greater dispersion of emitted VOCs (Rajabi et al., 2020). Data obtained from London Heathrow meteorological station confirmed that December 2023 mean and median wind speed were higher than November and September as shown in Table-3-3 (Defra, 2024). Figure 3-9 shows the monthly Windrose for London Heathrow Airport in 2023, illustrating the frequency distribution of hourly wind direction and wind speed. The radial bars represent the percentage of time the wind originates from each directional sector, while the colours indicate different wind speed classes (m s^{-1}).

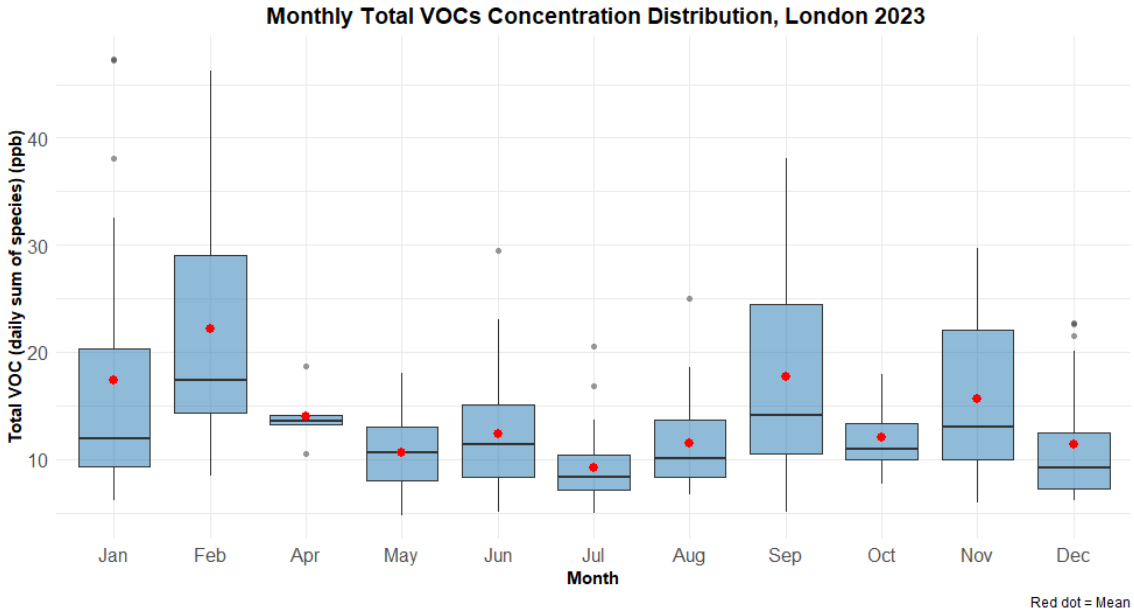

Figure 3-7 London 2023, monthly distribution of total VOCs concentrations (ppb), as sum of species' daily means, red dots: monthly mean concentrations, whiskers display the entire range, and boxes show the interquartile range (IQR).

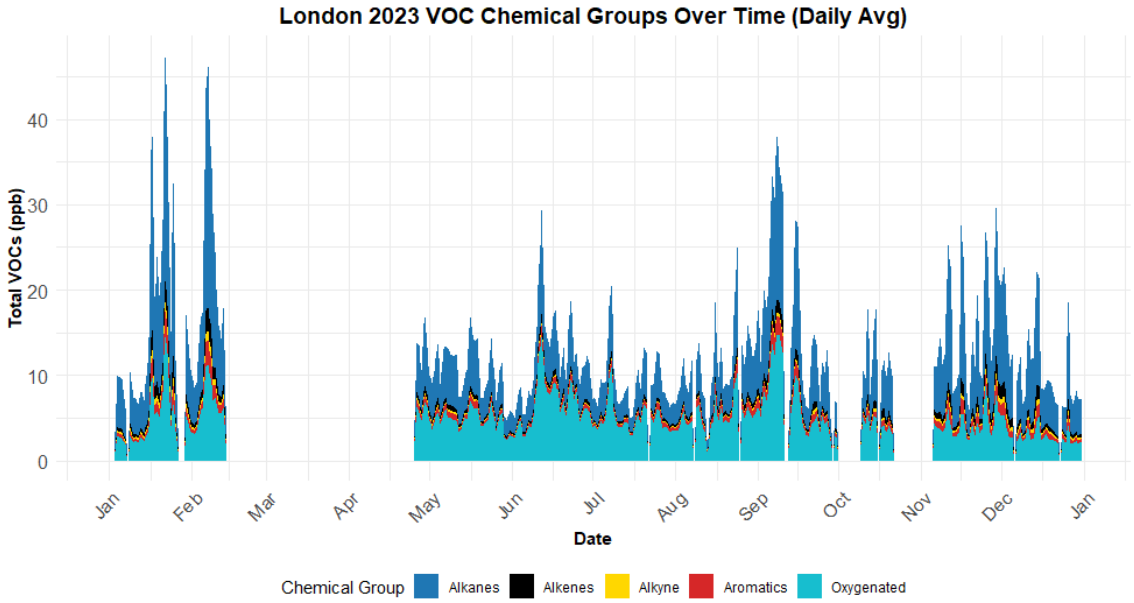

Figure 3-8 Time series of total VOCs, as sum of species' daily means (ppb), in London 2023, grouped by chemical group. Shaded areas represent the contribution of each group to the total VOC concentrations.

Table 3-3 Monthly mean and median wind speeds (m/s) at Heathrow airport (2023), with percentage differences showing the relative increase in December compared to September and November.

Month	Mean Wind Speed (m/s)	Median Wind Speed (m/s)	Mean Difference (%)	Median Difference (%)
September, 2023	3.58	3.27	+52	+62
November 2023	4.23	3.77	+28	+41
December, 2023	5.42	5.30	-	-

(Defra, 2024).

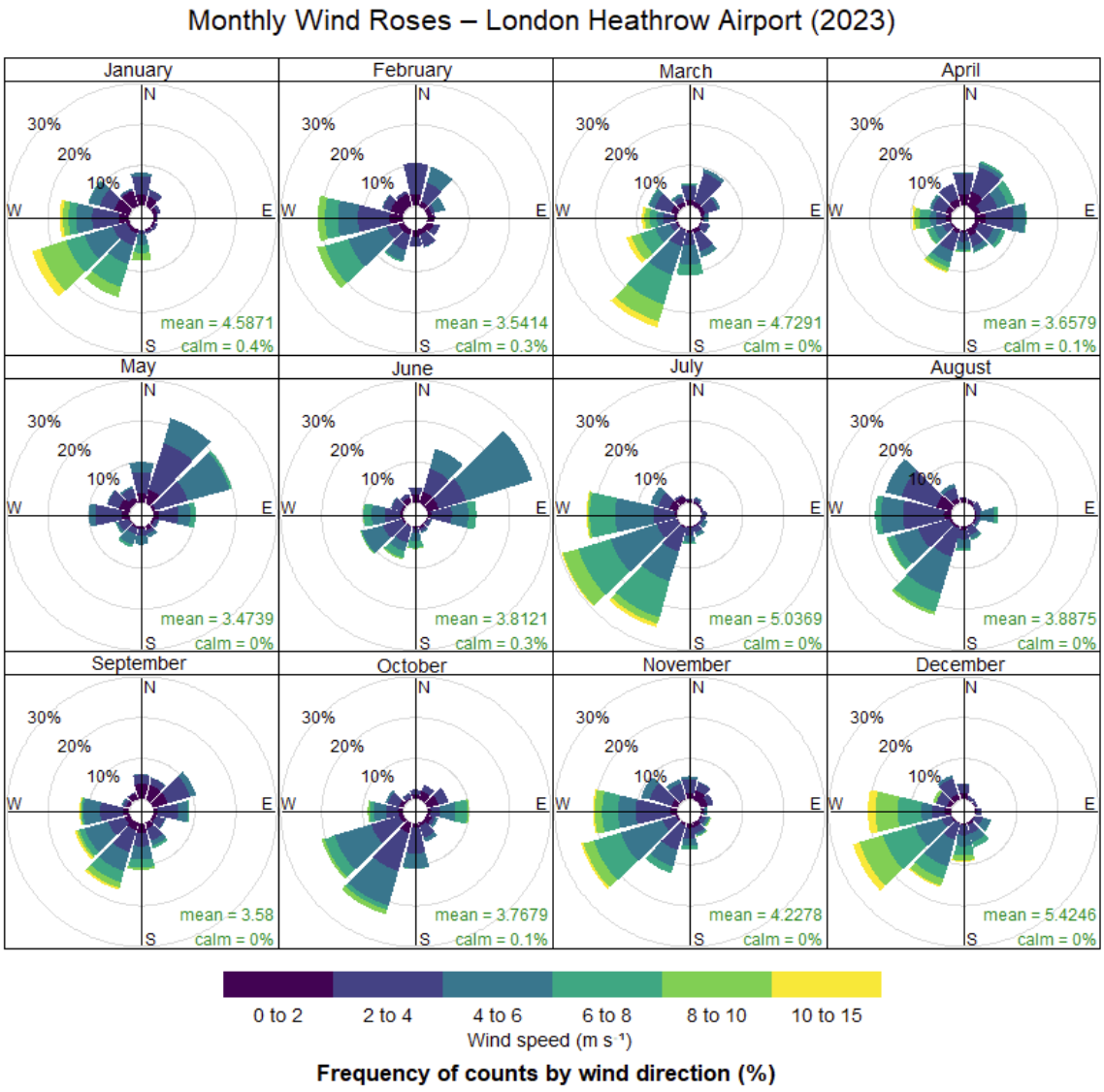

Figure 3-9 Monthly Windrose showing the frequency distribution of hourly wind direction and wind speed measured at London Heathrow Airport during 2023.

3.3.2 London 2023 Ten Most Abundant VOCs

The ten most abundant measured VOCs at the London urban background supersite in 2023, accounted for 89.7% of the total VOCs mixing ratio calculated as the sum of daily means mixing ratios of all the 32 species over the year, as illustrated in Table 3-4. Ethane, the most dominant VOC, accounted for 22.6% of the total observed mixing ratio, closely followed by ethanol, which contributed 19.8%, and acetone which accounted for 10.5% of the TVOCs concentration. These three species, accumulatively, had a share of more than half of the total VOCs levels at 52.9%. Other significant contributors were propane, acetaldehyde, and n-butane, which contributed for 9.0%, 8.1%, and 7.6% of the TVOCs concentrations,

respectively. Followed by less significant contributors to the TVOCs mixing ratio; iso-butane by 4.1%, ethene by 3.3%, iso-pentane by 2.6%, and toluene only by 2.0%.

These fractions indicate a substantial influence from non-combustion sources, with oxygenated VOCs (ethanol, acetone, and acetaldehyde) together representing 38.4% of the total VOCs, with secondary photochemical reactions, fuel evaporation, and solvent use all significantly contributing to the atmospheric levels of these oxygenated VOCs in urban areas (Dunmore et al., 2016; Jaimes-Palomera et al., 2016; Russo et al., 2010; Yáñez-Serrano et al., 2016), in addition to their emissions form incomplete fuel combustion sources. Moreover, non-combustion related alkanes (ethane, propane and n/iso butane, and iso-pentane) accounted for 45.9%, the presence of these alkanes mainly refers to natural gas handling, fuel evaporative and the use of non-aerosol personal products (AQEG, 2020), in addition to their minor combustion related sources. Alkenes (ethene) accounted only by 3%, pointing directly to combustion-related emissions (Cai et al., 2010; Gentner et al., 2013; Q. Zhang et al., 2018).

The seasonal analysis of these top ten VOCs, as presented in Figure 3-10, revealed distinct variations in composition between summer and winter. With mean concentrations of 4.2 ppb, ethane showed a significant winter enhancement and had the highest mixing ratio in this season. On the other hand, ethanol, even though it showed lower seasonal variability in its mean concentration indicating consistent emissions from various sources across the entire year, but slightly higher medians in summer, it was the most abundant VOC in summer with a mean concentration of 2.6 ppb. Acetone was notably elevated in summer, and similarly acetaldehyde was, indicating strong photochemical and secondary production. Propane, n-butane, iso-butane and ethene displayed higher winter means, reflecting stronger primary emissions. On the other hand, toluene and isopentane, the 9th and 10th most abundant VOCs, slightly varied between the two seasons, but still had higher winter means than summer ones, consistent with mixed traffic and solvent-related sources.

The seasonal variations suggest that winter VOC concentrations in London are predominantly affected by primary emissions and weak air dispersion. In contrast, summer enhancement in oxygenated VOCs indicates elevated photochemical activity and secondary production processes.

Table 3-4 The most ten abundant VOCs measured at the London urban background supersite in 2023, and their contribution to the total VOCs mixing ratio, calculated as the sum of daily mean mixing ratios of all 32 species over the year.

Rank	VOC	Contribution (%) to TVOCs	Cumulative (%)
1	Ethane	22.60%	22.60%
2	Ethanol	19.80%	42.40%
3	Acetone	10.50%	52.90%
4	Propane	9.00%	61.90%
5	Acetaldehyde	8.10%	70.00%
6	n-Butane	7.60%	77.60%
7	iso-Butane	4.10%	81.70%
8	Ethene	3.30%	85.00%
9	iso-Pentane	2.60%	87.60%
10	Toluene	2.00%	89.70%

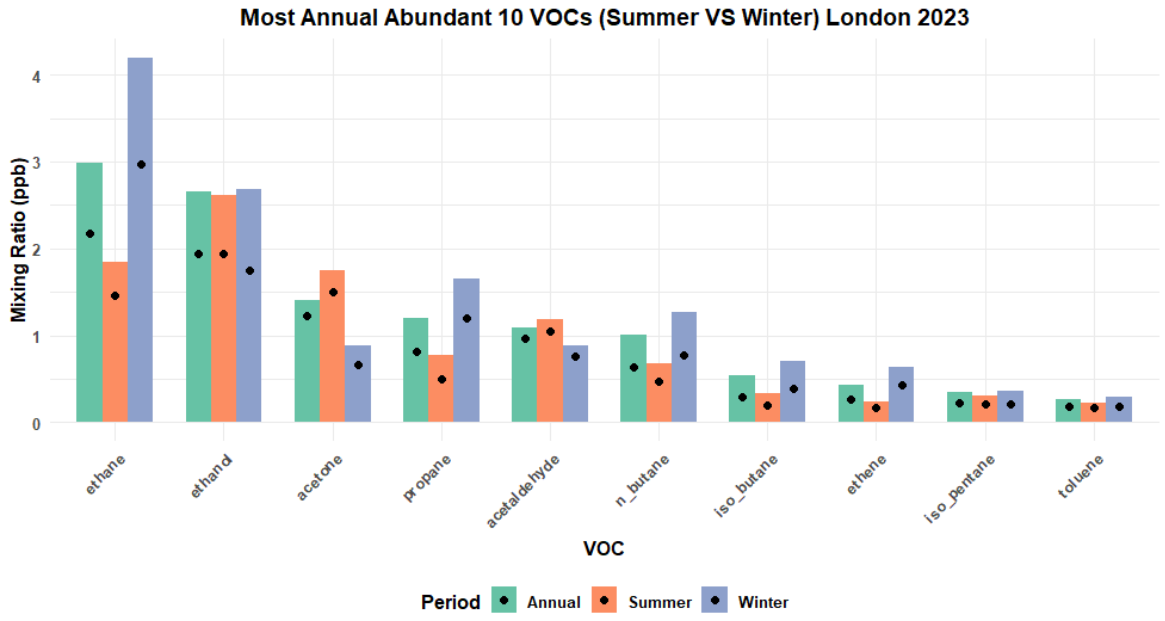

Figure 3-10 London 2023, Most 10 abundant VOCs, and their seasonal variation between summer and winter. Bars represent the daily means values, and black dots present daily medians for each VOC.

Although this chapter mainly focuses on the seasonal variability and inter-city comparison of VOCs concentrations between London and Birmingham, an additional analysis was conducted

to rank the ten most important VOC species based on their ozone formation potential (OFP) and secondary organic aerosol potential (SOA), in order to identify the key compounds that most strongly influence secondary pollutant formation. These calculations were conducted as described in 2.3.8 and 2.3.9 for each individual VOC. Table 3-5 presents the ten VOC species with the largest contributions to ozone formation potential (OFP) and secondary organic aerosol potential (SOAP), calculated using the 2023 annual mean VOC concentrations measured at the London supersite together with MIR and SOAP factor. Acetaldehyde dominates the OFP, contributing 22.3% of the total OFP. Along with ethanol, ethene, and toluene, these four VOCs account for 50% of the total OFP. Moreover, the ten VOCs with the largest contributions to OFP collectively account for 75.8% of the total OFP in London in 2023.

On the other hand, toluene dominates the SOAP, accounting for 35.7% of the total SOAP. This is followed by benzene and m-xylene, together cumulatively contribute 66% of the total SOAP. Moreover, the ten VOCs with the largest contributions to SOAP collectively account for 98.3% of the total SOAP in London in 2023.

It is worth noting that four VOCs (m-xylene, p-xylene, o-xylene, and propene) out of the most ten species contributing OFP, and seven VOCs (benzene, m-xylene, ethylbenzene, p-xylene, o-xylene, 1,2,4-trimethylbenzene, and 1,3,5-trimethylbenzene) out of the ten species contributing most to SOAP, are not among the ten most abundant VOCs measured at the London urban background supersite. Similar to our findings in sections 2.4.4, and 2.4.5, these results highlight the importance of considering VOC chemical reactivity and aerosol-forming efficiency, rather than ambient concentrations alone, when assessing their impacts on atmospheric chemistry and human health.

Table 3-5 Ranking of the ten most VOC species contributing to ozone formation potential (OFP) and secondary organic aerosol potential (SOAP), calculated using the annual mean VOC concentrations measured in London supersite in 2023 together with MIR and SOAP factor.

Ranking Based on OFP	**VOC**	**Contribution (%) to Total OFP**	**Ranking Based on SOAP**	**VOC**	**Contribution (%) to Total SOAP**
1	Acetaldehyde	22.3%	1	Toluene	35.7%
2	Ethanol	13.2%	2	Benzene	18.6%
3	Ethene	7.8%	3	m-Xylene	11.6%

Ranking Based on OFP	VOC	Contribution (%) to Total OFP	Ranking Based on SOAP	VOC	Contribution (%) to Total SOAP
4	Toluene	7.0%	4	Ethylbenzene	8.5%
5	m-Xylene	6.5%	5	p-Xylene	7.7%
6	n-Butane	4.8%	6	o-Xylene	7.3%
7	p-Xylene	4.4%	7	1,2,4-TMB	6.5%
8	Acetone	3.6%	8	Ethanol	1.1%
9	Propene	3.5%	9	1,3,5-TMB	0.8%
10	o-Xylene	2.9%	10	Acetaldehyde	0.4%

3.3.3 Birmingham 2022 VOCs Seasonality

The daily mean seasonal (summer and winter) and annual mean +/- standard deviation (SD) mixing ratios of measured VOC species in Birmingham 2022, grouped by chemical function, as presented in Table 3-6 shows that similar to the London case, winter concentrations were generally higher than summer for most VOC chemical groups, apart from OVOCs. However, this seasonal boost was stronger for light alkanes and fossil fuel combustion -related alkenes.

Ethane's daily mean almost doubled in winter increasing from 1.75 +/- 0.70 ppb in summer to 3.10 +/- 1.29 ppb in winter. Similarly, propane' daily mean rose from 0.60 +/- 0.30 ppb in summer to 1.32 +/- 0.56 ppb in winter. These trends were evident for n-butane, iso-butane, ethene, propene, and acetylene (the only measured alkyne). These species are well-known tracers of natural gas fugitive emissions, land transport emissions (both exhaust and fuel evaporative) (AQEG, 2020; Gentner et al., 2013; Stemmler et al., 2005; Tiwari et al., 2010).

In contrast, the daily means of all measured oxygenated VOCs were higher in summer than in winter. However, acetone and acetaldehyde summer levels 1.85 +/- 0.67 ppb and 0.96 +/- 0.37 ppb, respectively, were considerably higher than their winter levels, 0.77 +/- 0.18 ppb, and 0.65 +/- 0.19 ppb, respectively, indicating a strong impact from secondary photochemical production during warmer and sunnier days (Fischer et al., 2012; Russo et al., 2010). Unlike London 2023 where ethanol levels were slightly higher in winter than summer, Birmingham 2022 ethanol summer daily mean of 1.58 +/- 0.69 ppb were marginally higher than its winter value of 1.39 +/- 0.69 ppb, this can be explained by the combined contributions from both

combustion emissions from ethanol blended gasoline-powered vehicles that are often higher in winter, in addition to fuel evaporative emissions, and less importantly secondary atmospheric oxidation production that increase in the summer season (Kirstine & Galbally, 2012; Luecken et al., 2012).

Similar to London, aromatics followed the winter enrichment pattern with toluene level falling from 0.17 ± 0.11 ppb in winter to 0.13 ± 0.06 ppb in summer, and benzene dropping from 0.15 ± 0.07 ppb in winter to 0.06 ± 0.03 ppb in summer. This seasonal behaviour aligns with reduced photochemical removal rates in colder months, facilitating the accumulation of traffic and solvent use emissions (Debevec et al., 2021; Rajabi et al., 2020; Sadeghi et al., 2021).

As in London 2023, Birmingham 2022's alkanes had the highest contribution to the total observed VOCs mixing ratio, accounting for 50%, followed by oxygenated VOCs (OVOCs) at 37%. With a considerably lower contribution to Birmingham total VOCs, aromatics and alkenes only contributed by 5% and 6%, respectively, while acetylene, the only measured alkyne, had the lowest share at just 2% as illustrated in Figure 3-11.

However, as presented in Figure 3-12, these contributions varied between winter and summer. In winter alkanes significantly contributed (by 59%) to total VOCs levels, while in summer they only accounted for 39%. In contrast, summer oxygenated VOCs had the highest contribution, among all groups, (50%), whereas their winter contribution was only 27%. Alkenes, and aromatics had higher winter contribution of 7%, and 6% compared to 5% for each in summer, respectively. While alkyne contributed by 1% in both seasons. Overall, alkanes and OVOCs were the main contributors in summer and winter seasons. Birmingham 2022 VOCs chemical group contribution's proportion to the total measured VOCs mixing ratio were very close to London 2023 ones.

Figure 3-13 presents VOCs chemical groups daily means mixing ratio distributions. Alkanes exhibited the highest concentrations during winter reaching a peak daily mean of 12.5 ppb with a median concentration of just above 5 ppb, reflecting reduced atmospheric dispersion conditions and increased emissions from their main primary sources, natural gas leakage and traffic exhaust (Derwent et al., 2017; Salameh et al., 2016; Xue et al., 2017). In contrast, OVOCs had highest median and maximum values in summer, reflecting the enhanced

secondary formation from photochemical reactions in warmer months (Jacob et al., 2002; Millet et al., 2010). On the other hand, aromatics, alkenes, and alkynes, despite their smaller annual contributions, showed elevated distributions in winter compared to summer ones, mainly due to lower photochemical degradation rates and shallower mixing layers during colder months (Atkinson, 2000a; Grange et al., 2021).

Table 3-6 Birmingham 2022 Ambient VOCs Levels (daily mean +/- standard deviation).

Group	VOC	Summer (ppt)	Winter (ppt)	Annual (ppt)
Alkanes	ethane	1752 ± 703	3102 ± 1290	2349 ± 1075
	propane	601 ± 304	1321 ± 564	923 ± 488
	n-butane	445 ± 220	778 ± 445	587 ± 330
	isobutane	245 ± 128	445 ± 265	332 ± 196
	isopentane	152 ± 73	208 ± 112	170 ± 87
	n-pentane	75 ± 36	128 ± 62	94 ± 51
	methyl_2_pentane	41 ± 20	55 ± 33	46 ± 24
	methyl_3_pentane	25 ± 12	33 ± 20	27 ± 15
	iso-octane	16 ± 7	18 ± 13	17 ± 9
	n-hexane	26 ± 12	39 ± 19	30 ± 15
	cyclopentane	22 ± 11	28 ± 20	23 ± 14
Alkenes	ethene	263 ± 120	496 ± 326	365 ± 224
	propene	87 ± 37	125 ± 88	105 ± 61
	but_1_ene	14 ± 5	21 ± 14	17 ± 9
	isobutene	17 ± 8	19 ± 16	18 ± 11
	buta-1,3-diene	2 ± 1	4 ± 4	3 ± 3
	pent_1_ene	7 ± 3	10 ± 8	9 ± 5
	trans-2-butene	8 ± 3	7 ± 5	7 ± 4
	cis-2-butene	5 ± 3	14 ± 13	8 ± 8
	trans-2-pentene	2 ± 2	4 ± 5	3 ± 3
Alkyne	acetylene	107 ± 26	176 ± 75	145 ± 55
	toluene	129 ± 63	167 ± 111	141 ± 80
	benzene	64 ± 27	152 ± 66	102 ± 57
	m-xylene	64 ± 35	78 ± 71	70 ± 49
	o-xylene	37 ± 20	43 ± 36	39 ± 25
	p-xylene	36 ± 20	44 ± 37	39 ± 26

Group	VOC	Summer (ppt)	Winter (ppt)	Annual (ppt)
Aromatics	tmb_124	33 ± 18	39 ± 30	35 ± 22
	ethylbenzene	39 ± 21	48 ± 46	41 ± 31
	tmb_123	13 ± 6	15 ± 14	14 ± 9
	tmb_135	10 ± 5	11 ± 11	10 ± 7
Oxygenated	ethanol	1578 ± 693	1395 ± 692	1362 ± 644
	acetone	1846 ± 670	774 ± 176	1267 ± 612
	acetaldehyde	960 ± 374	653 ± 185	773 ± 299

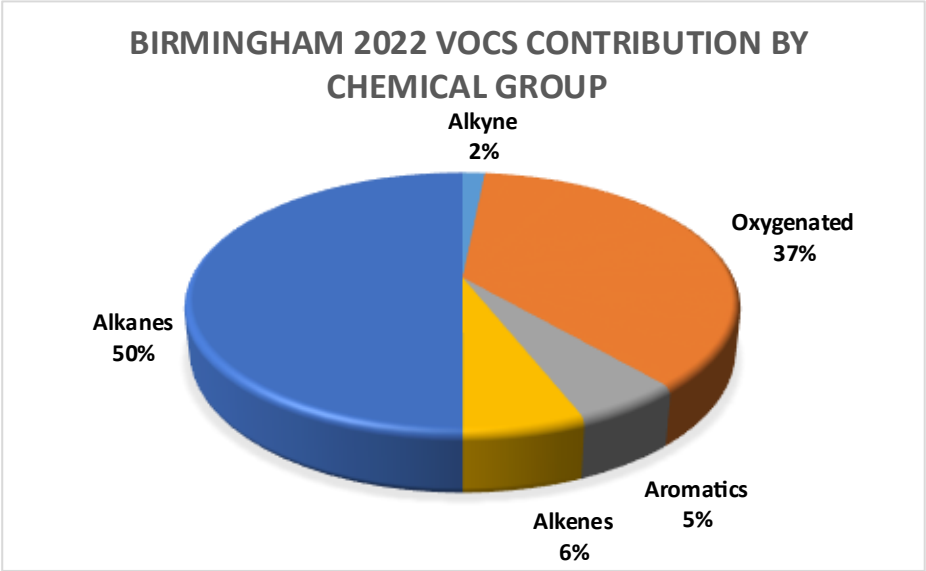

Figure 3-11 VOCs chemical groups contributions to the total VOC mixing ratio (based on the sum of VOCs daily means), Birmingham 2022.

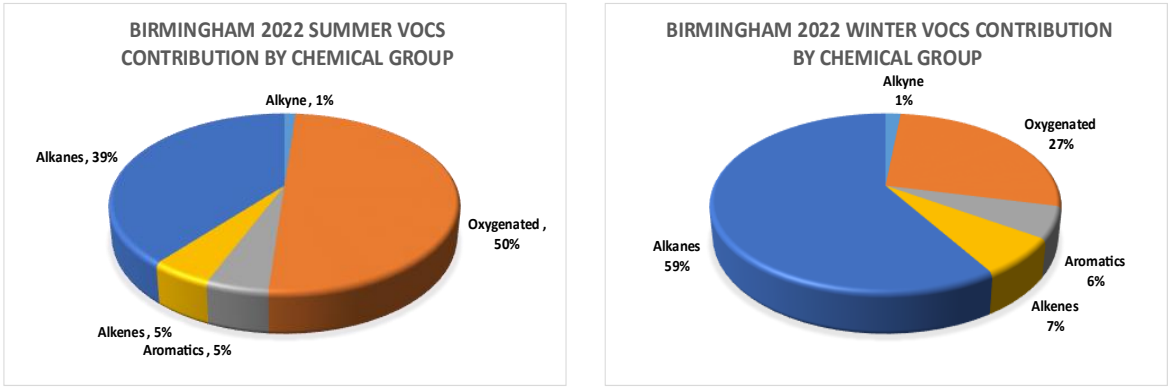

Figure 3-12 Summer and winter VOCs chemical groups contributions to the total VOC mixing ratio (based on the sum of VOCs daily means), Summer (to the left), Winter(to the right), Birmingham 2022.

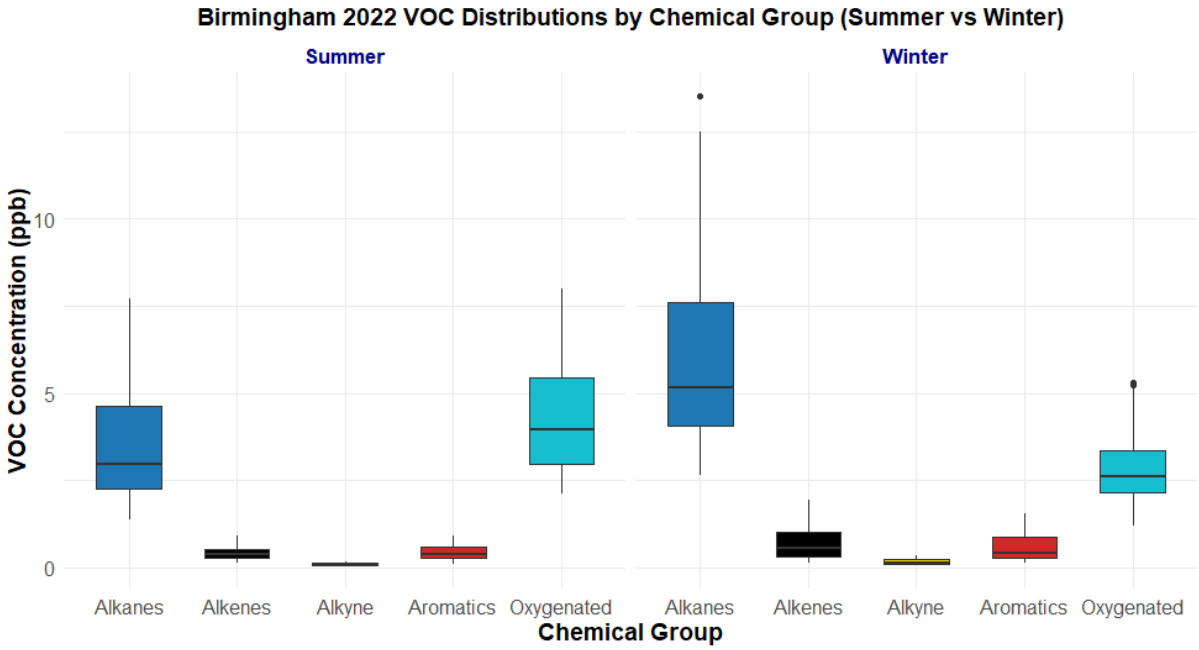

Figure 3-13 Summer vs. Winter VOCs chemical group daily means distribution (based on the sum of chemical group's VOCs daily means), Birmingham 2022.

Birmingham's 2022 monthly distribution of daily mean total VOC concentrations, presented in Figure 3-15, shows a clear seasonal pattern in TVOCs concentrations, with the highest concentrations and greatest variability taking place in the colder months, particularly January, March, and December. In contrast to the London case, December had the highest monthly median and mean concentrations of the year at 12 ppb and 12.6 ppb, respectively, with a maximum daily TVOCs concentration of 20.8 ppb. Similarly, January and March had considerably prominent levels of TVOCs, with wide ranges and means just below 12 ppb, mainly due to the combined effects of winter weather (lower boundary layer height, weaker vertical mixing, and lower temperature) and higher emissions from heating and traffic. (Debevec et al., 2021). These winter peaks were dominated by strong increases in alkane concentrations, particularly in January and December as illustrated in Figure 3-16. It is worth noting that the relatively low TVOCs mixing ratio distribution in February, compared to January and March levels, could be due to the high wind speed dispersion effects on the emitted VOCs, with mean wind speed in February being 51.4% and 28.8% higher than in January and March, respectively. Similarly, its median wind speed was 61.4% and 27.8% higher than in the above-mentioned months (Met Office, 2023). Figure 3-14 shows the monthly Windrose for Birmingham Airport in 2022, illustrating the frequency distribution of hourly wind direction and wind speed. The radial bars represent the percentage of time the

wind originates from each directional sector, while the colours indicate different wind speed classes (m s^{-1}).

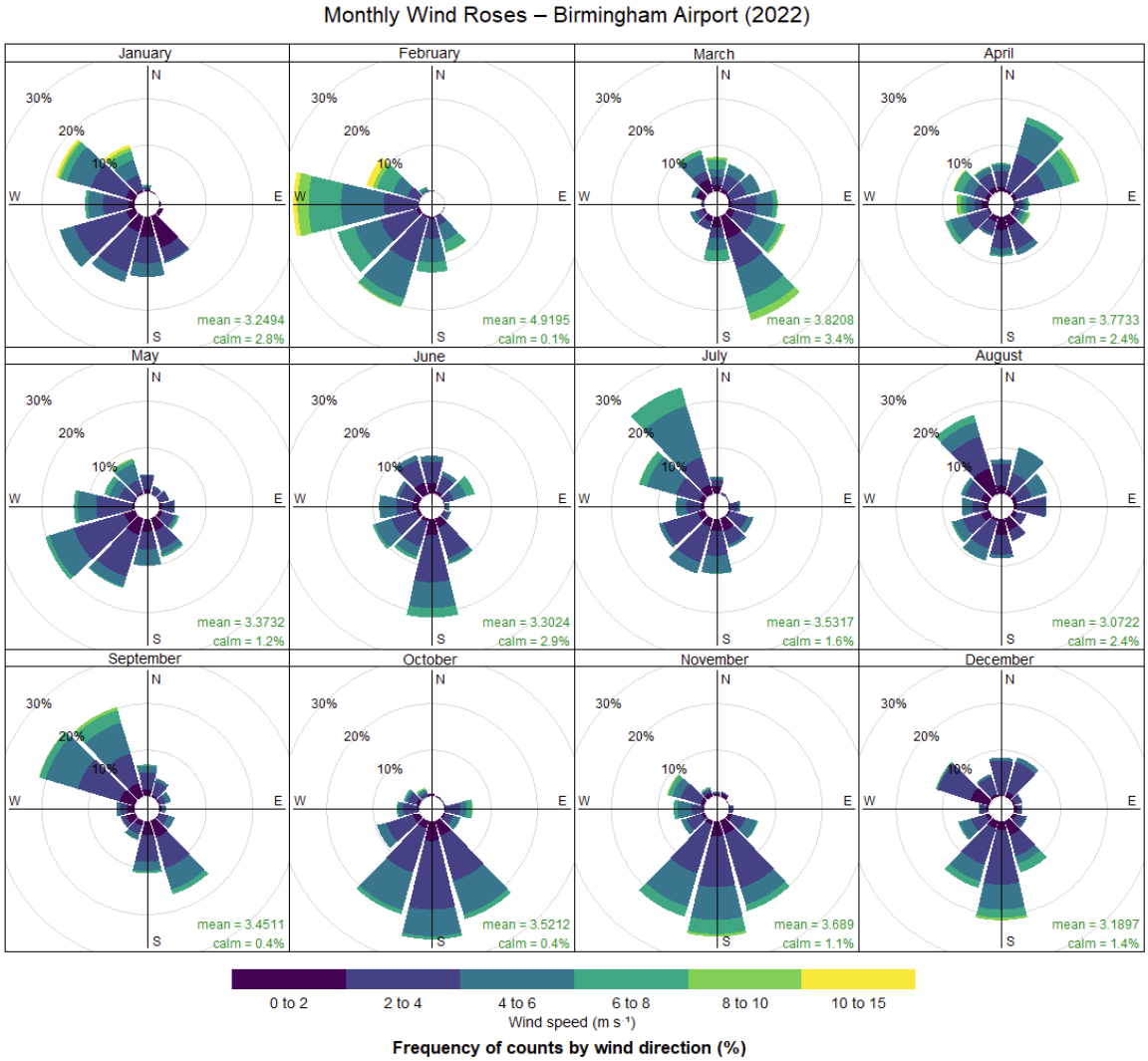

Figure 3-14 Monthly Windrose showing the frequency distribution of hourly wind direction and wind speed measured at Birmingham Airport (2022).

Winter TVOCs levels declined in April, with the median and mean just below 10 ppb, before dropping further in May, reaching the year's lowest monthly mean of about 7 ppb and the lowest maximum of 10.5 ppb. However, concentrations then gradually increased in summer, with June showing a wider distribution and the highest summer maximum of 17.1 ppb. Generally, summer (July to August) medians were similar at around 8 ppb, while August recorded the highest summer mean of 9.2 ppb, mainly driven by elevated OVOC contributions as shown in Figure 3-16.

In contrast to the London 2023 case, summer total volatile organic compounds (TVOCs), in Birmingham 2022, were relatively higher than autumn ones, specifically October and November, which could be a direct result of the reduced oxygenated VOCs formation under inadequate sunlight during these months (X. B. Li et al., 2022), in conjunction with the effects of meteorological variability (increased wind speed and air temperature) that enhance the dispersion of emitted VOCs (Rajabi et al., 2020).

The Birmingham 2022 pattern aligns with wintertime accumulation of VOCs under stationary conditions, summer dispersion and photochemical degradation, and variability during transitional seasons influenced by variations in emissions and meteorological conditions. However, summer concentrations were notably higher than those in the transitional seasons, largely due to the substantial photochemical production of oxygenated VOCs (OVOCs) in the presence of sunlight and warmer ambient temperatures.

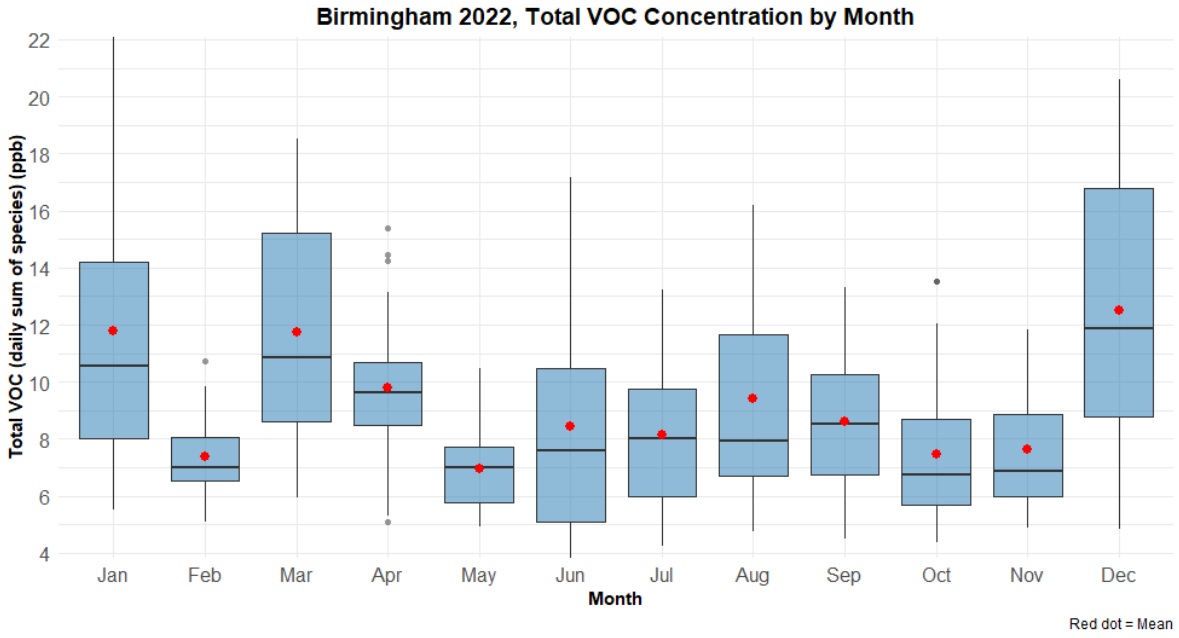

Figure 3-15 Birmingham 2022, monthly distribution of total VOCs concentrations (ppb), as sum of species' daily means, red dots: monthly mean concentrations, whiskers display the entire range, and boxes show the interquartile range (IQR).

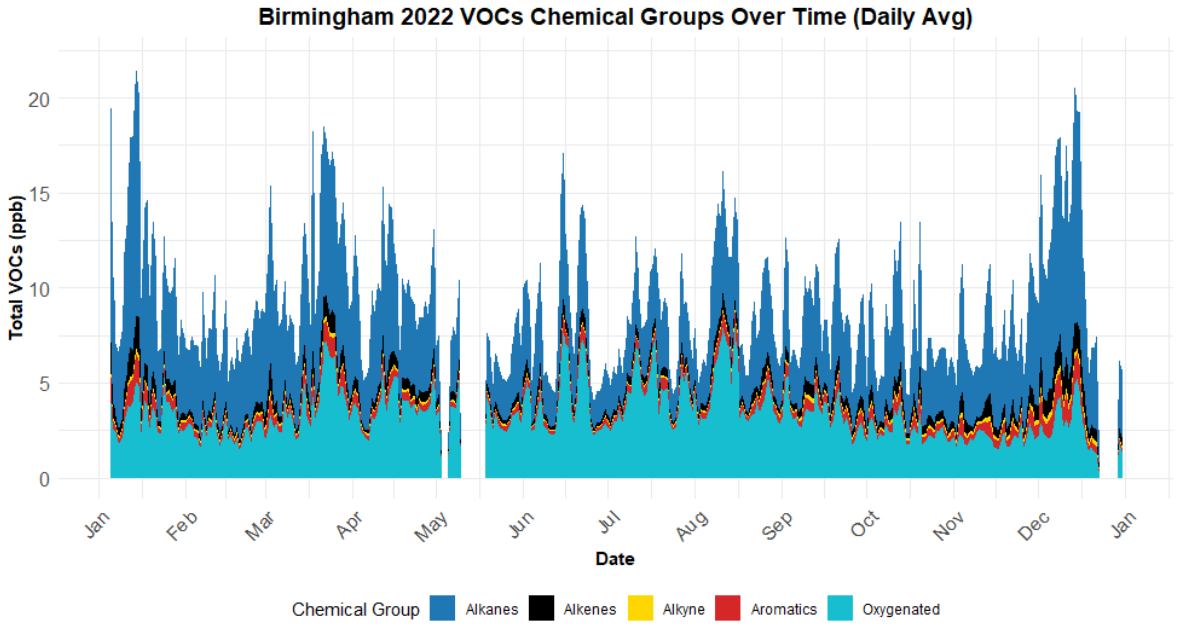

Figure 3-16 Time series of total VOCs, as sum of species' daily means (ppb), in Birmingham 2022, grouped by chemical group. Shaded areas represent the contribution of each group to the total VOC concentrations.

3.3.4 Birmingham 2022 Most ten Abundant VOCs

VOCs measurements at Birmingham Supersite 2022 show that the most ten abundant VOCs accounted for 90.2% of the total VOCs mixing ratio calculated as the sum of daily means mixing ratios of all the 32 species over the year, as illustrated in Table 3-7. Ethane, the most abundant VOC, accounted for slightly more than a quarter (25.9%) of the total VOCs concentrations, followed by ethanol, which had a 14.8% share, and acetone at 13.5%. Together, these three species contributed more than half of the total observed VOCs mixing ratio (54.2%). The other key contributors were propane, acetaldehyde and n-butane, accounted for 10.2%, 8.2%, and 6.4%, respectively, followed by ethene (4.0%), iso-butane (3.7%), iso-pentane (1.9%), and toluene (1.6%).

The above-mentioned ratios highlight the increased influence of non-combustion sources on atmospheric VOCs levels in Birmingham, with oxygenated VOCs (ethanol, acetone, and acetaldehyde) together representing 36.5% of total VOCs levels. The main sources of these oxygenated species are secondary photochemical production, solvent use emissions and evaporative losses from ethanol-blended fuels, especially during summer months, in addition to traffic combustion emissions (Dunmore et al., 2016; Jaimes-Palomera et al., 2016; Kirstine & Galbally, 2012; Yáñez-Serrano et al., 2016). Similarly, the elevated contribution of the light

alkanes (ethane, propane, n/iso-butane, and iso-pentane) at 48.1% to the total VOCs mixing ratio, considering their main sources in urban environments; natural gas handling, fuel evaporation, and emissions from non-aerosol personal care products (AQEG, 2020), in addition to their emissions from combustion related source, also reflects the importance of non-combustion VOCs sources. On the other hand, ethene, a key marker of fuel-combustion-related emission sources (Cai et al., 2010; Stemmler et al., 2005; Suthawaree et al., 2010; Toon et al., 2018), accounted for 4% of the total VOCs concentrations.

The seasonal analysis of the most ten abundant VOCs in Birmingham, as presented in Figure 3-17, illustrates clear seasonal compositional differences. Ethane, with an annual mean concentration of 2.4 ppb, reached 3.2 ppb in winter. Ethanol, on the other hand, showed relatively low seasonal variability, indicating a contribution from various sources over the year, however it had a slightly higher mean concentration in summer of 1.65 ppb compared to1.4 ppb in winter. While acetone had elevated summer levels, with a mean concentration of 1.85 ppb, slightly exceeding the ethane summer mean concentration of 1.83 ppb, indicating elevated photochemical and secondary production emissions associated with warmer conditions. Identical to acetone, acetaldehyde showed higher summer levels.

In contrast, propane, n-butane, iso-butane, and ethene had higher winter levels, mainly due to the accumulation of primary emitted VOCs under reduced atmospheric dispersion and decay conditions in colder months. Similarly, Iso-pentane and toluene, the 9th and 10th most 10 abundant VOCs had a relatively lower seasonal variation with slightly higher winter levels.

Birmingham's seasonal pattern shows that winter VOC concentrations are directly influenced by primary emissions in association with decreased atmospheric vertical mixing and degradation. In contrast, summer VOCs concentrations are directly influenced by the enhanced photochemical activity.

Table 3-7 The most ten abundant VOCs measured at Birmingham urban background supersite in 2022, and their contribution to the total VOCs mixing ratio, calculated as the sum of daily mean mixing ratios of all 32 species over the year.

Rank	VOC	Contribution (%) to TVOCs	Cumulative (%)
1	Ethane	25.90%	25.90%
2	Ethanol	14.80%	40.70%

Rank	VOC	Contribution (%) to TVOCs	Cumulative (%)
3	Acetone	13.50%	54.20%
4	Propane	10.20%	64.40%
5	Acetaldehyde	8.20%	72.60%
6	n-Butane	6.40%	79.00%
7	Ethene	4.00%	83.00%
8	Iso Butane	3.70%	86.70%
9	Iso Pentane	1.90%	88.60%
10	Toluene	1.60%	90.20%

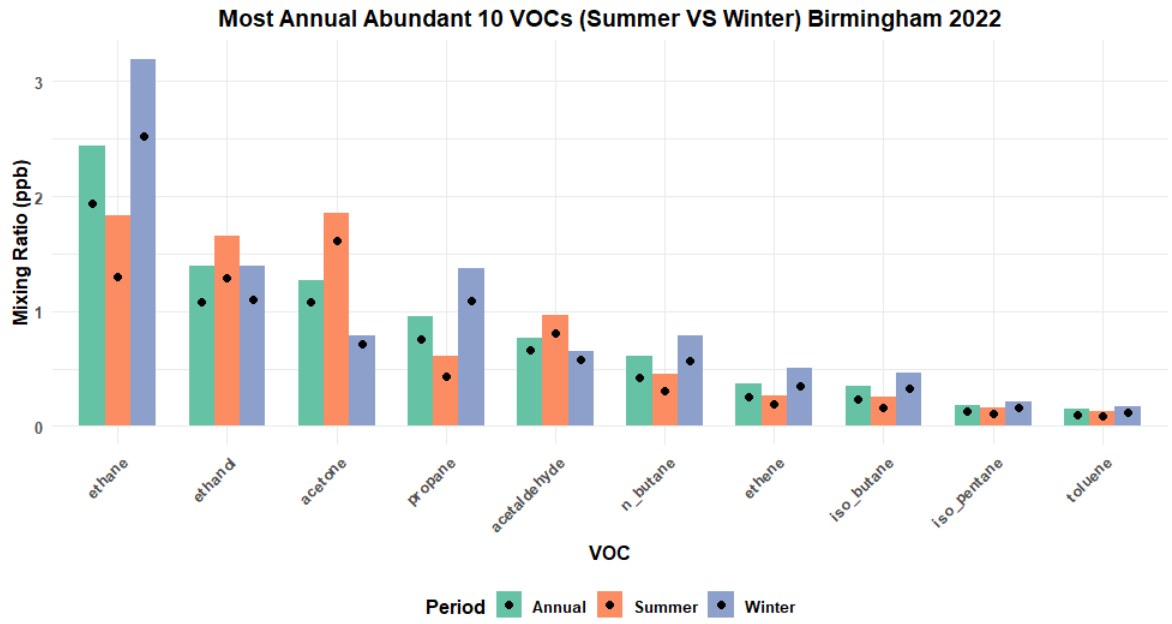

Figure 3-17 Birmingham 2022, Most 10 abundant VOCs, and their seasonal variation between summer and winter. Bars represent the daily means values, and black dots present daily medians for each VOC.

OFP and SOA analysis were conducted to rank the ten most important VOC species based on their influence on secondary pollutant formation. These calculations were conducted as described in 2.3.8 and 2.3.9 for each individual VOC. Table 3-8 shows that just four VOCs (acetaldehyde 22.8%, ethanol 9.8%, ethene 9.6%, and m-xylene 7.4%) account for 50% of the total OFP due to their high reactivity. The ten VOCs with the largest contributions to OFP collectively account for 76.3% of the total OFP in Birmingham in 2022.

On the other hand, the ten VOCs with the largest contributions to SOAP collectively account for 97.9% of the total SOAP in Birmingham in 2022. Among these, toluene (29.2%), benzene (16.3%), and m-xylene (14.2%) together account for 59.6% of the total SOAP in Birmingham in 2022.

It is worth noting that four VOCs (m-xylene, p-xylene, o-xylene, and propene) out of the most ten species contributing OFP, and eight VOCs (benzene, m-xylene, 1,2,4-trimethylbenzene, p-xylene, o-xylene, ethylbenzene, 1,3,5-trimethylbenzene , and 1,2,5-trimethylbenzene) out of the ten species contributing most to SOAP, are not among the ten most abundant VOCs measured at the Birmingham supersite. Similar to our findings in sections 2.4.4 and 2.4.5, these results highlight the importance of considering VOC chemical reactivity and aerosol-forming efficiency, rather than ambient concentrations alone, when assessing their impacts on atmospheric chemistry and human health.

Table 3-8 Ranking of the ten most VOC species contributing to ozone formation potential (OFP) and secondary organic aerosol potential (SOAP), calculated using the annual mean VOC concentrations measured in Birmingham supersite in 2022 together with MIR and SOAP factor.

Ranking Based on OFP	**VOC**	**Contribution (%) to Total OFP**	**Ranking Based on SOAP**	**VOC**	**Contribution (%) to Total SOAP**
1	Acetaldehyde	22.8%	1	Toluene	29.2%
2	Ethanol	9.8%	2	Benzene	16.3%
3	Ethene	9.6%	3	m-Xylene	14.2%
4	m-Xylene	7.4%	4	1,2,4-TMB	10.3%
5	Toluene	5.3%	5	p-Xylene	9.2%
6	Propene	5.0%	6	o-Xylene	8.1%
7	Acetone	4.7%	7	Ethylbenzene	8.0%
8	o-Xylene	4.2%	8	1,3,5-TMB	1.2%
9	n-Butane	4.0%	9	Ethanol	0.9%
10	p-Xylene	3.3%	10	1,2,3-TMB	0.6%

3.3.5 Summer 2023, Comparison of VOCs Profiles Between London and Birmingham

3.3.5.1 Summer most ten abundant VOCs

Table 3-9 presents the hourly mean mixing ratios for the most ten abundant VOCs during summer 2023 measured at the London and Birmingham urban background supersites. While both cities observed the same abundant VOCs species, their relative rankings reveal differences in key emission sources.

Ethanol, ethane, and acetone were the three most prevalent VOCs in London, accounting for 62% of the total top 10 VOC load, while in Birmingham, ethane ranked first, followed by acetone and then ethanol, collectively accounting for 61% of the total top 10 VOCs hourly mixing ratio, calculated as the sum of their hourly mean mixing ratios. The higher acetone ranking in Birmingham, compared with ethanol, could be due to the location of the Birmingham supersite, located only about 500 m to the northeast of the University of Birmingham Medical School, and just behind it the Queen Elizabeth Hospital Birmingham complex, all in which are associated with elevated indoor acetone levels, which eventually contribute to its ambient levels (Riveron et al., 2023).

Beyond the top three, acetaldehyde, propane, and n-butane had similar mid-table positions in both cities. Notably, there were obvious differences at the lower end of the rankings. Toluene ranked tenth in London's most 10 abundant VOCs list, but absent from Birmingham's, while acetylene, the seventh most abundant VOC in Birmingham, was not among the most abundant ten VOCs in London's atmosphere. Furthermore, ranked eighth, isopentane's hourly mean concentration was higher than ethene's in London, but it was the opposite in Birmingham where ethene ranked ninth and isopentane ranked tenth. This variation indicates a relatively greater impact of solvents and fuel evaporative emissions in London, while combustion tracers indicate the key role of combustion sources in Birmingham.

The results also show that London had consistently higher concentrations for almost all of most 10 abundant VOCs, with the largest absolute differences observed in oxygenated VOCs and ethane, at +1.60 ppb, +0.59 ppb, +0.59 ppb, and +0.52 ppb, for ethanol, acetone, acetaldehyde, and ethane, respectively. With a 157% increase over Birmingham, London experienced the highest relative increase in ethanol's hourly mean mixing ratio. Considering the higher solvent usage, traffic, and fuel evaporation emissions in a denser urban setting,

this significant percentage increase, compared to the rest of species' proportional increases, indicating a substantially stronger influence of ethanol sources in the capital. Likewise, the other two OVOCs were among the most proportionally increased species in London, with acetaldehyde, principally linked to secondary atmospheric oxidation formation (Russo et al., 2010b; Sommariva et al., 2011), demonstrating a 96.6% growth compared to Birmingham. The significant percentage rise in all OVOCs suggests variances in both direct emissions from vehicles and solvents, as well as changes in atmospheric oxidation, influenced by various photochemical conditions between the two cities. This variation is further supported by the difference in the relative OVOC contribution to the top 10 VOC concentrations, with OVOCs accounting for 56% of the total VOC load in London, while accounting for 49% in Birmingham. Generally, the elevated percentage of OVOCs in both cities during the summer months emphasises their essential influence on urban air quality and secondary pollutant formation, and hence the need to implement stricter control measures on their primary emission sources and precursors.

Surprisingly, iso-pentane, primarily emitted from petrol powered vehicles and fuel evaporation (Y. S. Huang & Hsieh, 2019; Kumar et al., 2020), showed an extraordinary percentage increase in London (+167.6%). Similarly, but to a lesser extent, n-butane, of which gasoline evaporation is one of its major sources in urban settings (Tiwari et al., 2010), increased by 91%, highlighting the critical significance of gasoline evaporative emissions in London, and therefore demanding further attention in VOCs and air quality legislation.

Finally, the relatively lower percentage increases in ethane, propane, and ethene in London by 39.9%, 32.4%, and 37.1%, respectively, compared with Birmingham, are considered expected, reflecting the combined impact of elevated traffic combustion activities and a more extensive natural gas network, associated with higher fugitive emissions, the main emission sources of these spices in urban areas (Chen et al., 2014; Derwent et al., 2017), in a larger and more populated city.

Table 3-9 Summer 2023, Comparison of the Hourly Mean Mixing Ratios (+/-SD) of the Most 10 Abundant VOCs (London VS Birmingham).

VOC	Ranking London/Birmingham	London Hourly mean mixing ratio (ppb)	Birmingham Hourly mean mixing ratio (ppb)	Difference (ppb)	Difference (%)
Ethanol	1/3	2.62 ± 1.92	1.02 ± 0.63	1.60	157.3
Ethane	2/1	1.84 ± 1.16	1.32 ± 0.97	0.52	39.9
Acetone	3/2	1.76 ± 0.79	1.17 ± 0.42	0.59	50.0
Acetaldehyde	4/4	1.19 ± 0.48	0.61 ± 0.24	0.59	96.6
Propane	5/5	0.78 ± 0.77	0.59 ± 0.51	0.19	32.4
n-butane	6/6	0.68 ± 0.62	0.35 ± 0.31	0.32	91.0
Iso-butane	7/8	0.33 ± 0.37	0.19 ± 0.17	0.14	73.5
Iso-pentane	8/10	0.31 ± 0.31	0.12 ± 0.11	0.19	167.6
Ethene	9/9	0.24 ± 0.20	0.18 ± 0.14	0.07	37.1
Toluene	10/-	0.22 ± 0.18	-	-	-
Acetylene	-/7	-	0.21 ± 0.11	-	-

3.3.5.2 Summer Correlation and diurnal analysis

Summer correlation matrix, presented in Figure 3-18, shows that C2 to C4 alkanes had significantly high positive correlation degree, although not necessarily from the identical sources, these species considerably co-vary. In Birmingham, the correlation between n-butane and iso-butane was strong ($r = 0.93$) and nearly perfect ($r \approx 0.99$) in London. Similarly, but slightly lower, ethane and propane showed elevated correlation levels ($r \approx 0.89$ and 0.91) in both cities, with robust associations of butanes with propane (0.86 in London and ≈0.90 in Birmingham), all confirming their common emission sources, natural gas leakage and traffic-related emissions, both combustion and evaporative (AQEG, 2020; J. Li et al., 2024). However, the relatively weaker positive correlations between butane and ethane (≈0.70 in London and ≈0.82 in Birmingham) demonstrate the greater regional background influence of ethane due to its longer atmospheric lifetime (Derwent et al., 2017). City variations are highlighted by different correlation's degrees between these alkanes and traffic emission tracers. While propane-ethene and butanes-ethene correlation values of 0.83, and 0.78, respectively in

London, were slightly higher than their correlation value in Birmingham, r= 0.74 each, which indicates a strongly association with vehicular exhaust emissions (Y. Liu et al., 2008). Propane-isopentane and butanes-isopentane correlations (r= 0.82 Birmingham, and 0.57 London), and (r= 0.86 Birmingham and 0.73 London), respectively, demonstrate Birmingham's stronger evaporative signature in this season, consistent with petrol-evaporation related sources (Cui et al., 2018).

Oxygenated VOCs also exhibited diverse behaviour. While ethanol in London had elevated correlation values with propane, ethane, ethene, and toluene r= 0.78, 0.75, 0.75 and 0.70, respectively, indicating links to solvent, fuel evaporative and combustion sources, ethanol in Birmingham was mostly associated with other oxygenates (acetone, r = 0.59; acetaldehyde, r = 0.73), indicating a more solvent and atmospheric oxidation driven signature. Both cities had high acetone to acetaldehyde correlations (r = 0.91 London, and 0.84 Birmingham) reflecting common sources. However, only in London acetaldehyde showed relatively high secondary associations with hydrocarbons, mainly with the gasoline evaporative marker isopentane (Y. Liu et al., 2008; Xue et al., 2017), (r = 0.74).

Acetylene exhibited a considerable variation among combustion tracers. In London, it showed a strong correlation with ethene (0.78) and a moderate correlation with the C2–C4 alkanes (r≈ 0.62), thereby supporting its traffic combustion origin. However, in Birmingham, acetylene had considerably low correlation with the rest of the VOC mixture, showing only a modest correlation with ethene (0.38) and negligible associations with OVOCs (r ≈ 0). This could be due to a separate source of acetylene in Birmingham.

Finally, toluene in London had a robust positive correlation with propane (0.78), butanes (0.75–0.76), and ethene (0.75), reinforcing its association with traffic emissions, while retaining associations with ethanol (0.70) and acetylene (0.62). In Birmingham, toluene had its strongest correlation with isopentane (r= 0.81) and the C3–C4 alkanes, while exhibiting low correlations with OVOCs and acetylene (r ≤ 0.4).

Together, correlation evidence aligns with the top 10 VOC rankings, where Birmingham's VOCs divide into two clusters: an oxygenate group (ethanol, acetone, acetaldehyde) and a hydrocarbon evaporative group (butanes, propane, isopentane, and toluene), with acetylene

mainly isolated. In contrast, London's VOCs form a united, traffic-influenced network with ethanol and OVOCs integrated into the hydrocarbon mix.

The diurnal patterns, presented in Figure 3-19, illustrate the temporal variations in the two cities' VOC behaviour. In London, n-butane and iso-butane concentrations surged dramatically in the morning (07:00–10:00), reflecting anthropogenic emissions, primarily linked to traffic activities under shallow boundary-layer conditions, and showed a secondary gradual increase after 18:00 linked to traffic activity and nocturnal accumulation. Birmingham had a comparable but slightly lower magnitude pattern. Propane, on the other hand, reached its peak in Birmingham between 04:00 and 06:00, while in London it peaked later between 05:00 and 08:00, and then concentrations in London dramatically declined reaching Birmingham levels by around 12:00, after which both cities showed comparable concentrations between 12:00 and 23:00, and then both increased sharply after 19:00. This daytime convergence could be due to the effect of stronger daytime boundary-layer growth in London, which dilutes local emissions more rapidly, combined with a relatively lower daytime emission pattern. Due to its relatively long lifetime (1 to 2 weeks), propane hourly variability is primarily controlled by boundary-layer mixing and emission timing rather than chemical loss (Atkinson, 2000a; Barlow et al., 2011; Xiao et al., 2008). At both locations, ethane had smoother cycles, reflecting its longer atmospheric lifespan and sensitivity to boundary-layer dynamics (Atkinson, 2000a; Derwent et al., 2017).

In contrast, the hourly mean concentrations of isopentane showed a completely different diurnal pattern, while London showed a clear afternoon maximum (14:00–15:00) reflecting temperature-driven volatilisation (Rubin et al., 2006), Birmingham peaked much later, at 22:00, with significantly lower daytime concentrations, indicating different emission pattern and nighttime mixing conditions. Toluene in Birmingham followed a similar pattern to iso-pentane hourly variation, reinforcing their shared evaporative and solvent-related sources. However, toluene in London peaked much earlier (04:00 to 05:00) and exhibited relatively sharper daytime decline in concentration, indicating stronger photochemical degradation under high OH conditions and dilution by the expanded daytime boundary layer height (Valach et al., 2015).

Ethene, on the other hand, exhibited strong traffic-related peaks in both cities, corresponding to the morning rush hour and evening congestion, distinguishing it from the more gradual

nighttime increase patterns noted in alkanes. However, the difference in magnitude between the two cities hit a low after 18:00, which again points to different emission patterns and nighttime mixing conditions. Although not among the top ten VOCs in London, acetylene was consistently higher in Birmingham. While both cities had afternoon minima (15:00–18:00) associated with enhanced mixing and higher photochemical removal rates, followed by a sharp evening increase, their early morning patterns varied. Birmingham exhibited a distinct early-morning maximum around 04:00, while London had a secondary rise between 06:00 and 09:00, indicating a different morning emission pattern.

Regarding OVOCs, acetaldehyde and acetone revealed substantial rises during the daytime in London, compared with Birmingham, where acetaldehyde increased steadily from 07:00 to hit a peak around 15:00, while acetone rose sharply after 09:00, peaking at the same time and then both declined. However, both hit a minimum between 03:00 and 07:00 and had a secondary increase after 21:00. The morning rise indicates strong secondary photochemical production under high summer oxidation conditions (Jacob et al., 2002; Millet et al., 2010; H. Singh et al., 1994). Similarly, ethanol cycles also diverged between the two cities. In London, concentrations peaked at night between 22:00 and 05:00, and then gradually dropped to a daytime minimum around 16:00, then it rose again in the evening. Given ethanol's main sources in urban areas, combustion emissions from ethanol-blended gasoline-powered vehicle exhaust and evaporative emissions from fuel use and storage (Dunmore et al., 2016; Florêncio et al., 2024) London's strong depletion reflects ethanol's short summer lifetime (<1 day under high OH), with photochemical loss and boundary-layer dilution outweighing its emissions (Atkinson, 2000a; Valach et al., 2015). However, ethanol was stable during daytime (07:00 to 17:00) in Birmingham, peaking just before midnight, around 23:00, indicating weaker OH driven removal and stronger nighttime accumulation, mainly due lower nocturnal boundary layer height.

Overall, the summer diurnal patterns revealed distinct key roles of chemistry, and atmospheric conditions in influencing VOC variability. Although London and Birmingham are geographically close and generally experience similar meteorological conditions, BLH and surface downward solar radiation data obtained from the ERA5 reanalysis for the supersite monitoring areas (Hersbach et al., 2026), along with wind speed data from London Heathrow and Birmingham airports during the study period (JJA 2023), retrieved from NOAA

meteorological records (NOAA, 2026), presented in Table 3-10 and Figure 3-20, show modest differences in atmospheric mixing and radiation that likely contributed to the observed VOC behaviour.

Table 3-10 shows that London's mean daytime BLH (1093 m) was 5.4% higher than the Birmingham one (1037 m), with a higher maximum daytime BLH (2418 m vs. 2207 m). In addition, daytime solar radiation was approximately 7% higher in London, indicating slightly stronger photolysis rates and OH production (Woodward-Massey et al., 2023). Moreover, daytime wind speeds in London (5.02 m s^{-1}) were 17.3% higher than in Birmingham (4.28 m s^{-1}), suggesting stronger atmospheric dispersion. Together, these factors likely contributed to sharper daytime reductions in VOC concentrations and enhanced OVOCs secondary formation in London. Conversely, Birmingham's lower mean nighttime wind speeds (3.00 m s^{-1}), compared with London's 3.60 m s^{-1} (20% higher), indicate greater meteorological stagnation. Despite a slightly higher mean nocturnal BLH, these weaker wind speed likely facilitated the observed nighttime accumulation of VOCs.

Figure 3-20 (a) BLH were very similar between the two sites throughout most of the day. However, between 10:00 and 15:00, London experienced slightly higher BLH, after which the BLH difference became negligible. This temporary enhancement in mixing height contribute to the sharper daytime decrease in VOC concentrations observed in London. For example, n-butane and iso-butane, Figure 3-19, show similar diurnal behaviour, with the largest concentration difference between the two sites occurring around 09:00, followed by a gradual reduction in this gap, until concentrations become nearly identical by 18:00.

Wind speed patterns show a comparable dispersion effect. London exhibited slightly higher wind speeds between 00:00 and 09:00, after which wind speeds became relatively higher from 10:00 to 23:00. This combination of marginally stronger mixing heights and higher wind speeds in London during daytime hours contributed to enhanced dispersion and a stronger daytime reduction in VOC concentrations compared with Birmingham.

Similarly, the solar radiation profile presented in Figure 3-20 (b) shows that London experienced relatively higher daytime solar radiation, with the largest differences occurring between approximately 09:00 and 15:00. After this period, the difference between the two sites became negligible. This enhanced daytime radiation in London contributed to stronger

photochemical activity and explains the relative enhancement in acetaldehyde concentrations observed in London, Figure 3-19, during these hours compared with Birmingham. Finally, the relatively higher daytime solar radiation in London, which promotes higher photolysis rates and OH radical production, likely enhanced the oxidative removal of primary VOCs, consequently contributing to both the observed reduction in their daytime concentrations and the formation of their secondary oxidation products.

Table 3-10 Comparison of key meteorological parameters influencing VOC dispersion and photochemical processing at the London and Birmingham supersites during Summer 2023 (JJA).

Parameter	**Period**	**London**	**Birmingham**	**Difference (%)**
BLH (m)	Daytime Mean	1093	1037	+5.4%
	Daytime Max	2418	2207	+9.5%
	Nighttime Mean	437	456	-4.1%
Wind Speed (ms^{-1})	Daytime Mean	5.02	4.28	+17.3%
	Nighttime Mean	3.60	3.00	+20.0%
Solar Radiation ($W\ m^{-2}$)	Daytime Mean	1.52M	1.42M	+7.0%

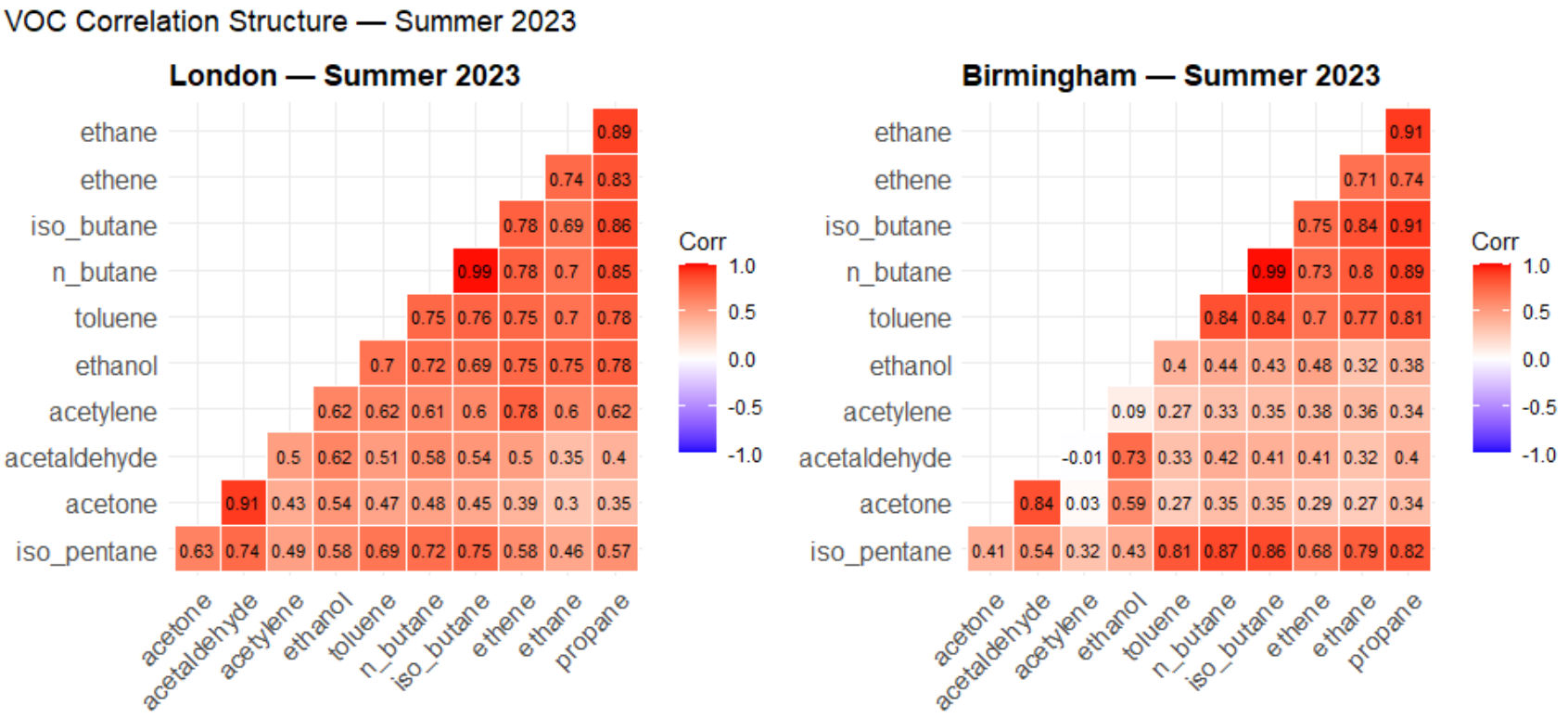

Figure 3-18 Summer 2023, correlation matrix of the most ten abundant VOCs at London and Birmingham.

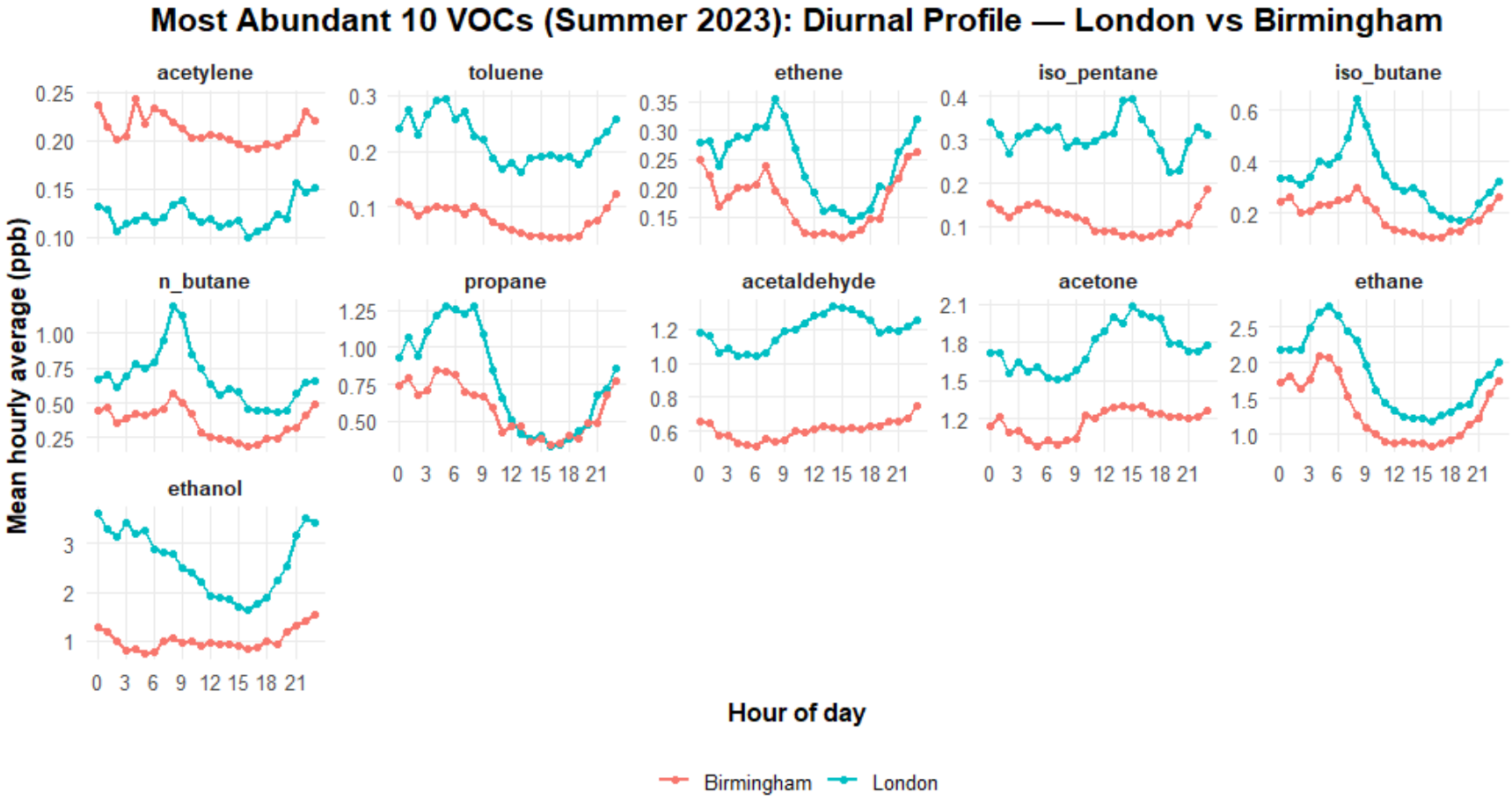

Figure 3-19 Hourly mean mixing ratio diurnal profiles of the most ten abundant VOCs at London and Birmingham, Summer 2023.

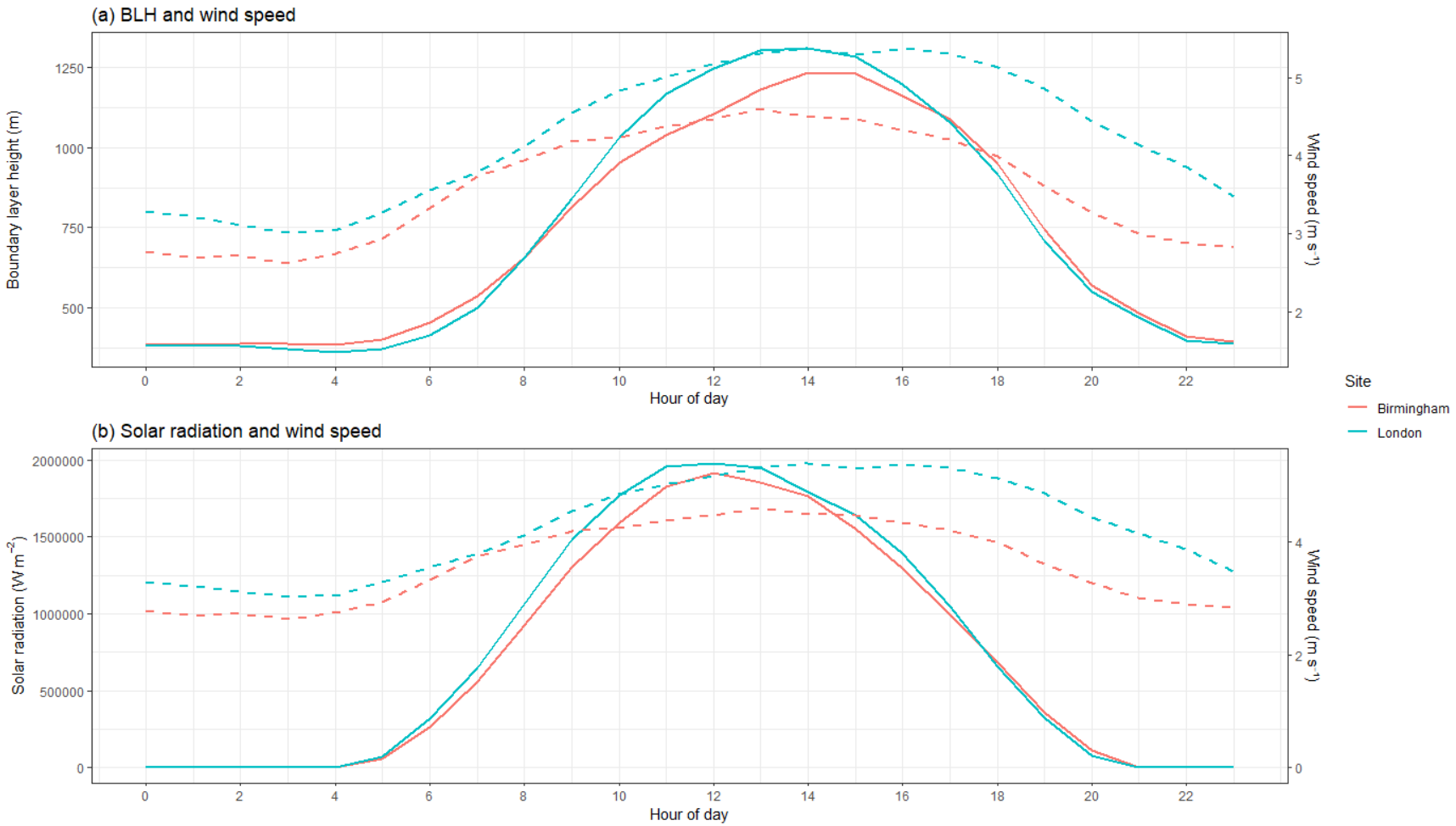

Figure 3-20 Diurnal variation of boundary layer height (BLH), solar radiation, and wind speed at the London and Birmingham monitoring supersites, JJA 2023

(a) hourly mean boundary layer height (solid lines) with hourly mean wind speed (dashed lines). (b) hourly mean surface solar radiation (solid lines) with hourly mean wind speed. London in blue and Birmingham in red.

3.3.6 Winter 2021-2022 (DJF), Comparison of VOCs Profiles Between London and Birmingham

3.3.6.1 Winter most ten abundant VOCs

Table 3-11 presents the hourly mean mixing ratios for the most ten abundant VOCs during winter (December 2021 to February 2022) observed at the London and Birmingham urban background supersites. While both cities were dominated by the same VOC species, however their relative rankings slightly varied. Ethane, ethanol, and propane were the three most prevalent VOCs in both urban environments, collectively accounting for 65% and 63% of the sum of top 10 VOCs hourly mixing ratios in London and Birmingham, respectively. On the other hand, acetone was the only VOC that had a different ranking between the two locations, being ranked sixth in London but fourth in Birmingham, and was the only specie with similar hourly mean concentrations between sites, due to the influence of the adjacent acetone emission sources near the Birmingham monitoring site.

Similar to the summer season, the results also show that London had consistently higher concentrations, apart from acetone, for nine out of the ten most abundant VOCs, with the largest absolute differences observed for ethanol (+1.04 ppb), ethane (+0.93 ppb), and propane (+0.44 ppb). London's hourly mean ethanol mixing ratio recorded the highest percentage change, compared with Birmingham's, followed by toluene, iso-butane, and iso-pentane, increasing by 78.7%, 76.1%, 60.8% and 58.1%, respectively. Interestingly, the winter proportional contribution of oxygenated VOCs (ethanol, acetaldehyde, and acetone) to the top 10 VOC concentrations was comparable, with 33.7% contribution in London and 32.5% in Birmingham, reflecting the key importance of their direct emission sources, under weakened atmospheric oxidation formation conditions in winter at both locations.

On the other hand, the relatively high percentage increases of toluene, iso-butane, and iso-pentane by 76.1%, 60.8%, and 58.1%, indicate a stronger relative influence of solvent use and petrol-related evaporative emissions in London during winter (Jaimes-Palomera et al., 2016; Mugica et al., 2002; Tiwari et al., 2010).

Finally, similar to the summer case, the relatively lower percentage increases in ethane, propane, and ethene in London by 33.2%, 38.2%, and 44.5%, respectively, compared with Birmingham, are considered normal and reflect the influence of elevated traffic combustion

activities and a more extensive natural gas network associated with higher fugitive emissions in London.

Table 3-11 Winter 2021-2022, Comparison of the Hourly Mean Mixing Ratios (+/-SD) of the Most 10 Abundant VOCs (London VS Birmingham).

VOC	Ranking London/Birmingham	London Hourly mean mixing ratio (ppb)	Birmingham Hourly mean mixing ratio (ppb)	Difference (ppb)	Difference (%)
Ethane	1/1	3.73 ± 1.16	2.80 ± 0.97	0.93	33.2
Ethanol	2/2	2.35 ± 1.92	1.32 ± 0.63	1.04	78.7
Propane	3/3	1.58 ± 0.77	1.15 ± 0.51	0.44	38.2
n-Butane	4/5	0.91 ± 0.62	0.63 ± 0.31	0.29	45.7
Acetaldehyde	5/6	0.87 ± 0.48	0.62 ± 0.24	0.26	41.6
Acetone	6/4	0.76 ± 0.79	0.76 ± 0.42	-0.01	-0.9
Iso-Butane	7/7	0.58 ± 0.37	0.36 ± 0.17	0.22	60.8
Ethene	8/8	0.52 ± 0.20	0.36 ± 0.14	0.16	44.5
Iso-Pentane	9/9	0.29 ± 0.31	0.18 ± 0.11	0.10	58.1
Toluene	10/10	0.23 ± 0.18	0.13 ± 0.07	0.10	76.1

3.3.6.2 Winter correlation and diurnal analysis

Winter correlation matrix, presented in Figure 3-21, shows that, similar to the summer season, C2–C4 alkanes had high correlation values in both cities, with the correlation values between n-butane and iso-butane very close to the full correlation scale of 1 in both urban environments (r = 0.99). Similarly, ethane and propane showed elevated correlation values (r = 0.89 in London and r = 0.84 in Birmingham), which was also supported by strong associations between propane and butanes (0.84, and 0.91) in both cities, expressing their common sources, mainly natural gas fugitive emissions, traffic fuel evaporative, and tailpipe emissions (J. Li et al., 2024). However, the relatively low correlations between ethane and butanes (r ≈ 0.74, 0.81 in London, 0.78, 0.82 in Birmingham) are because of the strong influence of regional background transport on ethane due to its longer atmospheric lifetime (Atkinson, 2000).

Similar winter correlation between alkanes and traffic tracers in both cities was revealed when examining these associations. Propane-ethene had an elevated correlation (r = 0.81),

and butanes-ethene correlations ranged between 0.72 and 0.79 in London. Similarly, in Birmingham, propane-ethene correlations were high but slightly lower than in London (r= 0.78), while butanes–ethene associations were marginally stronger (r= 0.82–0.84), suggesting that both cities exhibited clear traffic-related signatures, with Birmingham having relatively higher association between butanes and vehicular combustion. Moreover, London had marginally stronger evaporative associations, with propane–isopentane (r = 0.85 vs. 0.80 in Birmingham) and butanes–isopentane (r = 0.84–0.90 vs. 0.88–0.92 in Birmingham), pointing to the influence of petrol evaporation sources in both locations.

On the other hand, oxygenated VOCs experienced different behaviours between the two sites. In London, ethanol correlated with hydrocarbons including n-butane (r = 0.70), iso-butane (0.73), propane, and ethane (0.75 each), as well as with acetaldehyde (0.79), toluene (0.78), and acetone (0.81). This pattern suggests that London ethanol is more strongly linked to a mixture of traffic, solvent, and fuel-related evaporative emissions. By contrast, Birmingham ethanol was more mainly associated with acetaldehyde, r = 0.75, and toluene (0.62), pointing towards solvent use and secondary formation as more significant contributors. Acetaldehyde, exhibited secondary associations with hydrocarbons and aromatics in both cities, correlating with isopentane (r = 0.73), ethene (0.72), and toluene (0.80) in London, while in Birmingham it showed relatively higher correlation values; correlation with toluene (0.83), ethene (0.77), propane and n-butane (0.76), and isopentane (0.70). On the other hand, due to the direct effects of a nearby acetone emission source in Birmingham, acetone only exhibited a weak relationship with acetaldehyde (r = 0.51), whereas in London, acetone was well correlated with toluene (r = 0.85), isopentane (0.82), ethene (0.76), propane (0.79), ethanol (0.81), and acetaldehyde (0.80), emphasising its integration into the broader VOCs mixture.

The winter correlation structure revealed distinct inter-city variations. VOCs in Birmingham showed a clearer separation, with acetone remaining mostly separated due to a strong local source effect, whereas the other two OVOCs (ethanol and acetaldehyde) had moderate correlation with toluene and between each other. In contrast, a tightly packed cluster of hydrocarbons emerged, including toluene, propane, butanes, and isopentane, reflecting the unified traffic-influenced VOCs in the capital, where OVOCs (ethanol, acetaldehyde, and acetone) had robust correlations with alkanes, alkenes, and aromatics, in addition to each

other. Overall, this illustrates that while Birmingham's winter VOC mixture reflects stronger source separation, London's reflects a more unified blend of traffic, evaporative, and solvent-related emissions.

Figure 3-22 shows hourly mean mixing ratios diurnal patterns, illustrating the temporal variations in VOC levels between the two cities during the winter of 2021–2022. In London iso-butane, n-butane, and propane concentrations soared from 06:00, reaching a distinct morning peak at 09:00 reflecting the morning rush hours. Birmingham's morning increase, during the same period, was more gradual, with the concentration difference between the two cities being greatest at 09:00 due to the difference in anthropogenic emission intensity between the two cities. The morning peak in both cities was followed by a steady decline reaching a daytime minimum between 14:00 and 17:00, reflecting lower emission intensity and extended boundary layer mixing height. Meteorological data derived from the ERA5 reanalysis for the supersite monitoring areas (Dec 2021 to Feb 2022) indicate increased boundary layer heights during these hours , as illustrated in Figure 3-23 (Hersbach et al., 2026). After this daytime minimum, hourly mean concentrations increased sharply exhibiting a secondary peak around 19:00, due to the combination of evening rush-hour emissions and the accumulation of pollutants under a shallow nocturnal boundary layer, and then concentrations dropped significantly reaching their lowest levels between 03:00 and 06:00, as a result of negligible emissions. However, propane, in London only, remained at elevated levels between 20:00 and 22:00 before having a sharp nighttime decline, indicating a contribution from diverse sources. On the other hand, ethane had more uniform diurnal pattern, following the boundary layer height cycle, as evidenced by comparable peaks in the morning and late evening, and a midday minimum between 12:00 and 17:00.

Isopentane, on the other hand, exhibited a mixed temporal pattern. London isopentane concentrations peaked at 09:00, declined steadily until mid-afternoon, then fluctuated between 15:00 and 22:00 before decreasing to the lowest levels at 06:00, while in Birmingham, the evening maximum from 18:00 to 19:00 was slightly stronger than the morning peak, and the lowest values occurred around 02:00, which points to different local source contributions and nocturnal mixing conditions, as Birmingham showing greater enhancement of evaporative emissions during the evening.

Ethene, a representative marker of traffic emissions behaviour, showed clear diurnal patterns in both cities characterised by a notable morning peak from 07:00 to 09:00, and a more significant evening maximum at approximately 19:00, reflecting the urban traffic activity patterns reported by Department for transport report where road traffic volumes generally peak during the afternoon commuting period between 16:00 and 18:00, (Department for Transport, 2025), as shown in Figure 3-24. This was then followed by a sharp decrease overnight, reaching a minimum between 05:00 and 06:00. Notably, in Birmingham the morning peak was gentler, compared with the sharp peak observed in London, reflecting differences in traffic-related emissions intensity between the two cities.

In both cities, toluene showed significant morning rises from 06:00 to 09:00, peaking at 09:00, and then declining over the day until 14:00. While toluene levels in London fluctuated strongly in the afternoon and evening between 15:00 and 22:00, before falling to a minimum between 03:00 and 06:00, concentrations in Birmingham increased more smoothly to a comparable evening maximum from 17:00 to 19:00, aligning with solvent-related and traffic emission sources, with London's stronger fluctuations reflected a combined contribution of solvent use, fuel evaporative and traffic sources.

Among the OVOCs, acetaldehyde showed comparable general trends in both cities, but with varying timing. While concentrations in Birmingham increased significantly after 6:00, peaking at 10:00, then dipped slightly during midday before reaching a slightly stronger peak between 17:00 and 20:00 and thereafter decreased consistently until 4:00. In London it peaked later, between at 13:00, then decreased until mid-afternoon, before reaching a comparable evening maximum from 18:00 to 20:00 and then falling to early morning lows at 6:00. This reflects a similar acetaldehyde emission source in both locations. The second OVOC, acetone, showed generally similar levels in both cities but with differences in timing. Where acetone in London rose sharply after 07:00 to a late morning maximum at 11:00 and then fluctuated in the afternoon before hitting a maximum between 19:00 to 20:00 and thereafter dropping overnight to hit a minimum at 03:00. However, its levels in Birmingham increased steadily from 07:00 to hit a maximum between 14:00 and 17:00, exceeding London values due to strong localised emissions sources, before sharply declining into the lowest night levels without a secondary peak.

Similarly, ethanol followed comparable morning peaks (06:00 to 09:00) in both cities but deviated in the evening. London ethanol concentrations fluctuated after the morning rise, before increasing steadily from 17:00 to a strong evening maximum between 20:00 and 21:00, then decreasing overnight to reach minima at 06:00. Birmingham showed a steadier pattern, with concentrations plateauing after the morning peak, followed by an evening rise (19:00) of comparable strength, then declining gradually overnight. However, Birmingham ethanol concentrations showed a steadier pattern, with concentrations decreasing after the morning peak (09:00 to 10:00) but showing relatively stable levels during the day (11:00 to 18:00), followed by an evening rise at 19:00 comparable to the morning peak, then declining gradually overnight. Notably, ethanol diurnal pattern in London was identical to the ethene pattern, indicating stronger traffic combustion influence on ethanol levels during winter. In contrast, ethanol variability in Birmingham almost matched the acetaldehyde pattern, and did not follow the ethene pattern, indicating a major contribution from sources other than vehicular combustion emissions in Birmingham during the winter season.

In general, winter diurnal trends were characterised by traffic flow and boundary-layer patterns, with London exhibiting sharper peaks and stronger daytime fluctuations, whereas Birmingham had stable levels and stronger evening increase in evaporative and solvent-use related VOCs species.

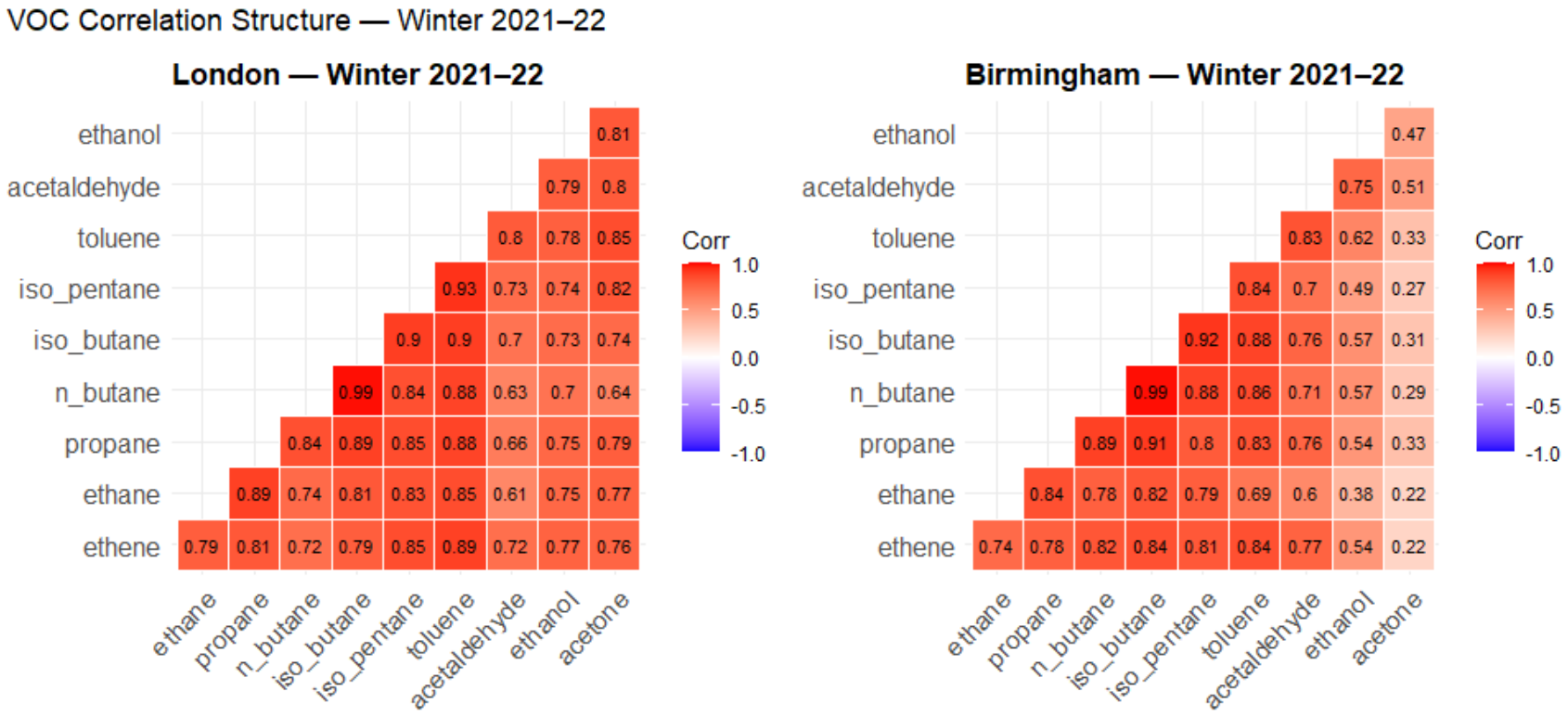

Figure 3-21 Winter 2021-2022, correlation matrix of the most ten abundant VOCs at London and Birmingham.

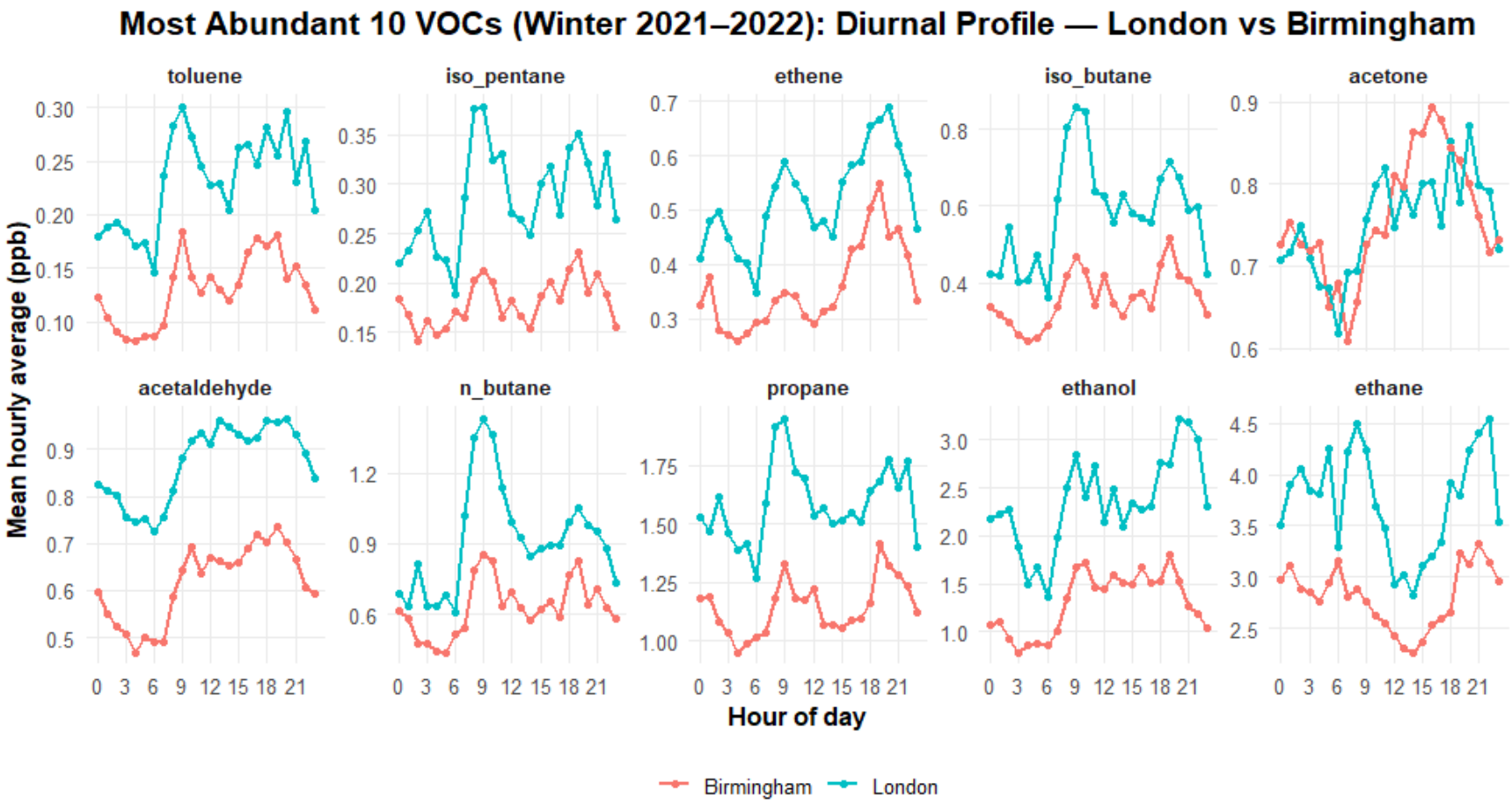

Figure 3-22 Hourly mean diurnal profiles of the most ten abundant VOCs at London and Birmingham, Winter 2021-2022.

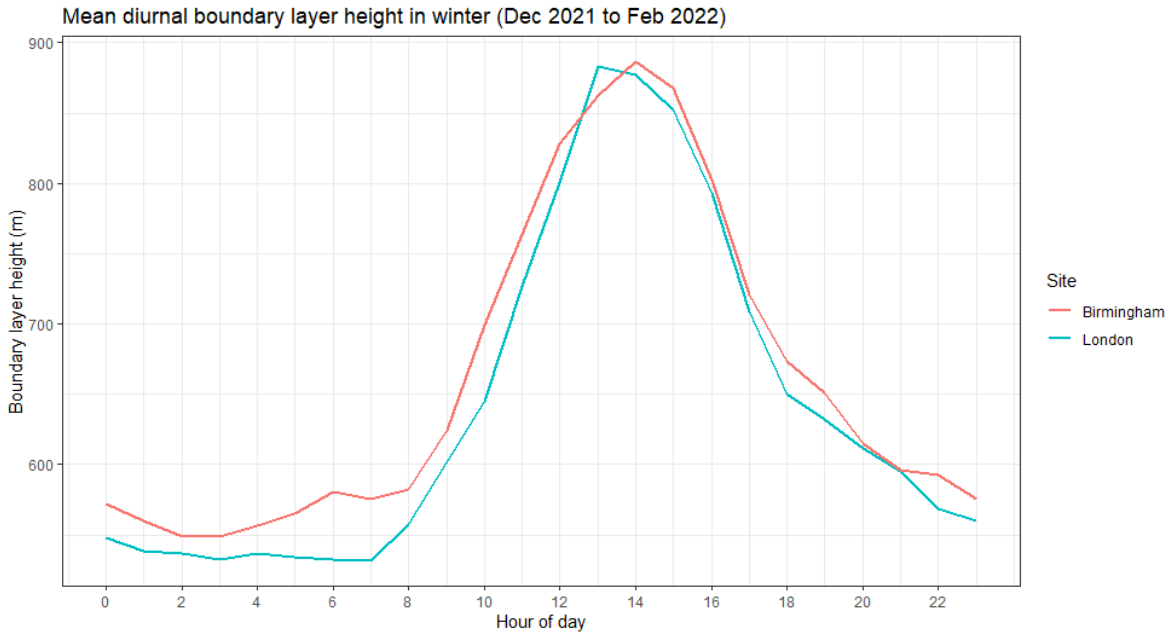

Figure 3-23 Hourly mean boundary layer height at the London and Birmingham monitoring supersites, Dec 2021 to Feb 2022. London in blue and Birmingham in red.

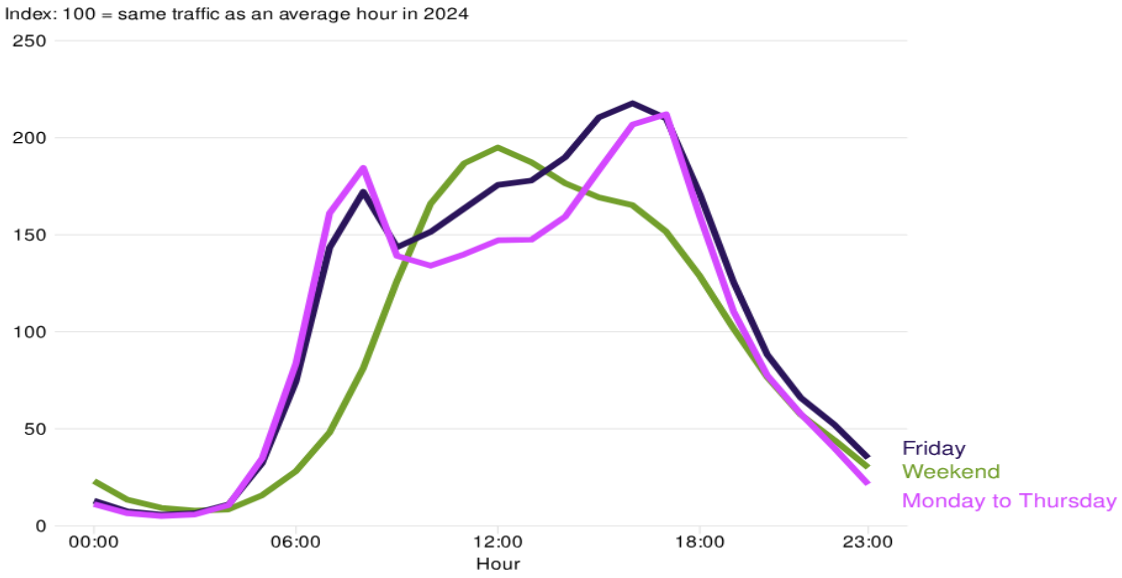

Figure 3-24 Hourly car and taxi traffic trends on all road types in Great Britain, 2024.

From (Department for Transport, 2025).

3.4 Conclusion

In this chapter, we examined the seasonal behaviour and inter-city contrasts of VOCs in London and Birmingham, two of the UK's largest urban centres with distinct demographic, geographic, and emission characteristics. Despite both cities having the same set of most 10 abundant VOCs, important seasonal and spatial differences were evident.

Interestingly, the most ten abundant VOCs accounted for nearly 90% of the total measured VOCs mixing ratio at both sites with ethane, ethanol, and acetone combined accounting for more than half of total VOC concentrations, emphasising the significant impact of non-combustion sources including evaporative losses, solvent usage, and natural gas, in addition to traffic emissions, on the urban atmospheric VOCs levels in the UK.

Winter concentrations in both London (2023) and Birmingham (2022) were generally higher than those observed in summer, particularly for light alkanes and combustion tracers, including propane, n- butane, iso-butane, ethene, and acetylene, all of which are primarily associated with natural gas leakage, vehicle exhaust, and fuel evaporation. Their elevated winter levels are a direct result of both decreased photochemical removal and higher emissions during stagnant weather. In contrast, OVOCs, particularly acetone and acetaldehyde, had elevated levels in summer, indicating the significant role of secondary photochemical production during this season. However, ethanol showed weaker seasonality due to the combined contribution from both vehicular emissions and fuel evaporation throughout the year. Generally, VOCs levels had higher levels during the studied seasons in London, mirroring the city's greater anthropogenic emission intensity, mainly from traffic related sources, solvent use, and natural gas fugitives.

Another distinct difference in the VOC profiles of these cities was noted, with London having elevated percentages of ethanol, iso-pentane, and toluene, compared with Birmingham, indicating a greater impact of solvent usage and evaporative sources. However, more distinct source separation was observed in Birmingham, with OVOCs clustering into one group, while hydrocarbons were more tightly clustered around combustion and evaporative sources.

Moreover, a comparison of the diurnal patterns in both cities showed that the variation of London VOCs was significantly influenced by boundary-layer dynamics and photochemistry leading to clearer daytime declines and increased secondary production of OVOCs during the

summer season. Conversely, the patterns observed in Birmingham were steadier. In summer, London showed sharp daytime declines and enhanced secondary OVOC formation under intense photochemistry. While Birmingham showed steadier daytime cycles and clear evening peaks specifically, during the same season, pointing to stronger nighttime accumulation. However, in winter, both cities had elevated levels of combustion and natural gas tracers, emphasising the impact of these sources on the winter VOCs concentrations, with sharper rush-hour peaks in London, and more gradual morning rise in Birmingham, reflecting differences in traffic intensity and boundary-layer dynamics.

All highlight the necessity for location-specific procedures: stricter regulation of solvent and evaporative emissions in London, and targeted management of combustion emissions in Birmingham.

Chapter 4

4 The Effects of UK Lockdown Measures on VOC Concentrations at London Marylebone Road, and Eltham Sites

4.1 Introduction

London, the capital of the United Kingdom, is one of the most diverse and dynamic capitals in the world, with a population of over 8.9 million in 2019, in which working-age individuals account for about 67.4% (National statistics, 2021). The population of the capital is projected to reach around 9.6 million in 2035, reflecting the steady increase in population since the beginning of the 1990s (Trust for London, 2022). Inner London, where boroughs like the City of London Westminster Southwark and Camden are located and host about 40% of the total population of Greater London (Office for National Statistics, 2022), represents the urban core of London. This is where the majority of London's financial and business activities, extensive busy transport network, and large-scale construction works come together, leading to the rise in concentration of air pollutants, mainly particulate matter (PM) and nitrogen oxides (NO_x), as a result of the significant residential, commercial, transport and construction activities (Mayor OF London, 2019).

In contrast, boroughs like Croydon, Richmond, Enfield, Bromley and 15 other boroughs out of the total 33 London local authorities are located in outer London, where the population density is about 4,000 residents per square kilometre compared to 10,660 residents in inner London (Centre for London, 2023), in addition to more green areas, leading to less transport congestion and consequently lower air pollution emissions. London's traffic emissions are the key source of air pollution accounting for almost 50% of total nitrogen oxides (Transport for London, 2020). Drivers in London lost on average 156 hours due to traffic congestion in 2021, hence the city was ranked the world's most congested city (INRIX, 2022).

In order to reduce the traffic related air pollution in London the Ultra Low Emission Zone (ULEZ) was introduced in central London in April 2019 and then expanded to cover all London local authorities in August 2023. It operates 24 hours per day in every single day of the week all around the year, apart from Christmas Day, discouraging those who drive noncompliant emission vehicles from using the roads in London. Its operation has led to a significant decrease in nitrogen dioxide levels which have decreased by about 53% in central London, 24% in inner London, and 21% in outer London (Mayor of London, 2023).

The air pollution reduction efforts, including the introduction of ULEZ in London in addition to many other air pollution reduction regulations, were crucial to tackling London's air

pollution issues. However, the unprecedented situation of the COVID-19 pandemic and its threat to mankind's life and lifestyle globally had a considerable impact on daily activities, consequently, reducing the anthropogenic emissions, especially the traffic-related ones, to a level that had never been achieved by any policy-driven interventions (Miyah et al., 2022). By 11th March 2020, there were almost twenty thousand cases of covid-19 reported worldwide and nearly four thousand and three hundred lives were lost due to its rapid spread (WHO, 2020). The World Health Organisation (WHO) subsequently advised governments to take serious measures to prevent the fast transmission of the virus, such as testing, isolating, tracing, and treating their citizens (WHO, 2020). In the UK, the first two cases were confirmed in York on January 29th, 2020, and the first death was recorded on February 28th, 2020. By March 16th, the total number of confirmed positive cases of Covid-19 reached about 1500, along with 55 resultant deaths (Office for National Statistics, 2020). In response to this rocketing increase in Covid-19 cases, social venues such as pubs, restaurants and cinemas were ordered to close on March 20th, and then full lockdown measures were taken on March 23rd, 2020 (Aspinall, 2022). These measures had a substantial impact on everyday life, especially on road traffic activities, limiting people's movement and travel to various degrees; the traffic flow dropped by 40% in April 2020 compared to pre-lockdown levels (SRN, 2020). Considering the traffic flow levels in 2019 as a reference, the traffic volumes in April 2020 dropped by 63%, May and June 2020 levels fell by 49% and 31%, respectively (Department of transport, 2021). The first lockdown ended on 14th August 2020 before a second lockdown was introduced in November 2020, during which traffic flows dropped by 27%. Bus miles travelled recorded the highest decrease, among all types of road traffic methods, followed by cars decreasing almost by 32% and 25% respectively in 2020, while the travelled distance by lorries and vans were only reduced by 5.7% and 9.1% respectively (Department of transport, 2021).

Many studies have been conducted to evaluate the impact of the serious drop in the industrial and transportation sectors on various air pollutants levels across the globe, mainly particulate matter (PM_{10} & $PM_{2.5}$), NOx, NO_2 and ground-level Ozone. In contrast, there is a lack of evaluating and understanding the effects of that drop on the non-methane hydrocarbons' ambient concentrations and species variation. Importantly, the land transport sector is one of the primary emission sources of VOCs in urban areas (C. Song et al., 2019), mainly due to

incomplete fuel combustion in vehicle engines (Arslan, 2020), where gasoline fuelled vehicles are the largest contributor to these emissions including exhaust emissions, fuel evaporations, and unburned fuel (David & William, 2009). The most abundant VOCs from this sector are C2 to C5 alkanes and aromatics; almost 40% of tailpipe VOCs emissions from gasoline-powered light-duty vehicles are aromatics, and 30% are alkanes. For light-duty diesel vehicles, alkanes dominate by about 70% of these emissions with aromatics accounting for less than 20% (Arslan, 2020). These VOCs play a vital role in the formation of secondary organic aerosol and/or tropospheric Ozone (Ou et al., 2015).

Hence the need to study and analyse the effects of the lockdown measures, mainly the massive drop in the land transport sector activities, on the measured VOC concentrations in different urban environments (The London Marylebone Road urban traffic site, and London Eltham suburban background monitoring site) from various angles. This includes examining the influence of meteorological conditions on the ambient VOC concentrations using machine learning techniques that analysed the partial dependence of VOC concentrations on individual meteorological variables over a five-year period (2015-2019) in order to explore their vital influence. Additionally, we investigated the impact of COVID-19 lockdown measures on VOC concentrations by comparing the VOC concentrations during lockdown periods against the predicted concentrations following the general trend - observed over the last five years before the pandemic. We then assessed post-lockdown VOC levels by comparing them with their projected concentrations as per their general trend. Finally, we utilized Random Forest models that considered the variation in VOC concentrations based on various explanatory variables (meteorological, seasonal, temporal, and long-term trend) to predict the concentration of VOCs in a business-as-usual scenario to precisely determine the actual impact of UK lockdown measures on VOC levels.

4.2 Methodology and Data

4.2.1 Sites information

4.2.1.1 London Marylebone Road

London Marylebone Road monitoring station, which was installed in June 1997, is an urban traffic monitoring site, UK-AIR ID: UKA00315, EU Site ID: GB0682A, Latitude/Longitude: 51.522530, -0.154611 with 35 metres altitude. The station is part of the automatic

hydrocarbon monitoring network; it monitors 29 VOC species in addition to various air pollutants (Ozone, Nitric oxide, Nitrogen dioxide, Nitrogen oxides as nitrogen dioxide, Sulphur dioxide, Carbon monoxide, PM_{10}, $PM_{2.5}$, Particle Concentrations and Numbers, Heavy Metals, and Polycyclic Aromatic Hydrocarbons (PAHs)) in addition to the following meteorological parameters: Modelled Wind Direction, Modelled Wind Speed, and Modelled Temperature. The station is located on the southern side of A501 road, 1 metre away from a bus lane; this road is generally congested as it is the main route to central London, heading north-east to south-west, serving about 90,000 vehicles on a daily basis (Road traffic statistics, 2019). The surrounding tall buildings, which include education, residential, markets, and tourist attractions buildings, form a relatively wide street canyon environment, nearly a width of 40 metres (Department for environment, 2008). These tall buildings on both sides of the road weaken the dispersion process of the emitted traffic pollutants by reducing the fresh air flow which traps the air pollution close to the emission sources (Buccolieri et al., 2018), Not only the street canyon environment that formed by the five-story buildings which surround the monitoring site limits both dilution and dispersion processes of the ground-level emitted pollutants, leading to high near-road pollutant concentrations (Park et al., 2004), but also the existence of the trees within this environment which reduces the velocity of the wind at the street level leading to more concentrated traffic pollutants (Vardoulakis et al., 2003), hence, Marylebone Road experiences some of the highest concentrations of traffic related pollutants in London (London Air, 2015).

The concentrations of traffic-related pollutants are known to peak directly at the roadside and then decay gradually up to a distance of 500 metres from the traffic emissions sources (Hagler et al., 2011). Therefore, London Marylebone Road monitoring site is ideally located to directly monitor traffic related emissions.

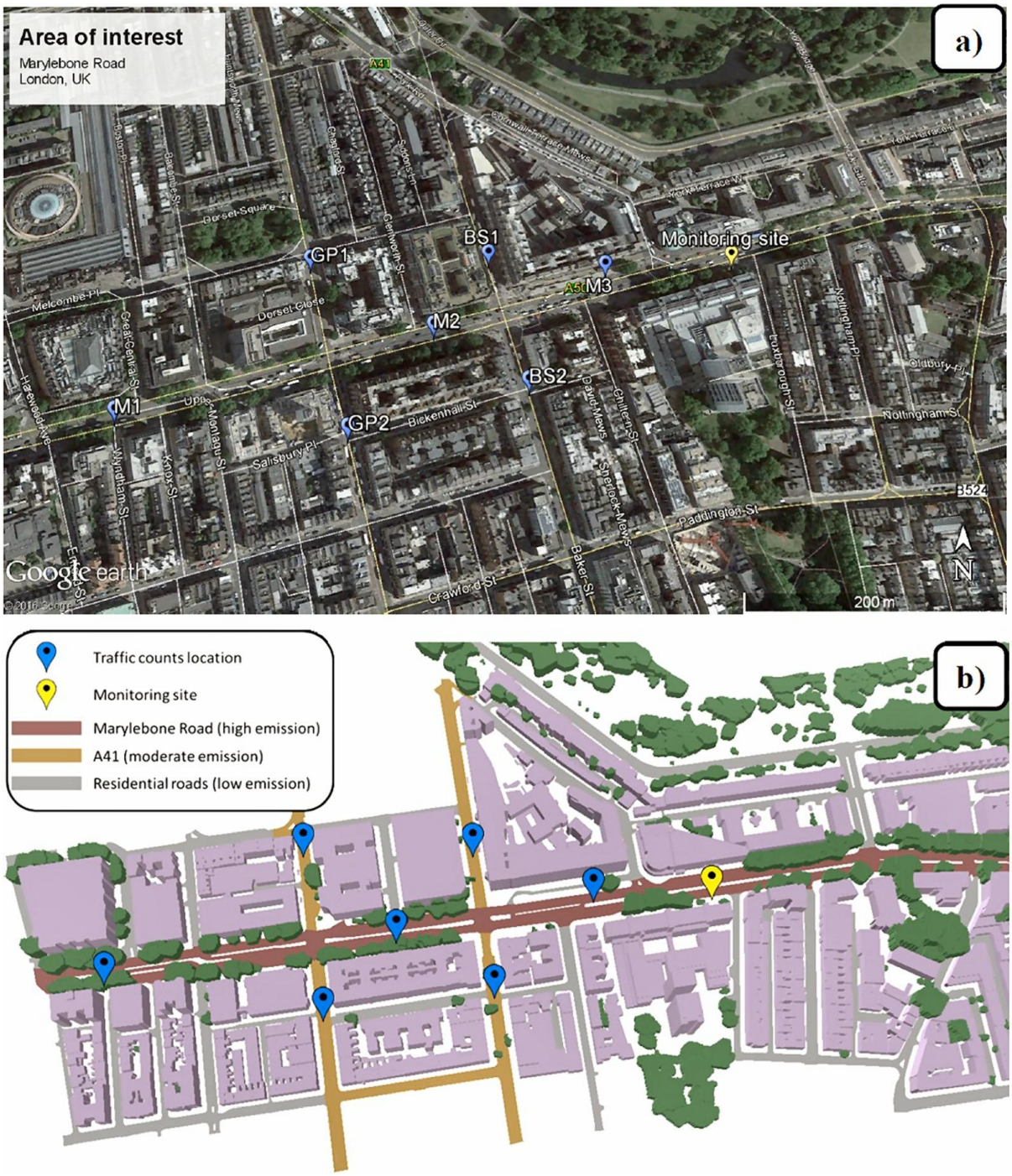

Figure 4-1 London Marylebone Road monitoring site. (a) Google Earth overview (b) 3D view including nearby streets and traffic count sites. (Buccolieri et al., 2018).
Traffic count locations are for contextual reference only and were not utilised in this study.

4.2.1.2 London Eltham monitoring station

London Eltham monitoring station is a suburban background monitoring site, UK-AIR ID: UKA00230, EU Site ID: GB0586A, Latitude/Longitude: 51.452580, 0.070766, with 60 meters altitude. The station is part of the automatic hydrocarbon monitoring network; it monitors 29 VOCs species in addition to many different air pollutants. The station is located on the ground

level of an environmental centre about 25 meters to the north of the A210 Bexley Road, the surrounding environment is relatively flat including open areas of grass, a golf course, trees, and residential housing. The monitoring process of most VOCs has started in October 1993 (DFRA, 2022). The traffic annual average daily flow (AADF), based on 2018 statistics, is nearly 13,500 vehicles (Department of transport, 2023). London Eltham monitoring station is about 17.5 km to the southeast of Marylebone Road monitoring station. Although it is quite far from industrial and road traffic emissions, compared to the London Marylebone Road site which is directly influenced by the traffic emissions, we can still consider it to fall within an urban area.

Figure 4-2 London Eltham Suburban monitoring site. Google Earth overview.

4.2.2 Data and Meteorological Variables Collection

The hourly VOC data were collected using an automated Perkin Elmer Gas chromatograph and obtained from the UK automatic hydrocarbon monitoring network, operated by DEFRA. Only ratified data were used in this study which unfortunately did not include 1,3-butadiene, a major traffic-related tailpipe emitted VOC in urban areas (Lewis et al., 2020d), for the period of this study as it was not ratified due to instrument issues. VOCs time series screening was conducted to identify and filter potential data quality issues, including extended periods of missing or invalid measurements. This screening was performed through visual inspection of high-resolution time series plots (hourly and daily averages), facilitating the identification of

long periods of missing data, and any instrument response issues, as presented in Figure 4-3 and Figure 4-4. As a result of this process, isoprene was excluded from further analysis due to substantial data gaps, particularly between 2015 and 2019 as shown in Figure 4-3, which would affect the quality and comparability of temporal and statistical analyses. The exclusion of species with insufficient temporal coverage is consistent with best practices in VOC source apportionment and time series analysis, where high data capture is vital for reliable and accurate analysis (Brown et al., 2015; Hopke, 2016).

Hourly meteorological data were obtained from London Heathrow airport meteorological station, the nearest available meteorological station to the studied site; Meteostat: 03772, coordinates: 51.4833, -0.45, 24 metres elevation (Metostat, 2022), and were downloaded from the national centre for environmental information(NOAA) (NOAA, 2022) VOC and meteorological data, including boundary layer height data from the Climate Data Store (CDS) (Climate Data Store, 2022) were combined in order to examine the role of these variables (air temperature, wind speed, wind direction, boundary layer height, relative humidity, atmospheric pressure, cloud cover, and the height of the cloud) on the variation of VOCs levels.

Although the distance between the London Marylebone Road monitoring station and London Heathrow airport meteorological station is relatively far (20 km), weather stations within a few kilometres from each other, due to the uniform weather conditions in the UK, generally generate comparable meteorological data (Arciszewska & McClatchey, 2001). In this context, the meteorological data that were obtained from Heathrow Airport meteorological station can be used confidently in this study. However, both local topography and microscale environment impact the meteorological variables' effects, mainly the wind speed, on the dispersion process of the locally emitted pollutants (Raj & Sharma, 2017). It is worth mentioning that VOC concentrations, especially for those with relatively short lifetimes, in urban areas are mainly driven by local traffic emissions (Yuan et al., 2012), this is thought to be particularly true for the Marylebone Road data due to the street canyon effect. While in suburban environments, in addition to the vehicular VOCs emission, various localised sources contribute to their ambient levels (S. Zheng et al., 2019). This study has mainly focused on the VOCs concentration changes and the percentage of these changes compared to the mean VOCs levels in previous years.

Table 4-1 and Table 4-2 present the measured mean VOC species concentrations for the pre-lockdown period (2019), the lockdown period (2020), and the percentage changes in mean concentrations between these periods at the Marylebone Road and Eltham sites.

Table 4-1 Measured mean VOCs species, pre lockdowns period 2019, lockdown period 2020 and the percentage changes of measured mean concentrations between these periods at London Marylebone Road.

VOCs	*Pre-LC1 2019 Mean Con +/-SD (µg/m³)*	*LC1, 2020 Mean Con +/-SD (µg/m³)*	*LC1 2019 VS 2020 Change (%)*	*Pre-LC2 2019 Mean Con +/-SD (µg/m³)*	*LC2 2020 Mean Con +/-SD (µg/m³)*	*LC2 2019VS 2020 change (%)*
Ethane	7.51 ± 2.19	7.57 ± 3.11	**0.63**	11.35±5.13	11.56 ± 7.10	**1.8**
Propane	4.39 ± 1.80	3.54 ± 1.90	-19.31	7.18 ± 2.67	7.25 ± 4.83	**0.9**
Iso-Butane	1.96 ± 0.77	1.49 ± 0.78	-23.60	3.17 ± 1.25	2.85 ± 1.95	-10.3
n-Butane	3.50 ± 1.42	2.52 ± 1.33	-27.70	5.61 ± 2.18	4.88 ± 3.44	-13
Iso-Octane	0.33 ± 0.13	0.19 ± 0.07	-41.96	0.39 ± 0.14	0.41 ± 0.20	6.0
n-Octane	0.17 ± 0.11	0.12 ± 0.04	-31.42	0.25 ± 0.08	0.20 ± 0.09	-16.9
Iso-Pentane	2.14 ± 0.94	1.40 ± 0.75	-34.20	2.22 ± 0.77	2.14 ± 1.31	**-3.8**
n-Pentane	0.89 ± 0.37	0.64 ± 0.32	-28.39	1.05 ± 0.35	1.00 ± 0.60	**-4.4**
n-Heptane	0.34 ± 0.21	0.18 ± 0.06	-46.87	0.46 ± 0.18	0.38 ± 0.22	-16.9
n-Hexane	0.27 ± 0.11	0.26 ± 0.22	-4.52	0.37 ± 0.15	0.36 ± 0.21	-2.4
Ethene	1.73 ± 0.63	1.04 ± 0.39	-39.58	2.80 ± 0.90	2.38 ± 1.48	-14.9
Propene	0.75 ± 0.26	0.80 ± 0.35	7.85	1.23 ± 0.36	1.28 ± 0.66	**4.2**
cis-2-Butene	0.07 ± 0.02	0.08 ± 0.02	12.85	0.09 ± 0.02	0.10 ± 0.03	**1.0**
trans-2-Butene	0.11 ± 0.03	0.09 ± 0.03	-15.21	0.16 ± 0.05	0.12 ± 0.04	-28.1
trans-2-Pentene	0.06 ± 0.04	0.06 ± 0.02	**3.37**	0.14 ± 0.04	0.08 ± 0.05	-40.2
1-Butene	0.21 ± 0.05	0.21 ± 0.06	4.17	0.29 ± 0.06	0.26 ± 0.12	-9.6
1-Pentene	0.05 ± 0.02	0.06 ± 0.02	10.28	0.10 ± 0.03	0.07 ± 0.03	-27.8
2Methylpentane	0.42 ± 0.27	0.35 ± 0.18	-17.65	0.46 ± 0.18	0.60 ± 0.38	28.9
Ethyne	0.74 ± 0.28	0.57 ± 0.13	-22.20	1.32 ± 0.42	1.00 ± 0.49	-24.3
Benzene	0.65 ± 0.20	0.56 ± 0.17	-14.20	0.95 ± 0.29	0.99 ± 0.57	**4.7**

VOCs	*Pre-LC1 2019 Mean Con +/-SD (µg/m³)*	*LC1, 2020 Mean Con +/-SD (µg/m³)*	*LC1 2019 VS 2020 Change (%)*	*Pre-LC2 2019 Mean Con +/-SD (µg/m³)*	*LC2 2020 Mean Con +/-SD (µg/m³)*	*LC2 2019VS 2020 change (%)*
Ethylbenzene	0.42 ± 0.18	0.29 ± 0.12	-29.10	0.50 ± 0.20	0.72 ± 0.45	42
m/p-Xylene	1.37 ± 0.61	0.95 ± 0.40	-29.68	1.78 ± 0.73	2.33 ± 1.46	31.1
o-Xylene	0.55 ± 0.23	0.40 ± 0.16	-25.77	0.72 ± 0.29	0.89 ± 0.57	22.2
Toluene	2.16 ± 1.15	1.36 ± 0.53	-36.34	2.59 ± 0.95	2.74 ± 1.55	**5.9**
1,2,4-TMB	0.46 ± 0.21	0.45 ± 0.17	-2.21	0.62 ± 0.24	0.75 ± 0.23	20.6
1,3,5-TMB	0.16 ± 0.07	0.13 ± 0.04	-17.64	0.27 ± 0.06	0.23 ± 0.08	-14.3

Con= Concertation, LC1= first lockdown, LC2= second lockdown, Red change(%) values indicate changes that are not statistically significant ($p \geq 0.05$).

Table 4-2 Measured mean VOCs species, pre lockdowns period 2019, lockdown period 2020 and the percentage changes of measured mean concentrations between these periods at Eltham site.

VOCs	Pre-LC1 2019 Mean Con +/-SD (µg/m³)	LC1, 2020 Mean Con +/-SD (µg/m³)	LC1 2019 VS 2020 Change (%)	Pre-LC2 2019 Mean Con +/-SD (µg/m³)	LC2 2020 Mean Con +/-SD (µg/m³)	LC2 2019VS 2020 change (%)
Ethane	4.86 ± 2.13	4.23 ± 1.55	-12.8	6.13 ± 2.67	6.33 ± 4.42	**3.4**
Propane	2.42 ± 1.38	2.18 ± 1.12	-10.0	3.75 ± 1.91	3.98 ± 3.18	**5.9**
Iso-Butane	1.32 ± 0.94	1.03 ± 0.60	-21.9	2.21 ± 1.31	2.30 ± 2.08	**4.0**
n-Butane	2.33 ± 1.48	2.05 ± 1.39	-11.9	4.13 ± 2.46	4.21 ± 3.81	**2.0**
Iso-Octane	0.07 ± 0.06	0.04 ± 0.03	-45.2	0.12 ± 0.09	0.25 ± 0.20	117.2
n-Octane	0.05 ± 0.03	0.05 ± 0.03	-7.7	0.06 ± 0.04	0.11 ± 0.06	89.3
Iso-Pentane	1.16 ± 0.91	0.96 ± 0.80	-17.5	1.47 ± 1.02	1.86 ± 2.40	26.8
n-Pentane	0.58 ± 0.46	0.47 ± 0.36	-17.9	0.73 ± 0.43	0.91 ± 1.13	25.1
n-Heptane	0.11 ± 0.07	0.17 ± 0.06	54.1	0.15 ± 0.08	0.27 ± 0.17	79.9
n-Hexane	0.24 ± 0.25	0.29 ± 0.33	22.0	0.28 ± 0.16	0.32 ± 0.29	16.7
2-Methylpentane	0.23 ± 0.16	0.25 ± 0.18	9.2	0.39 ± 0.21	0.46 ± 0.41	17.3
Ethene	0.66 ± 0.43	0.53 ± 0.25	-20.0	1.40 ± 0.68	1.66 ± 1.41	18.6
Propene	0.35 ± 0.22	0.30 ± 0.08	-14.8	0.49 ± 0.23	0.79 ± 0.70	59.4
cis-2-Butene	0.04 ± 0.02	0.03 ± 0.01	-30.4	0.07 ± 0.03	0.08 ± 0.07	16.0

VOCs	Pre-LC1 2019 Mean Con +/-SD ($\mu g/m^3$)	LC1, 2020 Mean Con +/-SD ($\mu g/m^3$)	LC1 2019 VS 2020 Change (%)	Pre-LC2 2019 Mean Con +/-SD ($\mu g/m^3$)	LC2 2020 Mean Con +/-SD ($\mu g/m^3$)	LC2 2019VS 2020 change (%)
trans-2-Butene	0.06 ± 0.02	0.03 ± 0.02	-41.4	0.08 ± 0.05	0.09 ± 0.08	9.2
trans-2-Pentene	0.03 ± 0.02	0.03 ± 0.02	7.6	0.07 ± 0.05	0.08 ± 0.08	11.3
1-Butene	0.08 ± 0.03	0.08 ± 0.02	-3.2	0.12 ± 0.05	0.16 ± 0.12	36.6
1-Pentene	0.04 ± 0.02	0.03 ± 0.01	-16.6	0.05 ± 0.02	0.06 ± 0.05	25.8
Ethyne	0.39 ± 0.20	0.30 ± 0.12	-23.1	0.52 ± 0.20	0.68 ± 0.42	31.0
Benzene	0.33 ± 0.20	0.30 ± 0.18	-10.2	0.54 ± 0.24	0.74 ± 0.53	37.2
Ethylbenzene	0.15 ± 0.09	0.14 ± 0.06	-7.7	0.26 ± 0.13	0.31 ± 0.24	19.5
m/p-Xylene	0.39 ± 0.26	0.30 ± 0.15	-23.8	0.74 ± 0.41	0.90 ± 0.78	22.4
o-Xylene	0.18 ± 0.11	0.12 ± 0.07	-30.8	0.29 ± 0.15	0.39 ± 0.32	34.4
Toluene	0.65 ± 0.36	0.49 ± 0.27	-25.7	1.17 ± 0.61	1.29 ± 0.98	10.7
1,2,4-TMB	0.12 ± 0.08	0.09 ± 0.06	-18.7	0.23 ± 0.12	0.33 ± 0.30	38.9
1,3,5-TMB	0.05 ± 0.03	0.04 ± 0.02	-19.7	0.07 ± 0.03	0.12 ± 0.10	67.5
1,3-Butadiene	0.04 ± 0.01	0.04 ± 0.01	**0.2**	0.09 ± 0.03	0.11 ± 0.08	21.6

Con= Concertation, LC1= first lockdown, LC2= second lockdown, Red change(%) values indicate changes that are not statistically significant ($p \geq 0.05$).

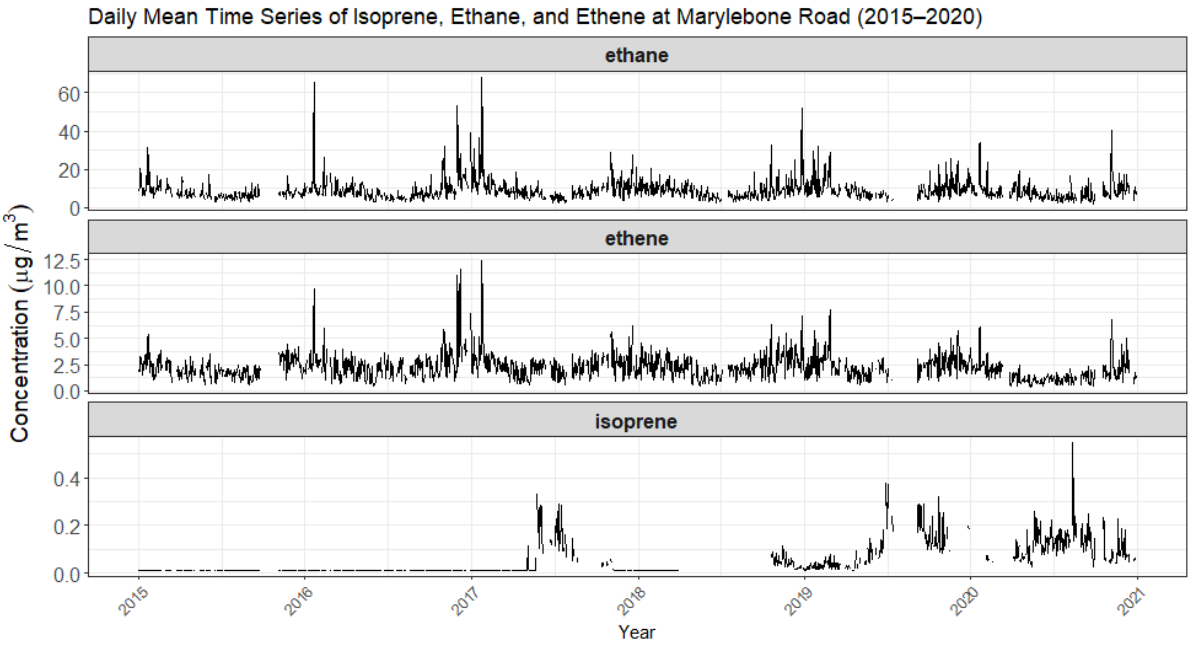

Figure 4-3 Daily mean time series of selected VOC species (isoprene, ethane, and ethene) measured at the Marylebone Road monitoring site between 2015 and 2020. Data are presented as daily averages with a 75% data capture threshold.

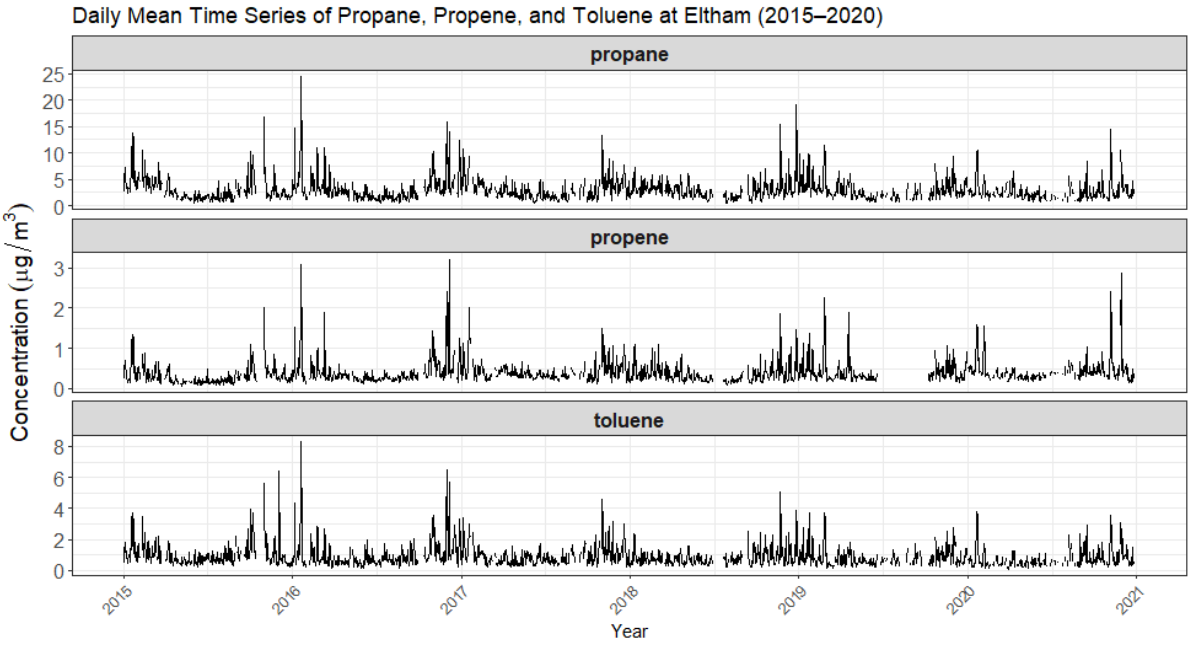

Figure 4-4 Daily mean time series of selected VOC species (propane, propene, and toluene) measured at the Eltham monitoring site between 2015 and 2020. Data are presented as daily averages with a 75% data capture threshold.

4.2.3 Data processing

The concentration arithmetic mean of each measured VOC was calculated for each UK lockdown period based on the VOCs' daily average, where VOCs daily means were calculated with a 75% data capture threshold . This means that at least 75% of the data in each day should be available and ratified, otherwise, the VOC mean concentration of that day will be ignored and not used in calculating the VOC arithmetic mean during any time scale. The arithmetic means of VOCs concentrations of each UK lockdown interval (first lockdown 23rd March 2020 to 23rd June 2020, second lockdown 5th November 2020 to 2nd December 2020), were then compared with the arithmetic mean VOC concentration at the same period between 2015 and 2019 to evaluate the historical change in VOCs concentrations due to UK lockdown measures. In addition to the arithmetic mean, the standard deviation (SD) of daily VOC concentrations was calculated for each period to characterise the natural of VOCs data, in order to evaluate whether the observed differences between lockdown and baseline conditions exceed the natural temporal scatter (Singh et al., 2023). Moreover, the statistical significance of the observed changes was evaluated using hypothesis testing, with a significance level of $p < 0.05$. Percentage change (%) values associated with $p \geq 0.05$ were classified as statistically non-significant, indicating that the observed differences fall within the natural variability of the dataset, hence, differences associated with $p < 0.05$ provide statistical evidence of lockdown-related effects (Çalik & Çetin Doğruparmak, 2024; do Nascimento et al., 2022).

Only those hourly average VOC concentrations associated with valid meteorological variables were used in evaluating the relationship between the meteorological conditions and the VOC levels. However, the highest daily 1% of values (99th percentile) for each VOC was excluded to avoid the undesirable influence of outliers on the model outcomes.

4.2.4 Trend analysis

A comparison between mean VOC concentrations during the two lockdown periods and their mean concentration over the previous five years minimises the probability of concentration changes due to the meteorological condition variation rather than the emission changes (Grange et al., 2021). However, it does not consider, or at least underestimates, the effects of the general trend in these concentrations particularly for measured pollutants at the Marylebone Road monitoring site, where these pollutants are expected to generally have a uniform decreasing trend as this site is highly influenced by traffic emissions that have been

strictly reduced by legislation since the late nineties of the last century (Lewis et al., 2020; Vaughan et al., 2017), leading to a steady downward trend in their levels over the last three decades.

However, this simplified analysis assumes that these uniform and linear trends will continue in the absence of any unexpected disruptions and based on various logical factors. These include the increased use of the electrical cars, the reduction in the number of old highly emitted vehicles on road, and the expansion of the ULEZ (Mayor of London, 2023). Furthermore, the shift toward more reliance on clean (heat pumps) and renewable energy sources (wind and solar sources) as the main heat and power provider (Mayor of London, 2025), which reduces fossil fuel combustion-related VOCs emissions. Finally, the continuous improvement of industrial pollution control and fugitive emissions technologies that reduce VOCs emissions from these sources.

In this study, we calculated the observed trend in individual VOCs, by examining their mean concentrations of the lockdown intervals over the last five years (the same period that was used when evaluating the historical changes in VOCs levels due to lockdown measures). We then assessed the timeframe required for the VOCs general trend to naturally reach the same VOC concentrations that were observed during the lockdown periods. We also assessed the mean concentration of each VOC in the following two years after the lockdown to evaluate post-lockdown recovery and to determine whether VOC concentrations returned to their normal declining trend, to assess if lockdown restrictions had a short term effect of VOCs levels, or if the VOCs lockdown levels were retained which may indicate to a shift in VOCs emission prior to lockdown measures.

4.2.5 Meteorological variables' effects on the VOCs levels over the last five years

The influence of meteorological conditions on air pollutant levels should not be underestimated, as they often have a more significant impact than pollution control efforts in many cases (Anh et al., 1997). From this perspective, it is essential to analyse the role of meteorological variables in the variation of VOC concentrations. This influence cannot be handled as one unit as we are dealing with almost 29 different species emitted from various sources, where the meteorological variables can affect the levels of each of these VOCs differently through their transportation, transformation, dispersion, and deposition. A

random forest model (RF), a non-parametric machine learning-based model (Breiman, 2001) (Tong et al., 2003), was used to explain how VOCs concentrations partially depend on different variables (air temperature, wind direction, relative humidity, wind speed, and boundary layer height). These variables were considered the explanatory ones (predictor variables).

Unlike other machine learning methods, such as kernel or artificial neural networks, the learning procedure of the RF can be explicated, tested, and interpreted (Kotsiantis, 2013). In RF, the observation data splits into pairs of homologous sets creating “pure” nodes by utilizing a bilateral recursive algorithm for classification. Then the purity of the nodes can be accomplished by repeating the splitting process, which is the core of the recursive algorithm. Each split creates a branch/node, and all splits accumulatively form the tree. The greedy nature of this recurrent algorithm aims to maximize node purity at each split, leading to a large tree where only a pair of observations is evaluated as a result of the last split (Biau et al., 2008). This called a “singleton node” which can lead to overfitting issue, where models will infrequently introduce to novel data that was not used in the training process. However, the RF minimises this issue by growing various single decision trees out of the training observations by bootstrap aggregation process known as bagging. Bagging is the random selection of observations with replacement from the training data as well as the selection of explanatory factors (Bbeiman, 1996). This process generates “in-bag” samples for training each tree and leaves out a portion known as out-of-bag data (OOB). While each tree is trained only on its respective in-bag sample, the OOB data serves as an internal validation set to estimate the forest's generalization error (Caruana, 2006). All of the individual trees (learner) outputs generated from the bagged observations by the RF model contribute to the prediction results. Hence, hundreds of trees, trained on different sub-groups out of the training group, together constitute a forest. Each tree has its own prediction, and combined predictions contribute to a sole prediction utilizing the mean predictions. This regression algorithm tackles the RF’s training set overfitting issue, normalising the predictive models and making RF one of the most reliable ML methods (Caruana, 2006).

Using RF method, we analysed the effect and the importance of the explanatory variables on the levels of four VOCs: ethane, ethene, i-pentane, and toluene, between 2015 and 2019 using the programming language R (rmweather package, version 0.2.4). The partial

dependence analysis explains the relationships between variables, allowing the importance of each predictor variable to be specified (Grange et al., 2018).

4.2.6 Business as usual scenario

In order to evaluate the actual influence of the lockdown measures on VOC concentrations, one first of all needs to eliminate the contribution of meteorological conditions in order to calculate a Business-as-usual (BAU) scenario (what VOC concentrations would have been if lockdowns had not occurred). VOC concentrations were projected by RF models. These models were trained over a pre-lockdown period of five years from 01/01/2015 to 31/01/2020; this extended training period enabled the model to analyse and capture the variation in VOC concentrations based on the variation in the explanatory variables, and the trained model was then used to predict BAU VOC concentrations during the lockdown periods.

We then compared the actual and predicted VOC concentrations to calculate the changes in VOC levels which could be attributed to the lockdown measures. The models' performance was statistically examined and validated over one month; 01/02/2020 to 28/02/2020, the last month before the formal lockdown measures were enforced, by comparing the predicted against the observed VOCs daily mean concentrations. Only VOC species whose daily mean predicted and measured concentrations achieved an $R^2 \geq 0.5$ were used to predict the BAU levels during the two lockdown periods, this ensured that predicted levels could be compared confidently with measured ones.

The meteorological explanatory variables (wind speed, wind direction, boundary layer height, relative humidity, atmospheric pressure, and air temperature), included in the model inputs were chosen based on their importance to the variation in VOCs concentrations, while variables with negligible influence during the five-year period were excluded.

Additionally, the hour of the day, the day of the week, the seasonal term (Julian day, ranging from 1 to 365), and the trend term (Unix time, providing a continuous and absolute measure of time since 1 January 1970 [UTC]). were included in this analysis.

4.3 Results and Discussions, Marylebone Road

4.3.1 VOCs Historical Change

Table 4-3 illustrates how VOC concentrations were radically affected by the UK's first lockdown measures at Marylebone Road. There was a substantial drop in total VOCs concentrations by 8.74 µg/m^3, which is equal to a 25.6% reduction. The majority of VOCs species has recorded a considerable reduction in their levels, compared to their mean concentrations of the same period over the last five years, varying between 9.3% and 58%.

Alkanes, those mainly emitted from traffic-related sources, both exhaust and evaporative emissions (i/n-pentane, i/n-octane, and n-heptane) (B. Li et al., 2017) were reduced by about 40% to 60%. Isopentane observed the highest reduction level in what concerns the absolute change at 1.33 µg/m^3 accounting for a 48.9% decrease in its level, while 2-methyl pentane, a VOC tracer for gasoline-powered exhaust emissions (Ho, Lee, Ho, Blake, Cheng, Li, Ho, et al., 2009) recorded the highest reduction percentage among all VOCs at 58% corresponding to a 0.48 µg/m^3 drop in its absolute concentration.

Aromatics, the most abundant tailpipe VOCs emission from gasoline-powered vehicles (Arslan, 2020), varied between a 28.5% to 41.6% reduction, close but did not reach the reduction percentages of the traffic-related alkanes. This could be due to the contribution of other combustion and/or solvent sources to the aromatic levels, as non-methane hydrocarbons emissions from the solvent production and use sector have become the most critical VOCs source recently in the UK (Ricardo Energy & Environment, 2020). Alkenes showed lower reductions than traffic-related alkanes, ranging between 9.3% to almost 36% decrease.

Alkanes emitted from natural gas (NG) related sources; propane and i/n butane (CRS Reports, 2020) were reduced by only by 19.5% to 32% which was relatively low when compared with the reduction levels in other alkanes.

Ethane, cis- and trans-2-butene, all are non-traffic related VOCs, were the only species that showed increases in concentration during the first lockdown period. Ethane is emitted mainly from the distribution, production, and consumption of natural gas (Franco et al., 2016), while butenes could be emitted from biogenic sources (L. Li et al., 2015). Although cis-2-butene

concentration increased by 60 %, its absolute change was only 0.03 µg/m^3. Similarly, a 0.01 µg/m^3 increase in trans-2-butene levels corresponds to a 15% increase in its concentration.

Both alkenes and aromatics species have high consideration in the ozone potential formation (OPF) due to their key role in the propagation of radicals and their reactivity with OH (Pinthong, Thepanondh, Kultan, et al., 2022). Alkenes rapidly oxidise by OH forming peroxy radicals (RO_2) eventually forming ozone throughout NOx cycle (Atkinson & Arey, 2003). While aromatics produce ozone precursors such as ketones and aldehydes due their oxidation process via OH radicals producing oxygenated VOCs (Calvert et al., 2002). The maximum incremental reactivity (MIR) value that directly related to species reactivity, explain the importance of the species in the ozone photochemical formation. propene (an alkene) has an MIR value of about 11.5, toluene (an aromatic) has an MIR value around 4, while propane (alkane) MIR value is only about 0.5 (Zou et al., 2021).

The results show that the first lockdown measures have had a significant impact on the VOCs levels at the road traffic site due to the significant drop in the land transport activities. All observed changes during the first lockdown were statistically significant ($p < 0.05$), indicating that the reductions exceeded the natural variability of the dataset and reflect a robust response to emission changes.

The second lockdown measures in the UK, as shown in Table 4-4, had less obvious effects on the total (sum) VOCs mean concentration at the urban traffic site dropping only by 0.86 µg/m^3 compared to their total mean concentration during the same period over the last five years, which is equal to a 1.86% reduction. The total reduction in VOCs levels, however, was weakened by the increase of the highly weighted NG-related VOCs, ethane, and propane, where the absolute increase of these two species equalled 2.14 µg/m^3.

There was a moderate reduction in traffic-related alkane concentrations ranging between 9% and 40%. As was the case in the first lockdown, iso pentane recorded the highest absolute reduction in its mean concentration by 0.75 µg/m^3. While 2-methyl pentane again recorded the highest proportional reduction of 42.6%. These findings highlight the decline in land transport activities, as these two VOCs are associated with traffic-related evaporative and exhaust emissions, respectively.

The drop in alkene levels was relatively similar to the alkanes case, ranging between 14% and 37%. A relatively small reduction in the mean concentration of aromatics was observed as well. Some aromatics (ethylbenzene, m-p xylene, and o-xylene) observed modest increase in their levels. Similarly, few alkenes such as propene and cis/trans-2-Butene showed increases in their mean concentrations. However, changes in iso-octane, propene, trans-2-butene, trans-2-pentene, and o-xylene during the second lockdown were statistically insignificant ($p \geq 0.05$), suggesting that these variations fall within the natural variability of the dataset and should be interpreted with caution.

The observed increase in the concentrations of ethane and propane during the second lockdown could be due to the enforced lockdown measures resulted in an increased number of individuals working from home, leading to heightened heating demands across residential areas. Additionally, the long atmospheric lifetimes of both ethane and propane compared to other VOCs could contribute to their elevated levels. This extended atmospheric persistence facilitates their transportation over wider geographical areas, amplifying the influence of domestic sources.

Table 4-3 Percentage and Absolute Change in VOCs Concentrations Due to 2020 First Lockdown Measures Compared to Their Mean Concentrations of the Same Period Between 2015 to 2019 at Marylebone Road.

VOCs	First Lockdown Period 2015-2019 Mean Con +/-SD (µg/m^3)	First Lockdown 2020 Mean Con +/-SD (µg/m^3)	Absolute Change (µg/m^3)	Change (%)
Ethane	7.41 ± 2.62	7.57 ± 3.11	0.15	2.09
Propane	4.40 ± 1.82	3.54 ± 1.90	-0.86	-19.52
Iso-Butane	2.08 ± 1.14	1.49 ± 0.78	-0.58	-28.11
n-Butane	3.72 ± 2.03	2.52 ± 1.33	-1.19	-32.09
Iso-Octane	0.36 ± 0.18	0.19 ± 0.07	-0.17	-46.68
n-Octane	0.21 ± 0.13	0.12 ± 0.04	-0.09	-43.53
Iso-Pentane	2.73 ± 1.72	1.40 ± 0.75	-1.33	-48.87
n-Pentane	1.08 ± 0.58	0.64 ± 0.32	-0.45	-41.25
n-Heptane	0.38 ± 0.28	0.18 ± 0.06	-0.2	-52.07
n-Hexane	0.35 ± 0.19	0.26 ± 0.22	-0.09	-25.01
2-Methylpentane	0.83 ± 0.55	0.35 ± 0.18	-0.48	-58.32
Ethene	1.83 ± 0.75	1.04 ± 0.39	-0.79	-42.95
Propene	0.89 ± 0.33	0.80 ± 0.35	-0.08	-9.49
cis-2-Butene	0.05 ± 0.05	0.08 ± 0.02	0.03	59.83

trans-2-Butene	0.08 ± 0.07	0.09 ± 0.03	0.01	14.91
trans-2-Pentene	0.09 ± 0.07	0.06 ± 0.02	-0.03	-36.68
1-Butene	0.24 ± 0.11	0.21 ± 0.06	-0.02	-10.24
1-Pentene	0.08 ± 0.05	0.06 ± 0.02	-0.02	-27.15
Ethyne	0.76 ± 0.34	0.57 ± 0.13	-0.19	-24.58
Benzene	0.78 ± 0.31	0.56 ± 0.17	-0.22	-28.61
Ethylbenzene	0.46 ± 0.23	0.29 ± 0.12	-0.17	-36.15
m/p-Xylene	1.61 ± 1.01	0.95 ± 0.40	-0.66	-40.84
o-Xylene	0.59 ± 0.30	0.40 ± 0.16	-0.19	-32.26
Toluene	2.35 ± 1.14	1.36 ± 0.53	-0.99	-42.13
1,2,4- TMB	0.56 ± 0.46	0.45 ± 0.17	-0.11	-19.64
1,3,5- TMB	0.22 ± 0.15	0.13 ± 0.04	-0.08	-38.45
Total VOCs	34.14 ± 4.79	25.40 ± 4.15	-8.74	-25.6

Red change(%) values indicate changes that are not statistically significant ($p \geq 0.05$).

Table 4-4 Percentage and Absolute Change in VOCs Concentrations Due to 2020 Second Lockdown Measures Compared to Their Mean Concentrations of the Same Period Between 2015 to 2019 at Marylebone Road.

VOCs	Second Lockdown Period 2015-2019 Mean Con +/-SD (µg/m^3)	Second Lockdown 2020 Mean Con +/-SD (µg/m^3)	Absolute Change (µg/m^3)	Change (%)
Ethane	10.43 ± 5.97	11.56 ± 7.10	1.34	12.80
Propane	6.57 ± 3.36	7.25 ± 4.83	0.79	12.15
Iso-Butane	3.14 ± 1.60	2.85 ± 1.95	-0.29	-9.29
n-Butane	5.40 ± 2.50	4.88 ± 3.44	-0.52	-9.67
Iso-Octane	0.42 ± 0.21	0.41 ± 0.20	0.01	**-0.64**
n-Octane	0.24 ± 0.18	0.20 ± 0.09	-0.04	-15.68
Iso-Pentane	2.88 ± 1.43	2.14 ± 1.31	-0.75	-25.89
n-Pentane	1.30 ± 0.58	1.00 ± 0.60	-0.28	-22.99
n-Heptane	0.48 ± 0.25	0.38 ± 0.22	-0.08	-20.55
n-Hexane	0.43 ± 0.23	0.36 ± 0.21	-0.07	-16.71
2-Methylpentane	1.04 ± 0.84	0.60 ± 0.38	-0.44	-42.61
Ethene	2.96 ± 1.28	2.38 ± 1.48	-0.57	-19.38
Propene	1.27 ± 0.36	1.28 ± 0.66	0.02	**1.22**
cis-2-Butene	0.08 ± 0.04	0.10 ± 0.03	0.02	20.3
trans-2-Butene	0.12 ± 0.08	0.12 ± 0.04	0.00	**-0.75**
trans-2-Pentene	0.13 ± 0.09	0.08 ± 0.05	-0.05	-38.83
1-Butene	0.32 ± 0.16	0.26 ± 0.12	-0.05	-17.36
1-Pentene	0.08 ± 0.04	0.07 ± 0.03	-0.01	-16.28
Ethyne	1.24 ± 0.52	1.00 ± 0.49	-0.24	-19.46
Benzene	1.11 ± 0.48	0.99 ± 0.57	-0.12	-10.58
Ethylbenzene	0.65 ± 0.34	0.72 ± 0.45	0.07	11.05

m/p-Xylene	2.11 ± 1.12	2.33 ± 1.46	0.22	10.61
o-Xylene	0.86 ± 0.44	0.89 ± 0.57	0.03	**3.05**
Toluene	3.11 ± 1.61	2.74 ± 1.55	-0.37	-11.86
1,2,4- TMB	0.81 ± 0.43	0.75 ± 0.23	-0.06	-7.2
1,3,5- TMB	0.31 ± 0.15	0.23 ± 0.08	-0.07	-23.83
Total VOCs	47.49 ± 8.53	46.63 ± 8.09	-0.86	-1.86

Red change(%) values indicate changes that are not statistically significant ($p \geq 0.05$).

4.3.2 Trend analysis

The trend analysis results show that the measured mean concentration of ethene, a VOC mainly emitted from diesel- and petrol-powered vehicle tailpipes (Morgott, 2015), declined significantly during the first lockdown period. When projected against the long-term trend (2015-2019), this reduction corresponds to concentration levels that would not have been expected until 2038, as shown in Figure 4-5, reflecting the massive drop in traffic activities. Surprisingly, during the equivalent lockdown period in 2021, there was a considerable increase in observed mean ethene concentration, exceeding the corresponding five-year baseline. This increase was driven by 11 unusual high concentrations measurements ranging between 4 µg/m^3 and about 10 µg/m^3, indicating episodic pollution events, which could be due to short-term traffic congestion, low dispersion conditions, or potential analyser data quality/sensitivity issue. This was confirmed by the median ethene concentration in 2021, as it remained marginally lower than the long-term trend, indicating that the overall distribution was not significantly shifted and that the elevated mean was disproportionately influenced by these extreme values. Conversely, ethene levels in 2022 displayed a marginal decline, deviating slightly from the prevailing trend.

The mean concentration of iso-pentane during the first lockdown in 2020 was forecasted to occur in 2025. Similarly, the mean concentration of toluene was projected to occur in 2024. Both toluene and iso-pentane levels in 2021 and 2022 returned to normal, following their general downward trends. Cis/trans-2-butene, the only alkenes that showed an increase in their levels during the first lockdown had very scattered distribution between 2015 and 2019, which explains why the trend analysis was not applicable to them.

Ethane showed a slight upward trend, primarily driven by a lower mean concentration observed in 2015, which explains the slight increase in its mean concentration during the first lockdown, However, it is worth noting that the ethane concentration in both 2018 and 2019

was nearly comparable to that observed during the lockdown. Notably, the mean concentrations of ethane in 2021 and 2022 declined, deviating from the previously established trend.

Hence, we can recognise the importance of the historical trend analysis in evaluating the impact of the Lockdown measures on the VOCs levels. The observed decrease in Ethene level during the first lockdown, associated with a 42.7% reduction, was predicted to occur almost after 20 years following its general downward trend. In contrast, 48.5%, and 41.6% drop in iso-Pentane and Toluene levels was equal only to five and four years, respectively, of their expected gradual decrease following their general backward trend. A 28.5% drop in benzene concentration was a normal result of its general downward trend suggesting that benzene was not significantly affected by the lockdown measures. Ethylbenzene mean concentration during the first lockdown was reduced by 35.2%, which was originally projected to occur in 2024 if the UK's first lockdown measures had not been implemented.

On the other hand, the trend analysis of the second lockdown has confirmed the weak correlation between the VOCs concentrations and the second lockdown implemented measures. Among analysed VOCs species, only ethene observed a decline greater than expected during the second lockdown period following its general backword trend. The 2020 ethene level was originally forecasted to take place in 2029, indicating a rapid reduction. However, ethene's mean concentrations over the last five years exhibited only slight variability compared to the first lockdown ones.

Following their general backward trends, iso pentane, and toluene were projected to have relatively lower mean concentrations during the second lockdown period rather than what were actually observed, likely influenced by a few elevated daily mean values during the lockdown. Similarly, benzene levels were affected in the same way.

In contrast, the high increase in ethane level, by 1.34 $\mu g/m^3$, during this lockdown, was a normal result of its historical forward trend.

This finding emphasises the difference in VOCs response to the lockdown interventions and highlight the importance of considering the historical trend analysis in differentiating between normal air pollutants variability and external measures related ones.

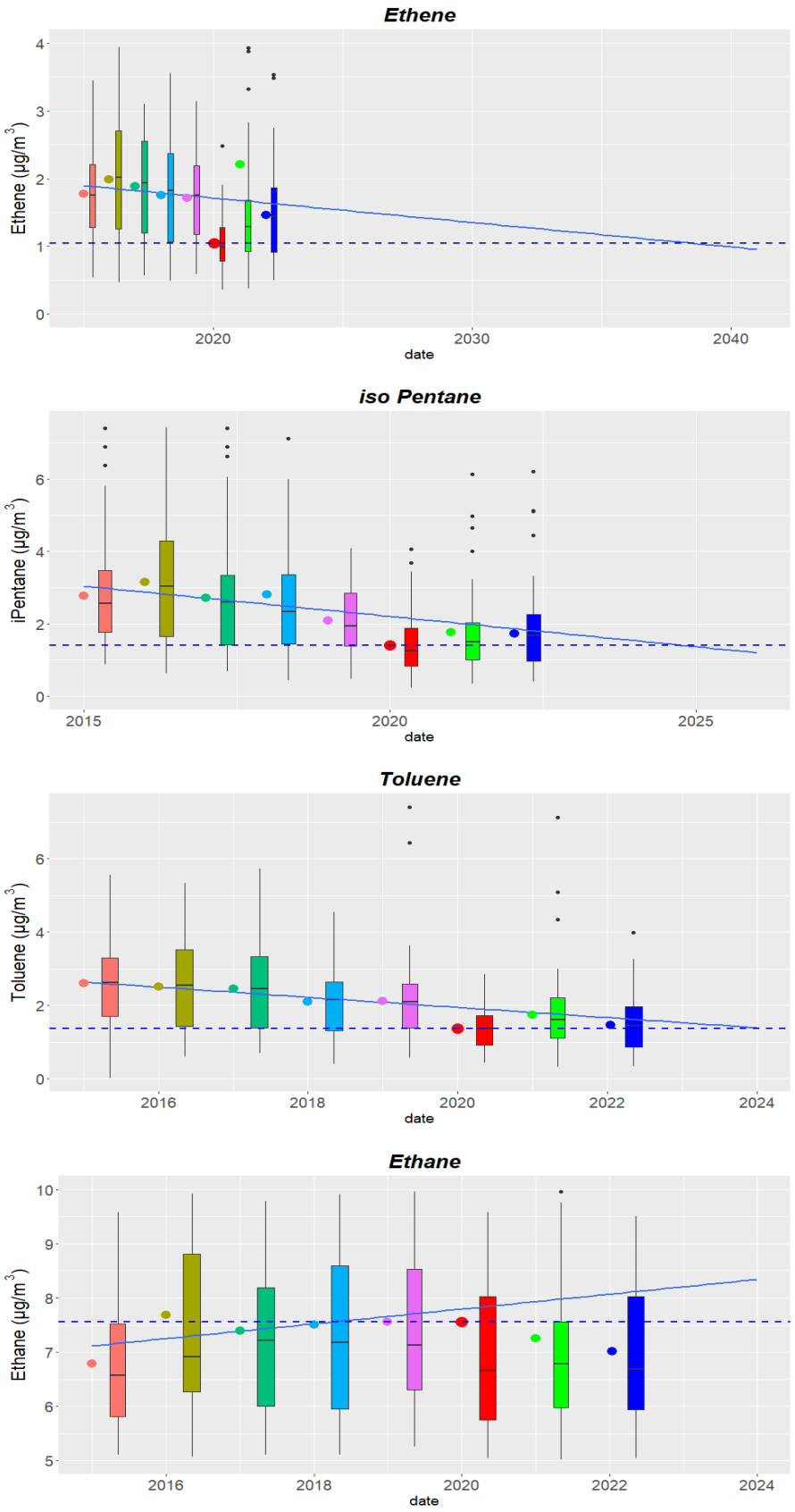

Figure 4-5 Marylebone Road , First Lockdown Trend analysis, Boxplots present daily means VOCs distributions, Red colour 2020 lockdown1, Coloured dots are VOCs mean concentrations, Solid blue line is the VOC historical trend, Doted blue line is lockdown1 mean concentrations level.

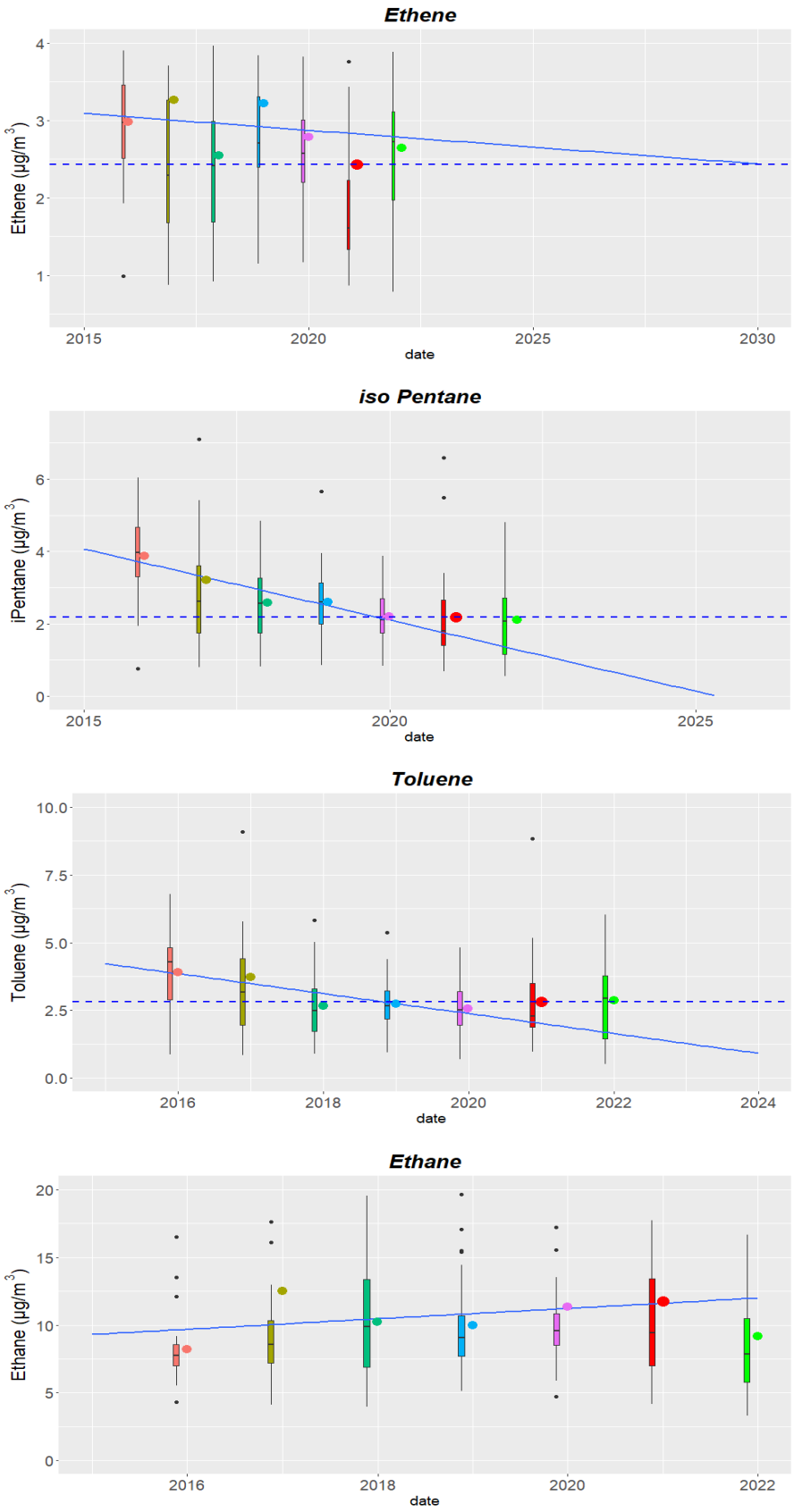

Figure 4-6 Marylebone Road, Second Lockdown Trend analysis, Boxplots present daily means VOCs distributions, Red colour 2020 lockdown2, Coloured dots are VOCs mean concentrations, Solid blue line is the VOC historical trend, Doted blue line is lockdown2 mean concentrations level.

4.3.3 Meteorological variables' effects on the VOCs levels

The results of the random forest analysis at London Marylebone Road revealed that air temperature was the most important variable in explaining the variation in iso-pentane and toluene levels, followed by the seasonal term (Julian day). For toluene, the seasonal term and wind direction contributed roughly equally to explaining its variability, whereas for iso-pentane the seasonal term had substantially greater weight than wind direction. For ethene, the seasonal term was the most crucial variable in predicting its concentrations, followed by the wind direction, and the boundary layer height Figure 4-7. The most heavily weighted variable in explaining the variation in Ethane levels during these five years was the boundary layer height, obtained from the ERA5 reanalysis for the monitoring site area (Hersbach et al., 2026), followed by air temperature and Julian day, with these two variables showing relatively similar importance.

Apart from ethane, where the cloud height variable was more important than the weekday in explaining the variation of its concentrations, the cloud cover, and the height of the cloud above the ground level had negligible importance to the levels of studied VOCs. Therefore, these two variables were excluded when predicting BAU concentrations in the next section. The importance of the rest of the tested variables varied between these VOCs. Although air temperature had a critical impact on some VOCs, it did not have the same type of effects on all of them. Iso Pentane concentrations recorded the lowest levels between -5 to 10 °C and then had a positive correlation with air temperature, hitting a top at 35 °C Figure 4-8. This was expected, as iso-pentane is mainly emitted from evaporative traffic-related sources. In contrast, ethane levels peaked at the lowest recorded temperature, having a reverse proportion with the air temperature between -5 and 15 and then levelled off. The nature of this relationship is due to the increase of NG (the primary atmospheric source of ethane) consumption, production, and distribution processes during the cold seasons. Ethene concentrations, a vehicle exhaust pollutant, peaked at -5°C under stable atmospheric conditions, where the convective vertical mixing is negligible. Ethen levels then showed a steady inverse relationship with temperature until reaching their lowest levels at 5 °C, followed by a gradual positive correlation between 10 to 30 °C. This positive correlation was unexpected but may be explained by the street canyon effects at this location. The relationship between the toluene levels and the air temperature was similar to the Ethene

between -5 to 5°C. However, there was a sharp increase in Toluene concentrations starting from 10°C, where these concentrations peaked at 30°C and then levelled off. The contribution of two key sources to the toluene levels at this site can explain this pattern; 1- traffic emissions, those levels increase under low air temperature (stable atmospheric conditions), and 2- the solvent sources, where the emissions increase by the increase of the air temperature.

The wind speed, despite its importance level, had a consistent effect across the four VOCs, all of them showed a negative correlation with wind speed up to 10 m/s, after which concentrations levelled off or gradually decreased, indicating the dominance of local emission sources. Similarly, the wind direction had the same impact on these VOCs concentrations; although the monitoring site is located on the southern side of the road, the highest concentrations were recorded when the wind blew between the East and SWW directions, which can be a result of the complexity of the street canyon environment where the pollutants are subjected to leeward accumulation and other complex flow dynamics (Grange & Carslaw, 2019).

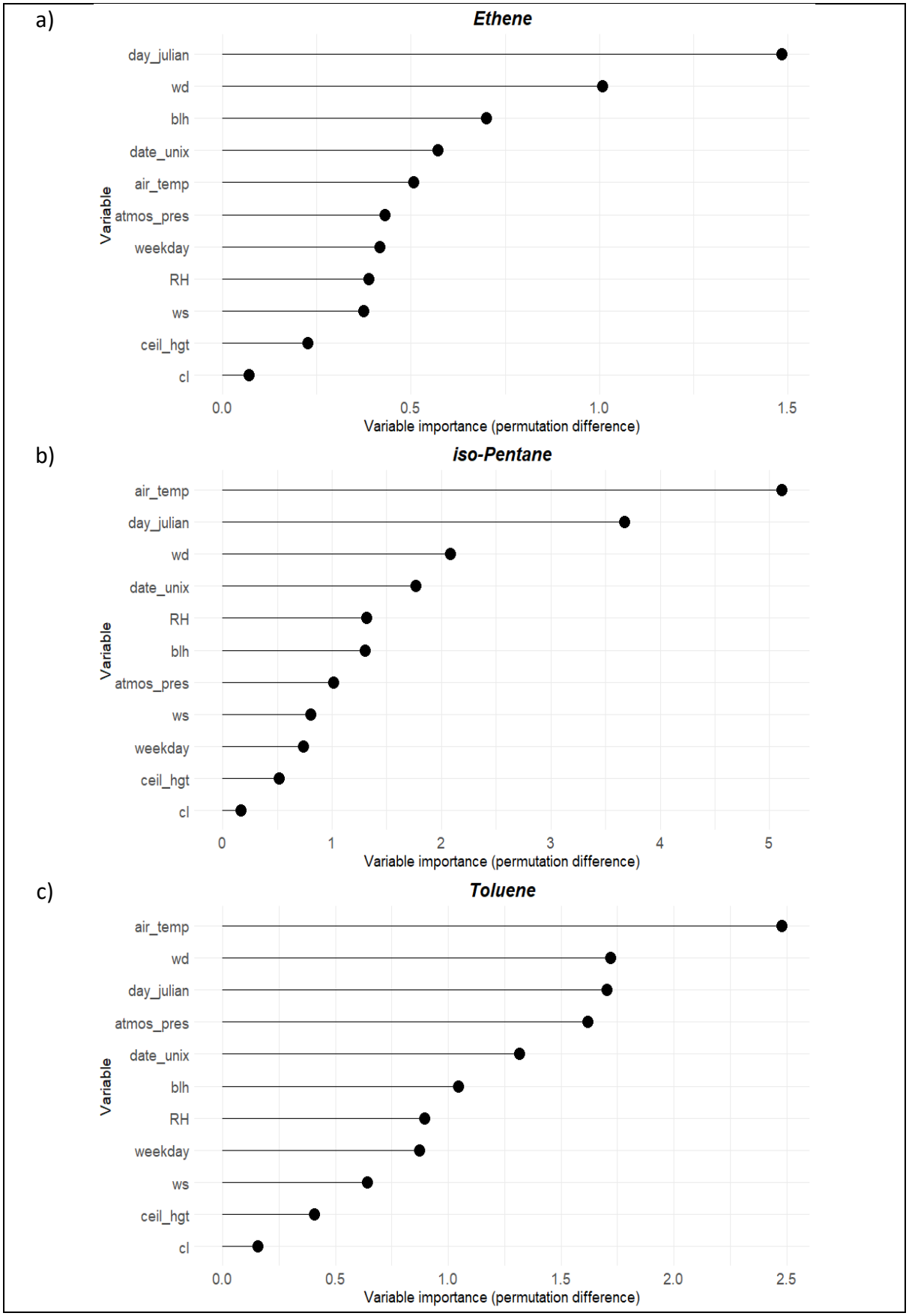
a)
Ethene
day_julian
wd
blh
date_unix
air_temp
atmos_pres
weekday
RH
ws
ceil_hgt
cl
Variable
0.0
0.5
1.0
1.5
Variable importance (permutation difference)
b)
iso-Pentane
air_temp
day_julian
wd
date_unix
RH
blh
atmos_pres
ws
weekday
ceil_hgt
cl
Variable
0
1
2
3
4
5
Variable importance (permutation difference)
c)
Toluene
air_temp
wd
day_julian
atmos_pres
date_unix
blh
RH
weekday
ws
ceil_hgt
cl
Variable
0.0
0.5
1.0
1.5
2.0
2.5
Variable importance (permutation difference)

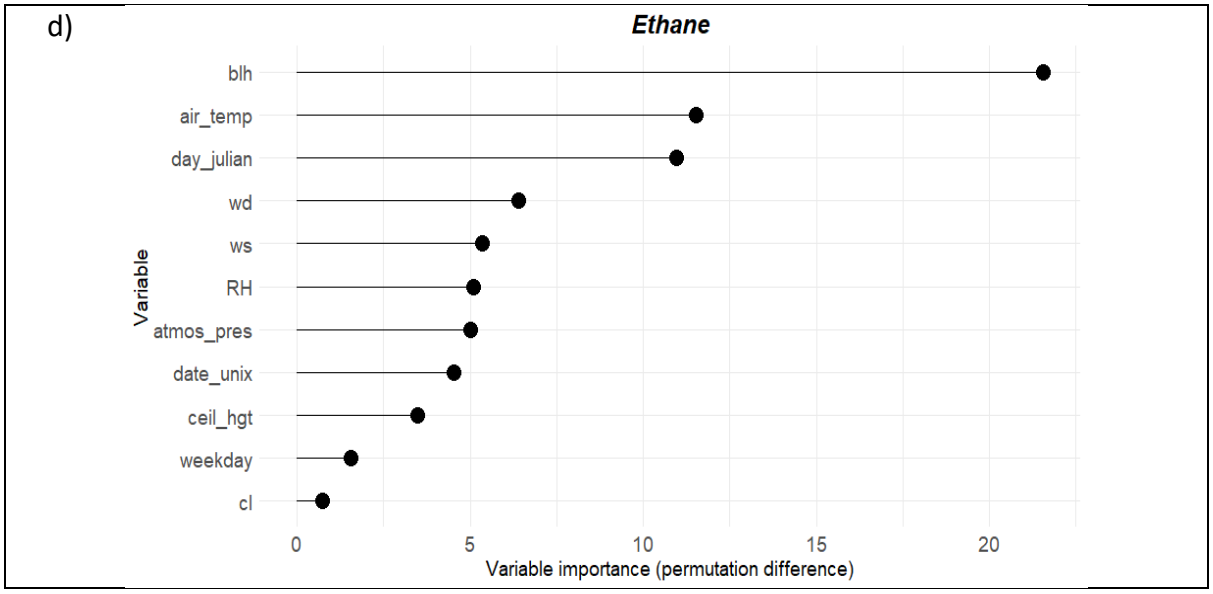

Figure 4-7 Variables importance to VOCs levels at Marylebone Road (2015-2019) . Predictor variables: day of year (day_julian), day of the week (weekday), timestamp (date_unix), wind direction (wd), wind speed (ws), boundary layer height (blh), air temperature (air_temp), atmospheric pressure (atmos_pres), relative humidity (RH), ceiling height (ceil_hgt), and cloud cover (cl). Panels show: (a) ethene, (b) isopentane, (c) toluene, and (d) ethane.

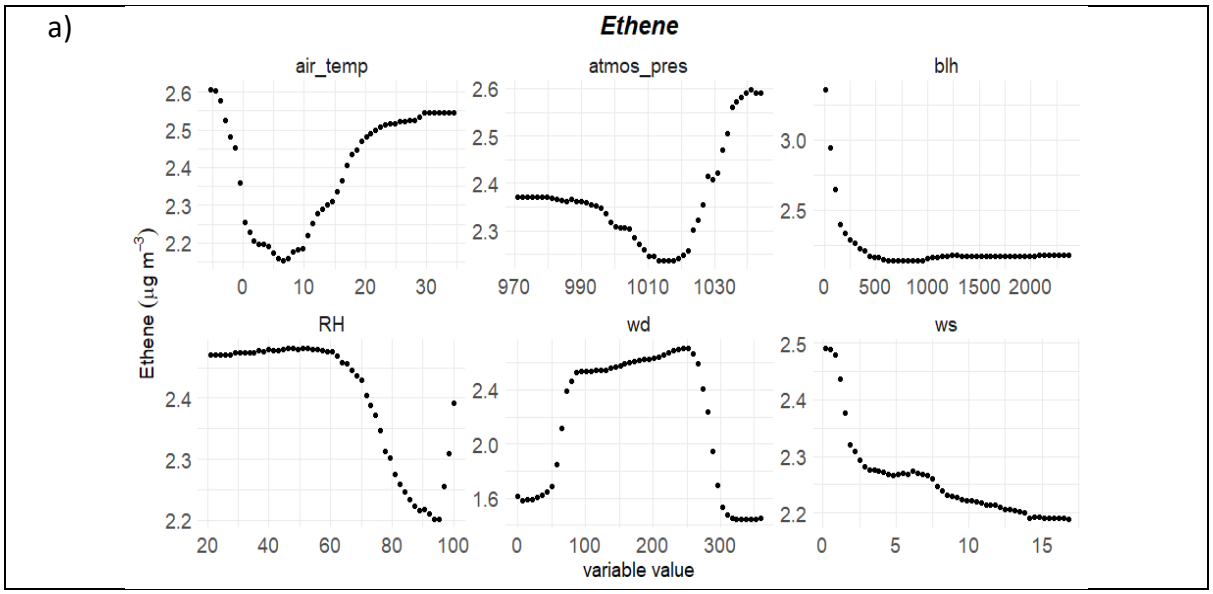

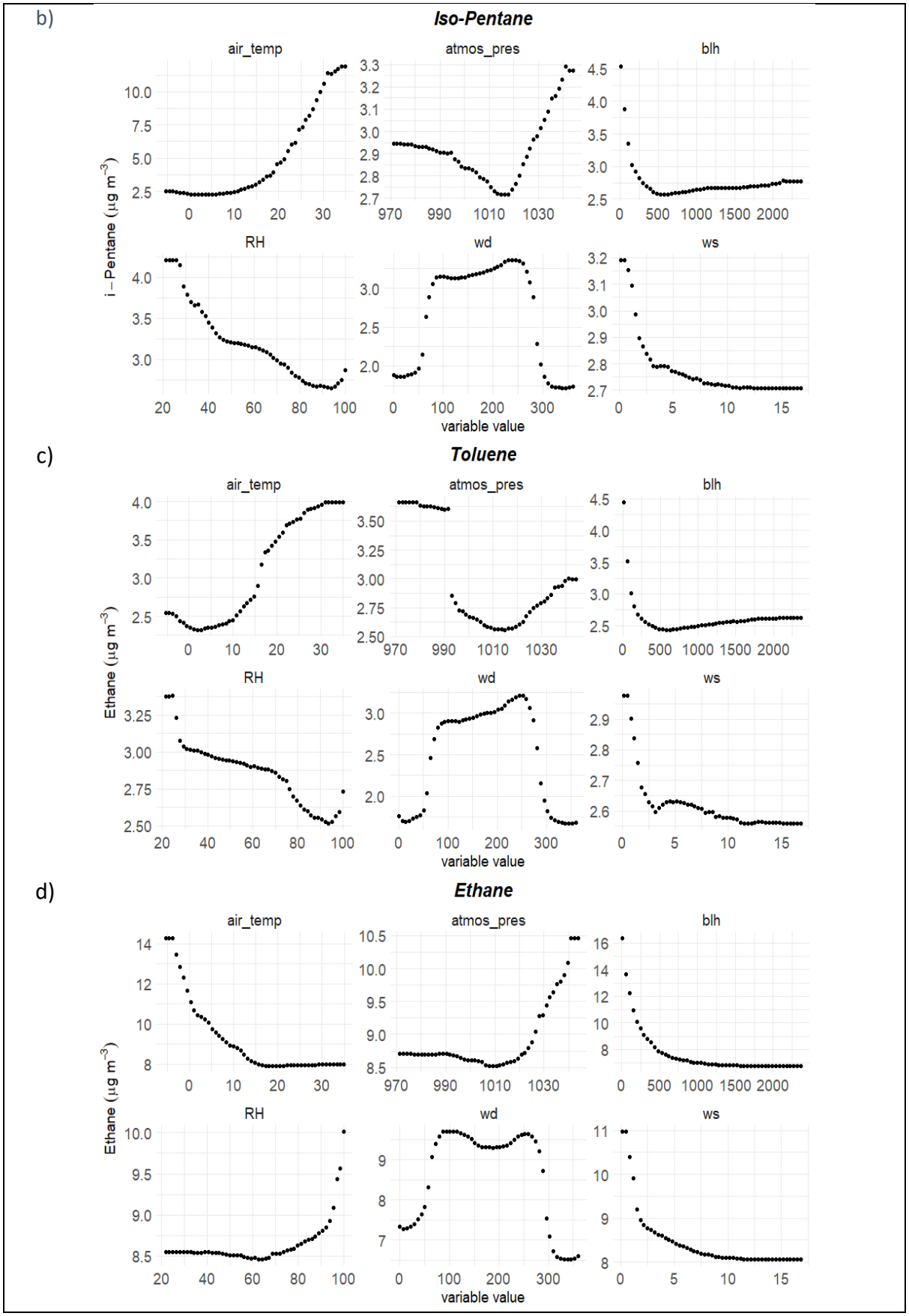

Figure 4-8 Partial dependent plots showing the relationship between selected VOCs concentrations and key meteorological variables at the Marylebone Road site (2015-2019). Y-axis represents the modelled VOC concentration (µg m^3), and X-axis shows the range of each predictor variable.

4.3.4 Business as usual scenario

In general, the model in the validation stage overpredicted the VOCs daily mean concentrations. During the validation month, the mean concentrations of the most abundant measured VOCs, including ethene, iso-pentane, toluene, benzene, ethane, propane, propene, ethyne, n-butane, iso-butane, n-pentane, m+p-xylene, and 2-methyl pentane, exhibited a tendency to be higher than the actual measurements. The magnitude of overestimation ranged from 0.01 to 0.75 µg/m^3, which represents a range of 0.17 to 18.4 per cent at 95% confidence intervals. This overpredicting trend in the model's performance could be due to two substantial reasons. The first one, is related to the variability of the meteorological variables, as February 2020 had the highest mean and median wind speed distribution compared to the whole training period as shown in Figure 4-9. The second one is the drop in social and industrial activities in February, even before the enforcement of the lockdown, leading to a reduction in the observed concentrations. We considered these two reasons were only applicable during the validation period, and they were not applicable during the prediction period. Therefore, these offsets were not corrected for the predicted VOCs daily mean concentrations.

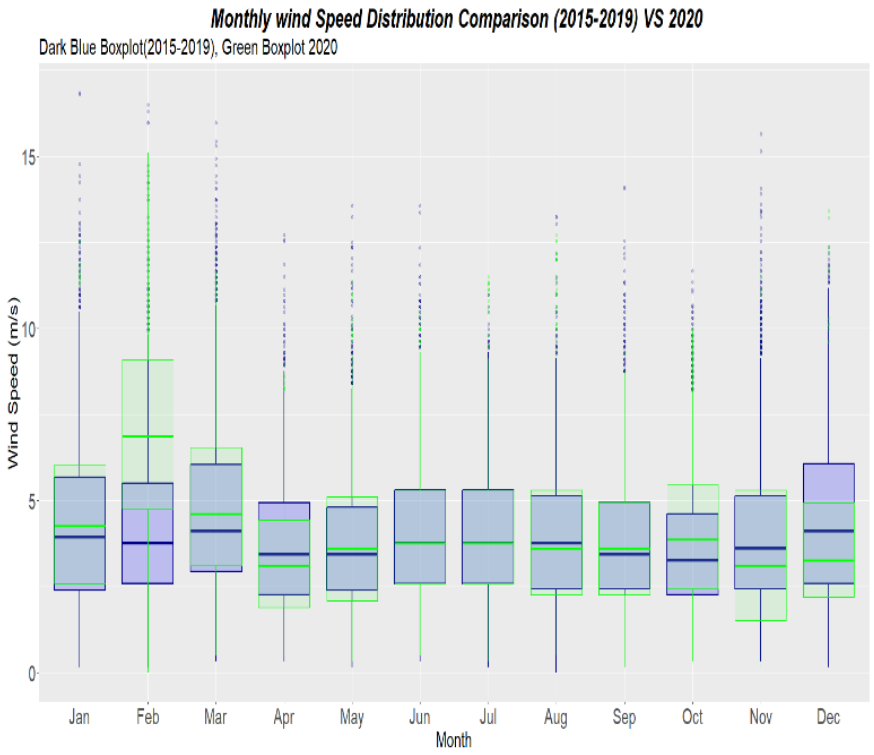

Figure 4-9 Comparison of Monthly Wind Speed Distribution from Heathrow airport (2015-2019) VS 2020, Dark Blue Boxplot (2015-2019), Green Boxplot 2020.

Figure 4-10 presents comparison between the measured (relative to the five-year baseline 2015-2019) and modelled BAU percentage changes in VOC concentrations at the Marylebone Road site during the UK lockdown periods (LC1) and (LC2). While Figure 4-11 presents the corresponding absolute changes in VOC concentrations (µg m³), allowing direct comparison between observed reductions and those expected under non-lockdown conditions.

The first lockdown measures had a stronger impact on natural gas-related VOCs levels following the BAU scenario output than what was calculated using the historical change method. The measured ethane mean concentration during the first lockdown was higher than its mean over the last five years by 0.15 µg/m^3 which represents a 2% increase during LC1, however, the predicted mean concentration of ethane during LC1 was higher than what was measured by 0.74 µg/m^3 indicating that ethane levels actually dropped by 9.3% during LC1.

Similarly, the reduction effects of LC1 on propane, and butane were relatively higher following the BAU scenario output than what was calculated using the historical change method. As per the BAU scenario propane, among all modelled VOCs levels, recorded the highest reduction in its mean concentration, dropping by 1.35 µg/m³ (-28.8%) during this lockdown, followed by n-butane, which dropped by 1.32 µg/m³ (-34.4%).

In contrast, iso-pentane, which recorded the highest drop in its concentrations during LC1 by 1.32 µg/m^3 following the historical change method, was reduced by only 0.95 µg/m³ in the predicted BAU scenario. The model predicted a slightly lower reduction in aromatics (benzene, mp-xylene, and toluene) during this lockdown dropping by 27.3%, 36.8% and 36.5%, compared with the historical method, where reductions were 28.5%, 40.2%, and 41.6%.

On the other hand, the modelled ethene mean concentration was higher than the measured one by 0.82 µg/m^3 recording the highest percentage reduction of 45.2% during LC1, while measured 2-methyl pentane concentration dropped by 39.7% compared to its modelled one, these two VOCs were reduced by 42.7% and 58% respectively, following the historical change method.

Similar to LC1, the model outcomes predicted a higher reduction in natural gas-related VOCs levels compared to the historical change method. Ethane and propane mean LC2 concentrations were higher than their historical levels by 12.8% and 12.1%, respectively.

However, the model results showed only 2.1% and 2.3% increases in these levels under the BAU scenario. Butane followed a similar trend as well.

In contrast, LC2 iso-pentane concentrations dropped by only 0.29 μg/m³ (-12.4%) compared with the BAU scenario, while they dropped by 0.7 μg/m³ (-24.3%) compared with the mean concentrations for the LC2 period over the last five years. On the other hand, the models predicted a reduction in ethene LC2 mean concentrations similar to that obtained with the historical method as shown in Figure 4-10, and Figure 4-11

The BAU results emphasize that the first lockdown had a greater effect in reducing VOC concentrations than the second lockdown, reflecting the stricter measures during LC1, when there was an almost complete pause in anthropogenic emissions, especially from traffic and industry. In contrast, LC2 involved only a partial economic pause and less strict measures, resulting in a more moderate drop in VOC concentrations.

The differences in the observed VOC reduction levels between the BAU model and the historical change analysis highlight the importance of conducting multiple analytical approaches when evaluating air pollution intervention strategies. The higher reductions in natural-gas-related VOCs following the BAU output suggest that energy consumption patterns were more affected by lockdown measures than previously estimated, whereas aromatic VOCs and iso-pentane experienced greater variability, mainly due to contributions from various non-traffic-related sources such as solvent use and industry.

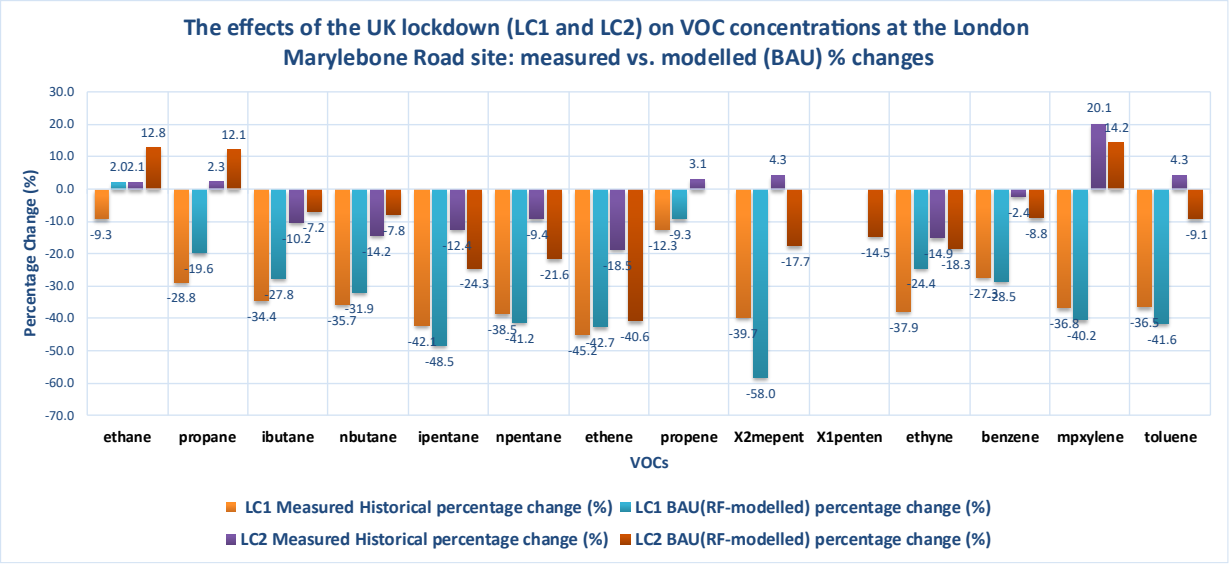

Figure 4-10 UK lockdown periods (LC1/LC2) measured versus modelled percentage changes in VOC concentrations at the Marylebone Road site. Measured changes are based on observed concentrations compared to the five-year baseline (2015–2019), while BAU changes are derived from Random Forest (RF) model predictions simulating business-as-usual conditions.

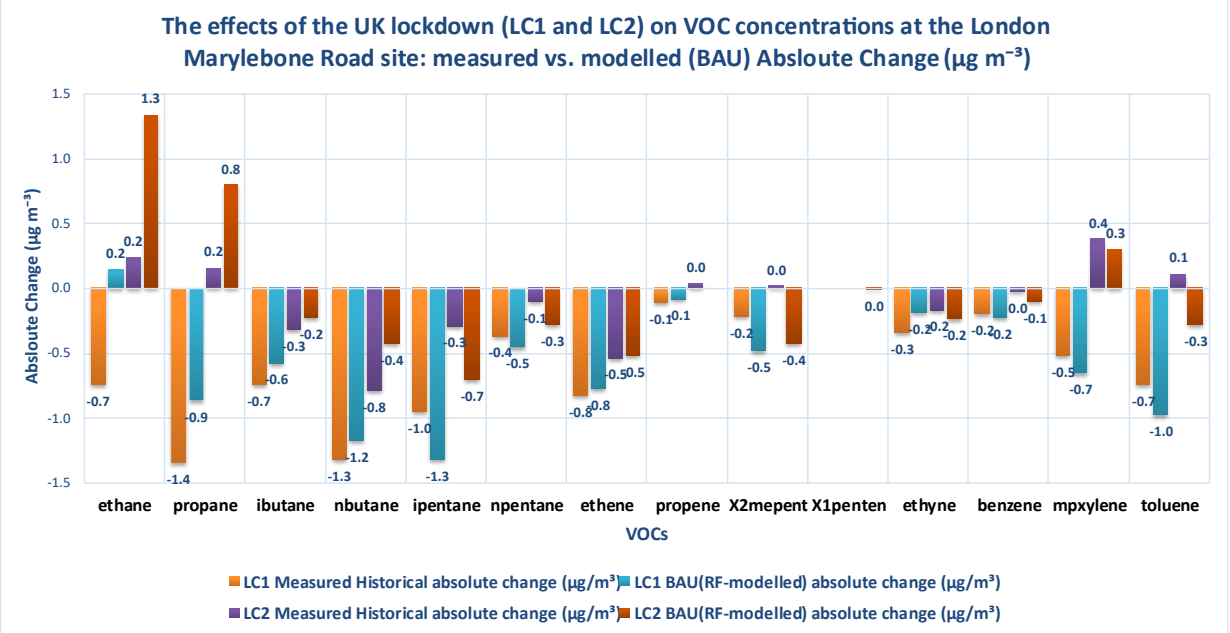

Figure 4-11 UK lockdown periods (LC1/LC2) measured versus modelled absolute changes in VOC concentrations at the Marylebone Road site. Measured changes are based on observed concentrations compared to the five-year baseline (2015–2019), while BAU changes are derived from Random Forest (RF) model predictions simulating business-as-usual conditions.

4.4 Results and Discussion, Eltham Site

The absolute and relative changes in VOC concentration at the London Eltham site during lockdown measures are presented in Table 4-5, the results show that the reduction in total VOCs concentrations was 8.51%. This drop was mainly driven by decreases in the highly weighted alkanes (ethane, propane, n-butane), where ethane levels fell by 0.28 µg/m^3 corresponding to a 6.2% drop. Similarly, the NG-related alkanes experienced a uniform weak reduction ranging between 4.9% to 8.2%. Given that natural gas consumption during the lockdown was expected to remain constant, this slight decrease could be mainly due to normal variations in background emissions or weather conditions variability rather than a lockdown-related effect. This emphasises the complexity of assessing VOC trends, as not all changes in VOCs concentrations resulted by emissions shift.

In what concerns the other alkanes, n-heptane and n-hexane levels were significantly higher than their averages over the past five years, while the average concentration of iso-octane, mainly associated with traffic emissions (Lan et al., 2014), plummeted by almost 60%. The rest of the alkanes recorded an average decrease of around 15%. On the other hand, the majority of aromatics recorded a considerable percentage drop between 18.5% to 39.4%, while alkenes showed uneven decrease. This illustrates that reactive VOCs, those have a vital impact on atmospheric chemistry through ozone production (Derwent- et al., 1998), are more vulnerable to human activity despite their lower concentrations. One important policy-related conclusion from this difference is that emission sources that are aimed for improving air quality might not be the same as those are crucial to carbon reduction and net-zero target.

During the second lockdown, there was a general increase almost in all species at the London Eltham site as shown in Table 4-6, consequently the total VOCs mean concertation increased by 18.2% compared to the reference period (2015 to 2019). In general, the second lockdown measures did not have any decreasing impact on the VOCs levels at the suburban site. In the contrast almost all species levels were increased, which could be due to number of factors. Firstly, the meteorological conditions had lower dispersion effects on air pollutants, both vertically by lower ambient temperature and spatially by slower wind speed during this lockdown, encouraging the accumulation of emitted VOCs. Secondly, human activities including the mobility were higher than the first lockdown under COVID-safe protocols that

enabled the partial reopening (Acosta-Ramírez & Higham, 2022). This also explains the lower impact of second lockdown on VOCs levels at London Marylebone Road.

Table 4-5 Percentage and Absolute Change in VOCs Concentrations Due to 2020 First Lockdown Measures Compared to Their Mean Concentrations of the Same Period Between 2015 to 2019 at Eltham Site.

VOCs	First Lockdown Period 2015-2019 Mean Con +/-SD (µg/m^3)	First Lockdown 2020 Mean Con +/-SD (µg/m^3)	Absolute Change (µg/m^3)	Change (%)
Ethane	*4.51 ± 1.72*	*4.23 ± 1.55*	*-0.28*	*-6.16*
Propane	*2.33 ± 1.18*	*2.18 ± 1.12*	*-0.14*	*-6.1*
Iso-Butane	*1.12 ± 0.70*	*1.03 ± 0.60*	*-0.09*	*-8.24*
n-Butane	*2.16 ± 1.27*	*2.05 ± 1.39*	*-0.11*	*-4.95*
Iso-Octane	*0.10 ± 0.06*	*0.04 ± 0.03*	*-0.06*	*-60.41*
n-Octane	*0.06 ± 0.03*	*0.05 ± 0.03*	*-0.01*	*-15.49*
Iso-Pentane	*1.13 ± 0.81*	*0.96 ± 0.80*	*-0.18*	*-15.52*
n-Pentane	*0.56 ± 0.42*	*0.47 ± 0.36*	*-0.09*	*-15.95*
n-Heptane	*0.12 ± 0.06*	*0.17 ± 0.06*	*0.06*	*49.63*
n-Hexane	*0.18 ± 0.19*	*0.29 ± 0.33*	*0.11*	*61.3*
2-Methylpentane	*0.27 ± 0.20*	*0.25 ± 0.18*	*-0.02*	*-6.22*
Ethene	*0.55 ± 0.31*	*0.53 ± 0.25*	*-0.02*	*-3.22*
Propene	*0.30 ± 0.15*	*0.30 ± 0.08*	*-0.01*	*-2.44*
cis-2-Butene	*0.06 ± 0.05*	*0.03 ± 0.01*	*-0.03*	*-50.38*
trans-2-Butene	*0.05 ± 0.02*	*0.03 ± 0.02*	*-0.02*	*-30.48*
trans-2-Pentene	*0.04 ± 0.02*	*0.03 ± 0.02*	*0*	*-5.86*
1-Butene	*0.08 ± 0.05*	*0.08 ± 0.02*	*0*	*4.5*
1-Pentene	*0.04 ± 0.02*	*0.03 ± 0.01*	*-0.01*	*-19.72*
Ethyne	*0.33 ± 0.18*	*0.30 ± 0.12*	*-0.04*	*-10.54*
Benzene	*0.37 ± 0.18*	*0.30 ± 0.18*	*-0.07*	*-18.5*

VOCs	First Lockdown Period 2015-2019 Mean Con +/-SD (µg/m^3)	First Lockdown 2020 Mean Con +/-SD (µg/m^3)	Absolute Change (µg/m^3)	Change (%)
Ethylbenzene	*0.15 ± 0.08*	*0.14 ± 0.06*	*-0.01*	*-3.79*
m/p-Xylene	*0.38 ± 0.23*	*0.30 ± 0.15*	*-0.08*	*-21.16*
o-Xylene	*0.17 ± 0.09*	*0.12 ± 0.07*	*-0.04*	*-24.88*
Toluene	*0.65 ± 0.34*	*0.49 ± 0.27*	*-0.17*	*-25.55*
1,2,4-TMB	*0.15 ± 0.10*	*0.09 ± 0.06*	*-0.05*	*-35.98*
1,3,5- TMB	*0.06 ± 0.03*	*0.04 ± 0.02*	*-0.02*	*-39.41*
1,3-Butadiene	*0.04 ± 0.03*	*0.04 ± 0.01*	*0.00*	*-2.53*
Total VOCs	*15.96 ± 3.07*	*14.61± 2.88*	*-1.36*	*-8.51*

Red change(%) values indicate changes that are not statistically significant ($p \geq 0.05$).

Table 4-6 Percentage and Absolute Change in VOCs Concentrations Due to 2020 Second Lockdown Measures Compared to Their Mean Concentrations of the Same Period Between 2015 to 2019 at Eltham Site.

VOCs	Second Lockdown Period 2015-2019 Mean Con +/-SD (µg/m^3)	Second Lockdown 2020 Mean Con +/-SD (µg/m^3)	Absolute Change (µg/m3)	Change (%)
Ethane	*5.89 ± 3.78*	*6.33 ± 4.42*	*0.44*	*7.39*
Propane	*3.59 ± 2.48*	*3.98 ± 3.18*	*0.39*	*10.71*
Iso-Butane	*1.92 ± 1.63*	*2.30 ± 2.08*	*0.38*	*18.95*
n-Butane	*3.48 ± 2.86*	*4.21 ± 3.81*	*0.73*	*20.37*
Iso-Octane	*0.14 ± 0.13*	*0.25 ± 0.20*	*0.11*	*73.94*
n-Octane	*0.07 ± 0.05*	*0.11 ± 0.06*	*0.04*	*58.7*
Iso-Pentane	*1.41 ± 1.19*	*1.86 ± 2.40*	*0.45*	*30.87*

VOCs	Second Lockdown Period 2015-2019 Mean Con +/-SD (µg/m^3)	Second Lockdown 2020 Mean Con +/-SD (µg/m^3)	Absolute Change (µg/m3)	Change (%)
n-Pentane	*0.73 ± 0.59*	*0.91 ± 1.13*	*0.18*	*24.15*
n-Heptane	*0.18 ± 0.15*	*0.27 ± 0.17*	*0.09*	*50.74*
n-Hexane	*0.23 ± 0.21*	*0.32 ± 0.29*	*0.09*	*35.14*
2-Methylpentane	*0.42 ± 0.45*	*0.46 ± 0.41*	*0.04*	*8.46*
Ethene	*1.25 ± 1.01*	*1.66 ± 1.41*	*0.41*	*32.46*
Propene	*0.51 ± 0.35*	*0.79 ± 0.70*	*0.28*	*55.49*
cis-2-Butene	*0.09 ± 0.11*	*0.08 ± 0.07*	*-0.01*	*-9.14*
trans-2-Butene	*0.07 ± 0.06*	*0.09 ± 0.08*	*0.02*	*20.13*
trans-2-Pentene	*0.06 ± 0.05*	*0.08 ± 0.08*	*0.02*	*28.69*
1-Butene	*0.15 ± 0.09*	*0.16 ± 0.12*	*0.01*	***4.68***
1-Pentene	*0.04 ± 0.03*	*0.06 ± 0.05*	*0.02*	*33.35*
Ethyne	*0.51 ± 0.39*	*0.68 ± 0.42*	*0.17*	*32.26*
Benzene	*0.62 ± 0.36*	*0.74 ± 0.53*	*0.12*	*18.82*
Ethylbenzene	*0.25 ± 0.21*	*0.31 ± 0.24*	*0.06*	*21.37*
m/p-Xylene	*0.73 ± 0.68*	*0.90 ± 0.78*	*0.17*	*22.69*
o-Xylene	*0.3 ± 0.26*	*0.39 ± 0.32*	*0.09*	*27.77*
Toluene	*1.12 ± 0.94*	*1.29 ± 0.98*	*0.17*	*14.44*
1,2,4-TMB	*0.29 ± 0.27*	*0.33 ± 0.30*	*0.04*	*13.11*
1,3,5- TMB	*0.11 ± 0.09*	*0.12 ± 0.10*	*0.02*	*15.89*
1,3-Butadiene	*0.09 ± 0.06*	*0.11 ± 0.08*	*0.02*	*18.78*
Total VOCs	*24.25 ± 6.02*	*28.79 ± 8.16*	*4.53*	*18.20*

Red change(%) values indicate changes that are not statistically significant ($p \geq 0.05$).

Regarding the trend analysis at this site, iso-octane, although the data were relatively scattered as shown in Figure *4-12*, had a general downward trend at the Eltham site, especially during the last three pre lockdown years, where first lockdown concentration appeared to be in-line with that trend. Interestingly, the variability of the iso-octane concentrations during the first lockdown was lower than in all previous (and subsequent) years, reflecting a significant in iso-octane emissions, primarily gasoline evaporation and vehicle exhaust (Lan et al., 2014). During the first lockdown period, the mean iso-octane concentration reduced by 60%, compared to its projected concentration based on the reference period trend (2015 to 2019). Using the reference period trend as a guide and assuming no other changes in emission, lockdown mean concentration was not predicted to occur until 2029.

On the other hand, even with its slight upward trend over the past five years, the increase in mean concentration of n-heptane during the first lockdown by 49.6% was dramatically sharp and was not projected to occur even by 2045, this increase in atmospheric n-heptane was unexpected, considering its primary emissions sources that include fuel evaporation and handling, vehicle exhaust, and emissions from petroleum refining and petrochemical processes (DEFRA, 2020; L. Zhang et al., 2021), occurred during a period of reduced traffic volumes and fuel consumption due to lockdown measures. However, the mean concentration in 2021 during the same period aligned with the predicted trend, and the 2022 mean concentration was even lower than what was projected.

In the contrast, benzene first lockdown mean concentration that dropped by 18.5% was completely projected by its trend over the past five years and did not affect by the lockdown measures at this site. Similarly, the benzene mean concentration in 2021 followed the predicted trend, while the 2022 benzene mean concentration was even lower.

In what concern the second lockdown, the 18.8% raise in benzene mean concentrations was against benzene general backward trend, as illustrated in Figure *4-13*, however, post lockdown 2021 and 2022 levels went back to follow the normal benzene trend at this site. This was exactly the same as in n- heptane case, as second lockdown mean concentration increased by 50% against the general trend, while post lockdown years levels back to follow their normal downward trend. However, the slight increase in ethane mean concentration during lockdown 2 was as predicted by its general trend for the same period over the past

five years. it worth mentioning that ethane mean concentration for the same period in 2019 and 2021 was remarkably close to the 2020 lockdown one, while 2022 levels dropped significantly compared with these years.

The results of the Random Forest (RF) model unveiled the key role of wind speed (WS) in predicting the analysed VOC concentrations (Ethane, Ethene, iso Pentane and Toluene), especially for ethane, at the London Eltham site, which is located in an open environment with almost no obstructions to wind movement. However, the most important variable for these species was the Julian day (day of year), indicating clear seasonal emission patterns. WS was the second most important variable for toluene, iso-pentane, and ethene, following the seasonal term directly. Eltham's wind direction was found to have less impact than at the Marylebone Road site, this is consistent with the lack of street canyon effects at this site, which explained the importance of WD at Marylebone Road.

At this suburban background location, there was strong negative correlation between VOC levels and WS, which indicates the dominance of local emissions rather than transported emissions. On the other hand, a negative correlation between ethane and ethene levels and air temperature was observed, up to about 10 °C, after which concentrations stabilised. Generally, VOC levels were higher under calm winds blowing from east and west directions, where nearby residential areas are located.

Finally, The Eltham site comparison presented in Figure *4-14*, revealed that the modelled business as usual (BAU) scenario's results were considerably different to the historical change ones. The historical changes explained in 4.3.1 did not match the RF models' prediction of a significantly higher drop in VOC levels during both lockdowns at Eltham site. This is mainly due to the strong influence of meteorological conditions on VOC concentrations at Eltham, compared with Marylebone Road, which is directly influenced by traffic emissions. Hence, the actual effect of the lockdown measures on VOC levels at Eltham site is accurately unveiled when this influence was scaled through the business-as-usual scenario.

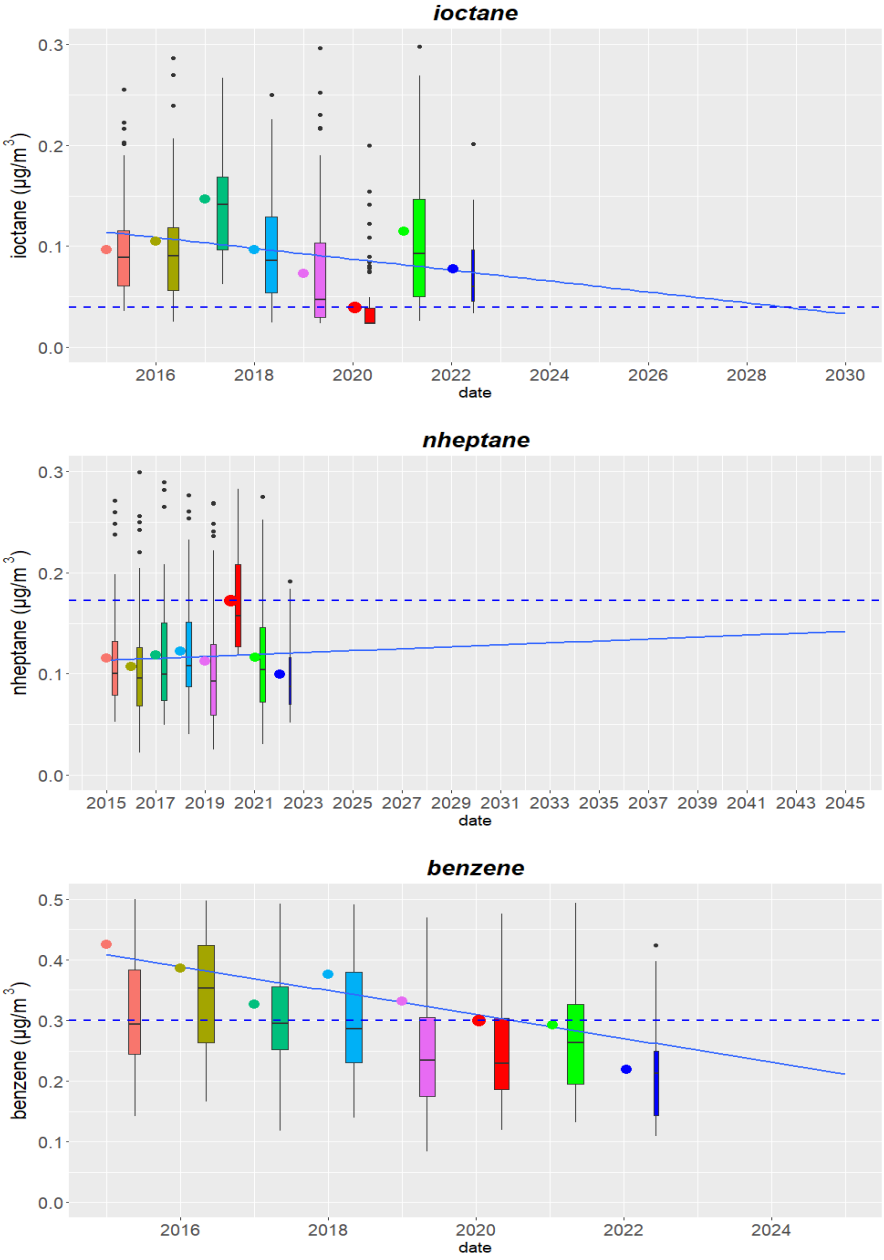

Figure 4-12 Eltham site, First Lockdown Trend analysis, Boxplots present daily means VOCs distributions, Red colour 2020 lockdown1, Coloured dots are VOCs mean concentrations, Solid blue line is the VOC historical trend, Doted blue line is lockdown1 mean concentrations level.

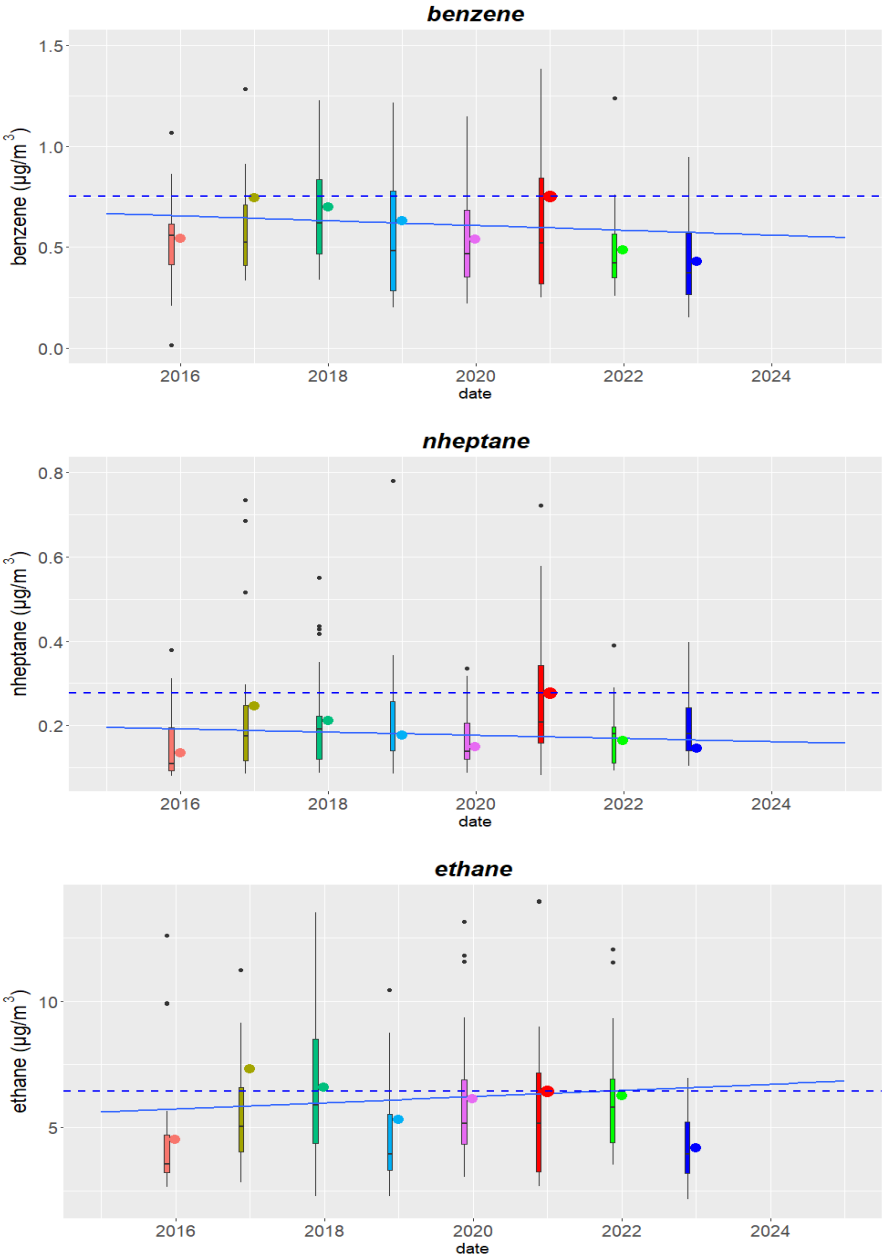

Figure 4-13 Eltham site, Second Lockdown Trend analysis, Boxplots present daily means VOCs distributions, Red colour 2020 lockdown1, Coloured dots are VOCs mean concentrations, Solid blue line is the VOC historical trend, Doted blue line is lockdown2 mean concentrations.

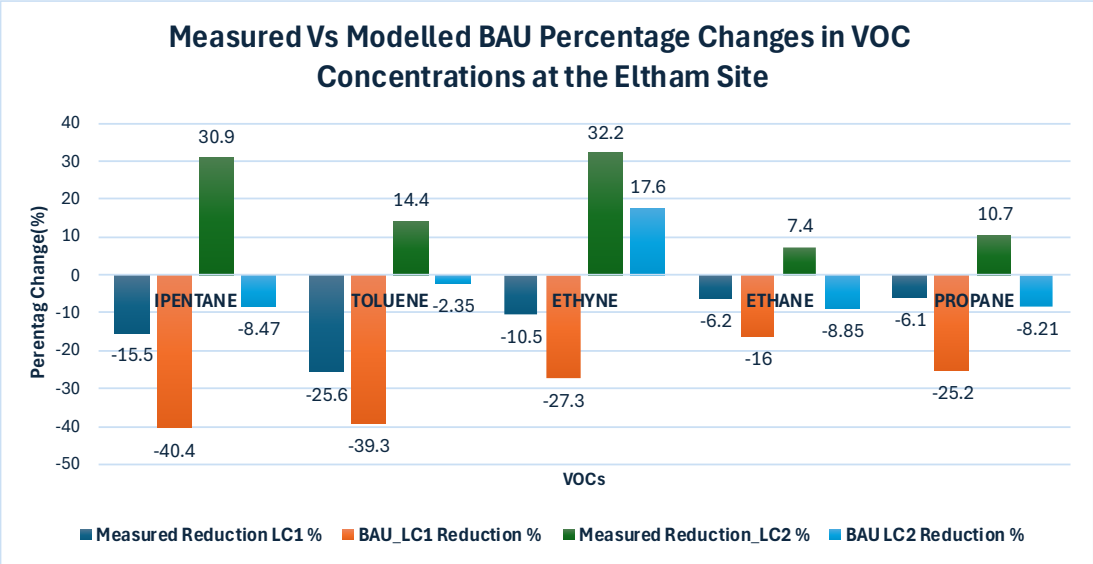

Figure 4-14 Measured versus modelled percentage changes in VOC concentrations at the Eltham suburban background site during the first (LC1) and second (LC2) UK lockdown periods. Measured changes are based on observed concentrations compared to the five-year baseline (2015–2019), while BAU changes are derived from Random Forest (RF) model predictions simulating business-as-usual conditions.

4.5 Conclusion

This study provides a comprehensive assessment of the impact of the UK's COVID-19 lockdown measures on VOCs concentrations at two different monitoring environments in London: Marylebone Road (urban traffic site) and Eltham (suburban background site). Utilising various analytical approaches, including historical comparisons, trend analysis, meteorological normalisation via Random Forest (RF) modelling, and business-as-usual (BAU) scenario forecasts, the findings present a thorough assessment of VOCs levels in response to the significant emission reductions during the pandemic.

At Marylebone Road, where local VOC concentrations are dominated by the adjacent traffic emissions, most VOC levels during the first lockdown, particularly traffic-related alkanes, and aromatics, observed a significant reduction, confirming the strong association between vehicular activity and ambient VOC concentrations in the urban settings. This was confirmed by the considerable reductions in iso-pentane and 2-methylpentane levels, reflecting significant emissions reduction from their main sources, gasoline evaporative and exhaust emissions. In contrast, non-traffic related alkanes (ethane, propane, and butanes) showed marginal changes, which could be due to the increased demand on domestic energy during

the lockdown period. However, the second lockdown, generally, had less significant impact on VOC levels at this site, as restriction measures were less strict.

At Eltham, a suburban area with more diversified and distributed VOC emission sources, the first lockdown measures slightly decreased the overall VOCs levels, while some species, particularly n-hexane and n-heptane, increased. Unexpectedly, the second lockdown was associated with increases in most VOC species, highlighting the importance of non-traffic sources and the vital weather impact on VOCs levels in suburban environments.

The trend analysis showed that the reduction in VOCs levels during the first lockdown at Marylebone Road, particularly for ethene, was greater than the projected levels based on their historical trends over the pre-lockdown five years, while the reduction in other VOCs levels, like benzene, was consistent with their normal backward trend. At Eltham, some changes, such as the sharp rise in n-heptane, deviated from expected trends, suggesting that emissions from non-traffic sources and the influence of complex meteorological conditions played a vital role at this site.

Meteorological normalisation using Random Forest models was crucial for revealing the actual effects of lockdown measures, independent of weather variability. Wind speed, seasonal variations, and temperature were important predictors of VOC levels, with a more noticeable meteorological impact at Eltham due to its open suburban environment. On the other hand, VOCs levels were more sensitive to wind direction at Marylebone Road because of the street canyon environment. BAU predictions revealed that meteorology masked a substantial reduction in VOCs mean concentrations, especially at Eltham.

The observed reductions in VOC concentrations alongside the changes in nitrogen oxides (NOx) due to significant reduction in anthropogenic activities , provide an important insight into urban atmospheric chemistry during the lockdown period. A recent study by Prof Lee from the University of York reported substantial decreases in NOx across the UK due to reduced traffic activity. However, ozone concentrations were found to increase across UK monitoring sites, with largest increase recorded at urban traffic sites (+48%) compared to (+11%) at urban backgrounds environments (Lee et al., 2020). This is consistent with VOC-limited (Nox-saturated) chemical regime in urban settings, where reduction in NOx levels reduce NO titration of ozone and enhance the net O_3 formation as detailed in section 1.4.1.

At Marylebone Road, the significant reduction in NO emissions likely reduced ozone titration, resulting in higher O_3 concentrations. Similarly, at Eltham, increases in ozone can be attributed to lower NOx levels combined with less consistent reductions in VOCs concentrations.

Evaluating VOC changes due to lockdown effects is more direct at Marylebone Road, located adjacent to direct traffic emissions, where VOCs levels are predominantly correlated with fresh traffic emissions. In the contrast, at Eltham, various geographically scattered emission sources contribute to VOCs level, including domestic combustion, fuel handling, and light industry, in addition to land transport-related emissions. The emission from these sources can be impacted by various weather conditions and photochemical reactions that occur during VOCs transport from the emission source to the monitoring site. Therefore, identifying the effects of lockdown measures out of the fluctuations caused by meteorological and photochemical factors cannot be confidently achieved only by comparing VOC levels, especially at Eltham.

Overall, the findings confirm the necessity of traffic emission regulations but also emphasise the need for more comprehensive strategies addressing non-traffic emission sources, particularly residential and energy-related VOC emissions. The integration of monitoring, trend analysis, and machine learning analysis proved to be crucial for understanding intervention effectiveness under real-world conditions.

Chapter 5

5 Conclusion

5.1 Overview and key findings.

We aimed in this project to investigate the sources, temporal variability, and policy-relevant impacts of VOCs on urban atmospheres in the UK, employing receptor modelling, inter-city comparative analysis, and an evaluation of a natural experiment (the COVID-19 lockdown) to provide a thorough assessment of VOCs levels responses to lockdown measures at roadside and urban background locations.

The research was organised into three primary chapters. First, a comprehensive source apportionment analysis for London was conducted using the EPA PMF 5.0 model, providing robust source profiles for a wide variety of emission sources. Second, a comparative analysis of seasonal and diurnal variability in London and Birmingham was undertaken, providing new insights into spatial heterogeneity. Third, the exceptional reduction in anthropogenic emissions during the 2020 lockdowns was investigated using data from a roadside (Marylebone Road) and an urban background site (Eltham), providing unique evidence on the sensitivity of VOC concentrations to sudden emission reductions.

All together, these chapters provide an integrated picture of urban VOC sources, emphasising the relative importance of traffic, solvent, fuel evaporative, and secondary sources, and demonstrating that, while traffic restrictions can deliver measurable improvements, other sources must also be addressed to achieve sustainable reduction.

The application of the US EPA PMF 5.0 model to the measured VOCs at the London Honor Oak Park urban background site provided a robust seven-factor solution, revealing the key sources of VOCs emissions in London: Regional Transport and Background Alkanes, Secondary Atmospheric Oxidation, Traffic Fuel Evaporation, Vehicular Combustion, Paint and Solvent, Industrial, and Commercial and Residential Fuel Combustion. Traffic related emissions, both fuel evaporative and tailpipe emissions, continued to be major VOCs source in urban atmosphere, accounting for 27% of the total VOCs mixing ratio, with fuel evaporative having grater VOCs emissions than vehicular combustion. Additionally, regional alkanes accounted for the largest proportion (28%) of total VOCs mixing ratio, however, due to the low reactivity of their components, they had marginal importance in secondary atmospheric pollutant formation, which includes Ozone Formation Potential (OFP) and Secondary Organic Aerosol Potential (SOAP). In contrast, paint and solvent emissions which accounted only for 9% of the

total VOCs mixing ratio, less than one third of regional alkanes contribution, had, due to their highly reactive compounds (aromatic VOCs), by far the greatest secondary organic aerosol potential. They were also the most significant contributors to atmospheric ozone formation. Secondary atmospheric oxidation source (acetone and acetaldehyde), accounted for 18% of the total VOCs mixing ratio, was the second highest source in OFP, which underscored the importance of photochemical processes, followed by vehicular combustion and traffic fuel evaporative sources. However, considering traffic related emissions as a single source would make it has the highest OFP among all sources.

A detailed comparison of London and Birmingham VOC species revealed both similarities and considerable differences. Both cites almost shared the ten most abundant VOCs species, those accounted for about 90% of the total observed VOCs mixing ratio, with ethane, ethanol, and acetone being the most three abundant VOCs species. However, there was a significant proportional increase in ethanol, iso-pentane, and toluene levels in London compared with Birmingham, indicating stronger contributions from solvent and evaporative emission sources. By contrast, combustion-related VOCs (ethene, and acetylene) were more prominent in Birmingham's VOCs profile, ranking higher than in London, in association with enhanced evening peaks. Generally, winter combustion tracers, in both cities, increased further, reflecting elevated VOCs emissions from combustion sources under weaker degradation and dispersion conditions. On the other hand, oxygenated VOCs contributed most to total VOCs levels, in summer, emphasising the importance of atmospheric secondary formation under improved photochemical conditions. Furthermore, diurnal patterns demonstrated the site-specific behaviours of VOCs species. In London VOCs levels showed sharp declines after the morning peaks followed by afternoon rises, reflecting the influence of photochemistry and boundary-layer dynamics. Birmingham, on the other hand, exhibited steadier patterns with evening enhancements driven by stronger nighttime accumulation.

The 2020 COVID-19 lockdown measures provided a unique natural experiment for assessing the impact of restricted human activity, primarily traffic, on VOC levels. At Marylebone Road, the first lockdown measures substantially decreased traffic-related VOCs, primarily alkanes and aromatics. On the other hand, non-traffic VOCs (ethane, propane, and butanes) only exhibited slight variations in their levels, reflecting increased residential heating demand during the same period. However, the second lockdown had weaker effects on VOC levels,

due to less strict lockdown measures. The results at Eltham were conflicting, where certain traffic related VOCs showed a slight decrease in their levels, others, namely, n-hexane and n-heptane, showed a considerable increase, emphasising the key importance of non-traffic and dispersed sources, compared with traffic-dominated sites. Trend and meteorological-normalisation analyses confirmed that declines in key traffic related species at Marylebone Road exceeded their general trends, confirming the direct impact of reduced traffic activity, while at Eltham, background influences and meteorological conditions masked the actual scale of change. The BAU scenario projection indicated that meteorological factors masked substantial reductions, especially at Eltham, underscoring the need for statistical methods to differentiate intervention impacts from natural variability.

5.2 Implications for Air Quality and Policy

The findings of this work show that UK urban VOC policies must consider the evolving urban VOCs sources in addition to vehicle tailpipe emissions. While vehicle exhaust controls have successfully reduced many combustion-related pollutants, the less strictly regulated sources, namely fuel evaporative losses, and solvent-related sources, have become more important than tailpipe emissions in contributing to total VOCs levels. These sources also play vital roles in the atmospheric formation of ozone and secondary organic aerosols.

The clear seasonal and spatial variation in VOCs sources and levels between London and Birmingham underscores the need for tailored VOCs mitigation strategies that consider the sources diversity in different urban areas, which could be underestimated in National-scale policies. London VOCs management plans should aim to reduce solvents and evaporative emissions more strictly, on the other hand, Birmingham strategies have to additionally address combustion and regional background sources. Consequently, aligning interventions to local VOCs sources will enhance their effectiveness and efficiency.

Additionally, traffic-focus measures' advantages and limitations were revealed by the lockdown analysis. While roadside VOCs concentrations were significantly reduced under limited mobility conditions, background concentrations remained relatively unaffected, and some compounds even increased, which emphasise that transport measures alone are insufficient to achieve comprehensive improvement in urban areas. However, targeted mobility measures, including expansion of Ultra Low Emission Zones, promotion of active

travel, and electrification of the fleet, remain vital interventions that should be coupled with broader package of measures.

Finally, our study revealed the key role of oxygenated and secondary VOCs in urban environments, indicating the vital need to integrate atmospheric chemistry considerations into air quality strategies, as reducing precursor and solvent-related emissions will not only decrease the primary VOC concentration but also efficiently limit secondary pollutant formation and, therefore, enhance public health benefits.

Overall, the findings illustrate the necessity of addressing VOCs emissions from transportation, solvent usage, fuel evaporative losses, and residential energy consumption. Additionally, secondary formation processes and localised variations between urban areas should be consider. Collectively, providing a comprehensive multi-source VOCs management strategies, which will provide co-benefits for air quality, climate objectives, and the protection of public health in the UK.

5.3 Limitations and Future Work

Although this research provides a comprehensive analysis of VOC sources and variability in UK urban environments, a few limitations should be acknowledged.

Firstly, our analysis was constrained by the species measured by the GC-FID system. While extensive, the current suite does not capture the full range of VOCs relevant to ozone and SOA formation. Ideally, measuring more oxygenated compounds, higher aldehydes, and biogenic species would improve both source apportionment and reactivity assessment.

Secondly, the receptor modelling results are fully dependent on the input dataset. While the main purpose of the London and Birmingham Supersites is to provide high resolution long-term data in order to characterise urban background conditions and they are not intended to capture street-level or industrial hot-spots, Birmingham supersite location in proximity to medical schools and the Queen Elizabeth Hospital complex, contributes to elevated acetone levels that may not reflect the wider urban background.

Moreover, the lockdown analysis was influenced by meteorological variability and the unique anthropogenic conditions of the COVID-19 pandemic. While meteorological normalisation

accounted for weather variability, the unique nature of the lockdown should be considered, and hence the results should be interpreted as indicative rather than applicable.

Future research should aim to expand the VOC library within routine monitoring. This can be achieved through the integration of gas chromatography coupled with mass spectrometry (GC-MS) in addition to the existing GC-FID systems, which will improve VOCs identification through molecular fragmentation patterns while maintaining robust quantification. Additionally, speciation of complex and co-eluting compounds, mainly oxygenated VOCs and biogenic species that are not fully resolved by FID alone, would be enhanced by utilising a MS. Moreover, the deployment of advanced real-time mass spectrometry techniques, such as proton-transfer-reaction time-of-flight mass spectrometry (PTR-TOF-MS), would further improve temporal resolution and reduce uncertainties in the quantification of key compounds such as isoprene and benzene.

Analyses should also be extended to other UK key cities in order to build a more representative national VOC profile. Further work should also combine the atmospheric science and health by linking VOC source apportionment with exposure models and epidemiological studies. Finally, upcoming interventions including ULEZ development and fleet electrification should be used as real-world experiments to evaluate VOC source responsiveness under evolving urban conditions.

6 References

Abeleira, A., Pollack, I. B., Sive, B., Zhou, Y., Fischer, E. V., & Farmer, D. K. (2017). Source characterization of volatile organic compounds in the Colorado Northern Front Range Metropolitan Area during spring and summer 2015. *Journal of Geophysical Research*, *122*(6), 3595–3613. https://doi.org/10.1002/2016JD026227

Acosta Navarro, J. C., Smolander, S., Struthers, H., Zorita, E., Ekman, A. M. L., Kaplan, J. O., Guenther, A., Arneth, A., & Riipinen, I. (2014). Global emissions of terpenoid VOCs from terrestrial vegetation in the last millennium. *Journal of Geophysical Research*, *119*(11), 6867–6885. https://doi.org/10.1002/2013JD021238

Acosta-Ramírez, C., & Higham, J. E. (2022). Effects of meteorology and human-mobility on UK's air quality during COVID-19. *Meteorological Applications*, *29*(3). https://doi.org/10.1002/met.2061

Agilent Technology. (2023). *Flame Ionization Detector*. https://www.agilent.com/en/product/gas-chromatography/gc-detectors/flame-ionization-detector

Alam, M. J., Rappenglueck, B., Retama, A., & Rivera-Hernández, O. (2024). Investigating the Complexities of VOC Sources in Mexico City in the Years 2016–2022. *Atmosphere*, *15*(2). https://doi.org/10.3390/atmos15020179

An, J., Zhu, B., Wang, H., Li, Y., Lin, X., & Yang, H. (2014). Characteristics and source apportionment of VOCs measured in an industrial area of Nanjing, Yangtze River Delta, China. *Atmospheric Environment*, *97*, 206–214. https://doi.org/10.1016/j.atmosenv.2014.08.021

Angot, H., Davel, C., Wiedinmyer, C., Pétron, G., Hueber, J., Blanchard, B., Bourgeois, I., Vimont, I., Montzka, S. A., Miller, B. R., Elkins, J. W., & Helmig, D. (2015). *Temporary pause in the growth of atmospheric ethane and*. https://doi.org/10.5194/acp-2021-285

Anh, V., Duc, H., & Azzi, M. (1997). Modeling anthropogenic trends in air quality data. *Journal of the Air and Waste Management Association*, *47*(1), 66–71. https://doi.org/10.1080/10473289.1997.10464406

AQEG. (2017). *The Potential Air Quality Impacts from Biomass Combustion*.

AQEG. (2020). *Non-methane Volatile Organic Compounds in the UK h*.

Araizaga, A. E., Mancilla, Y., & Mendoza, A. (2009). *Characterization of VOC Emissions from Light-Duty Vehicles in Monterrey, Mexico: Tunnel Study*.

Arciszewska, C., & McClatchey, J. (2001). The importance of meteorological data for modelling air pollution using ADMS-Urban. *Meteorol. Appl.*, 345–350.

Arsene, C., Mihalopoulos, N., Arsene, C., & Bougiatioti, A. (2009). Sources and variability of non-methane hydrocarbons in the Eastern Mediterranean. In *Global NEST Journal* (Vol. 11, Issue 3). https://www.researchgate.net/publication/228563106

Arslan, Ö. (2020). *Influence of Fuel Types and Combustion Environment on Emission of VOCs from Combustion Sources: A Review Influence of Fuel Types and Combustion Environment on Emission of VOCs from Combustion Sources: A Review View project*. https://www.researchgate.net/publication/342199243

Aspinall, E. (2022, April). *COVID-19 Timeline*. British Foreign Policy Group. https://bfpg.co.uk/2020/04/covid-19-timeline/

Atkinson, R. (2000). *Atmospheric chemistry of VOCs and NO V*.

Atkinson, R., & Arey, J. (2003). Atmospheric Degradation of Volatile Organic Compounds. *Chemical Reviews*, *103*(12), 4605–4638. https://doi.org/10.1021/cr0206420

AURN. (2020). *UK Automatic Urban and Rural Network (AURN)*. https://uk-air.defra.gov.uk/data/data_selector

Azuma, K., Uchiyama, I., Uchiyama, S., & Kunugita, N. (2016). Assessment of inhalation exposure to indoor air pollutants: Screening for health risks of multiple pollutants in Japanese dwellings. *Environmental Research*, *145*, 39–49. https://doi.org/10.1016/j.envres.2015.11.015

Baker, J., Arey, J., & Atkinson, R. (2005). Formation and reaction of hydroxycarbonyls from the reaction of OH radicals with 1,3-butadiene and isoprene. *Environmental Science and Technology*, *39*(11), 4091–4099. https://doi.org/10.1021/es047930t

Barletta, B., Meinardi, S., Rowland, F. S., Chan, C. Y., Wang, X., Zou, S., Lo, Y. C., & Blake, D. R. (2005). Volatile organic compounds in 43 Chinese cities. *Atmospheric Environment*, *39*(32), 5979–5990. https://doi.org/10.1016/j.atmosenv.2005.06.029

Barlow, J. F., Dunbar, T. M., Nemitz, E. G., Wood, C. R., Gallagher, M. W., Davies, F., O'Connor, E., & Harrison, R. M. (2011). Boundary layer dynamics over London, UK, as observed using Doppler lidar during REPARTEE-II. *Atmospheric Chemistry and Physics*, *11*(5), 2111–2125. https://doi.org/10.5194/acp-11-2111-2011

Barrefors, G., & Petersson, G. (1995). VOLATILE HYDROCARBONS FROM DOMESTIC WOOD BURNING. In *Chemosphere* (Vol. 30, Issue 8).

Bartle, K. D., & Myers, P. (2002). *History of gas chromatography +*.

Bauguitte, S. J.-B., Brough, N., Frey, M. M., Jones, A. E., Maxfield, D. J., Roscoe, H. K., Rose, M. C., & Wolff, E. W. (2010). *A network of autonomous surface ozone monitors in Antarctica: technical description and first results*. https://doi.org/10.5194/amtd-3-5795-2010

Bbeiman, L. (1996). *Bagging Predictors* (Vol. 24).

Beens, J., Adahchour, M., Vreuls, R. J., van Altena, K., & Th Brinkman, U. A. (2001). Simple, non-moving modulation interface for comprehensive two-dimensional gas chromatography. In *Journal of Chromatography A*. www.elsevier.com/locate/chroma

Beens, J., Blomberg, J., & Schoenmakers, P. J. (2000). Proper tuning of comprehensive two-dimensional gas chromatography (GC x GC) to optimize the separation of complex oil fractions. *HRC Journal of High Resolution Chromatography*, *23*(3), 182–188. https://doi.org/10.1002/(sici)1521-4168(20000301)23:3<182::aid-jhrc182>3.0.co;2-e

BEIS. (2020). *Energy Consumption in the UK (ECUK) 1970 to 2019, Department for Business, Energy, and for Business Strategy*. https://www.gov.uk/government/collections/digest-of-uk-energy-statistics-dukes

Bennett, N. D., Croke, B. F. W., Guariso, G., Guillaume, J. H. A., Hamilton, S. H., Jakeman, A. J., Marsili-Libelli, S., Newham, L. T. H., Norton, J. P., Perrin, C., Pierce, S. A., Robson, B., Seppelt, R., Voinov, A. A., Fath, B. D., & Andreassian, V. (2013). Characterising

performance of environmental models. *Environmental Modelling and Software*, *40*, 1–20. https://doi.org/10.1016/j.envsoft.2012.09.011

Biau, Luc Devroye, & G´abor Lugosi. (2008). Consistency of Random Forests and Other Averaging Classifiers Luc Devroye Gábor Lugosi. In *Journal of Machine Learning Research* (Vol. 9). http://www.stat.berkeley.edu/users/breiman/RandomForests

birmingham city council. (2022). *2021 Population Census in Birmingham-First Results*.

Birmingham city council. (2024). *Birmingham Population Mid-2022 estimate 2022 Mid-year Population Estimates in Birmingham*. www.birmingham.gov.uk/census

Blake, R. S., Monks, P. S., & Ellis, A. M. (2009). Proton-transfer reaction mass spectrometry. In *Chemical Reviews* (Vol. 109, Issue 3, pp. 861–896). https://doi.org/10.1021/cr800364q

Boeker, P., Leppert, J., Mysliwietz, B., & Lammers, P. S. (2013). Comprehensive theory of the deans' switch as a variable flow splitter: Fluid mechanics, mass balance, and system behavior. *Analytical Chemistry*, *85*(19), 9021–9030. https://doi.org/10.1021/ac401419j

Borbon, A., Gilman, J. B., Kuster, W. C., Grand, N., Chevaillier, S., Colomb, A., Dolgorouky, C., Gros, V., Lopez, M., Sarda-Esteve, R., Holloway, J., Stutz, J., Petetin, H., McKeen, S., Beekmann, M., Warneke, C., Parrish, D. D., & De Gouw, J. A. (2013). Emission ratios of anthropogenic volatile organic compounds in northern mid-latitude megacities: Observations versus emission inventories in Los Angeles and Paris. *Journal of Geophysical Research Atmospheres*, *118*(4), 2041–2057. https://doi.org/10.1002/jgrd.50059

Borbon, A., Locoge, N., Veillerot, M., Galloo, J. C., & Guillermo, R. (2002). Characterisation of NMHCs in a French urban atmosphere: overview of the main sources. In *The Science of the Total Environment* (Vol. 292). www.environnement.gouv.fry

Borlaza-Lacoste, L., Aynul Bari, M., Lu, C. H., & Hopke, P. K. (2024). Long-term contributions of VOC sources and their link to ozone pollution in Bronx, New York City. *Environment International*, *191*. https://doi.org/10.1016/j.envint.2024.108993

Breiman, L. (2001). *Random Forests* (Vol. 45).

Bressi, M., Sciare, J., Ghersi, V., Mihalopoulos, N., Petit, J. E., Nicolas, J. B., Moukhtar, S., Rosso, A., Féron, A., Bonnaire, N., Poulakis, E., & Theodosi, C. (2014). Sources and geographical origins of fine aerosols in Paris (France). *Atmospheric Chemistry and Physics*, *14*(16), 8813–8839. https://doi.org/10.5194/acp-14-8813-2014

Brown, S. G., Eberly, S., Paatero, P., & Norris, G. A. (2015). Methods for estimating uncertainty in PMF solutions: Examples with ambient air and water quality data and guidance on reporting PMF results. *Science of the Total Environment*, *518–519*, 626–635. https://doi.org/10.1016/j.scitotenv.2015.01.022

Brown, S. G., Frankel, A., & Hafner, H. R. (2007). Source apportionment of VOCs in the Los Angeles area using positive matrix factorization. *Atmospheric Environment*, *41*(2), 227–237. https://doi.org/10.1016/j.atmosenv.2006.08.021

Bryant, D. J., Nelson, B. S., Swift, S. J., Budisulistiorini, S. H., Drysdale, W. S., Vaughan, A. R., Newland, M. J., Hopkins, J. R., Cash, J. M., Langford, B., Nemitz, E., Acton, W. J. F., Hewitt, C. N., Mandal, T., Gurjar, B. R., Shivani, Gadi, R., Lee, J. D., Rickard, A. R., & Hamilton, J. F. (2023). Biogenic and anthropogenic sources of isoprene and monoterpenes and their secondary organic aerosol in Delhi, India. *Atmospheric Chemistry and Physics*, *23*(1), 61–83. https://doi.org/10.5194/acp-23-61-2023

Buccolieri, R., Jeanjean, A. P. R., Gatto, E., & Leigh, R. J. (2018). The impact of trees on street ventilation, NOx and PM2.5 concentrations across heights in Marylebone Rd street canyon, central London. *Sustainable Cities and Society*.

Cai, C., Geng, F., Tie, X., Yu, Q., & An, J. (2010). Characteristics and source apportionment of VOCs measured in Shanghai, China. *Atmospheric Environment*, 5005–5014. https://doi.org/10.1016/j.atmosenv.2010.07.059

Calvert, J. G., Atkinson, R., Becker, K. H., Kamens, R. M., Seinfeld, J. H., Wallington, T. J., & Yarwood, G. (2002). *The Mechanisms Of Atmospheric Oxidation Of Aromatic Hydrocarbons*. Oxford University Press. https://doi.org/10.1093/oso/9780195146288.001.0001

Carter, W. P. L. (2009). *UPDATED MAXIMUM INCREMENTAL REACTIVITY SCALE AND HYDROCARBON BIN REACTIVITIES FOR REGULATORY APPLICATIONS*.

Carter, W. P. L. (2010). Development of the SAPRC-07 chemical mechanism. *Atmospheric Environment*, *44*(40), 5324–5335. https://doi.org/https://doi.org/10.1016/j.atmosenv.2010.01.026

Caruana, R. (2006). *An Empirical Comparison of Supervised Learning Algorithms*. www.cs.cornell.edu

Centre for London. (2023). *Moving with the Times: Supporting sustainable travel in outer London*. https://centreforlondon.org/reader/sustainable-travel-outer-london/travel-matters/#reducing-greenhouse-gas-emissions

Chen, W. T., Shao, M., Lu, S. H., Wang, M., Zeng, L. M., Yuan, B., & Liu, Y. (2014). Understanding primary and secondary sources of ambient carbonyl compounds in Beijing using the PMF model. *Atmospheric Chemistry and Physics*, *14*(6), 3047–3062. https://doi.org/10.5194/acp-14-3047-2014

Claeys, M., Graham, B., Vas, G., & Wang, W. (2004). *Formation of Secondary Organic Aerosols Through Photooxidation of Isoprene*. https://www.science.org/doi/10.1126/science.1092805

Climate Data Store. (2022). *Datasets*. https://cds.climate.copernicus.eu/

CRS reports. (2020). https://crsreports.congress.gov

Cui, L., Wang, X. L., Ho, K. F., Gao, Y., Liu, C., Hang Ho, S. S., Li, H. W., Lee, S. C., Wang, X. M., Jiang, B. Q., Huang, Y., Chow, J. C., Watson, J. G., & Chen, L. W. (2018). Decrease of VOC emissions from vehicular emissions in Hong Kong from 2003 to 2015: Results from a tunnel study. *Atmospheric Environment*, *177*, 64–74. https://doi.org/10.1016/j.atmosenv.2018.01.020

Dash, C. S. K., Behera, A. K., Dehuri, S., & Ghosh, A. (2023). An outliers detection and elimination framework in classification task of data mining. *Decision Analytics Journal*, *6*. https://doi.org/10.1016/j.dajour.2023.100164

David, D. P., & William, C. K. (2009). Comparison of Air Pollutant Emissions among Mega-Cities. *Atmospheric Environment*, *43*(40), 6435–6441.

De Gouw, J., & Warneke, C. (2007). Measurements of volatile organic compounds in the earth's atmosphere using proton-transfer-reaction mass spectrometry. In *Mass Spectrometry Reviews* (Vol. 26, Issue 2, pp. 223–257). https://doi.org/10.1002/mas.20119

Debevec, C., Sauvage, S., Gros, V., Gros, V., Sciare, J., Dulac, F., & Locoge, N. (2021). Seasonal variation and origins of volatile organic compounds observed during 2 years at a western Mediterranean remote background site (Ersa, Cape Corsica). *Atmospheric Chemistry and Physics*, *21*(3), 1449–1484. https://doi.org/10.5194/acp-21-1449-2021

DEFRA. (2020). *Non-methane Volatile Organic Compounds in the UK h*.

Defra. (2024). *Automatic Urban and Rural Network (AURN).* https://uk-air.defra.gov.uk

Department for environment, food and rural affairs. (2008). *Marylebone Road, London - Non-Automatic Data*. UK AIR Air Information Resource. https://uk-air.defra.gov.uk/data/maryleboneroad

Department of transport. (2021). *Road Traffic Estimates in Great Britain: 2020*.

Department of transport. (2023). *Road traffic statistics*. https://roadtraffic.dft.gov.uk/manualcountpoints/56765

Department of Transport. (2025). *Summary statistics*. https://roadtraffic.dft.gov.uk/summary

Derwent, R. G., Field, R. A., Dumitrean, P., Murrells, T. P., & Telling, S. P. (2017). Origins and trends in ethane and propane in the United Kingdom from 1993 to 2012. *Atmospheric Environment*, *156*, 15–23. https://doi.org/10.1016/j.atmosenv.2017.02.030

Derwent-, R. G., Jenkin, M. E., Saundersm, S. M., & Pillingm, M. J. (1998). PHOTOCHEMICAL OZONE CREATION POTENTIALS FOR ORGANIC COMPOUNDS IN NORTHWEST EUROPE CALCULATED WITH A MASTER CHEMICAL MECHANISM. In *Atmospheric Environment* (Vol. 32, Issue 14). http://chem.leeds.ac.uk:80/Atmospheric/MCM/

Derwent, R. G., Jenkin, M. E., Utembe, S. R., Shallcross, D. E., Murrells, T. P., & Passant, N. R. (2010). Secondary organic aerosol formation from a large number of reactive man-made organic compounds. *Science of the Total Environment*, *408*(16), 3374–3381. https://doi.org/10.1016/j.scitotenv.2010.04.013

Derwent, R. G., Simmonds, P. G., O'Doherty, S., Grant, A., & Young, D. (2012). Seasonal cycles in short-lived hydrocarbons in baseline air masses arriving at Mace Head, Ireland. *Atmos. Environ*, 89–96.

DFRA. (2022). *Site Information for London Eltham (UKA00230)*. https://uk-air.defra.gov.uk/networks/site-info?uka_id=UKA00230&provider=

DIRECTIVE 2004/42/CE OF THE EUROPEAN PARLIAMENT AND OF THE COUNCIL. (2004). *on the limitation of emissions of volatile organic compounds due to the use of organic solvents certain paints and in varnishes and vehicle refinishing products and amending Directive 1999/13/EC*. Official Journal of the European Union. https://eur-lex.europa.eu/legal-content/EN/TXT/?uri=CELEX:32004L0042

Dollard, G. J., Dore, C. J., & Jenkin, M. E. (2001). Ambient concentrations of 1,3-butadiene in the UK. In *Chemico-Biological Interactions* (Vol. 135). www.elsevier.com/locate/chembiont

Dongre, P. K., Patel, V., Bhoi, U., & Maltare, N. N. (2025). An outlier detection framework for Air Quality Index prediction using linear and ensemble models. *Decision Analytics Journal*, *14*. https://doi.org/10.1016/j.dajour.2025.100546

Đorđević, D., Petrović, S., Relić, D., & Mihajlidi-Zelić, A. (2013). *Applying receptor models Unmix and PMF on real data set of elements in PM for sources evaluation of the sea coastal side region (Southeast Adriatic Sea)*. https://doi.org/10.5194/amtd-6-4941-2013

Dubois, D. W. (2008). *Ozone and its precursors in the Treasure Valley, Idaho*. https://www.researchgate.net/publication/268261225

Dunmore, R. E., Whalley, L. K., Sherwen, T., Evans, M. J., Heard, D. E., Hopkins, J. R., Lee, J. D., Lewis, A. C., Lidster, R. T., Rickard, A. R., & Hamilton, J. F. (2016). Atmospheric ethanol in London and the potential impacts of future fuel formulations. *Faraday Discussions*, *189*, 105–120. https://doi.org/10.1039/c5fd00190k

EDP. (2025). *Volatile Organic Compounds and Smog*. Environmental Protection Department, Hong Kong.

Ellis, A. M., & Mayhew, C. A. (2014). *Proton Transfer Reaction Mass Spectrometry Principles and Applications*.

Environment Agency. (2023). *State of the environment: health, people and the environment*. https://www.gov.uk/government/publications/state-of-the-environment/state-of-the-environment-health-people-and-the-environment?utm_source=chatgpt.com

European Environment Agency. (n.d.). *Background station (air monitoring)*. Retrieved March 28, 2025, from https://www.eea.europa.eu/help/glossary/eea-glossary/background-station-air-monitoring

European Environment Agency. (2016). *Tropospheric ozone: background information*.

Fan, M. Y., Zhang, Y. L., Lin, Y. C., Li, L., Xie, F., Hu, J., Mozaffar, A., & Cao, F. (2021). Source apportionments of atmospheric volatile organic compounds in Nanjing, China during high ozone pollution season. *Chemosphere*, *263*. https://doi.org/10.1016/j.chemosphere.2020.128025

Feldhausen, J., Bell, D. C., Yang, Z., Faulhaber, C., Boehm, R., & Heyne, J. (2022). Synthetic aromatic kerosene property prediction improvements with isomer specific characterization via GCxGC and vacuum ultraviolet spectroscopy. *Fuel*, *326*. https://doi.org/10.1016/j.fuel.2022.125002

Feng, T., Sun, M., Song, S., Zhuang, H., & Yao, L. (2019). 12 - Gas chromatography for food quality evaluation. In J. Zhong & X. Wang (Eds.), *Evaluation Technologies for Food Quality* (pp. 219–265). Woodhead Publishing. https://doi.org/https://doi.org/10.1016/B978-0-12-814217-2.00012-3

Fischer, E. V., Jacob, D. J., Millet, D. B., Yantosca, R. M., & Mao, J. (2012). The role of the ocean in the global atmospheric budget of acetone. *Geophysical Research Letters*, *39*(1). https://doi.org/10.1029/2011GL050086

Florêncio, J., Scaramboni, C., Giubbina, F. F., De Martinis, B. S., Fornaro, A., Felix, E. P., De Oliveira, T. C. S., & Campos, M. L. A. M. (2024). Ethanol, acetaldehyde, and methanol in the gas phase and rainwater in different biomes and urban regions of Brazil. *Science of the Total Environment*, *929*. https://doi.org/10.1016/j.scitotenv.2024.172629

Franco, B., Mahieu, E., Emmons, L. K., Tzompa-Sosa, Z. A., Fischer, E. V., Sudo, K., Bovy, B., Conway, S., Griffin, D., Hannigan, J. W., Strong, K., & Walker, K. A. (2016). Evaluating ethane and methane emissions associated with the development of oil and natural gas extraction in North America. *Environmental Research Letters*, *11*(4). https://doi.org/10.1088/1748-9326/11/4/044010

Fu, X., Wang, S., Zhao, B., Xing, J., Cheng, Z., Liu, H., & Hao, J. (2013). Emission inventory of primary pollutants and chemical speciation in 2010 for the Yangtze River Delta region, China. *Atmospheric Environment*, *70*, 39–50. https://doi.org/10.1016/j.atmosenv.2012.12.034

G. Fernández-Martínez, P. López-Mahía, P. López-Mahía, & Prada-Rodríguez. (2000). *Determination of volatile organic compounds in coal, fly ash and slag samples by direct thermal desorption/GC/MS*.

Geng, F., Cai, C., Tie, X., Yu, Q., An, J., Peng, L., Zhou, G., & Xu, J. (2009). Analysis of VOC emissions using PCA/APCS receptor model at city of Shanghai, China. *Journal of Atmospheric Chemistry*, *62*(3), 229–247. https://doi.org/10.1007/s10874-010-9150-5

Gentner, D. R., Harley, R. A., Miller, A. M., & Goldstein, A. H. (2009). Diurnal and seasonal variability of gasoline-related volatile organic compound emissions in Riverside, California. *Environmental Science and Technology*, *43*(12), 4247–4252. https://doi.org/10.1021/es9006228

Gentner, D. R., Worton, D. R., Isaacman, G., Davis, L. C., Dallmann, T. R., Wood, E. C., Herndon, S. C., Goldstein, A. H., & Harley, R. A. (2013). Chemical composition of gas-phase organic carbon emissions from motor vehicles and implications for ozone production. *Environmental Science and Technology*, *47*(20), 11837–11848. https://doi.org/10.1021/es401470e

Gilman, J. B., & Lerner, B. M. (2015). Biomass burning emissions and potential air quality impacts of volatile organic compounds and other trace gases from temperate fuels common in the United States FLAME-4 View project Fire Influence on Regional and Global Environments Experiment (FIREX) View project Carsten warneke National Oceanic

and Atmospheric Administration. *Article in Atmospheric Chemistry and Physics*. https://doi.org/10.5194/acpd-15-21713-2015

Gilman, J. B., Lerner, B. M., Kuster, W. C., & De Gouw, J. A. (2013). Source signature of volatile organic compounds from oil and natural gas operations in northeastern Colorado. *Environmental Science and Technology*, *47*(3), 1297–1305. https://doi.org/10.1021/es304119a

Global Atmosphere Watch. (n.d.). *Experts Workshop on Volatile Organic Compounds (VOCs)*. Retrieved March 23, 2025, from https://community.wmo.int/en/meetings/experts-workshop-volatile-organic-compounds-vocs

Grange, S. K., & Carslaw, D. C. (2019). Using meteorological normalisation to detect interventions in air quality time series. *Science of the Total Environment*, *653*, 578–588. https://doi.org/10.1016/j.scitotenv.2018.10.344

Grange, S. K., Carslaw, D. C., Lewis, A. C., Boleti, E., & Hueglin, C. (2018). Random forest meteorological normalisation models for Swiss PM10 trend analysis. *Atmospheric Chemistry and Physics*, *18*(9), 6223–6239. https://doi.org/10.5194/acp-18-6223-2018

Grange, S. K., Lee, J. D., Drysdale, W. S., Lewis, A. C., Hueglin, C., Emmenegger, L., & Carslaw, D. C. (2021). COVID-19 lockdowns highlight a risk of increasing ozone pollution in European urban areas. *Atmospheric Chemistry and Physics*, *21*(5), 4169–4185. https://doi.org/10.5194/acp-21-4169-2021

Grover, B. D., & Eatough, D. J. (2008). Source apportionment of one-hour semi-continuous data using positive matrix factorization with total mass (nonvolatile plus semi-volatile) measured by the R&P FDMS monitor. *Aerosol Science and Technology*, *42*(1), 28–39. https://doi.org/10.1080/02786820701787910

Gu, Y., Liu, B., Li, Y., Zhang, Y., Bi, X., Wu, J., Song, C., Dai, Q., Han, Y., Ren, G., & Feng, Y. (2020). Multi-scale volatile organic compound (VOC) source apportionment in Tianjin, China, using a receptor model coupled with 1-hr resolution data. *Environmental Pollution*, *265*. https://doi.org/10.1016/j.envpol.2020.115023

Guan, Y., Wang, L., Wang, S., Zhang, Y., Xiao, J., Wang, X., Duan, E., & Hou, L. (2020). Temporal variations and source apportionment of volatile organic compounds at an urban site in

Shijiazhuang, China. *Journal of Environmental Sciences*, *97*, 25–34. https://doi.org/https://doi.org/10.1016/j.jes.2020.04.022

Guicherit, R. (1997). Traffic as a source of volatile hydrocarbons in ambient air. In *The Science of the Total Environment* (Vol. 205).

Guo, X., Shen, Y., Liu, W., Chen, D., & Liu, J. (2021). Estimation and prediction of industrial VOC emissions in Hebei province, China. *Atmosphere*, *12*(5). https://doi.org/10.3390/atmos12050530

Hagler, G. S. W., Tang, W., Freeman, M. J., Heist, D. K., Perry, S. G., & Vette, A. F. (2011). Model evaluation of roadside barrier impact on near-road air pollution. *Atmospheric Environment*, *45*(15), 2522–2530. https://doi.org/10.1016/j.atmosenv.2011.02.030

Hallquist, M., Wenger, J. C., Baltensperger, U., Rudich, Y., Simpson, D., Claeys, M., Dommen, J., Donahue, N. M., George, C., Goldstein, A. H., Hamilton, J. F., Herrmann, H., Hoffmann, T., Iinuma, Y., Jang, M., Jenkin, M. E., Jimenez, J. L., Kiendler-Scharr, A., Maenhaut, W., … Wildt, J. (2009). The formation, properties and impact of secondary organic aerosol: current and emerging issues. In *Atmos. Chem. Phys* (Vol. 9). www.atmos-chem-phys.net/9/5155/2009/

Hanif, N. M., Hawari, N. S. S. L., Othman, M., Hamid, H. H. A., Ahamad, F., Uning, R., Ooi, M. C. G., Wahab, M. I. A., Sahani, M., & Latif, M. T. (2021). Ambient volatile organic compounds in tropical environments: Potential sources, composition and impacts – A review. *Chemosphere*, 131355. https://doi.org/10.1016/j.chemosphere.2021.131355

Hemann, J. G., Brinkman, G. L., Dutton, S. J., Hannigan, M. P., Milford, J. B., & Miller, S. L. (2008). A new method to estimate PMF model uncertainty Assessing positive matrix factorization model fit: a new method to estimate uncertainty and bias in factor contributions at the daily time scale A new method to estimate PMF model uncertainty. *Chem. Phys. Discuss*, *8*, 2977–3026. www.atmos-chem-phys-discuss.net/8/2977/2008/

Ho, K. F., Lee, S. C., Ho, W. K., Blake, D. R., Cheng, Y., Li, Y. S., Fung, K., Louie, P. K. K., & Park, D. (2009). *Vehicular emission of volatile organic compounds (VOCs) from a tunnel study in Hong Kong*. https://doi.org/10.5194/acpd-9-12645-2009

Hopke, P. K. (2016). Review of receptor modeling methods for source apportionment. In *Journal of the Air and Waste Management Association* (Vol. 66, Issue 3, pp. 237–259). Taylor and Francis Inc. https://doi.org/10.1080/10962247.2016.1140693

Hopke, P. K., Chen, Y., Rich, D. Q., Mooibroek, D., & Sofowote, U. M. (2023). The application of positive matrix factorization with diagnostics to BIG DATA. *Chemometrics and Intelligent Laboratory Systems*, *240*. https://doi.org/10.1016/j.chemolab.2023.104885

Hopkins, J. R., Lewis, A. C., & Read, K. A. (2003). A two-column method for long-term monitoring of non-methane hydrocarbons (NMHCs) and oxygenated volatile organic compounds (o-VOCs). *Journal of Environmental Monitoring*, *5*(1), 8–13. https://doi.org/10.1039/b202798d

Hou, S., Wang, Y., Duan, L., & Xiu, G. (2024). Health Risk Assessment from Exposure to Ambient Volatile Organic Compounds (VOCs) at a Truck Tire Factory in the Yangtze River Delta, China. *Atmosphere*, *15*(4). https://doi.org/10.3390/atmos15040458

Huang, D. D., Hu, Q., He, X., Huang, R. J., Ding, X., Ma, Y., Feng, X., Jing, S., Li, Y., Lu, J., Gao, Y., Chang, Y., Shi, X., Qian, C., Yan, C., Lou, S., Wang, H., & Huang, C. (2024). Obscured Contribution of Oxygenated Intermediate-Volatility Organic Compounds to Secondary Organic Aerosol Formation from Gasoline Vehicle Emissions. *Environmental Science and Technology*, *58*(24), 10652–10663. https://doi.org/10.1021/acs.est.3c08536

Huang, G., Brook, R., Crippa, M., Janssens-Maenhout, G., Schieberle, C., Dore, C., Guizzardi, D., Muntean, M., Schaaf, E., & Friedrich, R. (2017). Speciation of anthropogenic emissions of non-methane volatile organic compounds: A global gridded data set for 1970-2012. *Atmospheric Chemistry and Physics*, *17*(12), 7683–7701. https://doi.org/10.5194/acp-17-7683-2017

Huang, Y. S., & Hsieh, C. C. (2019). Ambient volatile organic compound presence in the highly urbanized city: source apportionment and emission position. *Atmospheric Environment*, *206*, 45–59. https://doi.org/10.1016/j.atmosenv.2019.02.046

Hughes, K. . (2001). *1,3-butadiene : human health aspects : first draft*. World Health Organization.

ICCP. (2014). *Climate change 2013 : the physical science basis*. Cambridge University Press.

INRIX. (2022). *London Tops List as Most Congested City, U.S. Cities Inch Closer*. https://inrix.com/press-releases/2022-global-traffic-scorecard-uk/

IPCC. (2023). Technical Summary. In *Climate Change 2021 – The Physical Science Basis* (pp. 35–144). Cambridge University Press. https://doi.org/10.1017/9781009157896.002

Isobel Simpson, & Claudia Volosciuk. (2019). *Changing Volatile Organic Compound Emissions in Urban Environments: Many Paths to Cleaner Air, 2019*. World Meteorological Organization . https://public.wmo.int/en/resources/bulletin/changing-volatile-organic-compound-emissions-urban-environments-many-paths

Jacob, D. J., Field, B. D., Jin, E. M., Bey, I., Li, Q., Logan, J. A., Yantosca, R. M., & Singh, H. B. (2002). Atmospheric budget of acetone. *Journal of Geophysical Research: Atmospheres*, *107*(9–10). https://doi.org/10.1029/2001jd000694

Jailson de Andrade, B. B., Andrade, M. V, & Pinheiro, H. L. (1998). Atmospheric Levels of Formaldehyde and Acetaldehyde and their Relationship with the Vehicular Fleet Composition in. In *J. Braz. Chem. Soc* (Vol. 9, Issue 3).

Jaimes-Palomera, M., Retama, A., Elias-Castro, G., Neria-Hernández, A., Rivera-Hernández, O., & Velasco, E. (2016). Non-methane hydrocarbons in the atmosphere of Mexico City: Results of the 2012 ozone-season campaign. *Atmospheric Environment*, *132*, 258–275. https://doi.org/10.1016/j.atmosenv.2016.02.047

Jobson, B. T., Berkowitz, C. M., Kuster, W. C., Goldan, P. D., Williams, E. J., Fesenfeld, F. C., Apel, E. C., Karl, T., Lonneman, W. A., & Riemer, D. (2004). Hydrocarbon source signatures in Houston, Texas: Influence of the petrochemical industry. *Journal of Geophysical Research D: Atmospheres*, *109*(24), 1–26. https://doi.org/10.1029/2004JD004887

Jordan, A., Haidacher, S., Hanel, G., Hartungen, E., Märk, L., Seehauser, H., Schottkowsky, R., Sulzer, P., & Märk, T. D. (2009). A high resolution and high sensitivity proton-transfer-reaction time-of-flight mass spectrometer (PTR-TOF-MS). *International Journal of Mass Spectrometry*, *286*(2), 122–128. https://doi.org/https://doi.org/10.1016/j.ijms.2009.07.005

Kampa, M., & Castanas, E. (2008). Human health effects of air pollution. In *Environmental Pollution* (Vol. 151, Issue 2, pp. 362–367). https://doi.org/10.1016/j.envpol.2007.06.012

Karl, T. G., Christian, T. J., Yokelson, R. J., Artaxo, P., Hao, W. M., & Guenther, A. (2007). The Tropical Forest and Fire Emissions Experiment: method evaluation of volatile organic compound emissions measured by PTR-MS, FTIR, and GC from tropical biomass burning. In *Atmos. Chem. Phys* (Vol. 7). www.atmos-chem-phys.net/7/5883/2007/

Karl, T., Guenther, A., Spirig, C., Hansel, A., & Fall, R. (2003). Seasonal variation of biogenic VOC emissions above a mixed hardwood forest in northern Michigan. *Geophysical Research Letters*, *30*(23). https://doi.org/10.1029/2003GL018432

Kesselmeier, J., & Staudt, M. (1999). Biogenic Volatile Organic Compounds (VOC): An Overview on Emission, Physiology and Ecology. In *Journal of Atmospheric Chemistry* (Vol. 33).

Kilty, P. A., & Sachtler, W. M. H. (1974). THE MECHANISM OF THE SELECTIVE OXIDATION OF ETHYLENE TO ETHYLENE OXIDE. *Catalysis Reviews*, *10*(1), 1–16. https://doi.org/10.1080/01614947408079624

Kim, H. Y., Lee, J. D., Kim, J. Y., Lee, J. Y., Bae, O. N., Choi, Y. K., Baek, E., Kang, S., Min, C., Seo, K., Choi, K., Lee, B. M., & Kim, K. B. (2019). Risk assessment of volatile organic compounds (VOCs) detected in sanitary pads. *Journal of Toxicology and Environmental Health - Part A: Current Issues*, *82*(11), 678–695. https://doi.org/10.1080/15287394.2019.1642607

Kirstine, W. V., & Galbally, I. E. (2012). The global atmospheric budget of ethanol revisited. *Atmospheric Chemistry and Physics*, *12*(1), 545–555. https://doi.org/10.5194/acp-12-545-2012

Korban, A., Čabala, R., Egorov, V., & Bosáková, Z. (2024). Variability of internal standard method calibration factors estimated with a multifactorial Taguchi experiment in the analysis of alcoholic products by gas chromatography with flame ionization detection. *Journal of Separation Science*, *47*(1). https://doi.org/10.1002/jssc.202300492

Korban, A., Čabala, R., Egorov, V., Bosáková, Z., & Charapitsa, S. (2022). Evaluation of the variation in relative response factors of GC-MS analysis with the internal standard

methods: Application for the alcoholic products quality control. *Talanta*, *246*. https://doi.org/10.1016/j.talanta.2022.123518

Koss, A. R., Sekimoto, K., Gilman, J. B., Selimovic, V., Coggon, M. M., Zarzana, K. J., Yuan, B., Lerner, B. M., Brown, S. S., Jimenez, J. L., Krechmer, J., Roberts, J. M., Warneke, C., Yokelson, R. J., & De Gouw, J. (2018). Non-methane organic gas emissions from biomass burning: Identification, quantification, and emission factors from PTR-ToF during the FIREX 2016 laboratory experiment. *Atmospheric Chemistry and Physics*, *18*(5), 3299–3319. https://doi.org/10.5194/acp-18-3299-2018

Kotsiantis, S. B. (2013). Decision trees: a recent overview. *Artificial Intelligence Review*, *39*(4), 261–283. https://doi.org/10.1007/s10462-011-9272-4

Kudo, S., Tanimoto, H., Inomata, S., Saito, S., Pan, X., Kanaya, Y., Taketani, F., Wang, Z., Chen, H., Dong, H., Zhang, M., & Yamaji, K. (2014). Emissions of nonmethane volatile organic compounds from open crop residue burning in the Yangtze River Delta region, China. *Journal of Geophysical Research*, *119*(12), 7684–7698. https://doi.org/10.1002/2013JD021044

Kudo, Y., Obayashi, K., Chu, X., Tanaka, K., Nakagawa, K., & Uchimura, T. (2023). Using an optimized relative response factor database to simplify a pyrolyzer/thermal desorption-gas chromatography-mass spectrometry method of screening for phthalate esters, polybrominated diphenyl ethers, and polybrominated biphenyls in polymers. *Journal of Analytical and Applied Pyrolysis*, *170*. https://doi.org/10.1016/j.jaap.2023.105925

Kumar, A., Sinha, V., Shabin, M., Hakkim, H., Bonsang, B., & Gros, V. (2020). Non-methane hydrocarbon (NMHC) fingerprints of major urban and agricultural emission sources for use in source apportionment studies. *Atmospheric Chemistry and Physics*, *20*(20), 12133–12152. https://doi.org/10.5194/acp-20-12133-2020

Kuo, C. P., Liao, H. T., Chou, C. C. K., & Wu, C. F. (2014). Source apportionment of particulate matter and selected volatile organic compounds with multiple time resolution data. *Science of the Total Environment*, *472*, 880–887. https://doi.org/10.1016/j.scitotenv.2013.11.114

Lan, C. H., Huang, Y. L., Ho, S. H., & Peng, C. Y. (2014). Volatile organic compound identification and characterization by PCA and mapping at a high-technology science park. *Environmental Pollution*, *193*, 156–164. https://doi.org/10.1016/j.envpol.2014.06.014

Langford, B., Nemitz, E., House, E., Phillips, G. J., Famulari, D., Davison, B., Hopkins, J. R., Lewis, A. C., & Hewitt, C. N. (2009). Fluxes and concentrations of volatile organic compounds above central London, UK. In *Chem. Phys. Discuss* (Vol. 9). www.atmos-chem-phys-discuss.net/9/17297/2009/

Langford, B., Nemitz, E., House, E., Phillips, G. J., Famulari, D., Davison, B., Hopkins, J. R., Lewis, A. C., & Hewitt, C. N. (2010). Fluxes and concentrations of volatile organic compounds above central London, UK. In *Atmos. Chem. Phys* (Vol. 10). www.atmos-chem-phys.net/10/627/2010/

Lee, S., Liu, W., Wang, Y., Russell, A. G., & Edgerton, E. S. (2008). Source apportionment of PM2.5: Comparing PMF and CMB results for four ambient monitoring sites in the southeastern United States. *Atmospheric Environment*, *42*(18), 4126–4137. https://doi.org/10.1016/j.atmosenv.2008.01.025

Lewis, A. C., Hopkins, J. R., Carslaw, D. C., Hamilton, J. F., Nelson, B. S., Stewart, G., Dernie, J., Passant, N., & Murrells, T. (2020). An increasing role for solvent emissions and implications for future measurements of volatile organic compounds: Solvent emissions of VOCs. *Philosophical Transactions of the Royal Society A: Mathematical, Physical and Engineering Sciences*, *378*(2183). https://doi.org/10.1098/rsta.2019.0328

Li, B., Ho, S. S. H., Xue, Y., Huang, Y., Wang, L., Cheng, Y., Dai, W., Zhong, H., Cao, J., & Lee, S. (2017). Characterizations of volatile organic compounds (VOCs) from vehicular emissions at roadside environment: The first comprehensive study in Northwestern China. *Atmospheric Environment*, *161*, 1–12. https://doi.org/10.1016/j.atmosenv.2017.04.029

Li, J., Lewis, A. C., Hopkins, J. R., Andrews, S. J., Murrells, T., Passant, N., Richmond, B., Hou, S., Bloss, W. J., Harrison, R. M., & Shi, Z. (2024). The impact of multi-decadal changes in VOC speciation on urban ozone chemistry: A case study in Birmingham, United Kingdom. *Atmospheric Chemistry and Physics*, *24*(10), 6219–6231. https://doi.org/10.5194/acp-24-6219-2024

Li, J., Zhai, C., Yu, J., Liu, R., Li, Y., Zeng, L., & Xie, S. (2018). Spatiotemporal variations of ambient volatile organic compounds and their sources in Chongqing, a mountainous megacity in China. *Science of the Total Environment*, *627*, 1442–1452. https://doi.org/10.1016/j.scitotenv.2018.02.010

Li, L., Xie, S., Zeng, L., Wu, R., & Li, J. (2015). Characteristics of volatile organic compounds and their role in ground-level ozone formation in the Beijing-Tianjin-Hebei region, China. *Atmospheric Environment*, *113*, 247–254. https://doi.org/10.1016/j.atmosenv.2015.05.021

Li, M., Pozzer, A., Lelieveld, J., & Williams, J. (2022). Northern hemispheric atmospheric ethane trends in the upper troposphere and lower stratosphere (2006-2016) with reference to methane and propane. *Earth System Science Data*, *14*(9), 4351–4364. https://doi.org/10.5194/essd-14-4351-2022

Li, N., Sun, T., Mudge, S., Zhang, Y., Gao, Z., Huang, L., & Lin, J. (2025). The role of atmospheric volatile organic compounds (VOCs) in ozone formation around China's largest plywood manufacturer. *Environmental Pollution*, *373*. https://doi.org/10.1016/j.envpol.2025.126197

Li, X. B., Yuan, B., Wang, S., Wang, C., Lan, J., Liu, Z., Song, Y., He, X., Huangfu, Y., Pei, C., Cheng, P., Yang, S., Qi, J., Wu, C., Huang, S., You, Y., Chang, M., Zheng, H., Yang, W., … Shao, M. (2022). Variations and sources of volatile organic compounds (VOCs) in urban region: insights from measurements on a tall tower. *Atmospheric Chemistry and Physics*, *22*(16), 10567–10587. https://doi.org/10.5194/acp-22-10567-2022

Liu, C., Ma, Z., Mu, Y., Liu, J., Zhang, C., Zhang, Y., Liu, P., & Zhang, H. (2017). The levels, variation characteristics, and sources of atmospheric non-methane hydrocarbon compounds during wintertime in Beijing, China. *Atmospheric Chemistry and Physics*, *17*(17), 10633–10649. https://doi.org/10.5194/acp-17-10633-2017

Liu, G., Xi, W., You, X., Zhi, Y., & Li, C. (2019). VOCs emission from an important industrial park in Tianjin, China. *IOP Conference Series: Earth and Environmental Science*, *227*(6). https://doi.org/10.1088/1755-1315/227/6/062037

Liu, L., Zhang, X., Wang, J., Yang, Y., Jia, W., Zhong, J., Jiang, X., & Wang, Y. (2022). Changes in the height of the pollution boundary layer and their meteorological effects on the distribution of surface ozone concentrations. *Frontiers in Environmental Science*, *10*. https://doi.org/10.3389/fenvs.2022.1094404

Liu, Y., Schallhart, S., Taipale, D., Tykkä, T., Räsänen, M., Merbold, L., Hellén, H., & Pellikka, P. (2021). *Seasonal and diurnal variations of biogenic volatile organic compounds in highland and lowland ecosystems in southern Kenya*. https://doi.org/10.5194/acp-2021-445

Liu, Y., Shao, M., Fu, L., Lu, S., Zeng, L., & Tang, D. (2008). Source profiles of volatile organic compounds (VOCs) measured in China: Part I. *Atmospheric Environment*, *42*(25), 6247–6260. https://doi.org/10.1016/j.atmosenv.2008.01.070

London Air. (2015). *BBC Radio London*. https://www.londonair.org.uk/LondonAir/general/news.aspx?newsId=6QAnez6FLEwekHVr1GZUn9&skip=30#:~:text=King's%20Environmental%20Research%20Group%20produced,most%20polluted%20streets%20in%20London.

London Data Store. (2024). *London's Population*. https://data.london.gov.uk/dataset/londons-population/

Luecken, D. J., Hutzell, W. T., Strum, M. L., & Pouliot, G. A. (2012). Regional sources of atmospheric formaldehyde and acetaldehyde, and implications for atmospheric modeling. *Atmospheric Environment*, *47*, 477–490. https://doi.org/10.1016/j.atmosenv.2011.10.005

Lv, D., Lu, S., Tan, X., Shao, M., Xie, S., & Wang, L. (2021). Source profiles, emission factors and associated contributions to secondary pollution of volatile organic compounds (VOCs) emitted from a local petroleum refinery in Shandong. *Environmental Pollution*, *274*. https://doi.org/10.1016/j.envpol.2021.116589

Lyu, X. P., Chen, N., Guo, H., Zhang, W. H., Wang, N., Wang, Y., & Liu, M. (2016). Ambient volatile organic compounds and their effect on ozone production in Wuhan, central China. *Science of the Total Environment*, *541*, 200–209. https://doi.org/10.1016/j.scitotenv.2015.09.093

Mayor OF London. (2019). *London Atmospheric Emissions Inventory (LAEI)* . Greater London Authority . https://data.london.gov.uk/dataset/london-atmospheric-emissions-inventory--laei--2019

Mayor of London. (2023). *The Ultra Low Emission Zone (ULEZ) for London*. https://www.london.gov.uk/programmes-strategies/environment-and-climate-change/pollution-and-air-quality/ultra-low-emission-zone-ulez-london

Mayor of London. (2025). *Energy supply*. https://www.london.gov.uk/programmes-and-strategies/environment-and-climate-change/energy/energy-supply

McFiggans, G., Mentel, T. F., Wildt, J., Pullinen, I., Kang, S., Kleist, E., Schmitt, S., Springer, M., Tillmann, R., Wu, C., Zhao, D., Hallquist, M., Faxon, C., Le Breton, M., Hallquist, Å. M., Simpson, D., Bergström, R., Jenkin, M. E., Ehn, M., … Kiendler-Scharr, A. (2019). Secondary organic aerosol reduced by mixture of atmospheric vapours. *Nature*, *565*(7741), 587–593. https://doi.org/10.1038/s41586-018-0871-y

McKeen, S. A., Gierczak, T., Burkholder, J. B., Wennberg, P. O., Hanisco, T. F., Keim, E. R., Gao, R. S., Liu, S. C., Ravishankara, A. R., & Fahey, D. W. (1997). The photochemistry of acetone in the upper troposphere: A source of odd-hydrogen radicals. *Geophysical Research Letters*, *24*(24), 3177–3180. https://doi.org/10.1029/97GL03349

McNabola, A., McCreddin, A., Gill, L. W., & Broderick, B. M. (2011). Analysis of the relationship between urban background air pollution concentrations and the personal exposure of office workers in Dublin, Ireland, using baseline separation techniques. *Atmospheric Pollution Research*, *2*(1), 80–88. https://doi.org/10.5094/APR.2011.010

Mcnair, H. M., & Miller, J. M. (2011). *BASIC GAS CHROMATOGRAPHY Second Edition*.

McNair, H. M., Miller, J. M., & Snow, N. H. (2019). Basic gas chromatography. *John Wiley & Sons*.

Melder, J., Zinsmeister, J., Grein, T., Jürgens, S., Köhler, M., & Oßwald, P. (2023). Comprehensive Two-Dimensional Gas Chromatography: A Universal Method for Composition-Based Prediction of Emission Characteristics of Complex Fuels. *Energy and Fuels*, *37*(6), 4580–4595. https://doi.org/10.1021/acs.energyfuels.2c04270

Mellouki, A., Wallington, T. J., & Chen, J. (2015). Atmospheric Chemistry of Oxygenated Volatile Organic Compounds: Impacts on Air Quality and Climate. In *Chemical Reviews* (Vol. 115, Issue 10, pp. 3984–4014). American Chemical Society. https://doi.org/10.1021/cr500549n

Met Office. (2023). *Met Office Integrated Data Archive System (MIDAS) Land and Marine Surface Stations Data (1853–present) [Data set]. Centre for Environmental Data Analysis (CEDA).* https://catalogue.ceda.ac.uk/uuid/220a65615218d5c9cc9e4785a3234bd0/

Metostat. (2022). *London Heathrow Airport*. https://meteostat.net/en/station/03772?t=2022-05-24/2022-05-31

Miller, L., Xu, X., Wheeler, A., Atari, D. O., Grgicak-Mannion, A., & Luginaah, I. (2011). Spatial variability and application of ratios between BTEX in two Canadian Cities. *TheScientificWorldJournal*, *11*, 2536–2549. https://doi.org/10.1100/2011/167973

Millet, D. B., Guenther, A., Siegel, D. A., Nelson, N. B., Singh, H. B., De Gouw, J. A., Warneke, C., Williams, J., Eerdekens, G., Sinha, V., Karl, T., Flocke, F., Apel, E., Riemer, D. D., Palmer, P. I., & Barkley, M. (2010). Atmospheric Chemistry and Physics Global atmospheric budget of acetaldehyde: 3-D model analysis and constraints from in-situ and satellite observations. In *Atmos. Chem. Phys* (Vol. 10). www.atmos-chem-phys.net/10/3405/2010/

Mishra, A. K., & Sinha, V. (2020). Emission drivers and variability of ambient isoprene, formaldehyde and acetaldehyde in north-west India during monsoon season. *Environmental Pollution*, *267*. https://doi.org/10.1016/j.envpol.2020.115538

Mondal, A., Saharan, U. S., Arya, R., Yadav, L., Ahlawat, S., Jangirh, R., Kotnala, G., Choudhary, N., Banoo, R., Rai, A., Yadav, P., Rani, M., Lal, S., Stewart, G. J., Nelson, B. S., Acton, W. J. F., Vaughan, A. R., Hamilton, J. F., Hopkins, J. R., … Mandal, T. K. (2021). Non-methane volatile organic compounds emitted from domestic fuels in Delhi: Emission factors and total city-wide emissions. *Atmospheric Environment: X*, *11*. https://doi.org/10.1016/j.aeaoa.2021.100127

Monks, P. S. (2005). NucleobasesGas-phase radical chemistry in the troposphere. *Chemical Society Reviews*, *34*(5), 376–395. https://doi.org/10.1039/b307982c

Montero-Montoya, R., López-Vargas, R., & Arellano-Aguilar, O. (2018). Volatile organic compounds in air: Sources, distribution, exposure and associated illnesses in children. In *Annals of Global Health* (Vol. 84, Issue 2, pp. 225–238). Levy Library Press. https://doi.org/10.29024/aogh.910

Morgott, D. A. (2015). Anthropogenic and biogenic sources of Ethylene and the potential for human exposure: A literature review. *Chemico-Biological Interactions*, *241*, 10–22. https://doi.org/10.1016/j.cbi.2015.08.012

Mugica, V., Watson, J., Vega, E., Reyes, E., Ruiz, M. E., & Chow, J. (2002). Receptor model source apportionment of nonmethane hydrocarbons in Mexico City. *TheScientificWorldJournal*, *2*, 844–860. https://doi.org/10.1100/tsw.2002.147

NAEI. (2024). *Non methane VOC*. https://naei.energysecurity.gov.uk/air-pollutants/non-methane-voc

NAEI. (2025). *UK Emissions Interactive Map*. https://naei.energysecurity.gov.uk/emissionsapp/

National Physical Laboratory (NPL). (n.d.). *Standard primary reference gases*. Retrieved March 23, 2025, from https://www.npl.co.uk/products-services/gas/primary-reference-gas-materials

National statistics. (2021). *Population estimates for the UK, England and Wales, Scotland and Northern Ireland, provisional: mid-2019*.

NOAA. (2022). *Data Tools: Find a Station*. https://www.ncei.noaa.gov/cdo-web/datatools/findstation

Norris, G., & Bai, S. (2014). *EPA Positive M atrix Factorization (PM F) 5.0 Fundamentals and User Guide*. www.epa.gov

Office for Health Improvement and Disparities. (2022, February). *Air pollution: applying All Our Health*. Https://Www.Gov.Uk/Government/Publications/Air-Pollution-Applying-All-Our-Health/Air-Pollution-Applying-All-Our-Health#:~:Text=In%20the%20UK%2C%20air%20pollution,And%2036%2C000%20deaths%20every%20year.

Office for National Statistics. (2022). *Estimates of the population for the UK, England, Wales*. https://www.ons.gov.uk/peoplepopulationandcommunity/populationandmigration/populationestimates/datasets/populationestimatesforukenglandandwalesscotlandandnorthernireland

Olivella, S., & Solé, A. (2004). Unimolecular decomposition of β-hydroxyethylperoxy radicals in the HȮ-initiated oxidation of ethene: A theoretical study. *Journal of Physical Chemistry A*, *108*(52), 11651–11663. https://doi.org/10.1021/jp045944f

Olumayede, E. G. (2014). Atmospheric Volatile Organic Compounds and Ozone Creation Potential in an Urban Center of Southern Nigeria. *International Journal of Atmospheric Sciences*, *2014*, 1–7. https://doi.org/10.1155/2014/764948

ONS. (2024). *Population estimates*. https://www.ons.gov.uk/peoplepopulationandcommunity/populationandmigration/populationestimates

Ortega, A. M., Hayes, P. L., Peng, Z., Palm, B. B., Hu, W., Day, D. A., Li, R., Cubison, M. J., Brune, W. H., Graus, M., Warneke, C., Gilman, J. B., Kuster, W. C., De Gouw, J., Gutiérrez-Montes, C., & Jimenez, J. L. (2016). Real-time measurements of secondary organic aerosol formation and aging from ambient air in an oxidation flow reactor in the Los Angeles area. *Atmospheric Chemistry and Physics*, *16*(11), 7411–7433. https://doi.org/10.5194/acp-16-7411-2016

Ou, J., Zheng, J., Li, R., Huang, X., Zhong, Z., Zhong, L., & Lin, H. (2015). Speciated OVOC and VOC emission inventories and their implications for reactivity-based ozone control strategy in the pearl river delta region, China. *Science of the Total Environment*, *530–531*, 393–402. https://doi.org/10.1016/j.scitotenv.2015.05.062

Paatero, P., & Tapper, U. (1994). Positive matrix factorization: A non-negative factor model with optimal utilization of error estimates of data values. *Environmetrics*, *5*(2), 111–126. https://doi.org/10.1002/env.3170050203

Pandit, G. G., Sahu, S. K., & Puranik, V. D. (2011). Distribution and source apportionment of atmospheric non-methane hydrocarbons in Mumbai, India. *Atmospheric Pollution Research*, *2*(2), 231–236. https://doi.org/10.5094/APR.2011.029

Park, S. K., Kim, S. Do, & Lee, H. (2004). Dispersion characteristics of vehicle emission in an urban street canyon. *Science of the Total Environment*, *323*(1–3), 263–271. https://doi.org/10.1016/j.scitotenv.2003.09.032

Pearson, J. K. (2019). European solvent VOC emission inventories based on industry-wide information. *Atmospheric Environment*, *204*, 118–124. https://doi.org/10.1016/j.atmosenv.2019.02.014

Pernov, J. B., Bossi, R., Lebourgeois, T., Nøjgaard, J. K., Holzinger, R., Hjorth, J. L., & Skov, H. (2021). Atmospheric VOC measurements at a High Arctic site: Characteristics and source apportionment. *Atmospheric Chemistry and Physics*, *21*(4), 2895–2916. https://doi.org/10.5194/acp-21-2895-2021

Pinthong, N., Thepanondh, S., & Kondo, A. (2022). Source Identification of VOCs and their Environmental Health Risk in a Petrochemical Industrial Area. *Aerosol and Air Quality Research*, *22*(2). https://doi.org/10.4209/aaqr.210064

Pinthong, N., Thepanondh, S., Kultan, V., & Keawboonchu, J. (2022). Characteristics and Impact of VOCs on Ozone Formation Potential in a Petrochemical Industrial Area, Thailand. *Atmosphere*, *13*(5). https://doi.org/10.3390/atmos13050732

Poole, C. F. (2015). Ionization-based detectors for gas chromatography. *Journal of Chromatography A*, *1421*, 137–153. https://doi.org/https://doi.org/10.1016/j.chroma.2015.02.061

Poole, C. F. (2019). Conventional Gas Chromatography: Basic Principles and Instrumental Aspects. In P. Q. Tranchida (Ed.), *Advanced Gas Chromatography in Food Analysis* (p. 0). The Royal Society of Chemistry. https://doi.org/10.1039/9781788015752-00083

Pravallika, S. (2016). Gas Chromatography a Mini Review. *Research and Reviews Journal of Pharmaceutical Analysis RRJPA |*, *5*(2).

Pripdeevech, P., Janta, R., Sripahco, T., Meesang, W., Aiyathiti, C., Prabamroong, T., Mahatheeranont, S., Poshyachinda, S., Pongpiachan, S., & Khruengsai, S. (2025). Seasonal volatile organic compound dynamics in urban and forest environments in Thailand: Implications for air quality and secondary pollutants. *Environmental Pollution*, *367*. https://doi.org/10.1016/j.envpol.2024.125565

Raj, N., & Sharma, B. (2017). Effect of meteorological condiation on NOx pollution of Kota city, India. *Indian Journal of Scientific Research*.

Rajabi, H., Mosleh, M. H., Mandal, P., Lea-Langton, A., & Sedighi, M. (2020). Emissions of volatile organic compounds from crude oil processing – Global emission inventory and environmental release. *Science of the Total Environment*, *727*(1). https://doi.org/10.1016/j.scitotenv.2020.138654

Ramirez-Gamboa, J., Paton-Walsh, C., Galbally, I., Simmons, J., Guerette, E. A., Griffith, A. D., Chambers, S. D., & Williams, A. G. (2021). Seasonal Variation of Biogenic and Anthropogenic VOCs in a Semi-Urban Area Near Sydney, Australia. *Atmosphere*, *12*(1). https://doi.org/10.3390/atmos12010047

Reff, A., Eberly, S. I., & Bhave, P. V. (2007). Receptor modeling of ambient particulate matter data using positive matrix factorization: Review of existing methods. *Journal of the Air and Waste Management Association*, *57*(2), 146–154. https://doi.org/10.1080/10473289.2007.10465319

Ren, J., Guo, F., & Xie, S. (2022). Diagnosing ozone-NOx-VOC sensitivity and revealing causes of ozone increases in China based on 2013-2021 satellite retrievals. *Atmospheric Chemistry and Physics*, *22*(22), 15035–15047. https://doi.org/10.5194/acp-22-15035-2022

Ren, Y., Qu, Z., Du, Y., Xu, R., Ma, D., Yang, G., Shi, Y., Fan, X., Tani, A., Guo, P., Ge, Y., & Chang, J. (2017). Air quality and health effects of biogenic volatile organic compounds emissions from urban green spaces and the mitigation strategies. *Environmental Pollution*, *230*, 849–861. https://doi.org/10.1016/j.envpol.2017.06.049

Ricardo Energy & Environment. (2020).

Richard K. Lattanzio. (2020). *Methane and Other Air Pollution Issues in Natural Gas Systems*. https://crsreports.congress.gov

Richmond, B. (2025). *NMVOC Speciation Information-NAEI23 README 1 Ricardo NMVOC Speciation Information-NAEI23 README*. https://www.eea.europa.eu/en/analysis/publications/emep-eea-guidebook-2023

Riveron, T. P., Wilde, M. J., Ibrahim, W., Carr, L., Monks, P. S., Greening, N. J., Gaillard, E. A., Brightling, C. E., Siddiqui, S., Hansell, A. L., & Cordell, R. L. (2023). Characterisation of volatile organic compounds in hospital indoor air and exposure health risk determination. *Building and Environment*, *242*. https://doi.org/10.1016/j.buildenv.2023.110513

Rosado-Reyes, C. M., & Francisco, J. S. (2007). Atmospheric oxidation pathways of propane and its by-products: Acetone, acetaldehyde, and propionaldehyde. *Journal of Geophysical Research Atmospheres*, *112*(14). https://doi.org/10.1029/2006JD007566

Rubin, J. I., Kean, A. J., Harley, R. A., Millet, D. B., & Goldstein, A. H. (2006). Temperature dependence of volatile organic compound evaporative emissions from motor vehicle. *Journal of Geophysical Research Atmospheres*, *111*(3). https://doi.org/10.1029/2005JD006458

Rudolph, J., & Ehhalt, D. (1981). Measurements of C2-C5 hydrocarbons over the North Atlantic. *J. Geophys. Res.: Oceans* , 11959–11964.

Russo, R. S., Zhou, Y., Haase, K. B., Wingenter, O. W., Frinak, E. K., Mao, H., Talbot, R. W., & Sive, B. C. (2010). Atmospheric Chemistry and Physics Temporal variability, sources, and sinks of C 1-C 5 alkyl nitrates in coastal New England. In *Atmos. Chem. Phys* (Vol. 10). www.atmos-chem-phys.net/10/1865/2010/

Sadeghi, B., Pouyaei, A., Choi, Y., & Rappenglueck, B. (2021). *Measurement report: Summertime and wintertime VOCs in Houston: Source apportionment and spatial distribution of source origins*. https://doi.org/10.5194/acp-2021-565

Sagebiel, J. C., Zielinska, B., Pierson, W. R., & Gertler, A. W. (1996). REAL-WORLD EMISSIONS AND CALCULATED REACTIVITIES OF ORGANIC SPECIES FROM MOTOR VEHICLES. In *Atmospheric Environment* (Vol. 30, Issue 12).

Salameh, T., Sauvage, S., Afif, C., Borbon, A., & Locoge, N. (2016). Source apportionment vs. emission inventories of non-methane hydrocarbons (NMHC) in an urban area of the Middle East: Local and global perspectives. *Atmospheric Chemistry and Physics*, *16*(5), 3595–3607. https://doi.org/10.5194/acp-16-3595-2016

Sangiorgi, G., Ferrero, L., Perrone, M. G., Bolzacchini, E., Duane, M., & Larsen, B. R. (2011). Vertical distribution of hydrocarbons in the low troposphere below and above the mixing height: Tethered balloon measurements in Milan, Italy. *Environmental Pollution*, *159*(12), 3545–3552. https://doi.org/10.1016/j.envpol.2011.08.012

Seinfeld, J. H., & Pandis, S. N. (2016). *From Air Pollution to Climate Change* (3rd ed.). Atmospheric Chemistry and Physics:

Shan, Y., Zhu, Y., Sui, H., Zhao, N., Li, H., Wen, L., Chen, T., Qi, Y., Qi, W., Wang, X., Zhang, Y., Xue, L., & Wang, W. (2025). Vertical distribution and regional transport of air pollution over Northeast China: Insights from an intensive aircraft study. *Atmospheric Environment*, *358*. https://doi.org/10.1016/j.atmosenv.2025.121327

Sharkey, T. D., Wiberley, A. E., & Donohue, A. R. (2008). Isoprene emission from plants: Why and how. In *Annals of Botany* (Vol. 101, Issue 1, pp. 5–18). https://doi.org/10.1093/aob/mcm240

Shen, L., Xiang, P., Liang, S., Chen, W., Wang, M., Lu, S., & Wang, Z. (2018). Sources profiles of volatile organic compounds (VOCs) measured in a typical industrial process in Wuhan, central China. *Atmosphere*, *9*(8). https://doi.org/10.3390/atmos9080297

Sigma-Aldrich. (n.d.). *Analytical Chemistry*. Retrieved March 23, 2025, from https://www.sigmaaldrich.com/GB/en/applications/analytical-chemistry

Sillman, S. (1999). Tropospheric ozone and photochemical smog. In *Atmos. Environ* (Vol. 9, Issue 11). Elsevier. http://www-personal.engin.umich.edu/~sillmanhttp://www-personal.engin.umich.edu/~sillman

Simpson, I. J., Andersen, M. P. S., Meinardi, S., Bruhwiler, L., Blake, N. J., Helmig, D., Sherwood Rowland, F., & Blake, D. R. (2012). Long-term decline of global atmospheric ethane concentrations and implications for methane. *Nature*, *488*(7412), 490–494. https://doi.org/10.1038/nature11342

Sindelarova, K., Granier, C., Bouarar, I., Guenther, A., Tilmes, S., Stavrakou, T., Müller, J. F., Kuhn, U., Stefani, P., & Knorr, W. (2014). Global data set of biogenic VOC emissions calculated by the MEGAN model over the last 30 years. *Atmospheric Chemistry and Physics*, *14*(17), 9317–9341. https://doi.org/10.5194/acp-14-9317-2014

Singh, H. B., O'Hara, D., Herlth, D., Sachse, W., Blake, D. R., Bradshaw, J. D., Kanakidou, M., & Crutzen, P. J. (1994). Acetone in the atmosphere: Distribution, sources, and sinks. *Journal of Geophysical Research: Atmospheres*, *99*(D1), 1805–1819. https://doi.org/https://doi.org/10.1029/93JD00764

Singh, H., Herlth, D., Sachse, W., Blake, D., Bradshaw, J., Kanakidou, M., Crutzen, P., Singh, H. B., Blake, D. R., Bradshaw, J. D., & Crutzen, P. J. (1994). Acetone in the atmosphere: Distribution, sources, and sinks. *Journal of Geophysical Research*, *99*(D1), 1805–1819. https://doi.org/10.1029/93JD00764ï

Smith, L. (2025). Air quality: policies, proposals and concerns. In *commonslibrary.parliament.uk Research Briefing* (Vol. 14).

Sokhi, R. S., Moussiopoulos, N., Baklanov, A., Bartzis, J., Coll, I., Finardi, S., Friedrich, R., Geels, C., Grönholm, T., Halenka, T., Ketzel, M., Maragkidou, A., Matthias, V., Moldanova, J., Ntziachristos, L., Schäfer, K., Suppan, P., Tsegas, G., Carmichael, G., … Kukkonen, J. (2022). Advances in air quality research - current and emerging challenges. In *Atmospheric Chemistry and Physics* (Vol. 22, Issue 7, pp. 4615–4703). Copernicus GmbH. https://doi.org/10.5194/acp-22-4615-2022

Sommariva, R., De Gouw, J. A., Trainer, M., Atlas, E., Goldan, P. D., Kuster, W. C., Warneke, C., & Fehsenfeld, F. C. (2011). Emissions and photochemistry of oxygenated VOCs in urban plumes in the Northeastern United States. *Atmospheric Chemistry and Physics*, *11*(14), 7081–7096. https://doi.org/10.5194/acp-11-7081-2011

Song, C., Liu, B., Dai, Q., Li, H., & Mao, H. (2019). Temperature dependence and source apportionment of volatile organic compounds (VOCs) at an urban site on the north China plain. *Atmospheric Environment*, *207*, 167–181. https://doi.org/10.1016/j.atmosenv.2019.03.030

Song, C., Liu, Y., Sun, L., Zhang, Q., & Mao, H. (2020). Emissions of volatile organic compounds (VOCs) from gasoline- and liquified natural gas (LNG)-fueled vehicles in tunnel studies. *Atmospheric Environment*, *234*. https://doi.org/10.1016/j.atmosenv.2020.117626

Song, M., Tan, Q., Feng, M., Qu, Y., Liu, X., An, J., & Zhang, Y. (2018). Source Apportionment and Secondary Transformation of Atmospheric Nonmethane Hydrocarbons in Chengdu,

Southwest China. *Journal of Geophysical Research: Atmospheres*, *123*(17), 9741–9763. https://doi.org/10.1029/2018JD028479

Song, S. K., Shon, Z. H., Kang, Y. H., Kim, K. H., Han, S. B., Kang, M., Bang, J. H., & Oh, I. (2019). Source apportionment of VOCs and their impact on air quality and health in the megacity of Seoul. *Environmental Pollution*, *247*, 763–774. https://doi.org/10.1016/j.envpol.2019.01.102

SRN. (2020, September). *Impact of the coronavirus (COVID-19) pandemic on travel time measures*. https://www.gov.uk/government/statistics/travel-time-measures-for-the-strategic-road-network-and-local-a-roads-july-2019-to-june-2020/impact-of-the-coronavirus-covid-19-pandemic-on-travel-time-measures

Steinemann, A. (2015). Volatile emissions from common consumer products. *Air Quality, Atmosphere and Health*, *8*(3), 273–281. https://doi.org/10.1007/s11869-015-0327-6

Stemmler, K., Bugmann, S., Buchmann, B., Reimann, S., & Staehelin, J. (2005). Large decrease of VOC emissions of Switzerland's car fleet during the past decade: Results from a highway tunnel study. *Atmospheric Environment*, *39*(6), 1009–1018. https://doi.org/10.1016/j.atmosenv.2004.10.010

Stockwell, C. E., Veres, P. R., Williams, J., & Yokelson, R. J. (2015). Characterization of biomass burning emissions from cooking fires, peat, crop residue, and other fuels with high-resolution proton-transfer-reaction time-of-flight mass spectrometry. *Atmospheric Chemistry and Physics*, *15*(2), 845–865. https://doi.org/10.5194/acp-15-845-2015

Su, Y. C., Chen, W. H., Fan, C. L., Tong, Y. H., Weng, T. H., Chen, S. P., Kuo, C. P., Wang, J. L., & Chang, J. S. (2019). Source Apportionment of Volatile Organic Compounds (VOCs) by Positive Matrix Factorization (PMF) supported by Model Simulation and Source Markers - Using Petrochemical Emissions as a Showcase. *Environmental Pollution*, *254*. https://doi.org/10.1016/j.envpol.2019.07.016

Suthawaree, J., Kato, S., Okuzawa, K., Kanaya, Y., Pochanart, P., Akimoto, H., Wang, Z., & Kajii, Y. (2010). Atmospheric Chemistry and Physics Measurements of volatile organic compounds in the middle of Central East China during Mount Tai Experiment 2006

(MTX2006): observation of regional background and impact of biomass burning. In *Atmos. Chem. Phys* (Vol. 10). www.atmos-chem-phys.net/10/1269/2010/

Swamy, Y. V., Venkanna, R., Nikhil, G. N., Chitanya, D. N. S. K., Sinha, P. R., Ramakrishna, M., & Rao, A. G. (2012). Impact of nitrogen oxides, volatile organic compounds and black carbon on atmospheric ozone levels at a semi Arid Urban Site in Hyderabad. *Aerosol and Air Quality Research*, *12*(4), 662–671. https://doi.org/10.4209/aaqr.2012.01.0019

TEXAS COMMISSION ON ENVIRONMENTAL QUALITY. (2008). *FACT SHEET 2-BUTENE (CIS AND TRANS)*.

Tham, Y. J., Wang, Z., Li, Q., Yun, H., Wang, W., Wang, X., Xue, L., Lu, K., Ma, N., Bohn, B., Li, X., Kecorius, S., Größ, J., Shao, M., Wiedensohler, A., Zhang, Y., & Wang, T. (2016). Significant concentrations of nitryl chloride sustained in the morning: Investigations of the causes and impacts on ozone production in a polluted region of northern China. *Atmospheric Chemistry and Physics*, *16*(23), 14959–14977. https://doi.org/10.5194/acp-16-14959-2016

Tiwari, V., Hanai, Y., & Masunaga, S. (2010). Ambient levels of volatile organic compounds in the vicinity of petrochemical industrial area of Yokohama, Japan. *Air Quality, Atmosphere and Health*, *3*(2), 65–75. https://doi.org/10.1007/s11869-009-0052-0

Tong, W., Hong, H., Fang, H., Xie, Q., & Perkins, R. (2003). Decision Forest: Combining the Predictions of Multiple Independent Decision Tree Models. *Journal of Chemical Information and Computer Sciences*, *43*(2), 525–531. https://doi.org/10.1021/ci020058s

Toon, G. C., Blavier, J. F. L., & Sung, K. (2018). Measurements of atmospheric ethene by solar absorption FTIR spectrometry. *Atmospheric Chemistry and Physics*, *18*(7), 5075–5088. https://doi.org/10.5194/acp-18-5075-2018

Tranchida, P. Q. (2019). *Advanced Gas Chromatography in Food Analysis* (P. Q. Tranchida, Ed.). The Royal Society of Chemistry. https://doi.org/10.1039/9781788015752

Transport for London. (2020). *Air quality*. https://tfl.gov.uk/corporate/about-tfl/air-quality

Trust For London. (2022). *Population changes over the decades*. https://trustforlondon.org.uk/data/population-over-time/

UK Air. (2023). *Air Information Resource*. https://uk-air.defra.gov.uk/networks/site-info?uka_id=UKA00656

Ulbrich, I. M., Canagaratna, M. R., Zhang, Q., Worsnop, D. R., & Jimenez, J. L. (2008). Interpretation of organic components from positive matrix factorization of aerosol mass spectrometric data Organic components from PMF of Q-AMS data. *Chem. Phys. Discuss*, *8*, 6729–6791. www.atmos-chem-phys-discuss.net/8/6729/2008/

University of Birmingham. (2023). *Birmingham Air Quality Supersite (BAQS)*. https://www.birmingham.ac.uk/research/centres-institutes/birmingham-air-quality-supersite#:~:text=The%20Birmingham%20Air%20Quality%20Supersite,liquid%20droplets%20suspended%20in%20air.

Uria-Tellaetxe, I., & Carslaw, D. C. (2014). Conditional bivariate probability function for source identification. *Environmental Modelling and Software*, *59*, 1–9. https://doi.org/10.1016/j.envsoft.2014.05.002

US EPA. (1997). *DETERMINATION OF GASEOUS ORGANIC COMPOUNDS BY DIRECT INTERFACE GAS CHROMATOGRAPHY-MASS SPECTROMETRY INTRODUCTION*.

USEPA. (2018). *Report on the Environment Volatile Organic Compounds Emissions*. https://www.epa.gov/sites/production/files/2018-07/documents/nei2014v2_tsd_05jul2018.pdf

Valach, A. C., Langford, B., Nemitz, E., Mackenzie, A. R., & Hewitt, C. N. (2015). Seasonal and diurnal trends in concentrations and fluxes of volatile organic compounds in central London. *Atmospheric Chemistry and Physics*, *15*(14), 7777–7796. https://doi.org/10.5194/acp-15-7777-2015

Vardoulakis, S., Fisher, B. E. A., Pericleous, K., & Gonzalez-Flesca, N. (2003). Modelling air quality in street canyons: a review. In *Atmospheric Environment* (Vol. 37).

Vaughan, A. R., Lee, J. D., Shaw, M. D., Misztal, P. K., Metzger, S., Vieno, M., Davison, B., Karl, T. G., Carpenter, L. J., Lewis, A. C., Purvis, R. M., Goldstein, A. H., & Hewitt, C. N. (2017). VOC emission rates over London and South East England obtained by airborne eddy covariance. In *Faraday Discussions* (Vol. 200, pp. 599–620). Royal Society of Chemistry. https://doi.org/10.1039/c7fd00002b

Vozka, P., Modereger, B. A., Park, A. C., Zhang, W. T. J., Trice, R. W., Kenttämaa, H. I., & Kilaz, G. (2019). Jet fuel density via GC × GC-FID. *Fuel*, *235*, 1052–1060. https://doi.org/https://doi.org/10.1016/j.fuel.2018.08.110

Wang, H., Lou, S., Huang, C., Qiao, L., Tang, X., Chen, C., Zeng, L., Wang, Q., Zhou, M., Lu, S., & Yu, X. (2014). Source profiles of volatile organic compounds from biomass burning in yangtze river Delta, China. *Aerosol and Air Quality Research*, *14*(3), 818–828. https://doi.org/10.4209/aaqr.2013.05.0174

Wang, H., Qiao, Y., Chen, C., Lu, J., Dai, H., Qiao, L., Lou, S., Huang, C., Li, L., Jing, S., & Wu, J. (2014). Source profiles and chemical reactivity of volatile organic compounds from solvent use in Shanghai, China. *Aerosol and Air Quality Research*, *14*(1), 301–310. https://doi.org/10.4209/aaqr.2013.03.0064

Wang, M., Li, S., Zhu, R., Zhang, R., Zu, L., Wang, Y., & Bao, X. (2020). On-road tailpipe emission characteristics and ozone formation potentials of VOCs from gasoline, diesel and liquefied petroleum gas fueled vehicles. *Atmospheric Environment*, *223*. https://doi.org/10.1016/j.atmosenv.2020.117294

Wang, M., Lu, S., Shao, M., Zeng, L., Zheng, J., Xie, F., Lin, H., Hu, K., & Lu, X. (2021). Impact of COVID-19 lockdown on ambient levels and sources of volatile organic compounds (VOCs) in Nanjing, China. *Science of the Total Environment*, *757*. https://doi.org/10.1016/j.scitotenv.2020.143823

Warneke, C., de Gouw, J. A., Goldan, P. D., Kuster, W. C., Williams, E. J., Lerner, B. M., Jakoubek, R., Brown, S. S., Stark, H., Aldener, M., Ravishankara, A. R., Roberts, J. M., Marchewka, M., Bertman, S., Sueper, D. T., McKeen, S. A., Meagher, J. F., & Fehsenfeld, F. C. (2004). Comparison of daytime and nighttime oxidation of biogenic and anthropogenic VOCs along the New England coast in summer during New England Air Quality Study 2002. *Journal of Geophysical Research D: Atmospheres*, *109*(10). https://doi.org/10.1029/2003JD004424

Warneke, C., Roberts, J. M., Veres, P., Gilman, J., Kuster, W. C., Burling, I., Yokelson, R., & De Gouw, J. A. (2011). VOC identification and inter-comparison from laboratory biomass

burning using PTR-MS and PIT-MS. *International Journal of Mass Spectrometry*, *303*(1), 6–14. https://doi.org/10.1016/j.ijms.2010.12.002

Watson, J. G., Chow, J. C., & Fujita, E. M. (2001). Review of volatile organic compound source apportionment by chemical mass balance. In *Atmospheric Environment* (Vol. 35).

WHO. (2020). *WHO Director-General's opening remarks at the media briefing on COVID-19 - 11 March 2020*. https://www.who.int/director-general/speeches/detail/who-director-general-s-opening-remarks-at-the-media-briefing-on-covid-19---11-march-2020

Wild, O. (2007). Atmospheric Chemistry and Physics Modelling the global tropospheric ozone budget: exploring the variability in current models. In *Atmos. Chem. Phys* (Vol. 7). www.atmos-chem-phys.net/7/2643/2007/

WMO. (2007). *WORLD METEOROLOGICAL ORGANIZATION GLOBAL ATMOSPHERE WATCH A WMO/GAW EXPERT WORKSHOP on GLOBAL LONG-TERM MEASUREMENTS of VOLATILE ORGANIC COMPOUNDS (VOCs)*.

Wu, C., Wang, C., Wang, S., Wang, W., Yuan, B., Qi, J., Wang, B., Wang, H., Wang, C., Song, W., Wang, X., Hu, W., Lou, S., Ye, C., Peng, Y., Wang, Z., Huangfu, Y., Xie, Y., Zhu, M., … Shao, M. (2020). Measurement report: Important contributions of oxygenated compounds to emissions and chemistry of volatile organic compounds in urban air. *Atmospheric Chemistry and Physics*, *20*(23), 14769–14785. https://doi.org/10.5194/acp-20-14769-2020

Wu, X., Huang, W., Zhang, Y., Zheng, C., Jiang, X., Gao, X., & Cen, K. (2015). Characteristics and uncertainty of industrial VOCs emissions in China. *Aerosol and Air Quality Research*, *15*(3), 1045–1058. https://doi.org/10.4209/aaqr.2014.10.0236

Xiao, Y., Jacob, D. J., & Turquety, S. (2007). Atmospheric acetylene and its relationship with CO as an indicator of air mass age. *Journal of Geophysical Research Atmospheres*, *112*(12). https://doi.org/10.1029/2006JD008268

Xiao, Y., Logan, J. A., Jacob, D. J., Hudman, R. C., Yantosca, R., & Blake, D. R. (2008). Global budget of ethane and regional constraints on U.S. sources. *Journal of Geophysical Research Atmospheres*, *113*(21). https://doi.org/10.1029/2007JD009415

Xiong, Y., Bari, M. A., Xing, Z., & Du, K. (2020). Ambient volatile organic compounds (VOCs) in two coastal cities in western Canada: Spatiotemporal variation, source apportionment, and health risk assessment. *Science of the Total Environment*, *706*. https://doi.org/10.1016/j.scitotenv.2019.135970

Xu, X., Van Stee, L. L. P., Williams, J., Beens, J., Adahchour, M., Vreuls, R. J. J., Brinkman, U. A. T., & Lelieveld, J. (2003). Atmospheric Chemistry and Physics Comprehensive two-dimensional gas chromatography (GC×GC) measurements of volatile organic compounds in the atmosphere. In *Atmos. Chem. Phys* (Vol. 3). www.atmos-chem-phys.org/acp/3/665/

Xu, Y., Yu, H., Yan, Y., Peng, L., Li, R., Wang, C., & Li, Z. (2021). Emission characteristics of volatile organic compounds from typical coal utilization sources: A case study in shanxi of Northern China. *Aerosol and Air Quality Research*, *21*(9). https://doi.org/10.4209/aaqr.210050

Xue, Y., Ho, S. S. H., Huang, Y., Li, B., Wang, L., Dai, W., Cao, J., & Lee, S. (2017). Source apportionment of VOCs and their impacts on surface ozone in an industry city of Baoji, Northwestern China. *Scientific Reports*, *7*(1). https://doi.org/10.1038/s41598-017-10631-4

Xue, Y., Huang, Y., Sai Hang Ho, S., Chen, L., Wang, L., Lee, S., & Cao, J. (2020). Origin and transformation of ambient volatile organic compounds during a dust-to-haze episode in northwest China. *Atmospheric Chemistry and Physics*, *20*(9), 5425–5436. https://doi.org/10.5194/acp-20-5425-2020

Yan, X., Qiu, X., Yao, Z., Liu, J., & Wang, L. (2024). Emissions of Oxygenated Volatile Organic Compounds and Their Roles in Ozone Formation in Beijing. *Atmosphere*, *15*(8). https://doi.org/10.3390/atmos15080970

Yáñez-Serrano, A. M., Nölscher, A. C., Bourtsoukidis, E., Derstroff, B., Zannoni, N., Gros, V., Lanza, M., Brito, J., Noe, S. M., House, E., Hewitt, C. N., Langford, B., Nemitz, E., Behrendt, T., Williams, J., Artaxo, P., Andreae, M. O., & Kesselmeier, J. (2016). Atmospheric mixing ratios of methyl ethyl ketone (2-butanone) in tropical, boreal, temperate and marine

environments. *Atmospheric Chemistry and Physics*, *16*(17), 10965–10984. https://doi.org/10.5194/acp-16-10965-2016

Yang, Y., Liu, B., Hua, J., Yang, T., Dai, Q., Wu, J., Feng, Y., & Hopke, P. K. (2022). Global review of source apportionment of volatile organic compounds based on highly time-resolved data from 2015 to 2021. In *Environment International* (Vol. 165). Elsevier Ltd. https://doi.org/10.1016/j.envint.2022.107330

Ye, Y., Galbally, -I E, Weeks, -I A, Duffy, -B L, & Nelson, P. F. (1998). EVAPORATIVE EMISSIONS OF 1,3-BUTADIENE FROM PETROL-FUELLED MOTOR VEHICLES. In *Atmospheric Environment* (Vol. 32, Issue 14).

Yeoman, A. M., & Lewis, A. C. (2021). Global emissions of VOCs from compressed aerosol products. *Elementa: Science of the Anthropocene*, *9*(1). https://doi.org/10.1525/elementa.2020.20.00177

Yeoman, A. M., Shaw, M., & Lewis, A. C. (2021). Estimating person-to-person variability in VOC emissions from personal care products used during showering. *Indoor Air*, *31*(4), 1281–1291. https://doi.org/10.1111/ina.12811

Yuan, B., Koss, A. R., Warneke, C., Coggon, M., Sekimoto, K., & De Gouw, J. A. (2017). Proton-Transfer-Reaction Mass Spectrometry: Applications in Atmospheric Sciences. *Chemical Reviews*, *117*(21), 13187–13229. https://doi.org/10.1021/acs.chemrev.7b00325

Yuan, B., Koss, A., Warneke, C., Gilman, J. B., Lerner, B. M., Stark, H., & De Gouw, J. A. (2016). A high-resolution time-of-flight chemical ionization mass spectrometer utilizing hydronium ions (H3O+ ToF-CIMS) for measurements of volatile organic compounds in the atmosphere. *Atmospheric Measurement Techniques*, *9*(6), 2735–2752. https://doi.org/10.5194/amt-9-2735-2016

Yuan, B., Shao, M., De Gouw, J., Parrish, D. D., Lu, S., Wang, M., Zeng, L., Zhang, Q., Song, Y., Zhang, J., & Hu, M. (2012). Volatile organic compounds (VOCs) in urban air: How chemistry affects the interpretation of positive matrix factorization (PMF) analysis. *Journal of Geophysical Research Atmospheres*, *117*(24). https://doi.org/10.1029/2012JD018236

Zhang, H., Li, H., Zhang, Q., Zhang, Y., Zhang, W., Wang, X., Bi, F., Chai, F., Gao, J., Meng, L., Yang, T., Chen, Y., Cheng, Q., & Xia, F. (2017). Atmospheric volatile organic compounds in a typical urban area of beijing: Pollution characterization, health risk assessment and source apportionment. *Atmosphere*, *8*(3). https://doi.org/10.3390/atmos8030061

Zhang, K., Xiu, G., Zhou, L., Bian, Q., Duan, Y., Fei, D., Wang, D., & Fu, Q. (2018). Vertical distribution of volatile organic compounds within the lower troposphere in late spring of Shanghai. *Atmospheric Environment*, *186*, 150–157. https://doi.org/10.1016/j.atmosenv.2018.03.044

Zhang, L., Wang, X., Li, H., Cheng, N., Zhang, Y., Zhang, K., & Li, L. (2021). Variations in levels and sources of atmospheric vocs during the continuous haze and non-haze episodes in the urban area of beijing: A case study in spring of 2019. *Atmosphere*, *12*(2), 1–15. https://doi.org/10.3390/atmos12020171

Zhang, Q., Wu, L., Fang, X., Liu, M., Zhang, J., Shao, M., Lu, S., & Mao, H. (2018). Emission factors of volatile organic compounds (VOCs) based on the detailed vehicle classification in a tunnel study. *Science of the Total Environment*, *624*, 878–886. https://doi.org/10.1016/j.scitotenv.2017.12.171

Zhang, Y., Wang, X., Zhang, Z., Lü, S., Shao, M., Lee, F. S. C., & Yu, J. (2013). Species profiles and normalized reactivity of volatile organic compounds from gasoline evaporation in China. *Atmospheric Environment*, *79*, 110–118. https://doi.org/10.1016/j.atmosenv.2013.06.029

Zhao, Q., Bi, J., Liu, Q., Ling, Z., Shen, G., Chen, F., Qiao, Y., Li, C., & Ma, Z. (2020). Sources of volatile organic compounds and policy implications for regional ozone pollution control in an urban location of Nanjing, East China. *Atmospheric Chemistry and Physics*, *20*(6), 3905–3919. https://doi.org/10.5194/acp-20-3905-2020

Zheng, H., Kong, S., Xing, X., Mao, Y., Hu, T., DIng, Y., Li, G., Liu, D., Li, S., & Qi, S. (2018). Monitoring of volatile organic compounds (VOCs) from an oil and gas station in northwest China for 1 year. *Atmospheric Chemistry and Physics*, *18*(7), 4567–4595. https://doi.org/10.5194/acp-18-4567-2018

Zheng, S., Xu, X., Zhang, Y., Wang, L., Yang, Y., Jin, S., & Yang, X. (2019). Characteristics and sources of VOCs in urban and suburban environments in Shanghai, China, during the 2016 G20 summit. *Atmospheric Pollution Research*, *10*(6), 1766–1779. https://doi.org/10.1016/j.apr.2019.07.008

Zou, Y., Charlesworth, E., Wang, N., Flores, R. M., Liu, Q. Q., Li, F., Deng, T., & Deng, X. J. (2021). Characterization and ozone formation potential (OFP) of non-methane hydrocarbons under the condition of chemical loss in Guangzhou, China. *Atmospheric Environment*, *262*. https://doi.org/10.1016/j.atmosenv.2021.118630

Acosta Navarro, J. C., Smolander, S., Struthers, H., Zorita, E., Ekman, A. M. L., Kaplan, J. O., Guenther, A., Arneth, A., & Riipinen, I. (2014). Global emissions of terpenoid VOCs from terrestrial vegetation in the last millennium. *Journal of Geophysical Research*, *119*(11), 6867–6885. https://doi.org/10.1002/2013JD021238

Arsene, C., Mihalopoulos, N., Arsene, C., & Bougiatioti, A. (2009). Sources and variability of non-methane hydrocarbons in the Eastern Mediterranean. In *Global NEST Journal* (Vol. 11, Number 3). https://www.researchgate.net/publication/228563106

Atkinson, R. (2000). *Atmospheric chemistry of VOCs and NO V*.

Atkinson, R., & Arey, J. (2003). Atmospheric Degradation of Volatile Organic Compounds. *Chemical Reviews*, *103*(12), 4605–4638. https://doi.org/10.1021/cr0206420

Beevers, S. D., Westmoreland, E., de Jong, M. C., Williams, M. L., & Carslaw, D. C. (2012). Trends in NOx and NO2 emissions from road traffic in Great Britain. *Atmospheric Environment*, *54*, 107–116. https://doi.org/10.1016/j.atmosenv.2012.02.028

Borbon, A., Locoge, N., Veillerot, M., Galloo, J. C., & Guillermo, R. (2002). Characterisation of NMHCs in a French urban atmosphere: overview of the main sources. In *The Science of the Total Environment* (Vol. 292). www.environnement.gouv.fry

Borlaza-Lacoste, L., Aynul Bari, M., Lu, C. H., & Hopke, P. K. (2024). Long-term contributions of VOC sources and their link to ozone pollution in Bronx, New York City. *Environment International*, *191*. https://doi.org/10.1016/j.envint.2024.108993

Çalik, Ö. N., & Çetin Doğruparmak, Ş. (2024). Effect of COVID-19 lockdown on ambient air quality. *Clean - Soil, Air, Water*, *52*(6). https://doi.org/10.1002/clen.202300101

Choi, S., Park, J. H., Kim, W., Kim, S. W., Lee, K. H., Chung, T., Park, J., Ryu, S. H., Shin, J., Koh, D. H., & Park, D. U. (2021). Black carbon exposure characteristics in diesel engine vehicle-related jobs. *Aerosol and Air Quality Research*, *21*(9). https://doi.org/10.4209/aaqr.200675

Collins, W. J., Derwent, R. G., Johnson, C. E., & Stevenson, D. S. (2002). *THE OXIDATION OF ORGANIC COMPOUNDS IN THE TROPOSPHERE AND THEIR GLOBAL WARMING POTENTIALS*.

De Hoffmann, E., & Stroobant, V. (2007). *Mass Spectrometry Principles and Applications Third Edition*.

DEFRA. (2020). *Non-methane Volatile Organic Compounds in the UK h*.

Department for Transport. (2025, June). *Road traffic estimates in Great Britain, 2024: Traffic in Great Britain by vehicle type*. https://www.gov.uk/government/statistics/road-traffic-estimates-in-great-britain-2024/road-traffic-estimates-in-great-britain-2024-traffic-in-great-britain-by-vehicle-type

Derwent, R. G., Jenkin, M. E., Utembe, S. R., Shallcross, D. E., Murrells, T. P., & Passant, N. R. (2010). Secondary organic aerosol formation from a large number of reactive man-made organic compounds. *Science of the Total Environment*, *408*(16), 3374–3381. https://doi.org/10.1016/j.scitotenv.2010.04.013

Diane Turner. (2024a, February 16). *GC-MS Principle, Instrument and Analyses and GC-MS/MS*. Technology Networks. https://www.technologynetworks.com/analysis/articles/gc-ms-principle-instrument-and-analyses-and-gc-msms-362513

Diane Turner. (2024b, March 24). *Gas Chromatography – How a Gas Chromatography Machine Works, How To Read a Chromatograph and GCxGC*. Technology Networks. https://www.technologynetworks.com/analysis/articles/gas-chromatography-how-a-gas-chromatography-machine-works-how-to-read-a-chromatograph-and-gcxgc-335168

Do Nascimento, C. M., de Oliveira, S. A., Santana, O. A., & Carvalho, H. (2022). Changes in air pollution due to COVID-19 lockdowns in 2020: Limited effect on NO2, PM2.5 and PM10 annual means compared to the new WHO Air Quality Guidelines. *Journal of Global Health*, *12*. https://doi.org/10.7189/JOGH.12.05043

Evans, R. L., Bryant, D. J., Voliotis, A., Hu, D., Wu, H., Syafira, S. A., Oghama, O. E., McFiggans, G., Hamilton, J. F., & Rickard, A. R. (2025). The importance of burning conditions on the composition of domestic biomass-burning organic aerosol and the impact of atmospheric ageing. *Atmospheric Chemistry and Physics*, *25*(8), 4367–4389. https://doi.org/10.5194/acp-25-4367-2025

Gentner, D. R., Jathar, S. H., Gordon, T. D., Bahreini, R., Day, D. A., El Haddad, I., Hayes, P. L., Pieber, S. M., Platt, S. M., De Gouw, J., Goldstein, A. H., Harley, R. A., Jimenez, J. L., Prévôt, A. S. H., & Robinson, A. L. (2017). Review of Urban Secondary Organic Aerosol Formation from Gasoline and Diesel Motor Vehicle Emissions. In *Environmental Science and Technology* (Vol. 51, Number 3, pp. 1074–1093). American Chemical Society. https://doi.org/10.1021/acs.est.6b04509

Gross, J. (2011). Mass Spectrometry—A Textbook. In *Mass Spectrometry: A Textbook, ISBN 978-3-642-10709-2. Springer-Verlag Berlin Heidelberg, 2011*. https://doi.org/10.1007/978-3-642-10711-5

Hajšlová, J., & Čajka, T. (2007). Chapter 12 - Gas chromatography–mass spectrometry (GC–MS). In Y. Picó (Ed.), *Food Toxicants Analysis* (pp. 419–473). Elsevier. https://doi.org/https://doi.org/10.1016/B978-044452843-8/50013-4

Hartikainen, A., Yli-Pirilä, P., Tiitta, P., Leskinen, A., Kortelainen, M., Orasche, J., Schnelle-Kreis, J., Lehtinen, K. E. J., Zimmermann, R., Jokiniemi, J., & Sippula, O. (2018). Volatile Organic Compounds from Logwood Combustion: Emissions and Transformation under Dark and Photochemical Aging Conditions in a Smog Chamber. *Environmental Science and Technology*, *52*(8), 4979–4988. https://doi.org/10.1021/acs.est.7b06269

Hersbach, H., Bell, B., Berrisford, P., Hirahara, S., Horányi, A., Muñoz-Sabater, J., Nicolas, J., Peubey, C., Radu, R., Schepers, D., Simmons, A., Soci, C., Abdalla, S., Abellan, X., Balsamo, G., Bechtold, P., Biavati, G., Bidlot, J., Bonavita, M. , …, & Thépaut, J.-N. (2026). *ERA5*

hourly data on single levels from 1940 to present [Data set]. Copernicus Climate Change Service (C3S) Climate Data Store (CDS). Doi.Org. https://cds.climate.copernicus.eu/datasets/reanalysis-era5-single-levels?tab=overview

Jacob, D. (1999). *INTRODUCTION TO ATMOSPHERIC CHEMISTRY:*

Johnson, D. K., & Marston, G. (2008). The gas-phase ozonolysis of unsaturated volatile organic compounds in the troposphere. *Chemical Society Reviews*, *37 4*, 699–716. https://api.semanticscholar.org/CorpusID:205703237

Kännaste, A., Copolovici, L., & Niinemets, Ü. (2014). Gas chromatography-mass spectrometry method for determination of biogenic volatile organic compounds emitted by plants. *Methods in Molecular Biology (Clifton, N.J.)*, *1153*, 161—169. https://doi.org/10.1007/978-1-4939-0606-2_11

Kelly, J. M., Marais, E. A., Lu, G., Obszynska, J., Mace, M., White, J., & Leigh, R. J. (2023). Diagnosing domestic and transboundary sources of fine particulate matter (PM2.5) in UK cities using GEOS-Chem. *City and Environment Interactions*, *18*, 100100. https://doi.org/https://doi.org/10.1016/j.cacint.2023.100100

Languille, B., Gros, V., Petit, J. E., Honoré, C., Baudic, A., Perrussel, O., Foret, G., Michoud, V., Truong, F., Bonnaire, N., Sarda-Estève, R., Delmotte, M., Feron, A., Maisonneuve, F., Gaimoz, C., Formenti, P., Kotthaus, S., Haeffelin, M., & Favez, O. (2020). Wood burning: A major source of Volatile Organic Compounds during wintertime in the Paris region. *Science of the Total Environment*, *711*. https://doi.org/10.1016/j.scitotenv.2019.135055

Lee, J. D., Drysdale, W. S., Finch, D. P., Wilde, S. E., & Palmer, P. I. (2020). UK surface NO2 levels dropped by 42 % during the COVID-19 lockdown: Impact on surface O3. *Atmospheric Chemistry and Physics*, *20*(24), 15743–15759. https://doi.org/10.5194/acp-20-15743-2020

Liu, B., Gu, Y., Wu, Y., Dai, Q., Song, S., Feng, Y., & Hopke, P. K. (2024). Review of source analyses of ambient volatile organic compounds considering reactive losses: methods of reducing loss effects, impacts of losses, and sources. *Atmospheric Chemistry and Physics*, *24*(22), 12861–12879. https://doi.org/10.5194/acp-24-12861-2024

Miyah, Y., Benjelloun, M., Lairini, S., & Lahrichi, A. (2022). COVID-19 Impact on Public Health, Environment, Human Psychology, Global Socioeconomy, and Education. In *Scientific World Journal* (Vol. 2022). Hindawi Limited. https://doi.org/10.1155/2022/5578284

NAEI. (2025). *AIR POLLUTANT INVENTORIES FOR ENGLAND, SCOTLAND, WALES AND NORTHERN IRELAND: 2005-2023*.

National Bureau of Statistics of China. (2024). *National Economy Pushed Forward with Innovation-led and High-quality Development and Expected Targets Achieved Successfully in 2025*. https://www.stats.gov.cn/english/

NCAC. (2024). *Why scientists are tracking wood burner emissions over the colder months*.

Newland, M. J., Mouchel-Vallon, C., Valorso, R., Aumont, B., Vereecken, L., Jenkin, M. E., & Rickard, A. R. (2022). Estimation of mechanistic parameters in the gas-phase reactions of ozone with alkenes for use in automated mechanism construction. *Atmospheric Chemistry and Physics*, *22*(9), 6167–6195. https://doi.org/10.5194/acp-22-6167-2022

NOAA. (2026). *Summer 2023 (Birmingham and London)* . National Oceanic and Atmospheric Administration (NOAA) National Centers for Environmental Information (NCEI).. Global Surface Summary of the Day . https://www.ncei.noaa.gov/

Office for National Statistics. (2020, May 1). *Deaths involving COVID-19 by local area and socioeconomic deprivation: deaths occurring between 1 March and 17 April 2020*. https://www.ons.gov.uk/peoplepopulationandcommunity/birthsdeathsandmarriages/deaths/bulletins/deathsinvolvingcovid19bylocalareasanddeprivation/deathsoccurringbetween1marchand17april

Pacchiarotta, T., Nevedomskaya, E., Carrasco-Pancorbo, A., Deelder, A. M., & Mayboroda, O. A. (2010). *Evaluation of GC-APCI/MS and GC-FID As a Complementary Platform*.

Patricia Atkins. (2022, June 2). *Looking with Light: Understanding Gas Chromatography, Part IV: Detectors*. Cannabis Science and Technology. https://www.cannabissciencetech.com/view/looking-with-light-understanding-gas-chromatography-part-iv-detectors

Road traffic statistics. (2019). *Average Annual Daily Flow*. https://roadtraffic.dft.gov.uk/count-points/57537#streetview

Shuttleworth, A., & Johnson, S. D. (2022). GC-MS/FID/EAD: A method for combining mass spectrometry with gas chromatography-electroantennographic detection. *Frontiers in Ecology and Evolution*, *Volume 10-2022*. https://doi.org/10.3389/fevo.2022.1042732

Singh, B. P., Sohrab, S. S., Athar, M., Alandijany, T. A., Kumari, S., Nair, A., Kumari, S., Mehra, K., Chowdhary, K., Rahman, S., & Azhar, E. I. (2023). Substantial Changes in Selected Volatile Organic Compounds (VOCs) and Associations with Health Risk Assessments in Industrial Areas during the COVID-19 Pandemic. *Toxics*, *11*(2). https://doi.org/10.3390/toxics11020165

Sobrado, L. A., Freije-Carrelo, L., Moldovan, M., Encinar, J. R., & Alonso, J. I. G. (2016). Comparison of gas chromatography-combustion-mass spectrometry and gas chromatography-flame ionization detector for the determination of fatty acid methyl esters in biodiesel without specific standards. *Journal of Chromatography A*, *1457*, 134–143. https://doi.org/https://doi.org/10.1016/j.chroma.2016.06.033

Vohra, K., Marais, E. A., Suckra, S., Kramer, L., Bloss, W. J., Sahu, R., Gaur, A., Tripathi, S. N., Van Damme, M., Clarisse, L., & Coheur, P.-F. (2021). Long-term trends in air quality in major cities in the UK and India: a view from space. *Atmospheric Chemistry and Physics*, *21*(8), 6275–6296. https://doi.org/10.5194/acp-21-6275-2021

WHO. (2008). *Health risks of ozone from long-range transboundary air pollution*. www.euro.who.int

Woodward-Massey, R., Sommariva, R., Whalley, L. K., Cryer, D. R., Ingham, T., Bloss, W. J., Ball, S. M., Cox, S., Lee, J. D., Reed, C. P., Crilley, L. R., Kramer, L. J., Bandy, B. J., Forster, G. L., Reeves, C. E., Monks, P. S., & Heard, D. E. (2023). Radical chemistry and ozone production at a UK coastal receptor site. *Atmospheric Chemistry and Physics*, *23*(22), 14393–14424. https://doi.org/10.5194/acp-23-14393-2023

Zhong, J., Harrison, R. M., James Bloss, W., Visschedijk, A., & Denier van der Gon, H. (2023). Modelling the dispersion of particle number concentrations in the West Midlands, UK

using the ADMS-Urban model. *Environment International*, *181*. https://doi.org/10.1016/j.envint.2023.108273